

Path–integral analysis of passive, graded–index waveguides
applicable to integrated optics.

by

Constantinos Christofi Constantinou.

A thesis submitted to the
Faculty of Engineering
of the
University of Birmingham
for the degree of
Doctor of Philosophy.

School of Electronic and Electrical Engineering,
University of Birmingham,
Birmingham B15 2TT,
United Kingdom.

September 1991.

UNIVERSITY OF
BIRMINGHAM

University of Birmingham Research Archive

e-theses repository

This unpublished thesis/dissertation is copyright of the author and/or third parties. The intellectual property rights of the author or third parties in respect of this work are as defined by The Copyright Designs and Patents Act 1988 or as modified by any successor legislation.

Any use made of information contained in this thesis/dissertation must be in accordance with that legislation and must be properly acknowledged. Further distribution or reproduction in any format is prohibited without the permission of the copyright holder.

1666892



Synopsis.

The Feynman path integral is used to describe paraxial, scalar wave propagation in weakly inhomogeneous media of the type encountered in passive integrated-optical communication devices.

Most of the devices considered in this work are simple models for graded-index waveguide structures, such as tapered and coupled waveguides of a wide variety of geometries. Tapered and coupled graded-index waveguides are the building blocks of waveguide junctions and tapered couplers, and have been mainly studied in the past through numerical simulations. Closed form expressions for the propagator and the coupling efficiency of symmetrically tapered graded-index waveguide sections are presented in this thesis for the first time. The tapered waveguide geometries considered are the general power-law geometry, the linear, parabolic, inverse-square-law, and exponential tapers. Closed form expressions describing the propagation of a centred Gaussian beam in these tapers have also been derived. The approximate propagator of two parallel, coupled graded-index waveguides has also been derived in closed form. An expression for the beat length of this system of coupled waveguides has also been obtained for the cases of strong and intermediate strength coupling. The propagator of two coupled waveguides with a variable spacing was also obtained in terms of an unknown function specified by a second order differential equation with simple boundary conditions.

The technique of path integration is finally used to study wave propagation in a number of dielectric media whose refractive index has a random component. A refractive index model of this type is relevant to dielectric waveguides formed using a process of diffusion, and is thus of interest in the study of integrated optical waveguides. We obtained closed form results for the average propagator and the density of propagation modes for Gaussian random media having either zero or infinite refractive-index-inhomogeneity correlation-length along the direction of wave propagation.

Contents.

	<u>Page</u>
Chapter 1. Introduction.	1
1.1 The history of integrated–optical technology.	1
1.2 Graded–index dielectric waveguides.	2
1.3 Graded–index dielectric waveguide analysis – the local normal mode analysis approach.	2
1.4 Numerical methods – the beam propagation method.	3
1.5 The derivation of the paraxial, scalar Helmholtz equation from Maxwell’s equations and a discussion of the validity of the assumptions made.	5
1.6 Analogy of paraxial, scalar wave–optics with non–relativistic quantum mechanics.	9
1.7 Thesis aims and outline.	11
Figures for chapter 1.	15
Chapter 2. Path Integration: general survey and application to the study of paraxial, scalar wave propagation in inhomogeneous media.	16
2.1 Definition and History of Path Integration.	16
2.2 The analogy between optics and mechanics revisited.	18
2.3 Path integration in quantum physics.	22
2.4 The transition from geometrical optics to wave optics and vice–versa.	25
2.5 Paraxial wave propagation in a homogeneous medium.	29
2.6 The uniform waveguide with a parabolic refractive index distribution.	34

Figures for chapter 2.	41
Chapter 3. Waveguides I: the straight and linearly tapering parabolic–refractive–index guides.	43
3.1 The straight, parabolic–refractive–index waveguide.	43
3.2 The propagation of a Gaussian beam in a straight, parabolic–refractive–index waveguide.	48
3.3 The linearly tapering parabolic–refractive–index waveguide.	53
3.4 The coupling efficiency of the linearly tapering parabolic–refractive–index waveguide.	58
3.5 The propagation of the total field $\psi(x, \zeta; z_0)$ in a linear taper.	62
3.6 The validity of the paraxial approximation.	64
3.7 Conclusions.	65
Figures for chapter 3.	66
Chapter 4. Waveguides II: parabolic–refractive–index guides of different geometries.	71
4.1 The symmetric, arbitrarily tapering parabolic–refractive– index waveguide.	71
4.2 The coupling efficiency of an arbitrary, symmetrical, parabolic–refractive–index taper.	75
4.3 The total field distribution in an arbitrary, symmetrical, parabolic–refractive–index taper.	77
4.4 Geometries for which the taper function $f(z, z_0)$ can be obtained in closed form.	78
4.5 The parabolic and inverse–square–law parabolic–refractive– index waveguides.	82

4.6	The exponential, parabolic–refractive–index waveguide.	87
4.7	Conclusions.	90
	Figures for chapter 4.	92
Chapter 5.	The coupling between two graded–index waveguides in close proximity.	96
5.1	Introduction.	96
5.2	The refractive index distribution used to model the two coupled waveguides.	96
5.3	The study of graded–index waveguides having a general transverse refractive index variation.	98
5.4	The propagator describing two coupled graded–index waveguides.	103
5.5	The derivation of an approximate closed form expression for the propagator of the coupled waveguides.	106
5.6	The approximate propagator describing two parallel, coupled, graded–index waveguides.	113
5.7	The functional form of the optimum function $c(z)$ for a system of two coupled waveguides with variable separation: speculations on a possible way forward?	121
5.8	Conclusions.	123
	Figures for chapter 5.	125
Chapter 6.	The random medium.	127
6.1	Introduction.	127
6.2	The definition of the random medium.	128
6.3	The averaged propagator.	131

6.4	The evaluation of the functional integral over the space of all random Gaussian refractive index functions $V(x,y,z)$.	133
6.5	The density of propagation modes.	136
6.6	The random medium which has a zero correlation length along the direction of propagation.	142
6.7	The random medium which is completely correlated along the direction of propagation.	146
6.8	The numerical calculation of the variational parameter ω of the propagator of the random medium which is completely correlated along the direction of propagation.	153
6.9	The density of modes of the random medium which is completely correlated along the direction of propagation.	155
6.10	Conclusions.	158
	Figures for chapter 6.	160
Chapter 7.	Conclusions and further work.	163
7.1	A general overview of the work presented in the thesis.	163
7.2	Suggested further work.	170
7.3	Conclusions.	172
Appendix A.		177
Appendix B.		181
Appendix C.		185
References.		189

Chapter 1

Introduction.

1.1 The history of integrated–optical technology.

The first demonstration of the laser around 1960 (Maiman, 1960) gave birth to a new area of telecommunications known today as lightwave technology. Originally it was envisaged that optical communication links could be realised by propagating laser beams in the atmosphere, but soon it became evident that the strong absorption of light by rain, snow, fog and smog severely restricted the length of optical atmospheric links. As a result such links could not be considered as serious alternatives to existing coaxial cable links. With the advent of compact, reliable, single–mode semiconductor lasers and low–loss optical fibres, it became possible to make optical communication links, which have larger bandwidth, better noise performance and smaller signal losses than any other conventional communications system known to date (Senior, 1985). In all communications systems there is a need to periodically re–amplify and reshape the optical signal in very long links, in order to ensure the integrity of the information contained in them. The only sensible way, from the engineering point of view, to make optical repeaters was suggested by Stuart E. Miller (1969) of the Bell Laboratories. This involved dispensing with electronic circuits as far as possible and making a miniature, all–optical repeater on a single chip. An integrated–optical repeater/circuit would have several advantages, such as improved noise performance, over conventional electronic devices. It would be capable of operating at higher speeds and hence have a larger bandwidth of operation. Furthermore, it would naturally have smaller connection losses when incorporated in an all–optical network. Miller’s idea marked the birth of integrated optics. The topics which integrated optics has grown to encompass are numerous: optical waveguiding, waveguide coupling, switching,

modulation, filtering and interferometry are just a few. Integrated optics is no longer concerned with optical repeaters only: it has found applications in optical transmitters, receivers, and signal processors (Boyd, 1991).

1.2 Graded-index dielectric waveguides.

In this thesis we will be exclusively concerned with the study of passive integrated optical dielectric waveguides. The most frequently encountered waveguide type in integrated optics is the dielectric waveguide whose permittivity (or equivalently whose refractive index) varies with position in a smooth, continuous fashion. Such a structure is commonly referred to as a graded-index waveguide. Graded-index waveguides are usually produced by modifying the refractive index of a crystalline or amorphous insulating substrate by diffusing certain atomic species into or out of the surface of the substrate (e.g. Silver ions in glass, or Titanium in Lithium Niobate) (Lee, 1986). Using a mask, it is easy to deposit a dopant substance onto the surface of the substrate in any geometrical configuration, thereby producing, after the diffusion process, very complicated networks of waveguides.

1.3 Graded-index dielectric waveguide analysis – the local mode analysis approach.

Even though the general theory of electromagnetic wave propagation in dielectric waveguides is well understood and has been studied intensely for over forty years, the number of waveguiding geometries which can be treated analytically (whether approximately or exactly) is very limited (Snyder and Love, 1983, Lee, 1986, Tamir, 1990). These include single waveguides or bundles of waveguides (coupled waveguides), whose cross-section and/or distance of separation are constant. Naturally, the

complicated waveguide networks used in integrated optics are not adequately described by those geometries which can be treated analytically. Practical geometries, such as the ones illustrated schematically in figure 1.1, include waveguide junctions, tapered waveguides and tapered couplers (non-parallel and/or bent waveguides in close proximity). The understanding of the operation of such waveguides is crucial in the successful design of integrated optical networks, but unfortunately most existing methods of analysis are numerical in nature and do not yield much insight into the propagation mechanism. The only exception to this statement is when the waveguide dimensions (width, separation, etc.) are sufficiently slowly varying that the modes of an infinitely long waveguide of the same dimensions at each longitudinal position may be assigned to each section of the non-uniform waveguide (Snyder and Love, 1983, Tamir, 1990). Such modes are called the **local modes** or **local normal modes** of the non-uniform waveguide. Strictly speaking, a non-uniform waveguide cannot have modes, which can only be defined for infinitely long, uniform waveguides (Snyder and Love, 1983). The analysis of the coupling between the local modes of the non-uniform waveguide or those of non-uniformly coupled waveguides is fairly complicated and the conditions for its validity are very restrictive. It is sufficient here to point out that the coupled local-mode theory is an approximate analysis applicable to waveguides with adiabatic transitions (Tamir, 1990). It must be stressed that unless a very small number of local modes is of importance, the problem soon becomes intractable because of the exceedingly complex task of considering simultaneously the propagation of, and coupling between, such a large number of modes. In this case the local normal mode method is unsuitable for gaining any insight into the propagation mechanism.

1.4 Numerical methods – the beam propagation method.

Alternative ways of studying wave propagation in graded-index dielectric waveguides are almost exclusively numerical. These involve the numerical solution of an

approximate form of Maxwell's equations on a computer. The most commonly used method of this kind is the **beam propagation method** (Feit and Fleck, 1978). The method is a numerical solution of the scalar, paraxial Helmholtz equation in a weakly inhomogeneous medium with an arbitrary refractive index distribution. The derivation and conditions of validity of this equation are considered in detail in the next section of this chapter. In this method, a given field amplitude and phase distribution are prescribed in some plane perpendicular to the direction of propagation. The field profile is then decomposed into its angular spectrum of uniform plane waves using a Fast Fourier Transform and each plane wave is propagated a very small distance δz along the direction of propagation, as if the surrounding medium had a constant refractive index. The inverse Fast Fourier Transform is then taken and the resultant field distribution phase is corrected according to the thin-lens law in order to account for the refractive index inhomogeneities. This procedure is repeated a large number of times in order to propagate the prescribed field distribution over a specified medium length.

The beam propagation method does not model polarisation (itself not a significant drawback as we shall see in the next section) and cannot account for abrupt and large refractive index changes in short distances compared to the wavelength. As a consequence, it does not take into account reflections from regions of rapid change in the refractive index. The assumptions of paraxial wave propagation and of a weakly inhomogeneous medium are not severe limitations as we shall soon see. They happen to be valid for most integrated-optical graded-index dielectric waveguides, as strongly guiding waveguides are very dispersive and therefore useless for communications purposes.

The main advantage of this method is that it can cope with a very wide range of waveguide cross-sectional refractive index profiles and waveguide geometries. The beam propagation method is therefore well suited to deal with tapered waveguides whose cross-section is an arbitrary function of position along the waveguide axis, and with non-uniformly coupled waveguides in which the distance of separation varies in an

arbitrary manner and for bent waveguides. Its main disadvantages are that it is computationally intensive and, being a numerical technique, yields little insight into the propagation mechanism and its linking to the various refractive index parameters.

1.5 The derivation of the paraxial, scalar Helmholtz equation from Maxwell's equations and a discussion of the validity of the assumptions made.

The medium in which we will formulate the propagation problem will be described by the following parameters. Its permittivity, $\epsilon(x,y,z)$, is a continuous, smooth scalar function of position, and its permeability, μ , is a scalar constant equal to that of free space, μ_0 . Its conductivity, σ , is taken to be zero. No free charges can exist in such a medium and we may, therefore, consider the free charge and free current densities to be zero.

An inhomogeneous medium which obeys the above description is a good approximation to the practical waveguiding structures used in integrated optics. Typical materials used in practical structures are silicate glasses (mixtures of SiO_2 with Li_2O , Na_2O , Al_2O_3 and K_2O) with ions such as Ag^+ , Tl^+ and K^+ diffused into the glass, and LiNbO_3 and LiTaO_3 crystal substrates, with Ti and Nb diffused into the crystal respectively, to form waveguides (Lee, 1986). The substrate refractive index values range between approximately 1.4 and 2.2, while the maximum refractive index change achieved by the diffusion process is between 0.3% and 3%. The propagation losses for successfully fabricated waveguides are less than 1dB/cm. These methods usually result in waveguides with typical cross-sectional dimensions ranging from $1\mu\text{m}$ to about $8\mu\text{m}$, which are used with light of free space wavelength ranging from $0.63\mu\text{m}$ to $1.55\mu\text{m}$. From this brief description of the materials used in the fabrication of integrated optical waveguides it can be seen that the propagation medium description given in the previous paragraph is fairly accurate.

Maxwell's equations in SI units for the medium described above are:

$$\nabla \times \mathbf{H} - \frac{\partial \mathbf{D}}{\partial t} = \mathbf{0}, \quad (1.1a)$$

$$\nabla \times \mathbf{E} + \frac{\partial \mathbf{B}}{\partial t} = \mathbf{0}, \quad (1.1b)$$

$$\nabla \cdot \mathbf{D} = 0, \quad (1.1c)$$

and

$$\nabla \cdot \mathbf{B} = 0, \quad (1.1d)$$

where \mathbf{E} and \mathbf{H} are the electric and magnetic field vectors respectively and \mathbf{D} and \mathbf{B} are the electric and magnetic displacement vectors respectively. The two sets of vectors are related by the constitutive relations,

$$\mathbf{D}(x, y, z) = \epsilon(x, y, z) \mathbf{E}(x, y, z), \quad (1.2a)$$

and

$$\mathbf{B}(x, y, z) = \mu_0 \mathbf{H}(x, y, z). \quad (1.2b)$$

We then use equations (1.2) to eliminate the electromagnetic field displacement vectors from Maxwell's equations (1.1), take the curl of equation (1.1b) and substitute for $\nabla \times \mathbf{H}$ from equation (1.1a) to obtain,

$$\nabla^2 \mathbf{E} - \epsilon(x, y, z) \mu_0 \frac{\partial^2 \mathbf{E}}{\partial t^2} - \nabla(\nabla \cdot \mathbf{E}) = \mathbf{0}. \quad (1.3)$$

The last term on the left-hand side of equation (1.3) can be rewritten with the aid of (1.1c), giving,

$$\nabla^2 \mathbf{E} - \epsilon(x, y, z) \mu_0 \frac{\partial^2 \mathbf{E}}{\partial t^2} + \nabla(\mathbf{E} \cdot \nabla[\ln \epsilon(x, y, z)]) = \mathbf{0}. \quad (1.4)$$

If we now concentrate our attention on a monochromatic wave of angular frequency ω , the above equation can be written as,

$$\nabla^2 \mathbf{E} + \omega^2 \epsilon(x, y, z) \mu_0 \mathbf{E} + \nabla(\mathbf{E} \cdot \nabla[\ln \epsilon(x, y, z)]) = \mathbf{0}. \quad (1.5)$$

The term $\omega^2 \epsilon(x, y, z) \mu_0$ is of the order of the square of the inverse wavelength of light. If the fractional change in the dielectric constant over distances of the order of the wavelength of light is at least a couple of orders of magnitude smaller than unity,

$$\left| \frac{\lambda \nabla \epsilon}{\epsilon} \right| \ll 1, \quad (1.6)$$

then the third term on the left-hand side of equation (1.5) can be neglected as being very small compared to the second term. Equation (1.6) is the criterion defining a weakly inhomogeneous medium. As we have already mentioned, weakly inhomogeneous media are

particularly relevant to integrated optics, because the waveguides involved are weakly guiding and are thus characterised by low dispersion and hence a higher bandwidth of operation. In this case, equation (1.4) simplifies to,

$$\nabla^2 \mathbf{E} - \epsilon(x, y, z) \mu_0 \frac{\partial^2 \mathbf{E}}{\partial t^2} = \mathbf{0}. \quad (1.7)$$

Therefore, all the Cartesian components of the electric field vector satisfy the wave equation. It is important to note that assumption (1.6) decouples the different linear polarisation states of the wave, which implies that a scalar wave theory is adequate as an analysis tool in integrated optics. Under assumption (1.6), it can be similarly shown that all the Cartesian components of the magnetic field vector, the magnetic vector potential and the electric scalar potential, satisfy equation (1.7). Any one of these components will be henceforth denoted by $\varphi(x, y, z)$. The power density of the corresponding propagating wave will then be proportional to $|\varphi|^2$.

Paraxial propagation is one in which the surfaces of constant phase of the propagating wave are approximately planar. The corresponding geometrical optics picture is that of a bundle of rays (defined to be normal to the wavefronts), which are nearly parallel to the direction of propagation (the angle θ between each of the rays and the propagation axis should not exceed the value $\pi/12$, so that the approximation $\sin\theta \simeq \theta$ is valid) (Born and Wolf, 1980). It is well known from other analyses (Lee, 1986) that the modes/local normal modes of weakly inhomogeneous waveguides satisfy the conditions of the paraxial approximation accurately. A simplistic way of looking at this statement is that the rays corresponding to the guided modes of the waveguide must be totally internally reflected at the guide boundaries. Since the change in the refractive index between the waveguide and the surrounding medium is small (weakly inhomogeneous medium), the ray must approach the guide boundary at almost grazing incidence (small θ). For this reason we will express the field amplitude $\varphi(x, y, z, t)$ of a monochromatic wave propagating paraxially along the z -axis of the chosen co-ordinate system in the form,

$$\varphi(x, y, z, t) = f(x, y, z) \exp(ik_0 n_0 z - i\omega t), \quad (1.8)$$

where n_0 is the maximum value of the refractive index (related to the permittivity function by equations (1.11) and (1.12) below), k_0 is the free space wavenumber related to the free space wavelength λ_0 , the angular frequency ω and the speed of light in vacuo c by,

$$k_0 = \omega/c = 2\pi/\lambda_0, \quad (1.9)$$

and the complex valued function $f(x, y, z)$ is a slowly varying function of z on a scale of $1/k_0 n_0$. The phase of f describes the departure of the phasefront of the wave from that of a plane wave.

Substituting equation (1.8) into equation (1.7) gives,

$$\frac{\partial^2 f}{\partial x^2} + \frac{\partial^2 f}{\partial y^2} + \frac{\partial^2 f}{\partial z^2} - k_0^2 n_0^2 f + 2ik_0 n_0 \frac{\partial f}{\partial z} + \omega^2 \mu_0 \epsilon f = 0. \quad (1.10)$$

The refractive index is related to the permittivity $\epsilon(x, y, z)$ by

$$n^2(x, y, z) = \epsilon(x, y, z)/\epsilon_0, \quad (1.11)$$

where ϵ_0 is the permittivity of free space. If we were to write the refractive index function in the form,

$$n(x, y, z) = n_0(1 - n'(x, y, z)), \quad (1.12)$$

where $n'(x, y, z)$ is a semi-definite, smooth, continuous function of position and n_0 is the maximum value of the refractive index in the medium, the weakly inhomogeneous medium criterion (1.6) imposes a restriction on the magnitude of $n'(x, y, z)$, namely,

$$n'(x, y, z) \ll 1. \quad (1.13)$$

Making use of the fact that $\epsilon_0 \mu_0 = 1/c^2$, equation (1.12) shows that equation (1.10) can be re-written as

$$\frac{\partial^2 f}{\partial x^2} + \frac{\partial^2 f}{\partial y^2} + \frac{\partial^2 f}{\partial z^2} + 2ik \frac{\partial f}{\partial z} + k_0^2 n_0^2 (n'^2 - 2n')f = 0. \quad (1.14)$$

Re-defining the wavenumber k in such a way as to absorb the n_0 term in it,

$$k = k_0 n_0, \quad (1.15)$$

and using $n' \gg n'^2$ (a consequence of (1.13)), equation (1.14) simplifies to,

$$\frac{\partial^2 f}{\partial x^2} + \frac{\partial^2 f}{\partial y^2} + \frac{\partial^2 f}{\partial z^2} + 2ik \frac{\partial f}{\partial z} - 2n' k^2 f = 0. \quad (1.16)$$

But by the assumption of paraxial propagation f is a slowly varying function of z on a

scale of $1/k$, and hence, $\frac{\partial^2 f}{\partial z^2} \ll k \frac{\partial f}{\partial z}$. This further simplifies equation (1.16) to,

$$\frac{\partial^2 f}{\partial x^2} + \frac{\partial^2 f}{\partial y^2} + 2ik \frac{\partial f}{\partial z} - 2n' k^2 f = 0, \quad (1.17)$$

which can be easily cast in the form

$$\frac{i}{k} \frac{\partial f}{\partial z}(x, y, z) + \frac{1}{2k^2} \nabla_{xy}^2 f(x, y, z) - n'(x, y, z) f(x, y, z) = 0, \quad (1.18)$$

where

$$\nabla_{xy}^2 \equiv \frac{\partial^2}{\partial x^2} + \frac{\partial^2}{\partial y^2} \quad (1.19)$$

Equation (1.18) will be referred to as the paraxial, scalar Helmholtz equation describing propagation in a weakly inhomogeneous medium (Marcuse, 1982). It will form the basis of our analysis in this work, but unlike the beam propagation method, we will not attempt to solve this numerically.

1.6 Analogy of paraxial, scalar wave-optics with non-relativistic quantum mechanics.

Equation (1.18) is identical in form to the Schrödinger equation describing the time-dependent, non-relativistic quantum-mechanical wavefunction $\psi(x, y, t)$ of a single zero-spin particle of mass, m , moving in two dimensions under the influence of a two-dimensional, time-dependent potential, $V(x, y, t)$ (Feynman and Hibbs, 1965).

$$i\hbar \frac{\partial \psi}{\partial t}(x, y, t) + \frac{\hbar^2}{2m} \nabla_{xy}^2 \psi(x, y, t) - V(x, y, t) \psi(x, y, t) = 0. \quad (1.20)$$

A direct comparison of equations (1.18) and (1.20) yields a number of useful analogies between paraxial, scalar wave optics and non-relativistic quantum mechanics. These are briefly discussed below and summarised in Table 1.1.

The problem of paraxial wave propagation in three dimensions corresponds to quantum-mechanical motion in two dimensions. The displacement variable, z , along the axis parallel to the direction of paraxial propagation, corresponds to the time variable, t , in the quantum-mechanical problem. The fact that the Schrödinger equation has a first order time-derivative term is due to its non-relativistic nature (we are to consider the

spin=0 case only), while the first order z -derivative term in the scalar wave equation is due to the paraxial approximation. A comparison of the simplest proposed version of a relativistic Schrödinger equation for spin=0 particles, known as the Klein-Gordon equation (Eisberg and Resnick, 1985), with equation (1.7) reveals that the time- and z -derivative terms now appear to second order. Therefore, the non-paraxial scalar wave optics problem corresponds to the spin=0, relativistic quantum-mechanical problem.

The analogy requires that the mass of the particle in the quantum-mechanical problem should be set to unity, and this yields a correspondence between the inverse scaled wavenumber $1/k$ and Planck's constant \hbar . Equations (1.9) and (1.15) show that the inverse scaled wavenumber is simply the minimum value of the wavelength in the medium, $\lambda \equiv \lambda_0/n_0$, divided by 2π .

Finally, the scaled position-dependent part of the refractive-index-inhomogeneity function $n'(x,y,z)$ is found to correspond to the time-dependent potential $V(x,y,t)$.

Scalar wave optics	Quantum mechanics (spin 0)
	particle mass $m \equiv 1$
3 space dimensions paraxial distance z transverse position x,y	3 space-time dimensions time t position x,y
paraxial	non-relativistic
reduced wavelength $\lambda \equiv 1/k \equiv \lambda_0/2\pi n_0$	Planck's constant $\hbar \equiv h/2\pi$
scaled refractive index inhomogeneity function n'	Potential V

Table 1.1

1.7 Thesis aims and outline.

In this thesis we will use the analogy between quantum mechanics and wave optics in order to study the propagation of paraxial, scalar waves in graded-index waveguides of various geometries. In order to do so, we will use the Feynman path-integral formalism of quantum mechanics (Feynman and Hibbs, 1965) in order to derive by analogy the propagator, or Green's function, of the paraxial, scalar wave equation, in an approximate but closed analytic form. Our aim is to produce results which do not suffer from the limitations of local normal mode theory and which, in contrast with the beam propagation method, are not numerical in nature and will, therefore, yield more insight into the propagation mechanism. In this sense, this work is intended to complement the beam propagation method as a tool for the analysis of waveguides.

The motivation behind this work is to model, using approximate closed form expressions, the propagation characteristics of dielectric graded-index waveguide junctions which in the past have been studied almost exclusively numerically. Any waveguide junction geometry can be seen to consist of two types of waveguides sections: tapered waveguide section, where two or more waveguides merge together, and coupled waveguide sections (waveguides in very close proximity) of an arbitrary geometrical arrangement, in regions just before the waveguides have merged. For this reason we will focus on two waveguide geometries, tapered waveguides and non-uniformly coupled waveguides.

An introduction to path integrals, including their definition and the application of path integration to problems in wave optics, forms the subject of chapter 2. Furthermore, we will briefly consider problems in other branches of physics which bear an analogy to non-relativistic quantum mechanics and to scalar, paraxial wave optics and we will, as far as possible, try to make use of these analogies to assist in the solution of the various problems we are going to consider. Finally, we will derive the propagator of an infinite uniform medium (free space) and of a model waveguide system whose cross-sectional

refractive index distribution has a quadratic dependence on the displacement from the waveguide axis (the corresponding quantum–mechanical problem is that of the harmonic oscillator) (Eisberg and Resnick, 1985). These two propagators are derived in exact, closed form. The quadratic refractive index waveguide is of great importance in modern optics, since it accurately models the refractive index distribution in the core of a multimode, graded–index fibre and a graded–index–rod lens (Senior, 1985, Wu and Barnes, 1991).

Chapter 3 is mainly concerned with the propagation of Gaussian beams (Yariv, 1991) in free space and quadratic refractive index waveguides. The results presented are well known, but the method of analysis used here allows us to express them in a more compact form than that previously available. The analysis of the linearly tapered quadratic refractive index waveguide forms the bulk of chapter 3. This is the single most important geometry for a tapered waveguide, as it naturally forms a part of waveguide junctions. The coupling efficiency of the first few local modes of the linearly tapered waveguide is investigated in detail, as well as the propagation of a Gaussian beam in such a taper. The coupling efficiency information presented here is new. A comparison is made with published predictions on the coupling efficiency of the linearly tapered waveguide, to illustrate the power of the method of analysis employed here. The linearly tapered quadratic–refractive–index waveguide analysis presented in this chapter has been published in Constantinou and Jones (1991a and 1991b).

Chapter 4 extends the work of chapter 3 to symmetrically tapered waveguides of arbitrary geometry. The general taper analysis is then applied to tapers with parabolic, inverse square law and exponential geometries. All the work in this chapter is, to the best of our knowledge, new. A comparison of the results with other published work is also presented.

A study of waveguide junctions requires not only the study of tapered waveguides but also the detailed understanding of coupled waveguides, whose separation is an

arbitrary function of paraxial propagation distance. Figure 1.2 shows schematically a pair of waveguide geometries of the type described above, where the coupling between the two waveguides is of importance. Chapter 5 presents the analysis of the two-coupled-waveguide problem of arbitrary geometry, and illustrates the power of the closed form but approximate results by applying them to the parallel and arbitrarily-tapered coupled waveguide problems. The work in this chapter is largely based on Feynman's variational principle (Feynman and Hibbs, 1965) which is presented as a tool for obtaining an approximate closed form expression for the propagator of a waveguide system with a cross-sectional refractive index profile for which it is not possible to evaluate the path integral in closed form. In the cases considered in this thesis, the variational method employs the quadratic refractive index waveguide as the archetypal waveguide model which can be used as the starting point in the calculation. The closed form expressions for the propagators of the arbitrarily, symmetrically tapered waveguide coupler and the parallel coupled waveguide are new. The expression derived for the beat length of two parallel, strongly coupled waveguides is also new.

As integrated-optical waveguides are formed by a process of diffusion, which is intrinsically a random process, the subject of propagation in a random medium/waveguide with random refractive index inhomogeneities is of particular relevance to this work. Random inhomogeneities act as scattering centres and tend to attenuate the propagating wave, as well as distort its phasefronts. The average propagator and density of wavenumber states (together with its engineering interpretation) are derived for media with different spatial correlation functions, in chapter 6. The work in this chapter uses the analogy with quantum mechanics extensively. The corresponding quantum-mechanical problem is that of electronic motion in disordered solids (Edwards, 1958, Jones and Lukes, 1969). Most, but not all, of the work presented in this chapter is original. The results for the density of wavenumber states are new, though.

Finally, chapter 7 summarises the work presented in the thesis, draws a number of

conclusions, including the suitability of path integration as an analytical tool in the study of wave optics, and proposes further work that can be carried out on this subject.

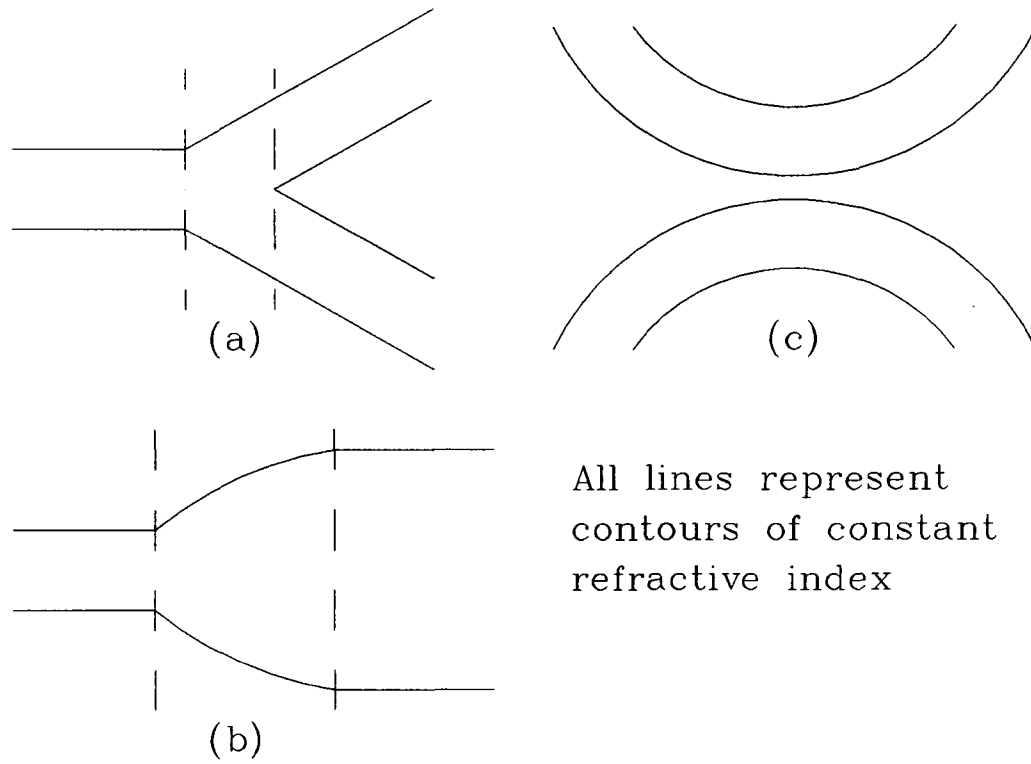


Figure 1.1: Examples of: (a) a waveguide junction, (b) a tapered waveguide section, and (c) a tapered coupler.

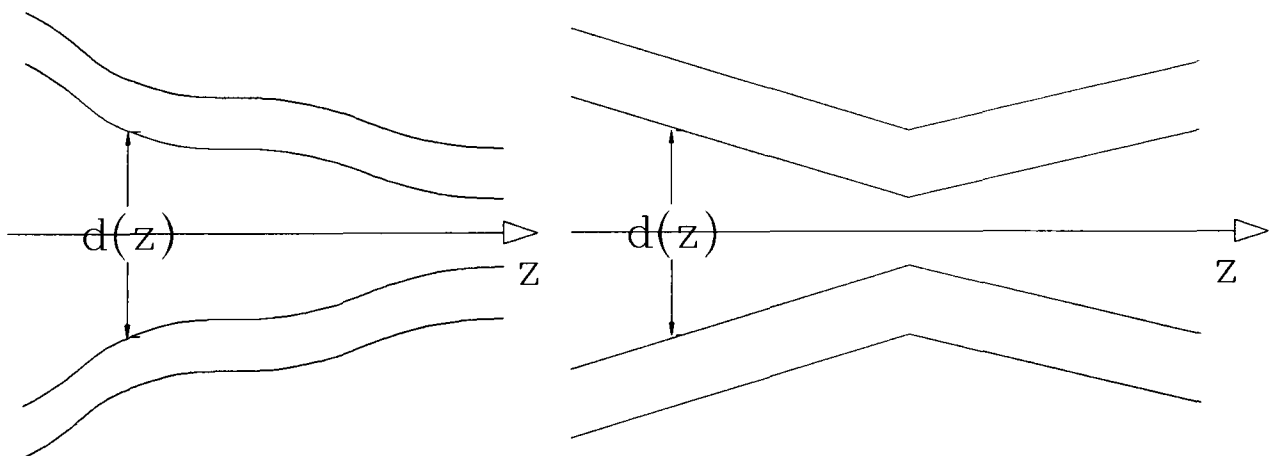


Figure 1.2: Two further examples of tapered couplers. The separation $d(z)$ of the two waveguides, and hence the coupling strength is variable.

Chapter 2

Path Integration: general survey and application to the study of paraxial, scalar wave propagation in inhomogeneous media.

2.1 Definition and history of path integration.

A path, or functional, integral is a generalisation of ordinary integral calculus to functionals. It can be defined as the limit of multiple ordinary Riemann integrals. We define

$$\int_{y(x_0)}^{y(x_N)} \delta y(x) F[y(x)] \quad (2.1)$$

to be a path integral, if $F[y(x)]$ is a functional, i.e. a function which depends not just on one value of y (which corresponds to one value of x), but depends on **all** values of $y(x)$ in the domain of interest. The limits in the integral (2.1) indicate that we are considering the space of functions $y(x)$ which have fixed endpoints $y(x_0) = y_0$ and $y(x_N) = y_N$. The integral is to be interpreted according to the following rule:

Divide the x -axis into N equal intervals whose end-points are x_{i-1} and x_i where $i \in \{1, 2, \dots, N\}$. For every single valued function $y(x)$ there corresponds a unique value of y to each x_i , which we will call $y_i = y(x_i)$. By joining each consecutive pair of points (y_{i+1}, x_{i+1}) and (y_i, x_i) by a straight line segment (see figure 2.1) the piecewise continuous curve formed is an approximation to the curve $y = y(x)$. This approximation is better and better as N becomes large, and in the limit as $N \rightarrow \infty$ the discrete representation of the function becomes exact. Replace the functional $F[y(x)]$ by a function of $(N+1)$ variables $F'(y_0, y_1, \dots, y_N)$ which is a discrete version of $F[y(x)]$ and compute the following $(N-1)$ -dimensional

integral:

$$A^{-N} \int_{-\infty}^{+\infty} \cdots \int_{-\infty}^{+\infty} dy_1 \cdots dy_{N-1} F'(y_0, y_1, \dots, y_N) \quad (2.2)$$

where y_0 and y_N are fixed and the constant A is a normalising factor depending on the number of intervals N , and which is chosen to allow one to take a proper limit as $N \rightarrow \infty$.

A^{-N} is called the measure of the functional space, and as we will see later it is formally infinite. What we have done in effect is to compute the sum of $F[y(x)]$ over all possible functions $y(x)$ subject to the boundary conditions $y(x_0) = y_0$ and $y(x_N) = y_N$. Then, the limit of the above multiple integral as $N \rightarrow \infty$ and $x_N - x_0 = \text{constant}$ is to be interpreted as the value of the path integral. The constant value of $x_N - x_0$ can be either finite and non-zero, as in the calculation of a propagator in Quantum Mechanics, or zero when, in statistical mechanics, one is trying to compute a partition function. It would also be zero in the evaluation of the density of states of a Quantum Mechanical system; an analogue of this latter problem will be considered in this thesis.

The first known attempt to integrate over a space of functions was by P.J. Daniell (1918, 1919, 1920), but this was unsuccessful because he refused to introduce an infinite measure into a functional space. A few years later, N. Wiener (1921a, 1921b, 1923, 1924, 1930) introduced the Wiener measure and used it to define the integral of a functional over a space of functions in his study of Brownian motion. This was the first successful attempt to use path integration to study a problem in physics. For more than a decade path integration found no further applications in theoretical physics. The paper which first suggested the use of path integration in most areas of quantum mechanics was by P.A.M. Dirac (1933) and was titled 'The Lagrangian in Quantum Mechanics'. Curiously, this paper had nothing to do with the techniques of path integration itself, but was an attempt to formulate quantum mechanics starting with the Lagrangian instead of the Hamiltonian description. The turning point in the use of path integration in physics came when

Feynman (1942, 1948), having read Dirac's paper, invented a representation for the propagator (Green's function) of the Schrödinger equation in terms of a path integral. Feynman then applied the path integral formalism of quantum mechanics to solve with relative ease very difficult problems, such as the propagation of a polaron (Feynman, 1955), which is an electron together with the disturbance it causes in an "elastic" crystal. He also successfully applied the path integral formalism to the study of liquid Helium (Feynman, 1957) and quantum electrodynamics (Feynman, 1950, 1951). Path integration soon found widespread use in other fields of theoretical physics. These include polymer dynamics (Edwards, 1965, 1967, 1975, de Gennes, 1969), solid state physics (Zittarz and Langer, 1966, Jones and Lukes, 1969, Edwards and Abram, 1972), statistical mechanics (Feynman, 1972, Wilson, 1971), fluid dynamics (Edwards, 1963), quantum field theory (Edwards and Peierls, 1954, Matthews and Salam, 1955), quantum gravity (Hawking, 1979), optics (Eichmann, 1971, Eve, 1976, Hannay, 1977, Hawkins, 1987, 1988, Troudet and Hawkins, 1988), and general propagation problems (Lee, 1978). Several excellent textbooks and review papers can be found on the subject, the most important ones being the books by Feynman and Hibbs (1965), by Kac (1959), and more recently the books by Schulman (1981) and Wiegand (1986), and the review papers of Gel'fand and Yaglom (1960), Sherrington (1971), Keller and McLaughlin (1975), and DeWitt–Morette, Low, Schulman and Shiekh (1986).

2.2 The analogy between optics and mechanics revisited.

In the previous chapter we developed the analogy between paraxial, scalar wave optics and non-relativistic, spin-0 quantum mechanics. The analogy between optics and mechanics is not confined to the wave aspects of the two subjects, but also extends to geometrical optics and classical mechanics. For the sake of completeness, we will now proceed to extend this analogy to paraxial geometrical optics and non-relativistic classical

mechanics. This analogy can be best seen if we approach the two subjects through Fermat's and Hamilton's principle respectively.

Fermat's principle, or the principle of least time (Born and Wolf, 1980), states that *'the time taken for a ray of light to travel between two fixed points in space is stationary with respect to small deviations of the ray path from its true value.'* If the light ray travels with a local speed $v(\mathbf{r})$, and s is the arc length along the ray path, the total time of travel between the two fixed endpoints can be written in the form of an integral as,

$$T[\mathbf{r}(s)] = \int_{s_0}^s d\sigma \frac{1}{v(\mathbf{r}(\sigma))} \quad (2.3)$$

Using the definition of the refractive index $n(\mathbf{r}) \equiv \frac{c}{v(\mathbf{r})}$, the total time of travel can be written as,

$$T[\mathbf{r}(s)] = \frac{1}{c} \int_{s_0}^s d\sigma n(\mathbf{r}(\sigma)). \quad (2.4)$$

The quantity $cT[\mathbf{r}(s)]$ is defined as the optical path length of the path $\mathbf{r}(s)$. Fermat's principle is then equivalent to the statement that the optical path length of a ray travelling between two points in space is extremal with respect to small deviations of the ray path from its true value. The optical path length $S[\mathbf{r}(s)]$

$$S[\mathbf{r}(s)] = \int_{s_0}^s d\sigma n(\mathbf{r}(\sigma)), \quad (2.5)$$

is a functional, since its value depends on the particular function $\mathbf{r}(s)$ chosen in $n(\mathbf{r}(\sigma))$ and has the dimensions of length.

In order to state Hamilton's principle, we first need to give the definitions of a small number of relevant physical quantities. The first of these is the Lagrangian, L , for a particle. This is defined to be the difference between its kinetic and potential energies,

$$L\left(\frac{d\mathbf{r}}{dt}, \mathbf{r}, t\right) = T\left(\mathbf{r}, \frac{d\mathbf{r}}{dt}\right) - V(\mathbf{r}, t) \quad (2.6)$$

where, the kinetic energy is given, in the non-relativistic limit, by

$$T\left(\mathbf{r}, \frac{d\mathbf{r}}{dt}\right) = \frac{1}{2} m \left[\frac{d\mathbf{r}}{dt}\right]^2, \quad (2.7)$$

and

$V(\mathbf{r}, t)$ is the potential energy of the particle.

The action integral is then defined to be the time integral of the Lagrangian,

$$S[\mathbf{r}(t)] = \int_{t_0}^t d\tau L\left(\frac{d\mathbf{r}}{dt}(\tau), \mathbf{r}(\tau), \tau\right) \quad (2.8)$$

The notation $S[\mathbf{r}(t)]$ indicates that the action is a functional, since it depends on all the values of $\mathbf{r}(t)$ in the domain $t_0 \leq \tau \leq t$. The dimensions of the action are those of angular momentum (in the SI system of units these are Joule–seconds [Js]). Hamilton’s principle (Goldstein, 1980), for a single particle moving under the influence of a potential field $V(\mathbf{r}, t)$, states that *‘the motion of the particle occurs so that the action integral S is stationary with respect to small deviations of the path from that which satisfies Newton’s laws, subject to the constraint of all considered paths having the same fixed endpoints.’*

It is evident that there exists a direct analogy between geometrical optics and classical mechanics, by virtue of the fact that both can be defined using an extremum principle. It may seem at first sight that some differences exist between the two physical problems, since the integrand in expression (2.8) has a definite functional form given by (2.6) and (2.7), while the functional form of the refractive index in (2.5) is completely arbitrary. The above statement is misleading though, because expression (2.7) is true in the non–relativistic approximation, while expression (2.5) is exact and not restricted to the paraxial approximation. As we have seen in chapter 1, the analogy strictly holds when we consider non–relativistic mechanics and paraxial wave optics. We will now proceed to show that in the paraxial approximation the functional form of the integrand in (2.5) has the same functional form as the Lagrangian given by (2.6) and (2.7).

In the paraxial approximation the angle θ which the ray of light makes with the axis of propagation (chosen to be the z –axis for consistency with chapter 1), is small. In the Cartesian co–ordinate system, we have,

$$\sin\theta = \frac{\sqrt{dx^2 + dy^2}}{ds} \simeq \theta \ll 1. \quad (2.9)$$

Making use of the Euclidean metric,

$$ds^2 = dx^2 + dy^2 + dz^2, \quad (2.10)$$

we have,
$$ds^2 \simeq dz^2 \gg dx^2 + dy^2. \quad (2.11)$$

Furthermore, we use expressions (1.12) and (1.13) in order to allow for a variation of refractive index with position (x, y, z) . This, as explained in chapter 1, is consistent with paraxial propagation, and we may then change the variable of integration in (2.5) from s to z , to get

$$S[\boldsymbol{\rho}(z)] = \int_{z_0}^z d\zeta n_0(1 - n'(x(\zeta), y(\zeta), \zeta)) \sqrt{1 + \left[\frac{dx}{d\zeta}(\zeta)\right]^2 + \left[\frac{dy}{d\zeta}(\zeta)\right]^2}, \quad (2.12)$$

where the two-dimensional position vector $\boldsymbol{\rho}$ is defined by

$$\boldsymbol{\rho} \equiv \begin{bmatrix} x \\ y \end{bmatrix}. \quad (2.13)$$

Expanding the square root in expression (2.12) into an infinite series, only terms which are up to second order in $\frac{dx}{dz}$ and $\frac{dy}{dz}$ are retained, by virtue of (2.11), which is a direct consequence of the paraxial approximation. When the multiplication of the resulting series with the expression for the refractive index is carried out, terms such as $n'(x, y, z) \left[\frac{dx}{dz}(z)\right]^2$ are neglected, since they are at least third order in small quantities, which in turn is a consequence of equations (1.13) and (2.11). The resulting approximate expression for the optical path length is then,

$$S[\boldsymbol{\rho}(z)] = n_0(z - z_0) + n_0 \int_{z_0}^z d\zeta \left\{ \frac{1}{2} \left[\frac{dx}{d\zeta}(\zeta)\right]^2 + \frac{1}{2} \left[\frac{dy}{d\zeta}(\zeta)\right]^2 - n'(x(\zeta), y(\zeta), \zeta) \right\}. \quad (2.14)$$

Apart from an irrelevant term $n_0(z - z_0)$, which is independent of the ray path $(x(\zeta), y(\zeta))$, and from the constant factor n_0 , the expression for the optical path length (2.14) has exactly the same functional dependence on the ray path and its derivatives, as expressions (2.6) to (2.8). Hence the analogy between paraxial wave optics and non-relativistic quantum mechanics as stated in Table 1.1 of chapter 1, also holds for paraxial geometrical optics and non-relativistic classical mechanics.

2.3 Path integration in quantum physics.

We briefly present the link between classical and quantum mechanics before considering the corresponding optics problem, so as to be able to continue the discussion on the analogy between optics and mechanics later in this chapter. The details of how classical and quantum mechanics are linked, are discussed in detail in Feynman and Hibbs (1965). To begin our discussion, we first need to define the meaning of the probability amplitude in quantum mechanics. The probability amplitude for a particle to go from position \mathbf{r}_0 at time t_0 to position \mathbf{r} at a later time t , is a complex valued function whose modulus squared gives the probability for this transition to occur. The phenomena of diffraction and interference observed in quantum mechanics make it necessary for us to postulate the linear superposition of probability amplitudes for mutually exclusive events, and not of the probabilities themselves (Feynman and Hibbs, 1965). Dirac (1933) showed that the probability amplitude for a particular path $\mathbf{r}(t)$ corresponds to $\exp\{iS[\mathbf{r}(t)]/\hbar\}$, where $S[\mathbf{r}(t)]$ is the classical action (2.8) for this path, and \hbar is Planck's constant, the fundamental constant of action in nature, divided by 2π .

Feynman (1942, 1948) made the conjecture that the word "corresponds" should translate to, "is proportional to". This led him to show that the transition amplitude, or propagator, $K(\mathbf{r}, t; \mathbf{r}_0, t_0)$, must be given by,

$$K(\mathbf{r}, t; \mathbf{r}_0, t_0) = \int_{\mathbf{r}_0, t_0}^{\mathbf{r}, t} \delta\mathbf{r}(t) \exp\left\{\frac{i}{\hbar} \int_{t_0}^t d\tau L\left(\frac{d\mathbf{r}}{dt}(\tau), \mathbf{r}(\tau), \tau\right)\right\}. \quad (2.15)$$

where the integral is a functional integral over the space of all paths, $\mathbf{r}(t)$, which are forward moving in time, with fixed end-points $\mathbf{r} \equiv \mathbf{r}(t)$ and $\mathbf{r}_0 \equiv \mathbf{r}(t_0)$. The integral (2.15) is often referred to as a Feynman path integral. It is defined in its limiting form using the procedure described in section 2.1, as,

$$K(\mathbf{r}, t; \mathbf{r}_0, t_0) = \lim_{\delta\tau \rightarrow 0} \left\{ A^{-N} \int_{-\infty}^{+\infty} \cdots \int_{-\infty}^{+\infty} d^D \mathbf{r}_1 \cdots d^D \mathbf{r}_{N-1} \exp \left\{ \frac{i}{\hbar} \delta\tau \sum_{n=0}^{N-1} L \left[\frac{\mathbf{r}_{n+1} - \mathbf{r}_n}{\delta\tau}, \frac{\mathbf{r}_{n+1} + \mathbf{r}_n}{2}, \frac{\tau_{n+1} + \tau_n}{2} \right] \right\} \right\}, \quad (2.16)$$

where $N \delta\tau = t - t_0$, a constant, (2.17)

$$A = \left[\frac{2\pi i \hbar \delta\tau}{m} \right]^{D/2} \quad (2.18)$$

is the normalising constant, and D is the dimensionality of the space we are working in. The measure of the Feynman path integral $1/A$ is formally infinite in the limit $\delta\tau \rightarrow 0$. A number of important properties of the propagator of a quantum mechanical particle are stated below. Their detailed derivation can be found in Feynman and Hibbs (1965). We will present the detailed derivation of a number of these properties in the case of optics later in this section.

The propagator is defined such that:

$$K(\mathbf{r}, t; \mathbf{r}_0, t_0) \equiv 0 \quad \text{for } t < t_0, \quad (2.19)$$

and $\lim_{t \rightarrow t_0} K(\mathbf{r}, t; \mathbf{r}_0, t_0) = \delta(\mathbf{r} - \mathbf{r}_0)$ (2.20)

It can be readily shown that the propagator is the Green's function of the Schrödinger equation:

$$\left[i\hbar \frac{\partial}{\partial t} + \frac{\hbar^2}{2m} \nabla^2 - V(\mathbf{r}, t) \right] K(\mathbf{r}, t; \mathbf{r}_0, t_0) = i\hbar \delta(t - t_0) \delta(\mathbf{r} - \mathbf{r}_0). \quad (2.21)$$

A direct consequence of the definition (2.16) is that, if $t_2 > t_1 > t_0$, then the propagator has the Markov property,

$$K(\mathbf{r}_2, t_2; \mathbf{r}_0, t_0) = \int d^D \mathbf{r}_1 K(\mathbf{r}_2, t_2; \mathbf{r}_1, t_1) K(\mathbf{r}_1, t_1; \mathbf{r}_0, t_0), \quad (2.22)$$

where the above integral extends over all possible values of \mathbf{r}_1 . The idea of a quantum mechanical wavefunction can be self-consistently introduced by using the following expression together with the probabilistic interpretation of the propagator.

$$\psi(\mathbf{r}, t) = \int d^D \mathbf{r}_0 K(\mathbf{r}, t; \mathbf{r}_0, t_0) \psi(\mathbf{r}_0, t_0). \quad (2.23)$$

It then follows that $\psi(\mathbf{r}, t)$ can be interpreted as the probability amplitude to find the

particle in a volume $d^D \mathbf{r}$, centred at position \mathbf{r} at time t , regardless of its previous history. If the particle is such that it cannot be annihilated, conservation of probability (or equivalently particle number), requires that,

$$\int d^D \mathbf{r}_0 \psi^*(\mathbf{r}_0, t_0) \psi(\mathbf{r}_0, t_0) = 1. \quad (2.24)$$

Using the defining expression for $\psi(\mathbf{r}, t)$ (2.23) and normalisation property (2.24), it follows that,

$$\int d^D \mathbf{r} K^*(\mathbf{r}, t; \mathbf{r}_1', t_1) K(\mathbf{r}, t; \mathbf{r}_1, t_1) = \delta(\mathbf{r}_1' - \mathbf{r}_1), \quad (2.25)$$

where $t > t_1$. From (2.25) it also follows that, if $t_0 < t$, then

$$K(\mathbf{r}_1, t_1; \mathbf{r}_0, t_0) = \int d^D \mathbf{r} K^*(\mathbf{r}, t; \mathbf{r}_1, t_1) K(\mathbf{r}, t; \mathbf{r}_0, t_0). \quad (2.26)$$

Since the time ordering of the above equation is $t > t_1 > t_0$, it follows that the complex conjugate of the propagator describes the evolution of the system backwards in time.

Before closing this section, a few words explaining how expression (2.15) links classical with quantum mechanics are in order. In the limit $\hbar \rightarrow 0$, the changes in the exponent in (2.15) corresponding to small deformations in the path $\mathbf{r}(t)$ are very large. The highly oscillatory behaviour of the imaginary exponential term in (2.15) results in the cancellation, on average, of the contributions to the path integral from adjacent paths, unless the particular path in question renders the exponent in (2.15) stationary. But the exponent in (2.15) is the classical action and therefore, the only paths that contribute to the propagator are, by definition, the paths described by classical mechanics. This statement indicates how the transition from quantum mechanics to classical mechanics can be made. Conversely, we can think of (2.15) as a rule for quantising classical mechanics. In this case, we can obtain the propagator of the particle by postulating that all paths which are forward moving in time contribute to the propagator. We then take a Feynman path integral over all these possible paths, with the weight term, w , assigned to each path, where,

$$w = \exp\left\{2\pi i \times \text{Classical action corresponding to the path} / \text{fundamental constant of action}\right\}.$$

2.4 The transition from geometrical optics to wave optics and vice-versa.

In this section we will link paraxial geometrical optics and paraxial, scalar wave optics using the approach of Feynman and Hibbs (1965), briefly outlined for the analogous cases of classical and quantum mechanics in the previous section. We will start from Fermat's principle and "quantise" geometrical optics using the rule described in the last paragraph of the previous section. This process will then enable us to arrive at an expression for the propagator of a ray of light, which we will then proceed to show is also the Green's function of the paraxial, scalar wave equation. The path-integral formalism used to describe paraxial, scalar wave propagation, will finally provide us with a way of linking geometrical to wave optics.

The question which first arises is what to use as a measure of the size of the optical path length (the equivalent of the measure of action, \hbar , in mechanics), in order to perform the quantisation. This information is provided in Table 1.1, where the minimum value of the wavelength, λ/n_0 , is shown to be equivalent to Planck's constant. Even if this information were not provided, we would only have to look at the dimensionality of the optical path length functional (2.14), to discover that it is measured in units of length. The question we should then ask ourselves is, what is the fundamental measure of length for waves, which affects their diffraction and interference properties. Experimentally, we know this measure to be their free space wavelength, λ_0 . Using the rest of the information shown in Table 1.1, we can then use the quantisation rule described above to write down the propagator of the rays which are forward moving along the z -axis (see figure 2.2), as

$$K(\boldsymbol{\rho}, z; \boldsymbol{\rho}_0, z_0) = \int \delta\boldsymbol{\rho}(z) \exp \left\{ \frac{2\pi i}{\lambda_0} \left[n_0(z-z_0) + n_0 \int_{z_0}^z d\zeta \left\{ \frac{1}{2} \left[\frac{dx}{d\zeta}(\zeta) \right]^2 + \frac{1}{2} \left[\frac{dy}{d\zeta}(\zeta) \right]^2 - n' (x(\zeta), y(\zeta), \zeta) \right\} \right] \right\},$$

for $z > z_0$ (2.27a)

and $K(\boldsymbol{\rho}, z; \boldsymbol{\rho}_0, z_0) = 0,$ for $z < z_0,$ (2.27b)

where by analogy with mechanics we may define an optical Lagrangian \mathfrak{L} to be given by,

$$\mathfrak{L}\left[\frac{d\rho}{dz}, \rho, z\right] = \frac{1}{2}\left[\frac{d\rho}{dz}\right]^2 - n'(\rho, z) \quad (2.27c)$$

Using the definitions (1.9) and (1.15), we may identify $\frac{2\pi n_0}{\lambda_0}$ with the maximum value of the wavenumber, k , in the inhomogeneous medium defined by (1.12), since n_0 is by definition the maximum value of the refractive index.

$$k = \frac{1}{\bar{\lambda}} = \frac{2\pi n_0}{\lambda_0} \quad (2.28)$$

Equation (2.27a) may be then written in the slightly more compact form,

$$K(\rho, z; \rho_0, z_0) = \exp[ik(z-z_0)] \times \int \delta\rho(z) \exp\left\{ik \int_{z_0}^z d\zeta \left[\frac{1}{2}\left[\frac{dx}{d\zeta}(\zeta)\right]^2 + \frac{1}{2}\left[\frac{dy}{d\zeta}(\zeta)\right]^2 - n'(x(\zeta), y(\zeta), \zeta) \right]\right\}. \quad (2.29)$$

We can also carry an analogue of the probabilistic interpretation of the propagator from quantum mechanics, and interpret $K(\rho, z; \rho_0, z_0)$ to be the probability amplitude for a ray of light starting at (ρ_0, z_0) to arrive at (ρ, z) . This probabilistic interpretation requires that

$$\lim_{z \rightarrow z_0} K(\rho, z; \rho_0, z_0) = \delta(\rho - \rho_0). \quad (2.30)$$

The rules (2.22), (2.25) and (2.26) describing the Markov property of the propagator still hold if we replace t by z and \mathbf{r} by ρ . Using (2.23) we can also define, in a consistent way, a field amplitude, $\varphi(\rho, z)$, which is to be interpreted as the probability amplitude for a ray of light to be found within an area $d^2\rho$, centred at the point ρ on the plane $\zeta = z$, regardless of its origin. In this sense, $|\varphi(\rho, z)|^2$, can also be interpreted as being proportional to the intensity of light, which, as shown in Born and Wolf (1980), is consistent with the idea that the intensity of light is proportional to the density of geometrical rays.

Equation (2.29) contains geometrical optics as the special case $\lambda \rightarrow 0$, or $k \rightarrow \infty$, as explained in the last paragraph of section 2.3. We will now proceed to show that $K(\rho, z; \rho_0, z_0)$ and hence $\varphi(\rho, z)$ obey the scalar, paraxial wave equation (1.18).

From (2.29) and (2.16) it follows that the propagator over an infinitesimally small displacement along the axis of paraxial propagation δz , is given by,

$$A^{-1} \exp\left\{i k \delta z \mathcal{L}\left[\frac{\rho_{n+1}^- \rho_n}{\delta z}, \frac{\rho_{n+1}^+ \rho_n}{2}, z_n\right]\right\}, \quad (2.31)$$

where the measure of the path integral A^{-1} is to be determined. We now consider the propagator K at three z -positions, z_0 , z_1 , and z_2 , such that $z_0 < z_1 < z_2$ and the planes $\zeta = z_1$ and $\zeta = z_2$ are only an infinitesimally small distance ϵ apart,

$$z_2 - z_1 = \delta z = \epsilon. \quad (2.32)$$

Then, using (2.22), (2.29) and (2.31) we have,

$$K(\rho_2, z_2; \rho_0, z_0) = \int d^2 \rho_1 \frac{1}{A} \exp\left\{i k \epsilon \mathcal{L}\left(\frac{\rho_2^+ \rho_1}{2}, \frac{\rho_2^- \rho_1}{\epsilon}, z_1\right)\right\} K(\rho_1, z_1; \rho_0, z_0). \quad (2.33)$$

Using (2.32),

$$K(\rho_2, z_1 + \epsilon; \rho_0, z_0) = \int d^2 \rho_1 \frac{1}{A} \exp\left\{i k \epsilon \mathcal{L}\left(\frac{\rho_2^+ \rho_1}{2}, \frac{\rho_2^- \rho_1}{\epsilon}, z_1\right)\right\} K(\rho_1, z_1; \rho_0, z_0). \quad (2.34)$$

Using (2.14) and changing the variable of integration to $\xi \equiv \rho_2 - \rho_1$, gives:

$$K(\rho_2, z_1 + \epsilon; \rho_0, z_0) = \exp[i k \epsilon] \int d^2 \xi \frac{1}{A} \exp\left\{\frac{i k \xi^2}{2 \epsilon}\right\} \exp\left\{-i k \epsilon n' \left(\frac{\rho_2^+ \rho_1}{2}, z_1\right)\right\} K(\rho_2 + \xi, z_1; \rho_0, z_0). \quad (2.35)$$

Using a stationary phase argument we can see that the significant contributions to the path integral are given by the values of ξ which satisfy:

$$\frac{i k ||\xi||^2}{2 \epsilon} \leq i \frac{\pi}{2}, \quad (2.36a)$$

or,
$$||\xi||_{\max} \sim \sqrt{\frac{\pi \epsilon}{k}}. \quad (2.36b)$$

Retaining only the terms up to first order in ϵ in the Taylor expansion of (2.35), gives

$$K + \epsilon \frac{\partial K}{\partial z_1} = (1 + i k \epsilon) \times \int d^2 \xi \frac{1}{A} \exp\left\{\frac{i k \xi^2}{2 \epsilon}\right\} \left\{1 - i k \epsilon n' \left(\frac{\rho_2^+ \rho_1}{2}, z_1\right)\right\} \left\{K + \xi \cdot (\nabla_{x_2 y_2} K) + \frac{1}{2} \xi^2 (\nabla_{x_2 y_2}^2 K)\right\}, \quad (2.37)$$

where

$$K \equiv K(\rho_2, z_1; \rho_0, z_0), \quad (2.38)$$

and

$$\nabla_{x_2 y_2}^2 \equiv \frac{\partial^2}{\partial x_2^2} + \frac{\partial^2}{\partial y_2^2}. \quad (2.39)$$

Since, by assumption, the refractive index inhomogeneity function $n'(\rho, z)$ is a smoothly varying function of position, then $ik\epsilon n'(\frac{\rho_2 + \rho_1}{2}, z_1) \approx ik\epsilon n'(\rho_2, z_1)$ to first order in ϵ . Making the simple change in symbols $z = z_1$ and $\rho = \rho_2$, equation (2.37) becomes:

$$K + \epsilon \frac{\partial K}{\partial z} = \int d^2\xi \frac{1}{A} \exp\left\{\frac{ik\xi^2}{2\epsilon}\right\} \left\{1 - ik\epsilon n'(\rho, z)\right\} \left\{K + \xi \cdot (\nabla_{xy} K) + \frac{1}{2}\xi^2 (\nabla_{xy}^2 K)\right\} \quad (2.40)$$

Equating the various terms which are of the same order in ϵ we obtain the following expressions: the terms which are of order ϵ^0 , give,

$$K = K \int d^2\xi \frac{1}{A} \exp\left\{\frac{ik\xi^2}{2\epsilon}\right\}, \quad (2.41a)$$

from which we can readily see that,

$$A = 2\pi i\epsilon/k. \quad (2.41b)$$

This is consistent with (2.18) when the analogies shown in Table 1.1 are used. The terms of order ϵ^1 must now be considered. In (2.37) the term $\xi^2 \nabla_{xy}^2 K$ on the right hand side is of order ϵ^1 , since according to (2.36) ξ^2 is of order ϵ in the region which significantly contributes to the ξ -integral. Thus,

$$\begin{aligned} \epsilon \frac{\partial K}{\partial z} = & ik\epsilon K \int d^2\xi \frac{1}{A} \exp\left\{\frac{ik\xi^2}{2\epsilon}\right\} + \\ & \int d^2\xi \frac{1}{A} \exp\left\{\frac{ik\xi^2}{2\epsilon}\right\} \left\{-ik\epsilon n'(\rho, z)\right\} K + \frac{1}{2} \int d^2\xi \frac{1}{A} \exp\left\{\frac{ik\xi^2}{2\epsilon}\right\} \xi^2 \nabla_{xy}^2 K. \end{aligned} \quad (2.42)$$

Evaluating the ξ integrals, and using equation (2.41) to substitute for A , results in,

$$\frac{i}{k} \frac{\partial K}{\partial z}(\rho, z; \rho_0, z_0) + \frac{1}{2k^2} \nabla_{xy}^2 K(\rho, z; \rho_0, z_0) + (1 - n'(\rho, z))K(\rho, z; \rho_0, z_0) = 0. \quad (2.43)$$

Equation (2.43) is of course valid for $z = z_1 > z_0$. Using the definition of the propagator in (2.27a) and (2.27b) and the property (2.30), we may infer the behaviour of the propagator $K(\rho, z; \rho_0, z_0)$ as $z_1 \rightarrow z_0$. It is a straightforward matter to show that the case where $z_1 \rightarrow z_0$ is correctly described by the equation,

$$\frac{i}{k} \frac{\partial K}{\partial z}(\rho, z; \rho_0, z_0) + \frac{1}{2k^2} \nabla_{xy}^2 K(\rho, z; \rho_0, z_0) + (1 - n'(\rho, z))K(\rho, z; \rho_0, z_0) = \frac{i}{k} \delta(z_1 - z_0) \delta(\rho_1 - \rho_0). \quad (2.44)$$

Therefore, the propagator $K(\boldsymbol{\rho}, z; \boldsymbol{\rho}_0, z_0)$ is the Green's function of the scalar, paraxial wave equation (1.18). Equation (2.44) differs from the Schrödinger equation (2.21) and the paraxial wave equation (1.18) in one respect: The term $(1 - n'(\boldsymbol{\rho}, z))K(\boldsymbol{\rho}, z; \boldsymbol{\rho}_0, z_0)$ which appears in (2.44), appears as $-n'(\boldsymbol{\rho}, z)f(\boldsymbol{\rho}, z)$ in (1.18) and $-V(\mathbf{r}, t)K(\mathbf{r}, t; \mathbf{r}_0, t_0)$ in (2.21). This is due to the fact that the optical path length expression (2.14) contains the term $n_0(z-z_0)$ in addition to the functional integral. In quantum mechanics the inclusion of such a term would redefine the ground state energy of the system, which is completely arbitrary. In optics it defines the absolute phase of a wave, which is again a completely arbitrary quantity. The reason this extra term does not appear in (1.18) is because we have already taken it into account in equation (1.8). For this reason $f(\boldsymbol{\rho}, z)$ is defined by (1.8), whilst $\varphi(\boldsymbol{\rho}, z)$ satisfies (2.44) with the right hand side equal to zero.

The fact that the propagator (2.27) satisfies the scalar, paraxial wave equation (2.44) concludes the argument that one can "quantise" geometrical optics to arrive at scalar, paraxial wave optics. The analogy between optics and mechanics extends, therefore, to both the wave theories and to geometrical optics and classical mechanics. Figure 2.3 contains a diagram summarising this analogy, which is quantified in Table 1.1.

2.5 Paraxial wave propagation in a homogeneous medium.

The simplest possible medium we can consider is the homogeneous medium, or equivalently, free space. We will therefore use the homogeneous medium propagator to examine the propagation characteristics of a Gaussian beam (Yariv, 1991). A Gaussian beam is a scalar wave whose wavefronts are predominantly transverse to some direction of propagation (which we will take to be the z -axis) and whose transverse amplitude distribution is Gaussian. It is a good approximation to the electric field amplitude at the output of lasers and laser diodes, as well as to the electric field amplitude in weakly guiding waveguides (Yariv, 1991). In free space the refractive index is identically equal to

unity (since the speed of light is everywhere c). Therefore,

$$n(x, y, z) = 1. \quad (2.45)$$

In the case of a homogeneous medium of refractive index n_0 , we simply have to replace k_0 by $k \equiv k_0 n_0$. The optical path length expression (2.14) then becomes,

$$S[\rho(z)] = z - z_0 + \frac{1}{2} \int_{z_0}^z d\zeta [\dot{x}^2(\zeta) + \dot{y}^2(\zeta)], \quad (2.46)$$

where a dot represents a differentiation with respect to ζ . The expression for the propagator (2.27) then becomes,

$$K_0(x, y, z; x_0, y_0, z_0) = \exp[ik_0(z - z_0)] \int \int \delta x(z) \delta y(z) \exp\left\{\frac{ik_0}{2} \int_{z_0}^z d\zeta [\dot{x}^2(\zeta) + \dot{y}^2(\zeta)]\right\} \quad (2.47)$$

The above expression is in a form which is readily separable, giving,

$$K_0(x, y, z; x_0, y_0, z_0) = \exp[ik_0(z - z_0)] \int \delta x(z) \exp\left\{\frac{ik_0}{2} \int_{z_0}^z d\zeta \dot{x}^2(\zeta)\right\} \int \delta y(z) \exp\left\{\frac{ik_0}{2} \int_{z_0}^z d\zeta \dot{y}^2(\zeta)\right\}. \quad (2.48)$$

Thus we now only need to evaluate a single, one dimensional path integral in order to find an explicit form for the propagator. Let us concentrate on the $x(z)$ path integral only,

$$I_x \equiv \int \delta x(z) \exp\left\{\frac{ik_0}{2} \int_{z_0}^z d\zeta \dot{x}^2(\zeta)\right\}. \quad (2.49)$$

In order to evaluate this, we make use of the definition of a functional integral given in section 2.1. We divide the interval $[z_0, z]$ into N equal intervals each of width ϵ . We can then approximate the path integral of (2.49) as the limit of an $(N-1)$ -dimensional Riemann integral, as shown below:

$$I_x = \lim_{\substack{N \rightarrow \infty \\ \epsilon \rightarrow 0}} \prod_{n=1}^{N-1} \left\{ \frac{1}{\sqrt{A}} \int_{-\infty}^{+\infty} dx_i \right\} \frac{1}{\sqrt{A}} \exp\left\{\frac{ik_0}{2} \sum_{n=1}^N \frac{(x_n - x_{n-1})^2}{\epsilon}\right\}, \quad (2.50)$$

where A is the normalizing factor (2.41b). All the integrals in (2.50) are of the standard form (Feynman and Hibbs, 1965)

$$\int_{-\infty}^{+\infty} dx \exp[-ax^2 + bx] = \sqrt{\frac{\pi}{a}} \exp\left[\frac{b^2}{4a}\right], \quad (2.51)$$

and can thus be evaluated one at a time. Since the result of each Gaussian integration is also a Gaussian expression, (2.51) can be used iteratively $(N-1)$ times to give:

$$I_x = \lim_{\substack{N \rightarrow \infty \\ \epsilon \rightarrow 0}} \sqrt{\frac{k_0}{2\pi i N \epsilon}} \exp\left\{\frac{i k_0}{2} \frac{(x-x_0)^2}{N \epsilon}\right\}. \quad (2.52)$$

Taking the limit on the right hand side of (2.52), while bearing in mind that $N\epsilon = z-z_0$, a constant, we arrive at

$$I_x = \sqrt{\frac{k_0}{2\pi i (z-z_0)}} \exp\left\{\frac{i k_0}{2(z-z_0)} (x-x_0)^2\right\}. \quad (2.53)$$

The total free space propagator is then given by

$$K_0(x, y, z; x_0, y_0, z_0) = \frac{k_0}{2\pi i (z-z_0)} \exp\left\{i k_0 (z-z_0) + \frac{i k_0}{2(z-z_0)} \left[(x-x_0)^2 + (y-y_0)^2\right]\right\}. \quad (2.54)$$

We now show that (2.54) is an approximate form of a spherical wave whose origin is at the point (x_0, y_0, z_0) . The approximation involved is in the spirit of the paraxial approximation introduced in chapter 1 and section 2.2 of this chapter, where we implicitly assumed that,

$$(x-x_0)^2, (y-y_0)^2 \ll (z-z_0)^2. \quad (2.55)$$

An outgoing spherical wave centred at the origin of the chosen coordinate system is described by the equation,

$$\varphi(x, y, z, t) \propto \frac{1}{r} \exp[i(k_0 r - \omega t)], \quad (2.56a)$$

where,

$$r = \sqrt{x^2 + y^2 + z^2}. \quad (2.56b)$$

Using the approximation (2.55), r may be approximated by the following series expansion of the square root,

$$r \simeq z + \frac{x^2 + y^2}{2z} - \frac{(x^2 + y^2)^2}{8z^3} + \dots \quad (2.57)$$

If the inequality described by equation (2.55) holds, only the first two terms in the expansion (2.57) make any significant contribution to the phase term in (2.56). The factor $\frac{1}{r}$ can be approximated by using the first term in the expansion (2.57) only, with very little error. Hence, equation (2.57) can be written as,

$$\varphi(x, y, z, t) \propto \frac{1}{z} \exp\left\{i k_0 z + \frac{i k_0}{2z} (x^2 + y^2) - i \omega t\right\}. \quad (2.58)$$

It can be seen that equations (2.54) and (2.58) are of the same form if one omits the time dependent part of the exponential and the constant of proportionality in (2.54). The expression in (2.58) is a good model for a spherical wave with a surface of constant phase (wavefront) having a radius of curvature much larger than the wavelength, i.e. for observation points very far away from the source of the wave and close to the axis of propagation. This is precisely the context in which we discussed the paraxial approximation as applied to waves in chapter 1.

It is of interest to see what equation (2.54) predicts for the propagation of a Gaussian beam in free space. The spot size, or beam waist, of a Gaussian beam is defined to be the distance from the optical axis at which the amplitude of the beam falls by a factor of $\frac{1}{e}$. A Gaussian beam of spot size w_0 and a radius of curvature of the surface of constant phase R_0 , at $\zeta = z_0$, is described by (Yariv, 1991),

$$\psi(x_0, y_0, z_0) = \psi_0 \exp\left\{-\frac{x_0^2 + y_0^2}{w_0^2}\right\} \exp\left\{\frac{ik_0(x_0^2 + y_0^2)}{2R_0}\right\}. \quad (2.59)$$

In order to find what this transverse field profile looks like after a distance $(z - z_0)$ of propagation through free space, one must use the propagation rule given by equation (2.23) to get,

$$\psi(x, y, z) = \int K_0(x, y, z; x_0, y_0, z_0) \psi(x_0, y_0, z_0) dx_0 dy_0. \quad (2.60)$$

Substituting equations (2.54) and (2.59) into equation (2.60), yields:

$$\begin{aligned} \psi(x, y, z) = \frac{\psi_0 k_0}{2\pi i (z - z_0)} \exp[ik_0(z - z_0)] \int_{-\infty}^{+\infty} \int_{-\infty}^{+\infty} dx_0 dy_0 \exp\left\{\frac{ik_0}{2(z - z_0)} \left[(x - x_0)^2 + (y - y_0)^2 \right]\right\} \times \\ \exp\left\{-\frac{x_0^2 + y_0^2}{w_0^2}\right\} \exp\left\{\frac{ik_0(x_0^2 + y_0^2)}{2R_0}\right\}. \end{aligned} \quad (2.61)$$

The double integral in (2.61) is separable and can be evaluated using (2.51) to give,

$$\begin{aligned} \psi(x, y, z) = \frac{\psi_0 k_0}{2\pi i (z - z_0)} \exp[ik_0(z - z_0)] \exp\left\{\frac{ik_0 x^2}{2(z - z_0)}\right\} \sqrt{\frac{\pi}{1/w_0^2 - ik_0[1/R_0 + 1/(z - z_0)]/2}} \times \\ \exp\left\{\frac{-k_0^2 x^2}{4(z - z_0)[1/w_0^2 - ik_0[1/R_0 + 1/(z - z_0)]/2]}\right\} \exp\left\{\frac{ik_0 y^2}{2(z - z_0)}\right\} \times \\ \sqrt{\frac{\pi}{1/w_0^2 - ik_0[1/R_0 + 1/(z - z_0)]/2}} \exp\left\{\frac{-k_0^2 y^2}{4(z - z_0)[1/w_0^2 - ik_0[1/R_0 + 1/(z - z_0)]/2]}\right\}. \end{aligned} \quad (2.62)$$

After a considerable number of algebraic manipulations, equation (2.62) can be cast into the form,

$$\begin{aligned} \psi(x,y,z) = & \frac{\psi_0}{\sqrt{1 + 2(z-z_0)/R_0 + (z-z_0)^2[1/R_0^2 + 4/(k^2w_0^4)]}} \times \\ & \exp\left\{ik_0(z-z_0) - i \arctan\left[\frac{1}{(k_0w_0^2/2)[1/R_0 + 1/(z-z_0)]}\right]\right\} \times \\ & \exp\left\{\frac{-(x^2+y^2)}{w_0^2[(z-z_0)^2[1/R_0 + 1/(z-z_0)]^2 + 4(z-z_0)^2/(k_0^2w_0^4)]}\right\} \times \\ & \exp\left\{\frac{ik_0(x^2+y^2)[1 + (k_0^2w_0^4)[1/R_0 + 1/(z-z_0)]/(4R_0)]}{2(z-z_0)[1 + (k_0^2w_0^4)[1/R_0 + 1/(z-z_0)]^2/4]}\right\}. \end{aligned} \quad (2.63a)$$

Equation (2.63a) multiplied by an $\exp(-i\omega t)$ term completely describes the paraxial propagation of a Gaussian beam through free space. From this expression, and by direct comparison with the standard form for a Gaussian beam of equation (2.59), one can read the expressions for the new beam waist, $w(z)$, and wavefront radius of curvature, $R(z)$, directly. These are given by,

$$w(z) = w_0 (z-z_0) \sqrt{\left[\frac{1}{R_0} + \frac{1}{z-z_0}\right]^2 + \frac{4}{k^2w_0^4}}, \quad (2.63b)$$

and

$$R(z) = (z-z_0) \frac{1 + k_0^2w_0^4[1/R_0 + 1/(z-z_0)]^2/4}{1 + k_0^2w_0^4[1/R_0 + 1/(z-z_0)]/(4R_0)}, \quad (2.63c)$$

respectively. The beam waist increases with propagation distance, whilst the wavefront radius of curvature decreases. The variation of the Gaussian beam waist size versus propagation distance is shown in the plot of figure 2.4. We believe that the result given by equation (2.63) is new, in spite of the fact that the work on path integrals presented in this section is well known (Feynman and Hibbs, 1965, Schulman, 1980).

The special case of infinite initial radius of curvature R_0 has, however, been studied by a number of people and can be found in most textbooks of optics. If one lets $R_0 \rightarrow \infty$ and sets $z_0 = 0$, equation (2.63) simplifies to,

$$\begin{aligned} \psi(x,y,z) = & \frac{\psi_0}{\sqrt{1 + \frac{z^2}{[k_0w_0^2/2]^2}}} \exp\left\{ik_0(z - \arctan\left[\frac{z}{k_0w_0^2/2}\right])\right\} \times \\ & \exp\left\{-(x^2+y^2)\left[\frac{1}{w_0^2[1+z^2/(k_0w_0^2/2)^2]} - \frac{ik_0}{2z[1+(k_0w_0^2/2)^2/z^2]}\right]\right\}, \end{aligned} \quad (2.64)$$

which is identical to equations (2.5–11) to (2.5–14) given by Yariv (1991). The general result we have derived in equation (2.63) should prove more useful than the particular case given in (2.64) in the study of the output light from lasers. As we have mentioned earlier in this chapter, the light emitted by lasers can be modeled to a good degree of accuracy by a Gaussian beam. The plane of zero wavefront curvature usually lies in the middle of the laser cavity, and as a rule we can determine the field distribution on the output aperture of the laser. For this reason, the general result derived in (2.63a) is more suitable for use in describing the propagating field distribution outside the laser cavity than (2.64). Detailed knowledge of the field distribution in the space in the front of the laser aperture is necessary for determining the optimum way in which the laser light can be coupled to waveguides of varied geometries and sizes.

2.6 The uniform waveguide with a parabolic refractive index distribution.

A more complicated medium for which a closed form solution exists is the one described by a refractive index variation which has the functional form shown below.

$$n(x,y,z) = n_0 \left(1 - \frac{1}{2}(a^2x^2 + b^2y^2) \right). \quad (2.65)$$

Such a model is of some significance in graded index optics, since it describes approximately a number of waveguides of practical importance. A graded-index optical fibre (Senior, 1985) is an example of this. In fact a number of practical waveguides and devices have a refractive index variation described by equation (2.65) exactly: Examples of these are the core region of selfoc fibres and graded index (GRIN) rod lenses. Bundles of such waveguides have found use in medical imaging, and the GRIN rod lenses are extensively used in imaging devices and waveguide couplers. The following analysis applies only to a medium of quadratic refractive index variation which extends infinitely in all directions. It is a very simple model for a waveguide, such as an optical fibre without cladding, whose core region extends to infinity. Such a medium cannot physically exist

since its refractive index is a negative number outside the ellipse defined by $a^2x^2 + b^2y^2 = 2$. In order to see whether such a refractive index distribution can realistically be expected to model real waveguides, we briefly need to consider the typical values of the various refractive index parameters encountered in practice. What is important to check, is whether the typical size of this ellipse is of the order of, say, a hundred wavelengths or more, so that virtually all the light energy is concentrated in the region near the z -axis, where the refractive index model (2.65) is realistic.

Typically, for a graded index rod lens the value of the parameters a and b are equal and lie between 0.25mm^{-1} and 0.60mm^{-1} , n_0 is approximately 1.5, and the operating free space wavelength varies between 630nm and 1550nm (Melles Griot Optics Guide 5, 1990). The distance away from the z -axis at which equation (2.65) ceases to describe the true refractive index distribution is of the order of thousands of wavelengths (λ/n_0). The refractive index described by equation (2.65) takes non-physical values for distances of the order of one million wavelengths or more, and we may therefore conclude that the refractive index model is accurate for GRIN rod lenses.

For a multimode graded index fibre of typical diameter $50\text{--}100\mu\text{m}$ and operating free space wavelength $1\mu\text{m}$, equation (2.65) will cease to describe the true refractive index distribution of the fibre core at a distance of approximately 38–75 wavelengths (Senior 1985). Since n_0 for such a fibre is approximately 1.5 and $a \simeq 7.5\text{mm}^{-1}$ (Senior 1985), the refractive index described by equation (2.65) will acquire non-physical values for distances of the order of approximately 280 wavelengths. Once again, the refractive index model (2.65) is appropriate to the description of graded-index multimode fibres. Our work is not appropriate though, for the description of a single mode fibre, whose refractive index profile is approximately constant across its core, and whose diameter is approximately $3\text{--}8\mu\text{m}$ (Senior 1985).

The optical path length for such quadratic refractive index medium is then given by substituting equation (2.65) in (2.14).

$$S[x(z), y(z)] = n_0(z-z_0) + n_0/2 \int_{z_0}^z d\zeta \left[\dot{x}^2(\zeta) + \dot{y}^2(\zeta) - a^2 x^2(\zeta) - b^2 y^2(\zeta) \right]. \quad (2.66)$$

The corresponding expression for the propagator (2.29), is,

$$K_0(x, y, z; x_0, y_0, z_0) = \exp[ik(z-z_0)] \star \iint \delta x(z) \delta y(z) \exp \left\{ ik/2 \int_{z_0}^z d\zeta \left[\dot{x}^2(\zeta) + \dot{y}^2(\zeta) - a^2 x^2(\zeta) - b^2 y^2(\zeta) \right] \right\}. \quad (2.67)$$

This expression separated can be into two simpler path integrals (by virtue of the fact that the exponential term in the integrand is separable) in the $x(\zeta)$ and $y(\zeta)$ variables respectively. Thus, we need only to evaluate one path integral of the form:

$$J_x = \int \delta x(z) \exp \left\{ ik/2 \int_{z_0}^z d\zeta \left[\dot{x}^2(\zeta) - a^2 x^2(\zeta) \right] \right\}. \quad (2.68)$$

This path integral is usually identified with that for the one dimensional quantum mechanical oscillator and its solution is well known (Feynman and Hibbs, 1965, Schulman, 1980, Wiegell, 1986). It can be evaluated using the method used for the free space propagator, since the individual ordinary Riemann integrals which occur in the limiting form of the path integral (2.16) are of the standard Gaussian form of equation (2.51). Alternatively, one may exploit the fact that the exponential is quadratic in the path and use Fermat's Principle to compute the above path integral. This latter method was introduced by Feynman (Feynman and Hibbs, 1965). We define the geometrical optics (or ray) path, $X(\zeta)$, to be the one which makes the optical path length in the xz -plane, $S[x(z)]$, extremal. We also define $\xi(\zeta)$ to be the deviation of a particular path $x(\zeta)$ from the geometrical optics path $X(\zeta)$. Thus we have,

$$x(\zeta) = X(\zeta) + \xi(\zeta). \quad (2.69)$$

Since $X(\zeta)$ is a function independent of the path variation $\xi(\zeta)$ (the variation is *about* $X(\zeta)$), the Jacobian involved in the change of the variable of path integration from $x(z)$ to $\xi(z)$ is unity, and therefore,

$$\delta x(\zeta) = \delta \xi(\zeta). \quad (2.70)$$

Substituting (2.69) and (2.70) in equation (2.68), we obtain,

$$J_x = \exp\left\{ik/2 \int_{z_0}^z d\zeta [\dot{X}^2(\zeta) - a^2 X^2(\zeta)]\right\} \int \delta \xi(z) \exp\left\{ik/2 \int_{z_0}^z d\zeta [\dot{\xi}^2(\zeta) - a^2 \xi^2(\zeta)]\right\}, \quad (2.71)$$

where, by virtue of the defining extremal property of $X(\zeta)$, the integrals of the terms in the exponent which are linear in $\xi(z)$ are all equal to zero. Since $\xi(\zeta)$ is the deviation from the geometrical optics path, we must have,

$$\xi(z) = \xi(z_0) = 0. \quad (2.72)$$

Therefore, $\xi(\zeta)$ can be written in terms of a Fourier sine series,

$$\xi(\zeta) = \sum_{n=1}^{\infty} a_n \sin\left\{\frac{n\pi(\zeta - z_0)}{(z - z_0)}\right\}. \quad (2.73)$$

By virtue of the fact that $\xi(\zeta)$ vanishes at the endpoints $\zeta = z_0$ and $\zeta = z$, the path integral in (2.71) is taken over all paths beginning and ending at the origin. For this reason, we use the different notation for the path integral,

$$J_x = \exp\left\{ik/2 \int_{z_0}^z d\zeta [\dot{X}^2(\zeta) - a^2 X^2(\zeta)]\right\} \oint \delta \xi(z) \exp\left\{ik/2 \int_{z_0}^z d\zeta [\dot{\xi}^2(\zeta) - a^2 \xi^2(\zeta)]\right\}. \quad (2.74)$$

to denote that the path integral is now taken over the space of all closed paths beginning and ending at the same origin. The exponential term pre-multiplying the path integral depends only upon the optical path length between the two fixed end points, as given by geometrical optics. This is the optical path length along the extremum path and is given by,

$$S_{G0} = 1/2 \int_{z_0}^z d\zeta [\dot{X}^2(\zeta) - a^2 X^2(\zeta)]. \quad (2.75)$$

where $X(\zeta)$ is the solution of the Euler–Lagrange equation for the corresponding geometrical optics problem (Marchand, 1978). Now, the integration over the space of all closed paths can be replaced by a multiple integral over the Fourier coefficients a_n of

$\xi(z)$ in equation (2.73). Varying the coefficients independently in the interval $(-\infty, +\infty)$ is equivalent to considering all the possible functions $\xi(z)$ obeying the boundary conditions given by (2.72). If one considers the linear transformation from the $\{\xi_i\}$ to the $\{a_n\}$ as a change of the variable of integration, the Jacobian J is the determinant of the transformation matrix and will be a constant, depending on k and $(z-z_0)$ only. The Fourier representation of an exact periodic function, such as $\xi(\zeta)$, is itself exact when an infinite number of Fourier coefficients are taken into account. A consequence of making this transformation, i.e. changing the variables of integration to the Fourier coefficients, is that the result below is exact. Equation (2.74) now becomes,

$$J_x = J \exp[ikS_{G0}] \prod_{n=1}^{\infty} \left[\int_{-\infty}^{+\infty} da_n \right] \exp \left\{ \frac{ik}{2} \sum_{m=1}^{\infty} a_m^2 \frac{z-z_0}{4} \left[\frac{n^2 \pi^2}{(z-z_0)^2} - a^2 \right] \right\}, \quad (2.76)$$

where we have replaced $\xi(\zeta)$ by its Fourier series (2.73) and evaluated the ζ -integral. Equation (2.76) is easy to evaluate, since it is the product of simple Gaussian integrals.

$$J_x = J \exp[ikS_{G0}] \prod_{n=1}^{\infty} \frac{\sqrt{8\pi}}{\sqrt{-ik(z-z_0) \left[\frac{n^2 \pi^2}{(z-z_0)^2} - a^2 \right]}}. \quad (2.77)$$

Using the continued product representation (Arfken, 1985),

$$\frac{\sin x}{x} = \prod_{n=1}^{\infty} \left[1 - \frac{x^2}{n^2 \pi^2} \right], \quad (2.78)$$

equation (2.77) becomes

$$J_x = J \exp[ikS_{G0}] C \left[\frac{a(z-z_0)}{\sin a(z-z_0)} \right]^{1/2}, \quad (2.79)$$

where C is a constant depending on k and $z-z_0$. Defining a new constant, $B = J C$, equation (2.79) becomes:

$$J_x = B \exp[ikS_{G0}] \left[\frac{a(z-z_0)}{\sin a(z-z_0)} \right]^{1/2}. \quad (2.80)$$

The remaining quantity needed to determine the propagator completely is S_{G0} . In order to determine its value, we have to use the Euler-Lagrange equation (Goldstein, 1980) to

determine the geometric optics path, and then substitute this path in (2.75) to find the corresponding optical path length. The optical Lagrangian defined in (2.27c) is then given by,

$$L = (\dot{X}^2 - a^2 X^2)/2. \quad (2.81)$$

The corresponding Euler–Lagrange equation for this problem is (Goldstein, 1980),

$$\partial L/\partial X = \frac{d}{d\zeta}(\partial L/\partial \dot{X}). \quad (2.82)$$

Equations (2.81) and (2.82) give,

$$\frac{d^2 X}{d\zeta^2} + a^2 X = 0, \quad (2.83)$$

whose solution subject to the boundary conditions $X(z) = x$ and $X(z_0) = x_0$ is,

$$X(\zeta) = \frac{x_0 \sin(a[z-\zeta]) + x \sin(a[\zeta-z_0])}{\sin(a[z-z_0])}. \quad (2.84)$$

The optical path length (2.75) corresponding to the ray path (2.84) is,

$$S_{G0} = \frac{a}{2\sin(a[z-z_0])} [(x^2+x_0^2)\cos(a[z-z_0]) - 2xx_0]. \quad (2.85)$$

Using equation (2.85) the partial propagator (2.80) becomes,

$$J_x = B \left[\frac{a(z-z_0)}{\sin a(z-z_0)} \right]^{1/2} \exp \left\{ \frac{ika}{2\sin a(z-z_0)} [(x^2+x_0^2)\cos a(z-z_0) - 2xx_0] \right\}. \quad (2.86)$$

In order now to determine B one must notice that as $a \rightarrow 0$ the partial propagator (2.86) must reduce to (2.53), which is the corresponding expression for the homogeneous medium.

Thus,

$$B = \sqrt{\frac{k}{2\pi i(z-z_0)}}. \quad (2.87)$$

If we combine the partial propagator (2.86), (2.87) with the corresponding expression for the y -variable, then equation (2.67) becomes,

$$K(x,y,z;x_0,y_0,z_0) = \frac{k}{2\pi i} \left[\frac{ab}{\sin a(z-z_0) \sin b(z-z_0)} \right]^{1/2} \exp[ik(z-z_0)] \times \\ \exp \left\{ \frac{ika}{2\sin a(z-z_0)} [(x^2+x_0^2)\cos a(z-z_0) - 2xx_0] + \frac{ikb}{2\sin b(z-z_0)} [(y^2+y_0^2)\cos b(z-z_0) - 2yy_0] \right\}. \quad (2.88)$$

The above expression completely describes paraxial scalar wave propagation in a medium

of quadratic refractive index variation. In chapter 3 we will examine the propagation of a Gaussian beam in such a medium, as well as ways of extracting useful information from the closed form propagator expression. As a closing remark, we would like to point out that all of the work presented in this section is well known in quantum mechanics, but has never found widespread application in optics.

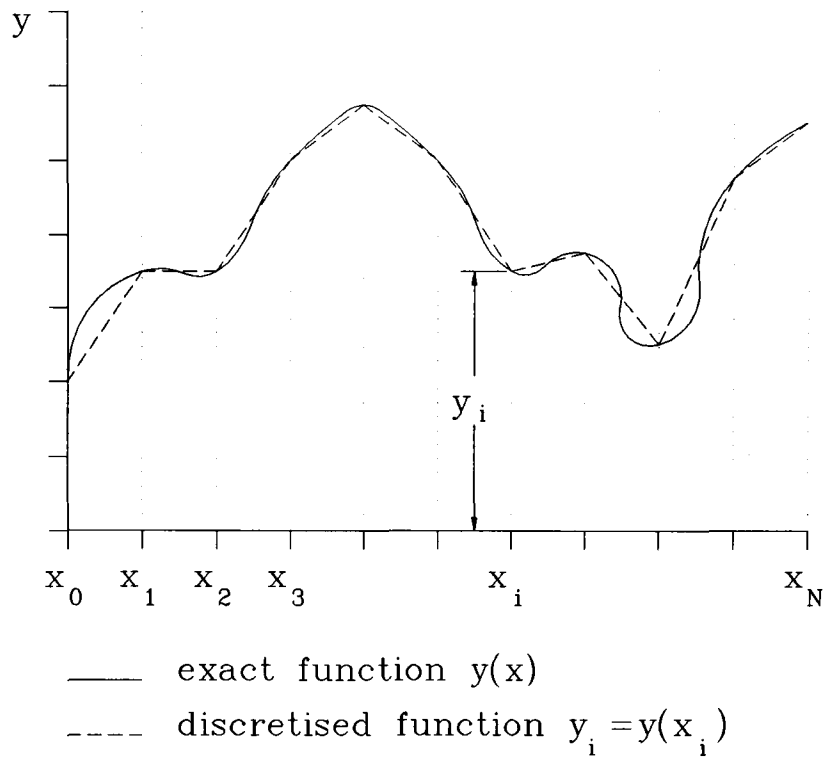


Figure 2.1: The piecewise linear approximation $\{x_i, y_i\}$ to a continuous path $y(x)$ becomes exact in the limit $x_i - x_{i-1} \rightarrow 0$.

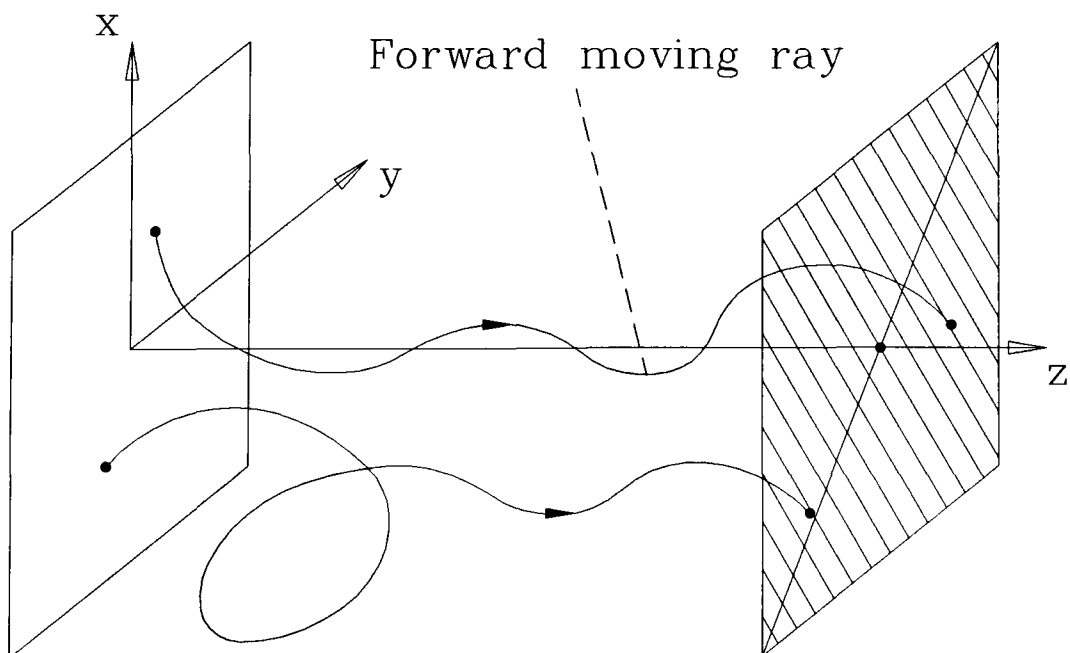


Figure 2.2: A forward moving ray is one for which the coordinate z increases monotonically with time.

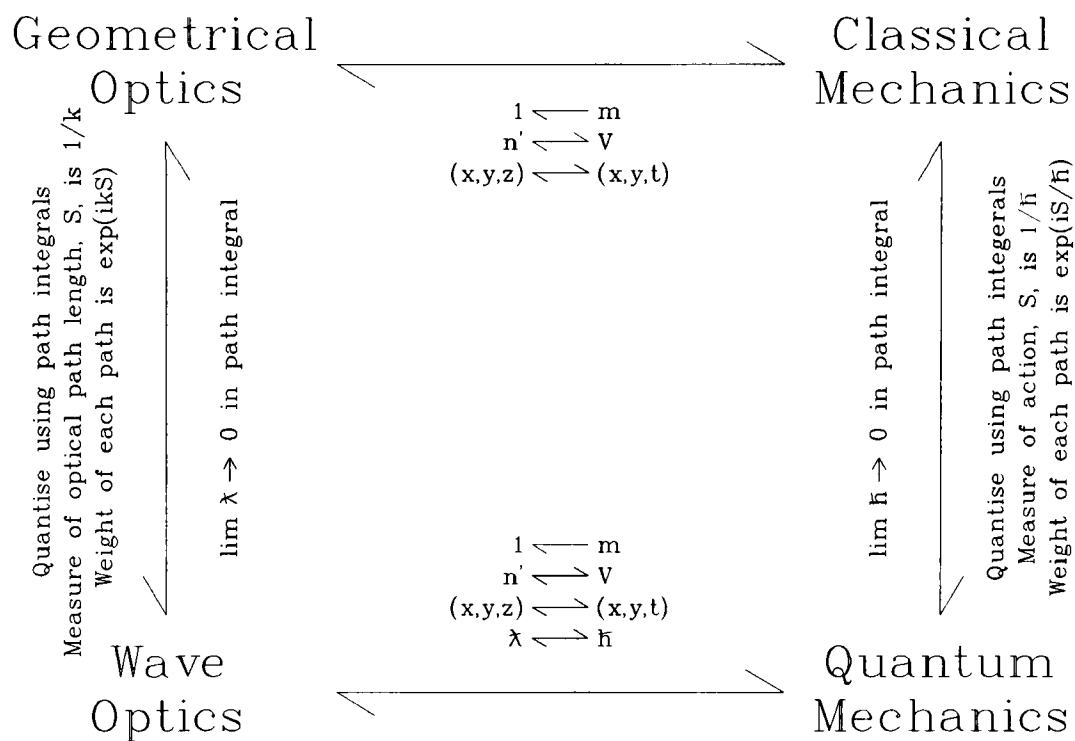


Figure 2.3: A summary of the analogy between optics and mechanics and the transition between geometrical and wave optics, and classical and quantum mechanics.

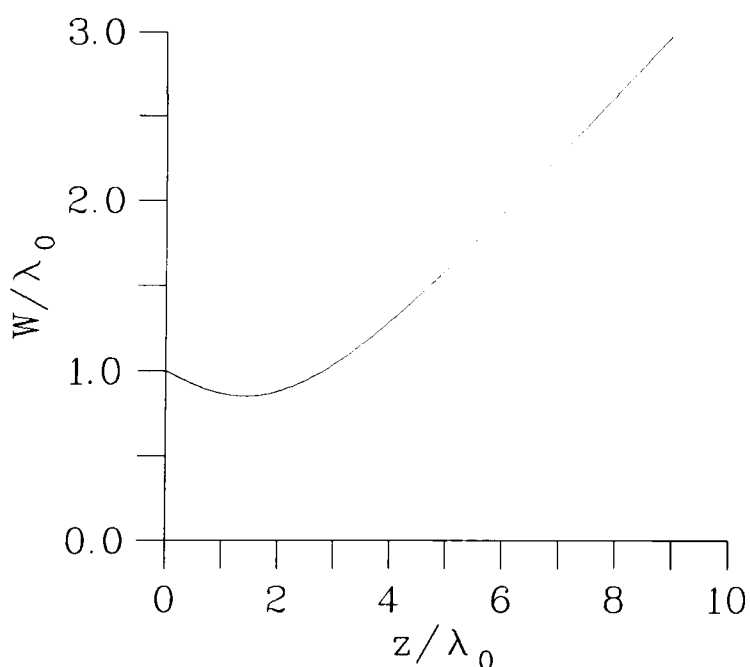


Figure 2.4: The variation of the beam waist W of a Gaussian beam in free space. Initial beam waist and phasefront radius of curvature are $W_0 = \lambda_0$ and $R_0 = -5\lambda_0$ respectively.

Chapter 3

Waveguides I:

the straight and linearly tapering parabolic–refractive–index guides.

3.1 The straight, parabolic–refractive–index waveguide.

The propagator (2.88) of our model of the straight, parabolic–refractive–index waveguide, defined by the refractive index distribution (2.65), has already been discussed in detail in chapter 2. In this section we will proceed to extract useful engineering information on the waveguide, from expression (2.88) for the propagator. A study of the propagation of a Gaussian beam in such a waveguide will be presented in section 3.2.

The traditional way of studying wave propagation in waveguides in engineering is to consider the propagation of each mode of the waveguide separately. A waveguide mode is given by a standing wave pattern, $\varphi_{nm}(x,y)$, in the plane transverse to the direction of propagation which we call the z -axis. This latter is the waveguide axis. The field amplitude, $\psi_{nm}(x,y,z)$, of a wave travelling unaltered along the waveguide axis with a given propagation constant, β_{nm} , is then given by,

$$\psi_{nm}(x,y,z) = \varphi_{nm}(x,y) \exp[i(\beta_{nm}z - \omega t)] \quad (3.1)$$

where $\varphi_{nm}(x,y)$ obeys the homogeneous paraxial, scalar wave equation (2.44). Substituting (3.1) into (2.44) then yields,

$$\frac{1}{2k^2} \nabla_{xy}^2 \varphi_{nm}(x,y) + (1 - n'(x,y)) \varphi_{nm}(x,y) = \frac{\beta_{nm}}{k} \varphi_{nm}(x,y). \quad (3.2)$$

Clearly, equation (3.2) defines a Sturm–Liouville eigenvalue problem with suitable radiation boundary conditions for $\varphi_{nm}(x,y)$ at infinity (Morse and Feshbach, 1953). The modal field amplitudes, $\varphi_{nm}(x,y)$ are the eigenfunctions of the problem, and the scaled propagation constants β_{nm}/k the corresponding eigenvalues. The Green's function of the paraxial, scalar wave equation (2.44) can be written in terms of the mode amplitudes

(Morse and Feshbach, 1953) as,

$$K(x, y, z; x_0, y_0, z_0) = \sum_{n=0}^{\infty} \sum_{m=0}^{\infty} \varphi_{nm}(x, y) \varphi_{nm}^*(x_0, y_0) \exp[i\beta_{nm}(z-z_0)]. \quad (3.3)$$

In the quantum mechanical analogue of the optical problem, a mode corresponds to an eigenfunction of the potential well $n'(x, y)$ and the corresponding propagation constant corresponds to the energy level. Using the analogy with quantum mechanics, it is a simple matter to show that the energy eigenvalues of the harmonic oscillator are bounded from below (Dirac, 1958) and, as a consequence of the fact that the minimum in the potential well corresponds to the maximum in the refractive index, the propagation numbers β_{nm} are bounded from above.

We will now examine two methods which can be used to extract useful information on mode field profiles and propagation constants from the propagator expression (2.88). The first method is a direct expansion of the exponential terms in the expression for the propagator (2.88) into their Maclaurin series in the variables $\exp[ia(z-z_0)]$ and $\exp[ib(z-z_0)]$. In order to get the answer in the desired form use must be made of the following identities:

$$\cos[a(z-z_0)] = \frac{1}{2} e^{ia(z-z_0)} (1 + e^{-2ia(z-z_0)}) \quad (3.4)$$

$$i \sin[a(z-z_0)] = \frac{1}{2} e^{ia(z-z_0)} (1 - e^{-2ia(z-z_0)}) \quad (3.5)$$

Using the above identities (3.4) and (3.5), the expression for the propagator (2.88) can be re-written as,

$$K(x, y, z; x_0, y_0, z_0) = \left[\frac{k^2 ab}{\pi^2 e^{ia(z-z_0)} (1 - e^{-2ia(z-z_0)}) e^{ib(z-z_0)} (1 - e^{-2ib(z-z_0)})} \right]^{1/2} \times \\ \exp \left\{ \frac{-ka}{e^{ia(z-z_0)} (1 - e^{-2ia(z-z_0)})} \left[\frac{(x^2 + x_0^2)}{2} e^{ia(z-z_0)} (1 + e^{-2ia(z-z_0)}) - 2xx_0 \right] \right\} \times \\ \exp \left\{ \frac{-kb}{e^{ib(z-z_0)} (1 - e^{-2ib(z-z_0)})} \left[\frac{(y^2 + y_0^2)}{2} e^{ib(z-z_0)} (1 + e^{-2ib(z-z_0)}) - 2yy_0 \right] \right\} \times \\ \exp[ik(z-z_0)]. \quad (3.6)$$

Expression (3.6) can be further simplified to,

$$\begin{aligned}
K(x, y, z; x_0, y_0, z_0) &= \exp[ik(z-z_0)] \times \\
&\left[\frac{ka}{\pi} \right]^{1/2} \exp\left\{ \frac{-ia(z-z_0)}{2} \right\} \left[1 - e^{-2ia(z-z_0)} \right]^{-1/2} \times \\
&\exp\left\{ -\frac{ka}{2} \left[(x^2+x_0^2) \frac{1 + e^{-2ia(z-z_0)}}{1 - e^{-2ia(z-z_0)}} - \frac{4xx_0 e^{-ia(z-z_0)}}{1 - e^{-2ia(z-z_0)}} \right] \right\} \times \\
&\left[\frac{kb}{\pi} \right]^{1/2} \exp\left\{ \frac{-ib(z-z_0)}{2} \right\} \left[1 - e^{-2ib(z-z_0)} \right]^{-1/2} \times \\
&\exp\left\{ -\frac{kb}{2} \left[(y^2+y_0^2) \frac{1 + e^{-2ib(z-z_0)}}{1 - e^{-2ib(z-z_0)}} - \frac{4yy_0 e^{-ib(z-z_0)}}{1 - e^{-2ib(z-z_0)}} \right] \right\}. \tag{3.7}
\end{aligned}$$

Expanding all the terms in the variables $\exp[-ia(z-z_0)]$ and $\exp[-ib(z-z_0)]$ into their Maclaurin series (Feynman and Hibbs, 1965), gives,

$$\left[1 - e^{-2ia(z-z_0)} \right]^{-1/2} = 1 + \frac{1}{2} e^{-2ia(z-z_0)} + \dots \tag{3.8}$$

$$\frac{e^{-ia(z-z_0)}}{1 - e^{-2ia(z-z_0)}} = e^{-ia(z-z_0)} + e^{-3ia(z-z_0)} + \dots \tag{3.9}$$

$$\frac{1 + e^{-2ia(z-z_0)}}{1 - e^{-2ia(z-z_0)}} = 1 + \frac{1}{2} e^{-2ia(z-z_0)} + \dots \tag{3.10}$$

Substituting equations (3.8) to (3.10) into the expression for the propagator (3.7), carrying out the multiplications and grouping the appropriate terms together finally yields,

$$\begin{aligned}
K(x, y, z; x_0, y_0, z_0) &= \frac{k\sqrt{ab}}{\pi} e^{-k(ax^2+by^2)/2} e^{-k(ax_0^2+by_0^2)/2} e^{i(k-a/2-b/2)(z-z_0)} + \\
&\frac{2k^2\sqrt{a^3b}}{\pi} x e^{-k(ax^2+by^2)/2} x_0 e^{-k(ax_0^2+by_0^2)/2} e^{i(k-3a/2-b/2)(z-z_0)} + \\
&\frac{2k^2\sqrt{ab^3}}{\pi} y e^{-k(ax^2+by^2)/2} y_0 e^{-k(ax_0^2+by_0^2)/2} e^{i(k-a/2-3b/2)(z-z_0)} + \\
&\frac{4k^3\sqrt{(ab)^3}}{\pi} xy e^{-k(ax^2+by^2)/2} x_0 y_0 e^{-k(ax_0^2+by_0^2)/2} e^{i(k-3a/2-3b/2)(z-z_0)} \\
&+ \dots \tag{3.11}
\end{aligned}$$

A direct comparison of equations (3.3) and (3.11) yields,

$$\begin{aligned}
\beta_{00} &= k - a/2 - b/2 \quad \text{and} \quad \varphi_{00}(x, y) = \sqrt{\frac{k\sqrt{ab}}{\pi}} e^{-k(ax^2+by^2)/2} \\
\beta_{10} &= k - 3a/2 - b/2 \quad \text{and} \quad \varphi_{10}(x, y) = \sqrt{\frac{2k\sqrt{a^3b}}{\pi}} x e^{-k(ax^2+by^2)/2} \\
\beta_{01} &= k - a/2 - 3b/2 \quad \text{and} \quad \varphi_{01}(x, y) = \sqrt{\frac{2k\sqrt{ab^3}}{\pi}} y e^{-k(ax^2+by^2)/2}
\end{aligned}$$

$$\beta_{11} = k - 3a/2 - 3b/2 \text{ and } \varphi_{11}(x,y) = 2\sqrt{\frac{k^3\sqrt{a^3b^3}}{\pi}} xy e^{-k(ax^2+by^2)/2}$$

etc. (3.12)

The mode profile and propagation constant results in (3.12) are well known (Marcuse, 1982, Yariv, 1991), but have been derived here in order to illustrate the way they can be extracted from the propagator.

The second way of extracting the above information from the propagator is suitable only for obtaining the lowest order mode, but has the advantage of being easy to adapt for use on a computer. In order to proceed further, the definition of the trace of the propagator must be presented first. In the Heisenberg picture of quantum mechanics (Sakurai, 1985) all operators can be represented by matrices. The trace or spur of a matrix is defined to be the sum of all its diagonal elements, i.e. $Tr A = \sum_i A_{ii}$, and has the property that it is invariant under orthogonal basis vector (coordinate) transformations (Morse and Feshbach, 1953). The trace of an operator is the continuous analogue of this, and is defined by setting $x_0 = x$, $y_0 = y$ and integrating over all possible values of x and y (Morse and Feshbach, 1953, Feynman and Hibbs, 1965). Thus,

$$Tr K(z-z_0) = \int_{-\infty}^{+\infty} dx \int_{-\infty}^{+\infty} dy K(x,y,z;x,y,z_0). \quad (3.13)$$

Equations (3.3) and (3.13), together with the fact that the eigenfunctions $\varphi_{nm}(x,y)$ are orthonormal, imply that,

$$Tr K(z-z_0) = \sum_{n=0}^{\infty} \sum_{m=0}^{\infty} \exp[i\beta_{nm}(z-z_0)]. \quad (3.14)$$

Using the analytic continuation

$$z-z_0 = i\mu, \quad (3.15)$$

and the fact that the propagation constants β_{nm} are bounded from above, we may extract the lowest order mode propagation constant β_{00} from the trace of the propagator, since in the limit $\mu \rightarrow -\infty$, the term $\exp(-\mu\beta_{00})$ dominates the sum in (3.14). Thus,

$$\beta_{00} = \lim_{\mu \rightarrow -\infty} \left(-\frac{1}{\mu} \ln[\text{Tr } K(i\mu)] \right). \quad (3.16)$$

In the same limit, and using equation (3.3) we may write,

$$\varphi_{00}(x, y) \varphi_{00}^*(x_0, y_0) = \lim_{\mu \rightarrow -\infty} \left(\frac{K(x, y, i\mu; x_0, y_0, 0)}{\text{Tr } K(i\mu)} \right). \quad (3.17)$$

Let us now use expression (2.88) for the propagator in equations (3.16) and (3.17). The trace of the propagator (2.88) is,

$$\begin{aligned} \text{Tr } K(z-z_0) &= \exp[ik(z-z_0)] \times \\ &\int_{-\infty}^{+\infty} dx \left[\frac{ka}{2\pi i \sin[a(z-z_0)]} \right]^{1/2} \exp\left\{ \frac{2ikax^2}{2\sin[a(z-z_0)]} [\cos[a(z-z_0)] - 1] \right\} \times \\ &\int_{-\infty}^{+\infty} dy \left[\frac{kb}{2\pi i \sin[b(z-z_0)]} \right]^{1/2} \exp\left\{ \frac{2ikby^2}{2\sin[b(z-z_0)]} [\cos[b(z-z_0)] - 1] \right\}. \end{aligned} \quad (3.18)$$

Evaluating the integrals in (3.18) then gives,

$$\text{Tr } K(z-z_0) = \frac{\exp[ik(z-z_0)]}{\sqrt{2[\cos[a(z-z_0)]-1]} \sqrt{2[\cos[b(z-z_0)]-1]}}. \quad (3.19)$$

We may now extract directly the lowest order mode propagation constant from the trace of the propagator (3.19) using (3.16).

$$\beta_{00} = \lim_{\mu \rightarrow -\infty} -\frac{1}{\mu} \left[-k\mu - \frac{1}{2} \ln[2[\cosh(a\mu)-1]] - \frac{1}{2} \ln[2[\cosh(b\mu)-1]] \right] \quad (3.20)$$

or,

$$\beta_{00} = k + \lim_{\mu \rightarrow -\infty} \frac{\ln(e^{-a\mu}) + \ln(e^{-b\mu})}{2\mu}. \quad (3.21)$$

Hence,

$$\beta_{00} = k - a/2 - b/2, \quad (3.22)$$

which is in agreement with (3.12). We now substitute the expression for the trace of the propagator (3.19) into (3.17) to obtain the lowest order mode field profile.

$$\begin{aligned} \varphi_{00}(x, y) \varphi_{00}^*(x_0, y_0) &= \lim_{\mu \rightarrow -\infty} \left\{ \sqrt{\frac{2ka/\cos(i a \mu) - 1}{2\pi i \sin(i a \mu)}} \sqrt{\frac{2kb/\cos(i b \mu) - 1}{2\pi i \sin(i b \mu)}} \times \right. \\ &\left. \exp\left\{ \frac{ika(x^2+x_0^2)[\cos(i a \mu) - 1]}{2\sin(i a \mu)} + \frac{ika(x-x_0)^2}{2\sin(i a \mu)} \right\} \exp\left\{ \frac{ikb(y^2+y_0^2)[\cos(i b \mu) - 1]}{2\sin(i b \mu)} + \frac{ikb(y-y_0)^2}{2\sin(i b \mu)} \right\} \right\} \end{aligned} \quad (3.23)$$

Using

$$\lim_{\mu \rightarrow -\infty} \frac{\cos(i a \mu) - 1}{i \sin(i a \mu)} = \lim_{\mu \rightarrow -\infty} \frac{\cosh(a\mu) - 1}{\sinh(a\mu)} = 1 \quad (3.24)$$

and

$$\lim_{\mu \rightarrow -\infty} \frac{1}{i \sin(i a \mu)} = \lim_{\mu \rightarrow -\infty} \frac{1}{\sinh(a \mu)} = 0, \quad (3.25)$$

equation (3.23) yields,

$$\varphi_{00}(x, y) \varphi_{00}^*(x_0, y_0) = \frac{k\sqrt{ab}}{\pi} e^{-k(ax^2+by^2)/2} e^{-k(ax_0^2+by_0^2)/2}. \quad (3.26)$$

The fundamental mode profile is, therefore, given by,

$$\varphi_{00}(x, y) = \sqrt{\frac{k\sqrt{ab}}{\pi}} e^{-k(ax^2+by^2)/2}, \quad (3.27)$$

which, once again, is in agreement with (3.12).

Although the two methods presented above have concentrated on the parabolic refractive index waveguide, they are not restricted to it. The main shortcoming of the first of the two methods is that it requires knowledge of the closed form expression for the propagator, while the second does not rely on this. In fact, the second method has been used (Hawkins, 1987, 1988, Troudet and Hawkins, 1988) to obtain numerically the propagation constants of waveguides of different cross-sectional refractive index profiles.

3.2 The propagation of a Gaussian beam in a straight, parabolic-refractive-index waveguide.

Let us now turn our attention to the study of the propagation of a Gaussian beam through a medium with a parabolic refractive index variation. In what follows the Gaussian beam contours of constant amplitude will be assumed to be elliptic in the plane transverse to the direction of propagation and centred on the axis of the guiding medium. An off-centre Gaussian beam is not much more difficult to analyse, but as the calculations are lengthier, only the final results are presented here for the sake of compactness. The phasefront of the Gaussian beam considered will be assumed to be a plane wave, i.e. have an infinite radius of curvature initially, again in order to keep the calculation simple. The Gaussian beam amplitude is described in the plane $z = z_0$ by the equation (Yariv, 1991),

$$\psi(x_0, y_0; z_0) = \psi_0 \exp\left\{-\frac{x_0^2}{w_x^2} - \frac{y_0^2}{w_y^2}\right\}. \quad (3.28)$$

w_x is the known beam waist (i.e. the beam width) along the x -axis on this plane, and w_y is the corresponding beam waist along the y -axis. Using the propagation rule (2.60) and substituting for the propagator (2.88), the field amplitude at a distance of propagation $z-z_0$ will be given by,

$$\begin{aligned} \psi(x, y, z) = & \int_{-\infty}^{+\infty} dx_0 \int_{-\infty}^{+\infty} dy_0 \psi_0 \exp\left\{-\frac{x_0^2}{w_x^2} - \frac{y_0^2}{w_y^2}\right\} \frac{k}{2\pi i} \left[\frac{ab}{\sin[a(z-z_0)] \sin[b(z-z_0)]} \right]^{1/2} \times \\ & \exp\left\{\frac{ika}{2\sin[a(z-z_0)]} \left[(x^2+x_0^2)\cos[a(z-z_0)] - 2xx_0 \right] + \frac{ikb}{2\sin[b(z-z_0)]} \left[(y^2+y_0^2)\cos[b(z-z_0)] - 2yy_0 \right]\right\} \\ & \times \exp[ik(z-z_0)]. \end{aligned} \quad (3.29)$$

We now need to compute two integrals of the form,

$$I_x = \int_{-\infty}^{+\infty} dx_0 \exp\left\{-\frac{x_0^2}{w_x^2} + \frac{ika}{2\sin[a(z-z_0)]} \left[(x^2+x_0^2)\cos[a(z-z_0)] - 2xx_0 \right]\right\}. \quad (3.30)$$

The integral (3.30) can be cast in the standard form (2.51) and hence simplifies to,

$$\begin{aligned} I_x = & \exp\left\{\frac{ika}{2}x^2\cot[a(z-z_0)]\right\} \sqrt{\frac{\pi}{\frac{1}{w_x^2} - \frac{ika}{2}\cot[a(z-z_0)]}} \times \\ & \exp\left\{\frac{-k^2a^2x^2}{4\sin^2[a(z-z_0)]\left[\frac{1}{w_x^2} - \frac{ika}{2}\cot[a(z-z_0)]\right]}\right\}. \end{aligned} \quad (3.31)$$

After some algebraic manipulation (3.31) further simplifies to,

$$\begin{aligned} I_x = & \frac{\sqrt{\pi}}{4\sqrt{\frac{1}{w_x^2} + \frac{k^2a^2}{4}\cot^2[a(z-z_0)]}} \exp\left\{\frac{i}{2}\arctan\left[\frac{w_x^2ka}{2}\cot[a(z-z_0)]\right]\right\} \times \\ & \exp\left\{\frac{-x^2}{\frac{4\sin^2[a(z-z_0)]}{k^2a^2w_x^2} + w_x^2\cos^2[a(z-z_0)]} + \frac{ikx^2/2}{\frac{\sin^2[a(z-z_0)]}{(a/2)\sin[2a(z-z_0)]} + \frac{k^2a^2w_x^4\cos^2[a(z-z_0)]}{(1-k^2a^2w_x^4/4)}}\right\}. \end{aligned} \quad (3.32)$$

Using the result in (3.32) the full expression for the complex Gaussian beam amplitude (3.29) is then given by,

$$\begin{aligned}
\psi(x,y,z) = & \frac{\psi_0}{i} \left[\frac{w_x^2}{\frac{4\sin^2|a(z-z_0)|}{k^2 a^2 w_x^2} + w_x^2 \cos^2[a(z-z_0)]} \frac{w_y^2}{\frac{4\sin^2|b(z-z_0)|}{k^2 b^2 w_y^2} + w_y^2 \cos^2[b(z-z_0)]} \right]^{1/4} \times \\
& \exp \left\{ ik(z-z_0) + \frac{i}{2} \arctan \left[\frac{w_x^2 ka}{2} \cot[a(z-z_0)] \right] + \frac{i}{2} \arctan \left[\frac{w_y^2 kb}{2} \cot[b(z-z_0)] \right] \right\} \times \\
& \exp \left\{ \frac{-x^2}{\frac{4\sin^2|a(z-z_0)|}{k^2 a^2 w_x^2} + w_x^2 \cos^2[a(z-z_0)]} + \frac{ikx^2/2}{\frac{\sin^2|a(z-z_0)| + k^2 a^2 w_x^4 \cos^2|a(z-z_0)|}{(a/2)\sin[2a(z-z_0)](1 - k^2 a^2 w_x^4/4)}} \right\} \times \\
& \exp \left\{ \frac{-y^2}{\frac{4\sin^2|b(z-z_0)|}{k^2 b^2 w_y^2} + w_y^2 \cos^2[b(z-z_0)]} + \frac{iky^2/2}{\frac{\sin^2|b(z-z_0)| + k^2 b^2 w_y^4 \cos^2|b(z-z_0)|}{(b/2)\sin[2b(z-z_0)](1 - k^2 b^2 w_y^4/4)}} \right\}.
\end{aligned} \tag{3.33}$$

Equation (3.33) completely describes the paraxial propagation of a centred, elliptic Gaussian beam in a medium of parabolic refractive index variation. The above result is consistent with the predictions on the propagation of a Gaussian beam in a medium of parabolic refractive index variation found elsewhere in the literature (Yariv, 1991). Our result though, is presented in a closed form which is new. The above result is of great importance in engineering since it describes the propagation of a paraxial wave in a weakly guiding waveguide, not in terms of each individual mode, but in terms of the total field. A propagation of a Gaussian beam is a good approximation to the propagation of TEM waves in weakly guiding waveguides, and as such it is a good description of a real field. This ties in well with the discussion at the beginning of section 2.6 in chapter 2, where it was argued that the graded index waveguide with a parabolic transverse refractive index distribution can be regarded as an archetypal waveguide model for paraxial wave propagation in graded index waveguides. The closed form in which the above result appears is a slightly more general form of the results quoted elsewhere. It should be pointed out that a general Gaussian beam, such as an off-centre beam with different initial radii of curvature along the x and y -axes, can easily be investigated by following exactly the same steps in the calculation as above, and the results can be obtained in closed form, though the detailed calculation will be considerably lengthier.

By comparing the expression for the Gaussian beam amplitude in (3.33) to that in

(2.59), we can immediately observe that the phasefront of the beam is in general an ellipsoid, while its beam waist varies periodically, as expected for propagation in a medium which acts as a waveguide. The z -coordinates of the foci of the medium can be easily found if one considers that at these foci the beam waist along the x and y -axes, $w_x(z)$ and $w_y(z)$ respectively, should be a minimum in the x and y -axis directions simultaneously. In order to avoid confusion, a clear distinction should be made between the function $w_x(z)$ and w_x , its initial value at the plane $z = z_0$. In the event $w_x(z)$ and $w_y(z)$ do not have a minimum on the same z -plane, the medium focuses the beam astigmatically and the focal points are defined to be the ones at which the function $\sqrt{w_x(z)w_y(z)}$ has a minimum (Marchand, 1978).

Using the direct comparison between (3.28) and (3.33), $w_x(z)$ is seen to be given by,

$$w_x(z) = \sqrt{w_x^2 \cos^2[a(z-z_0)] + \frac{4 \sin^2[a(z-z_0)]}{k^2 a^2 w_x^2}}. \quad (3.34)$$

A similar expression can be obtained for $w_y(z)$ by replacing a and w_x with b and w_y respectively. A plot of $w_x(z)$ against propagation distance $(z-z_0)$ is shown in the graph of figure 3.1. In the particular case presented in figure 3.1, the initial beam waist $w_x(z_0)$ was larger than $\sqrt{2/ka}$, the beam waist of the lowest order mode of the model waveguide, and in this case the focusing property of the parabolic-refractive-index waveguide dominates over diffraction, resulting in an initial decrease of the beam waist towards a minimum. Depending on the exact value of the beam waist, diffraction and focusing become the dominant propagation mechanisms alternately, which accounts for the oscillatory behaviour of the beam waist observed in figure 3.1. In contrast to this, if the initial beam waist $w_x(z_0)$ were smaller than $\sqrt{2/ka}$, diffraction would initially dominate the propagation mechanism and the beam waist would begin to increase, but would otherwise oscillate in exactly the same way as described above. The radius of curvature $R_x(z)$, along the x -direction can also be obtained in the same way as the expression (3.34)

for the beam waist and is given by,

$$R_x(z) = \frac{\sin^2[a(z-z_0)] + k^2 a^2 w_x^4 \cos^2[a(z-z_0)]}{(a/2) \sin[2a(z-z_0)] / (1 - k^2 a^2 w_x^4 / 4)}. \quad (3.35)$$

As expected, the radius of curvature also varies periodically with propagation distance. The wavefront radius of curvature ranges from infinity (a plane wave), to a minimum value which depends on the parameters of the medium and the initial beam shape. The reciprocal of the radius of curvature, i.e. the wavefront curvature, is plotted against propagation distance in the graph of figure 3.2. The radius of curvature of the wavefront is positive when the beam diverges and negative when the beam converges towards a point. The results shown in figure 3.2 confirm that the Gaussian beam converges towards and diverges from the focal points of the medium periodically, i.e. the medium acts as a waveguide. Knowledge of the radius of curvature of the propagating field distribution is of importance in the calculation of the coupling efficiency between different waveguide sections (Yariv, 1991, Snyder and Love, 1983).

The result corresponding to (3.34) for an off-centre Gaussian beam, initially centred at (x_i, y_i) with radii of curvature R_x and R_y along the x and y -axes respectively, was calculated with the aid of the computer algebra package DERIVETM, and was found to be

$$w_x(z) = \sqrt{w_x^2 \cos^2[a(z-z_0)] + \left[\frac{4}{k^2 a^2 w_x^2} + \frac{w_x^2}{a^2 R_x^2} \right] \sin^2[a(z-z_0)] + \frac{w_x^2 \sin[2a(z-z_0)]}{a R_x}}. \quad (3.36)$$

The centre (point of maximum amplitude) of the Gaussian beam, $(x_i(z), y_i(z))$, was also determined and is given by,

$$x_i(z) = x_i \cos[a(z-z_0)]. \quad (3.37)$$

The results for $w_y(z)$ and $y_i(z)$ are given by similar expressions to (3.36) and (3.37), when we replace x_i , w_x and R_x by y_i , w_y and R_y respectively. Using the computer algebra package DERIVETM, it is also possible to obtain expressions for the evolution with propagation distance, of the radii of curvature of the beam phasefront and the coordinates

of the point of stationary phase of the Gaussian beam. The coordinates of the point of stationary phase, $\tilde{x}_i(z)$, of the Gaussian beam are given by,

$$\tilde{x}_i(z) = x_i \frac{\cos[a(z-z_0)]}{\cos[2a(z-z_0)]} \frac{1 + \frac{1}{2} \left[\frac{1}{R_x a} + \frac{4R_x}{k^2 w_x^2 a^2} \right] \tan[a(z-z_0)]}{1 + \frac{1}{2} \left[\frac{1}{R_x a} + \frac{4R_x}{k^2 w_x^2 a^2} - R_x a \right] \tan[2a(z-z_0)]}. \quad (3.38)$$

Evidently, the point of stationary phase and the point of maximum amplitude do not coincide for the above Gaussian beam. The radius of curvature of the phasefront is finally given by,

$$R_x(z) = R_x \times \frac{1 + \frac{1}{R_x a} \tan[2a(z-z_0)] + \frac{1}{2R_x a} \left[\frac{1}{R_x a} + \frac{2R_x}{k^2 w_x^2 a} - R_x a \right] \left[\frac{1}{\cos[2a(z-z_0)]} - 1 \right]}{1 + \frac{1}{2} \left[\frac{1}{R_x a} + \frac{4R_x}{k^2 w_x^2 a^2} - R_x a \right] \tan[2a(z-z_0)]}. \quad (3.39)$$

where R_x is the initial radius of curvature of the phasefront of the Gaussian beam. Again, the corresponding results for $y_i'(z)$ and $R_y(z)$ can be found using the substitutions mentioned before in equations (3.38) and (3.39). All of the above results (3.36) to (3.39) concerning the propagation of an off-centre, Gaussian beam in a parabolic refractive index waveguide are both exact and new. The only other similar results known, are those given by Marcuse (1982), which are however only an approximation.

3.3 The linearly tapering parabolic-refractive-index waveguide.

In the last two sections of chapter 2 and in all of this chapter so far, we have been concerned with the study of graded-index optical waveguides of constant cross-sectional shape and area. There exist a fair number of techniques for analysing wave propagation in such waveguides (Snyder and Love, 1983) and path integration is just one of them. The advantages of the use of path integration become more evident when we consider waveguide junctions and tapered waveguides. In section 1.3 of chapter 1 we have

explained the importance of understanding the propagation mechanism of optical waves in graded-index waveguide tapers and junctions, in the context of integrated optics. Here we will be concerned with the analysis of a parabolic-refractive-index, linearly-tapering waveguide, using path integration. In the next chapter we will examine tapered waveguides of more general geometries and in chapter 5 we will concentrate on the analysis of waveguide junctions.

The refractive index distribution we choose to model a waveguide which tapers in the xz plane only, is of the form,

$$n(x, y, z) = n_0 \left(1 - \frac{1}{2} c^2(z) x^2 - \frac{1}{2} b^2 y^2 \right). \quad (3.40)$$

The constant refractive index contour line $n(x, 0, z) = n_0/2$ has the equation

$$x(z) = \pm 1/c(z), \quad (3.41)$$

and henceforth we shall use this equation to describe the geometry of the waveguide. Although there does not exist a universally accepted convention for specifying the dimensions of graded-index waveguides in the absence of step-refractive-index interfaces, all the definitions known to us (see e.g. Snyder and Love, 1983, Tamir, 1990) make use of some contour of constant refractive index in order to define waveguide sizes and/or scale lengths. Our approach to naming graded-index waveguide geometries is a natural extension of the existing schemes. When $c(z)$ is a real constant the contours of constant refractive index in the xz plane are pairs of parallel straight lines, and the refractive index distribution (3.40) describes a straight waveguide of uniform cross-section. By allowing $c(z)$ to vary with the distance along the waveguide axis z , we are deforming the contours of constant refractive index into pairs of non-parallel, and possibly curved lines. Clearly, if we choose

$$c(z) = \frac{1}{z \tan \theta}, \quad (3.42)$$

the contour of refractive index $n(x, 0, z) = n_0/2$ is the pair of straight lines $x = \pm z \tan \theta$. Henceforth, we shall call such a refractive index distribution a linear taper. Such a taper can be created by employing a linearly tapering mask in the deposition stage of the

manufacturing process, prior to diffusion (Lee, 1986). The angle θ above cannot be related in a simple way to the corresponding angle on the mask, as θ will depend on non-geometrical parameters such as the total diffusion time. The surfaces of constant refractive index in this case are right elliptical cones centred on the z -axis. The refractive index distribution in xz plane for such a taper is shown in figure 3.3. A more general waveguide model, which describes a waveguide tapering independently in the xz and yz planes can be described by allowing b in equation (3.40) to be a function of z . As we have seen in chapter 2, equation (2.67) which describes the propagator of a parabolic refractive index waveguide, is separable in the $x(\zeta)$ and $y(\zeta)$ variables, regardless of whether the coefficients a and b are functions of z or not. Hence, no new information will be gained by letting b vary with z .

The propagator of the paraxial wave equation for a medium with the refractive index distribution (3.40) is given by

$$K(x, y, z; x_0, y_0, z_0) = \exp[ik(z-z_0)] \int \delta x(z) \exp\left\{ ik/2 \int_{z_0}^z d\zeta [\dot{x}^2(\zeta) - c^2(\zeta)x^2(\zeta)] \right\} \times \\ \left[\frac{kb}{2\pi i \sin[b(z-z_0)]} \right]^{1/2} \exp\left\{ \frac{ikb}{2\sin[b(z-z_0)]} [(y^2+y_0^2)\cos[b(z-z_0)] - 2yy_0] \right\}, \quad (3.43)$$

where we have made use of the result (2.88). We now only need to consider the path integral over $x(z)$, which we define as the partial propagator $K(x, z; x_0, z_0)$:

$$K(x, z; x_0, z_0) \equiv \int \delta x(z) \exp\left\{ ik/2 \int_{z_0}^z d\zeta [\dot{x}^2(\zeta) - c^2(\zeta)x^2(\zeta)] \right\}. \quad (3.44)$$

The path integral in (3.44) can be evaluated in closed form by virtue of the fact that it is quadratic in the path $x(\zeta)$ and its derivative. The method for evaluating a path integral of the form (3.44) with an arbitrary function $c(z)$ is presented in appendix A and closely follows that suggested by Schulman (1981) (see also Gel'fand and Yaglom, 1960). The partial propagator (3.44) is shown in appendix A to be equal to

$$K(x, z; x_0, z_0) = \left[\frac{k}{2\pi i} \right]^{1/2} \left[\frac{1}{f(z, z_0)} \right]^{1/2} \exp \left\{ ik/2 \int_{z_0}^z d\zeta [\dot{X}^2(\zeta) - c^2(\zeta)X^2(\zeta)] \right\}, \quad (3.45)$$

where $X(\zeta)$ is the path of the ray described by geometrical optics and has fixed endpoints (x, z) and (x_0, z_0) . By Fermat's principle $X(\zeta)$ renders the exponent in (3.44) extremal, and as shown in appendix A is the solution of the Euler–Lagrange equation,

$$\frac{d^2 X(\zeta)}{d\zeta^2} + c^2(\zeta)X(\zeta) = 0, \quad (3.46a)$$

with boundary conditions

$$X(z_0) = x_0 \quad \& \quad X(z) = x. \quad (3.46b)$$

The function $f(z, z_0)$ obeys the same differential equation with respect to the variable z as does $X(\zeta)$,

$$\frac{\partial^2 f(z, z_0)}{\partial z^2} + c^2(z)f(z, z_0) = 0, \quad (3.47a)$$

but satisfies different boundary conditions given by,

$$f(z=z_0, z_0) = 0 \quad \text{and} \quad \left. \frac{\partial f(z, z_0)}{\partial z} \right|_{z=z_0} = 1. \quad (3.47b)$$

For the linear taper described by (3.40) and (3.42), the ray path $X(z)$ described by geometrical optics is given by the solution to

$$\frac{d^2 X(\zeta)}{d\zeta^2} + \frac{1}{\zeta^2 \tan^2 \theta} X(\zeta) = 0. \quad (3.48)$$

The above differential equation is just a special case of the Euler–Cauchy equation (Kreyszig, 1983),

$$\zeta^2 \frac{d^2 X}{d\zeta^2} + a\zeta \frac{dX}{d\zeta} + bX = 0, \quad (3.49)$$

the general solution to which has the form

$$X(\zeta) = \zeta^m, \quad (3.50)$$

where m satisfies the quadratic indicial equation

$$m^2 - m + \frac{1}{\tan^2 \theta} = 0. \quad (3.51)$$

In practice θ is a small angle (Milton and Burns, 1977), of the order of 5° – 20° , and therefore the relevant solution of (3.51) appropriate to small taper angles ($\theta \leq \arctan(2)$) is

$$m_1 = m_2^* = \frac{1}{2} + qi, \quad (3.52)$$

where

$$q \equiv \frac{\sqrt{4 - \tan^2 \theta}}{2 \tan \theta}. \quad (3.53)$$

The general solution of equation (3.48) is then given by

$$X(\zeta) = A\sqrt{\zeta} \cos(q \ln \zeta) + B\sqrt{\zeta} \sin(q \ln \zeta). \quad (3.54)$$

Fitting the boundary conditions (3.46b) completely determines $X(\zeta)$ to be,

$$X(\zeta) = \frac{x \sqrt{\zeta z_0} \sin[q \ln(\zeta/z_0)] + x_0 \sqrt{z\zeta} \sin[q \ln(z/\zeta)]}{\sqrt{zz_0} \sin[q \ln(z/z_0)]}. \quad (3.55)$$

Similarly, we may determine $f(z, z_0)$, which is found to be given by

$$f(z, z_0) = \frac{\sqrt{zz_0}}{q} \sin[q \ln(z/z_0)]. \quad (3.56)$$

Substituting equations (3.55) and (3.56) into the expression for the partial propagator (3.45) and after some considerable, but straight-forward algebraic manipulations we find that

$$K(x, z; x_0, z_0) = \left[\frac{kq}{2\pi i \sqrt{zz_0} \sin[q \ln(z/z_0)]} \right]^{1/2} \times \exp \left\{ ik \left[\frac{x^2}{2z} \left(\frac{1}{2} + \cot[q \ln(z/z_0)] \right) + \frac{x_0^2}{2z} \left(\frac{1}{2} + \cot[q \ln(z/z_0)] \right) - \frac{qx x_0}{\sqrt{zz_0} \sin[q \ln(z/z_0)]} \right] \right\}. \quad (3.57)$$

It is important to note that the propagator depends not on the propagation distance $(z-z_0)$, but on the absolute values of both z and z_0 . This is because the refractive index distribution chosen to model the linear taper is such that the initial taper width depends on the absolute value of z_0 (≥ 0). The propagator of the linearly tapering waveguide is therefore completely specified by equations (3.43) (3.44) and (3.57). This exact result describing paraxial propagation in a linear taper is new and we are now in position to use it to study the coupling properties of such a taper analytically.

3.4 The coupling efficiency of the linearly tapering parabolic–refractive–index waveguide.

Suppose we connect the linearly tapering waveguide to two uniform, semi–infinite parabolic–refractive–index waveguides whose transverse refractive index distribution completely matches that of the taper at $\zeta = z_0$ and $\zeta = z$ respectively. We will refer to the waveguide which exists for $\zeta \leq z_0$ as the input waveguide, and the one which exists for $\zeta \geq z$ as the output waveguide. The refractive index distributions which describe these two straight, uniform waveguides are

$$n_{\text{in}}(x_0, y_0) = n_0 \left(1 - \frac{1}{2} a_0^2 x_0^2 - \frac{1}{2} b^2 y_0^2 \right) \quad \text{for } \zeta \leq z_0, \quad (3.58a)$$

and

$$n_{\text{out}}(x, y) = n_0 \left(1 - \frac{1}{2} a^2 x^2 - \frac{1}{2} b^2 y^2 \right) \quad \text{for } \zeta \geq z. \quad (3.58b)$$

The matched refractive index condition at $\zeta = z_0$ and $\zeta = z$ implies that

$$a_0 = c(z_0) = \frac{1}{z_0 \tan \theta} \quad (3.59a)$$

and

$$a = c(z) = \frac{1}{z \tan \theta} \quad (3.59b)$$

The modes of the input and output waveguides $\psi_{nk}(x_0, y_0)$ and $\varphi_{ml}(x, y)$ respectively are given by equations (3.12) and are normalised to correspond to unit power.

Since in our model we have chosen all three waveguide sections of interest (input waveguide, taper and output waveguide) to have an identical y –dependence of refractive–index, we may suppress all the y –dependent parts of the expressions that follow (including the corresponding mode indices k and l) for the sake of simplicity. We must bear in mind though, that as a consequence of the mode eigenfunction orthonormality and the uniformity of all three waveguides in the y –direction, the input waveguide mode $\psi_{nk}(x_0, y_0)$ cannot excite the output waveguide mode $\varphi_{ml}(x, y)$, unless $k = l$. Henceforth we suppress the y –dependence and use $\psi_n(x_0)$ and $\varphi_m(x)$ to denote $\psi_{nk}(x_0, y_0)$ and $\varphi_{ml}(x, y)$ respectively.

If we excite the taper at $\zeta = z_0$ with the n^{th} mode, $\psi_n(x_0)$, of the input graded–index waveguide, the total field amplitude at any ζ –plane $z_0 \leq \zeta \leq z$ along the

taper will be given by the Markov property of the propagator (2.23),

$$\psi(x, \zeta; z_0) = \int_{-\infty}^{+\infty} dx_0 K(x, \zeta; x_0, z_0) \psi_n(x_0). \quad (3.60)$$

Making use of the fact that the mode eigenfunctions $\varphi_m(x)$ of a uniform waveguide form a complete orthonormal set of basis functions (Morse and Feshbach, 1953), we may determine the extent by which the total field (3.60) at $\zeta = z$ excites the m^{th} mode of the output waveguide $\varphi_m(x)$, by considering the amplitude coupling coefficient

$$C_{mn}(z, z_0) = \int_{-\infty}^{+\infty} dx \varphi_m^*(x) \psi(x, z; z_0) = \int_{-\infty}^{+\infty} dx \int_{-\infty}^{+\infty} dx_0 \varphi_m^*(x) K(x, z; x_0, z_0) \psi_n(x_0). \quad (3.61)$$

We can interpret the amplitude coupling coefficient, $C_{mn}(z, z_0)$, to be the amount by which the m^{th} mode of the output waveguide is contained in the n^{th} mode of the input waveguide, after the latter has been propagated along the length of the taper. The amplitude coupling coefficient would be described in the language of quantum mechanics as the transition amplitude between two quantum states. Since all $\psi_n(x_0)$, $\varphi_m(x)$ and $K(x, z; x_0, z_0)$ are normalised as explained in chapter 2, the power coupling efficiency is simply given by $|C_{mn}|^2$. Using the equations for the mode field profiles (3.12), the partial propagator expression (3.57), the refractive index matching conditions (3.59) and the definition of the coupling coefficient (3.61), we can arrive at closed form expressions for the power coupling efficiencies $|C_{00}|^2$, $|C_{01}|^2$, $|C_{10}|^2$, $|C_{02}|^2$ and $|C_{20}|^2$. All the integrals involved in the calculations are of the form (2.51), which is easy to evaluate. After considerable simplification, the expressions for the above coupling efficiencies are found to be,

$$|C_{00}|^2 = \frac{1}{\sqrt{1 + \left[\frac{\sin[q \ln(z/z_0)]}{2q} \right]^2}}, \quad (3.62)$$

$$|C_{01}|^2 = |C_{10}|^2 = 0, \quad (3.63)$$

and

$$|C_{02}|^2 = |C_{20}|^2 = \frac{\left[\frac{\sin[q \ln(z/z_0)]}{2q} \right]^2}{2 \left\{ \sqrt{1 + \left[\frac{\sin[q \ln(z/z_0)]}{2q} \right]^2} \right\}^3}. \quad (3.64)$$

Other coupling efficiencies such as $|C_{11}|^2$ and $|C_{22}|^2$ can be computed with equal ease. The result given in (3.63) expresses the fact that the even and odd modes of a symmetrical waveguide structure cannot couple to each other. The coupling efficiency expressions (3.62) and (3.64) are plotted against θ and $d \equiv z/z_0$ in figures 3.4 and 3.5 respectively. Since the width of a parabolic–refractive–index waveguide is inversely proportional to the parameter a , the ratio $d \equiv z/z_0 = a_0/a$ is equal to the ratio of the width of the output waveguide at $\zeta = z$ to the width of the input waveguide at $\zeta = z_0$. Both the above results are new.

As a check, it can be seen that as $\theta \rightarrow 0$ or $d \rightarrow 1$, $|C_{00}|^2 \rightarrow 1$ and $|C_{02}|^2 \rightarrow 0$, which is the mathematical statement of the fact that an infinitely long and/or an infinitely shallow linear taper operates adiabatically. This result has been known through other methods of analysis (Milton and Burns, 1977). The path integral analysis makes the further prediction that, even under non–adiabatic operation, $|C_{00}|^2 = 1$ and $|C_{02}|^2 = 0$ when the condition

$$q \ln(d) = m\pi \quad (3.65)$$

is satisfied with $m \in \{1, 2, 3, \dots\}$. Equations (3.53) and (3.65) give the relation which must be satisfied by the angle θ , given the waveguide width ratio d , in order to ensure optimum single mode operation:

$$\theta = \arctan \frac{2}{\sqrt{1 + \left[\frac{2m\pi}{\ln(d)} \right]^2}}. \quad (3.66)$$

The largest value of θ for a given d is given by $m = 1$. It can be seen from figure 3.4 that this largest value of θ for $1 \leq d < \infty$, describes the outermost ripple of the surface $|C_{00}(\theta, d)|^2$ for which $|C_{00}|^2 = 1$. All the other 100% coupling efficiency ripples correspond to higher values of m and lie between the $m = 1$ ripple and the d -axis, in a region where the coupling efficiency oscillates between the values 1.00 and approximately 0.95. This region of high coupling efficiency quantifies what is meant by small values of θ , and is a new result:

$$\text{Small } \theta \rightarrow \theta \leq \arctan \frac{2}{\sqrt{1 + \left[\frac{2\pi}{\ln(d)} \right]^2}}. \quad (3.67)$$

Beyond the critical value of θ given by (3.67) the lowest-order-mode to lowest-order-mode coupling efficiency decreases monotonically with increasing θ and d . The main limitation of the above result is that it is independent of the wavenumber k . This is because we have been considering a waveguide with an infinite parabolic refractive index profile, and this waveguide does not possess a characteristic length scale. As a consequence, the infinite parabolic refractive index waveguide does not possess a finite mode cut-off (Snyder and Love, 1983), that is, it can support an infinite number of modes. We therefore expect the criterion (3.67) to be valid for multimode waveguides only.

By comparing figures 3.4 and 3.5 it can be seen that in the region where $|C_{00}|^2$ is low, $|C_{02}|^2$ is relatively high. We may now make use of the idea of local normal modes explained in chapter 1, and interpret the values of $|C_{00}|^2$ and $|C_{02}|^2$ as the energy contained in the lowest order local normal mode $\psi_0(x;\zeta)$ at $z = \zeta$, and the second excited local normal mode, $\psi_2(x;\zeta)$, respectively. It is evident from figures 3.4 and 3.5 that for values of θ greater than that specified by equation (3.67) the energy of the lowest order local mode is transferred to higher order modes, especially the second excited local normal mode. Most of the energy in the linearly tapered waveguide (over 85%) remains within the lowest two even excited modes, for the range of the parameters θ and d shown in figures 3.4 and 3.5.

It should be noted that, to the best of our knowledge, no other analysis of the linearly tapering waveguide has produced information about the detailed behaviour of the coupling coefficient in the region of small θ . Experimental measurements of the radiation loss due to mode conversion of a Y-junction (see figure 1.1(a)) involving a linear taper (Cullen and Wilkinson, 1984) have shown such ripples to be present (Figure 4b in Cullen and Wilkinson, 1984). Strictly speaking though, in the case of a Y-junction the mode

conversion due to the coupling of the branch arms must also be taken into account.

3.5 The propagation of the total field $\psi(x, \zeta; z_0)$ in a linear taper.

If we excite the taper with the lowest order mode of the input waveguide, $\psi_0(x_0)$, the total field amplitude (3.60) must be a centred Gaussian beam. Here we will endeavour to compare the total field amplitude with the corresponding local normal mode field. If we compare the total field (3.57) excited in the linear taper by the lowest order mode of the matched input waveguide (3.12) to the standard form for a Gaussian beam (2.59), we may easily obtain its beam waist and phasefront curvature at an arbitrary position ζ . These are given by,

$$w(\zeta) = w(z_0) \sqrt{\frac{\zeta}{z_0} \left[1 + \frac{1}{4q^2} - \frac{1}{2q} \sin[2q \ln(\zeta/z_0)] - \frac{1}{4q^2} \cos[2q \ln(\zeta/z_0)] \right]^{1/2}}, \quad (3.68)$$

and

$$\frac{1}{R(\zeta)} = \frac{1}{\zeta} \left[\frac{\sin^2[q \ln(\zeta/z_0)]}{1 - \frac{1}{(4q^2+1)} \cos[2q \ln(\zeta/z_0)] - \frac{2q}{(4q^2+1)} \sin[2q \ln(\zeta/z_0)]} \right], \quad (3.69)$$

where $w(z_0) = \sqrt{\frac{2}{ka_0}}$ is the beam waist of the lowest order mode of the input waveguide, $\psi_0(x_0)$. The beam waist, $w_{1nm}(\zeta)$, and curvature, $1/R_{1nm}(\zeta)$, of a local normal mode at a plane ζ can both be directly obtained from equation (3.12), and are given by,

$$w_{1nm}(\zeta) = \sqrt{\frac{2}{k a}} = \sqrt{\frac{2}{ka_0}} \sqrt{\frac{\zeta}{z_0}} = w(z_0) \sqrt{\frac{\zeta}{z_0}}, \quad (3.70)$$

and

$$\frac{1}{R_{1nm}(\zeta)} = 0, \quad (3.71)$$

respectively.

It can be readily seen that $w(\zeta) = w_{1nm}(\zeta)$ and $R(\zeta) = R_{1nm}(\zeta)$ only when the condition $q \ln(d) = m\pi$ of equation (3.65) is satisfied. Furthermore, the above equalities

are approximately satisfied when q is large and hence θ is small, in accordance with the criterion (3.67). Our analysis shows that the local normal mode description is not always a good approximation to the paraxial wave propagation in a linear graded-index taper. Finally, we have shown that the local normal mode analysis is an accurate method of studying propagation in graded-index linear tapers, provided that the taper geometry satisfies the criterion (3.67). Figure 3.6 shows a plot of $w(z)/w_{1nm}(z)$ against z/z_0 , when $\theta = 10^\circ$. Since the curvature depends on the absolute dimensions of the taper, we have chosen to plot the dimensionless parameter $z_0/R(z)$ (which is proportional to both the curvature and the initial width of the taper), against z/z_0 , for $\theta = 10^\circ$. This latter plot is shown in figure 3.7.

As has been mentioned in section 3.4 above, we do not know of any analysis of the wave propagation mechanism in a linearly tapering parabolic-refractive-index waveguide. The weakly guiding step-index linearly tapering waveguide has been analysed by Marcuse (1970), using a local normal mode analysis. Although the step-index and graded-index linear tapers are strictly speaking two different problems, we have produced a comparison of Marcuse's results to ours, in order to enable some comparison between the path integral and local normal mode analyses to take place. We have plotted in figure 3.8 the coupling efficiency of a linear taper with $d \equiv w/w_0 = 2$, as a function of the taper half-angle θ' corresponding to the contour chosen for convenience to be $n(x, y=0, z) = n_0/1.432$. The two curves which appear on the graph of figure 3.8 are the predictions of equation (3.62) and the local normal mode analysis of Marcuse (1970). In order to reproduce the results shown in figure 3.8, we have matched the transverse refractive index distributions of the step and graded index waveguides at their maximum value (on the z -axis), and on the refractive index contour $n(x, y=0, z) = n_0/1.432$. Finally, we have made use of the equation $\tan\theta' = \frac{2}{dL/w}$, where L is the length of the taper, to convert Marcuse's results to a form which allows comparison with our results. The angle θ' between the constant refractive index contours $n = n_0/p$, ($1 < p < \infty$) can be related to the angle θ

corresponding to the constant refractive index contour $n = n_0/2$ by $\tan\theta' = \tan\theta \sqrt{2(1-1/p)}$. The oscillations in the coupling efficiency which appear at small taper angles on our curve, are not predicted by the local normal mode analysis, which also predicts a slightly lower coupling efficiency than the path integral analysis. The lower coupling efficiency prediction of the local normal mode analysis can be partly explained by the fact that Marcuse has considered the lowest order TM mode of a step index, single mode waveguide taper (not appropriate to integrated optical structures), while we have considered the scalar wave analysis of a multimode graded index waveguide.

3.6 The validity of the paraxial approximation.

The angle φ between the normal to the wave phasefront and the axis of propagation (z -axis) can be used to investigate the validity of the paraxial approximation. Since the paraxial approximation assumes that propagation occurs predominantly along the z -direction, the smallness of the angle φ is a useful measure of its validity. The tangent of the angle φ can be found by elementary geometrical considerations and is given by $x(\zeta)/R(\zeta)$. For large $x(\zeta)$ the wave amplitude and hence the power density carried by the wave rapidly diminishes. It follows that in the region of negligible power density, φ may be large without violating the paraxial approximation. If we choose a point away from the z -axis at which the power density falls to approximately 0.034% of its peak value on the z -axis (see figure 3.9), the standard Gaussian beam expression (2.59) gives, $x(\zeta) \simeq 2w(\zeta)$. We therefore need to investigate whether the values of φ given by

$$\varphi(\zeta) = \arctan\left[2\frac{w(\zeta)}{R(\zeta)}\right] \quad (3.72)$$

are small, say less than $1/\sqrt{3}$. We have found that, for values of $k \geq 10a$, the inequality $\varphi \ll 1/\sqrt{3}$ is satisfied to a very good accuracy for all $\tan\theta \leq 2$. Note that the definition of a weakly guiding medium (c.f. chapter 1) requires k to be much greater than the parameter a . This verifies a posteriori that the paraxial approximation has yielded consistent results.

3.7 Conclusions.

In this chapter we have seen two ways in which information on the modal field profiles and propagation constants can be extracted from the expression for the propagator of a waveguiding graded-index structure. The application of both these methods was illustrated for the uniform parabolic-refractive-index waveguide. The propagation of a Gaussian beam in such a waveguide was also considered at some length and new compact results for the beam waist and radius of curvature of the propagating Gaussian beam were derived.

The propagator of the linearly tapering parabolic-refractive-index waveguide was then derived in closed form and was used to study the expressions for the coupling efficiencies between the two even lowest order local normal modes at the ends of such a tapered waveguide. The expression for the linear taper propagator was also used to study the propagation of a Gaussian beam in a linear taper, excited by the lowest order local normal mode at its narrow end. New results for the coupling efficiency and the optimal lowest order mode operation of a multimode linear taper were obtained. The information obtained on the propagating Gaussian beam was finally employed to verify a posteriori the validity of the paraxial approximation.

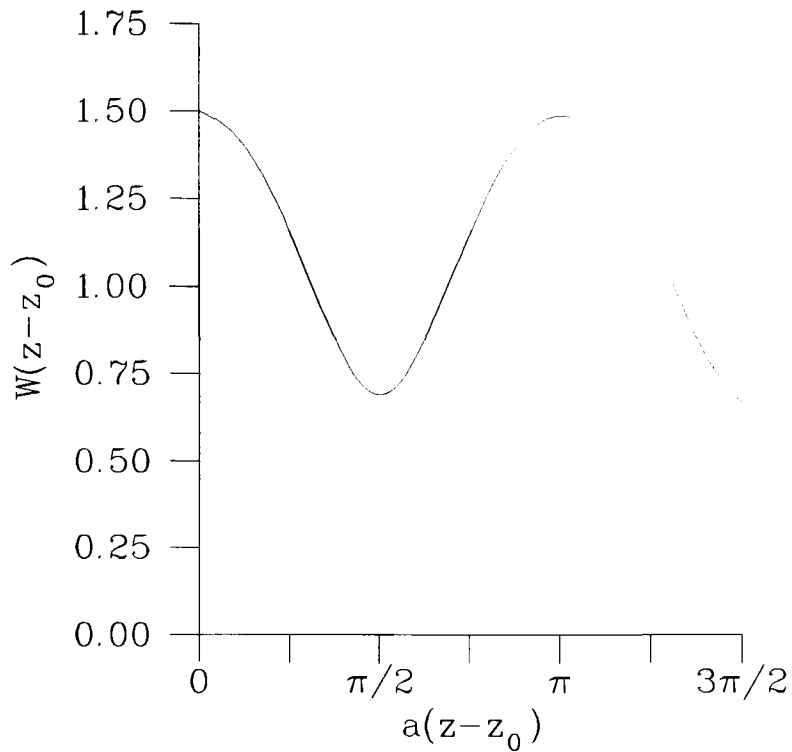


Figure 3.1: The variation of the beam waist (in units of $\sqrt{2/\kappa a}$) of a Gaussian beam with propagation distance in a parabolic refractive index guide.

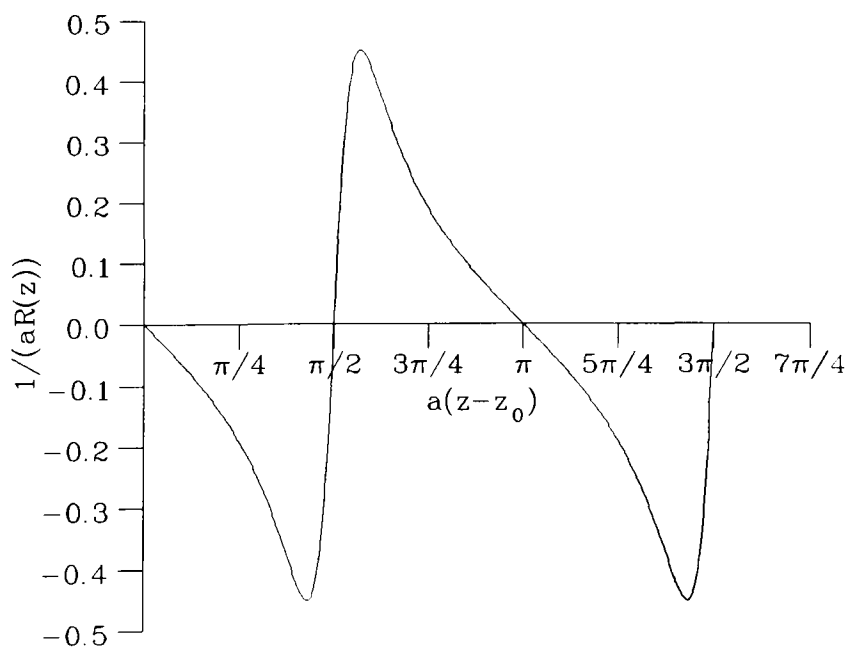


Figure 3.2: The variation of the phasefront curvature (in units of a) of a Gaussian beam with propagation distance in a parabolic refractive index guide.

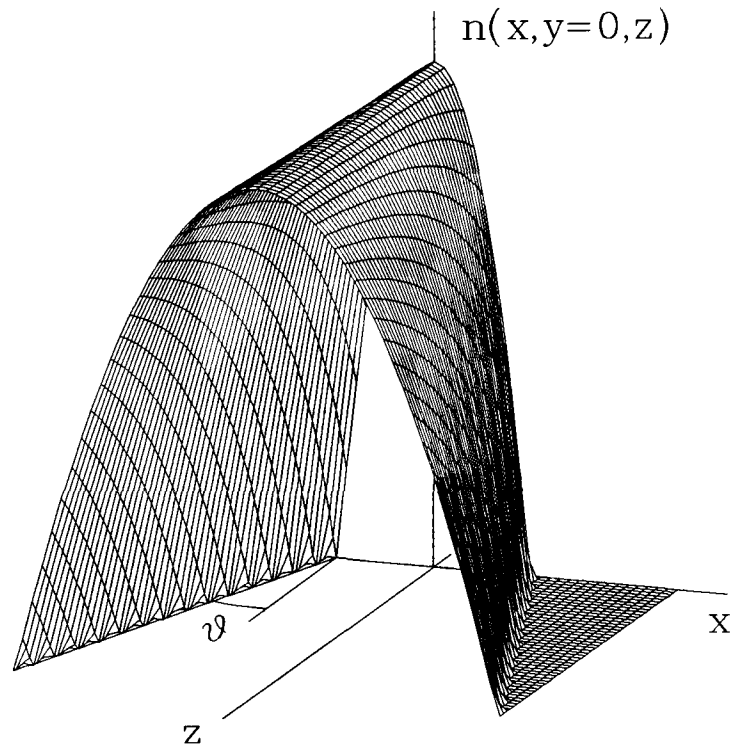


Figure 3.3: The refractive index distribution of a linearly tapering parabolic refractive index waveguide in the xz plane.

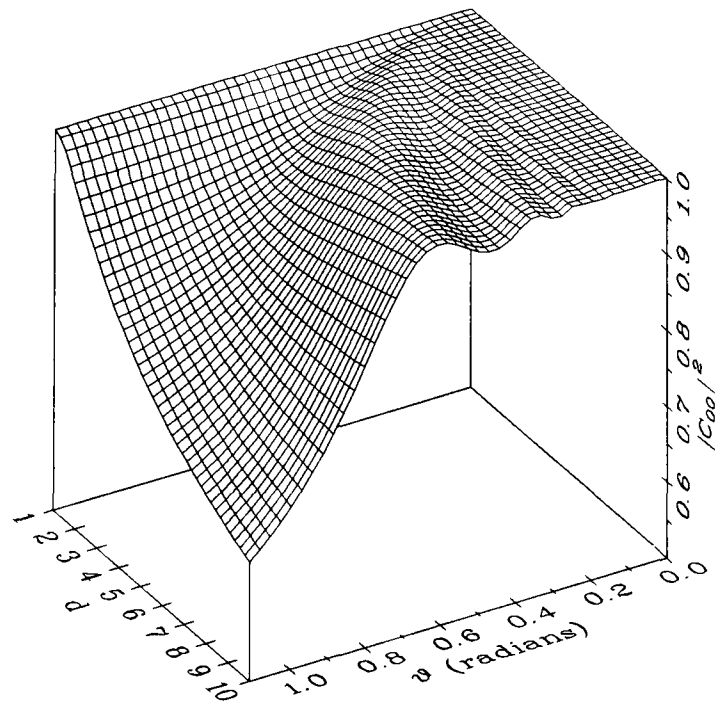


Figure 3.4: The lowest-order-mode to lowest-order-mode power coupling efficiency graph for a linear taper, plotted against θ and $d = z/z_0$.

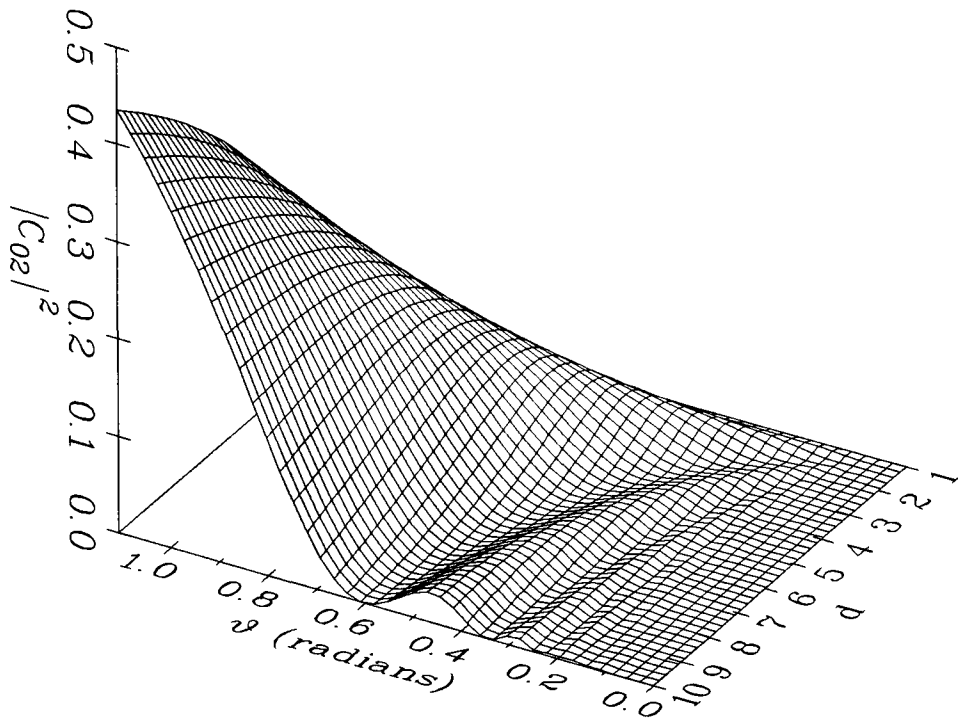


Figure 3.5: The lowest-order-mode to second-excited-mode power coupling efficiency graph for a linear taper, plotted against θ and $d \equiv z/z_0$.

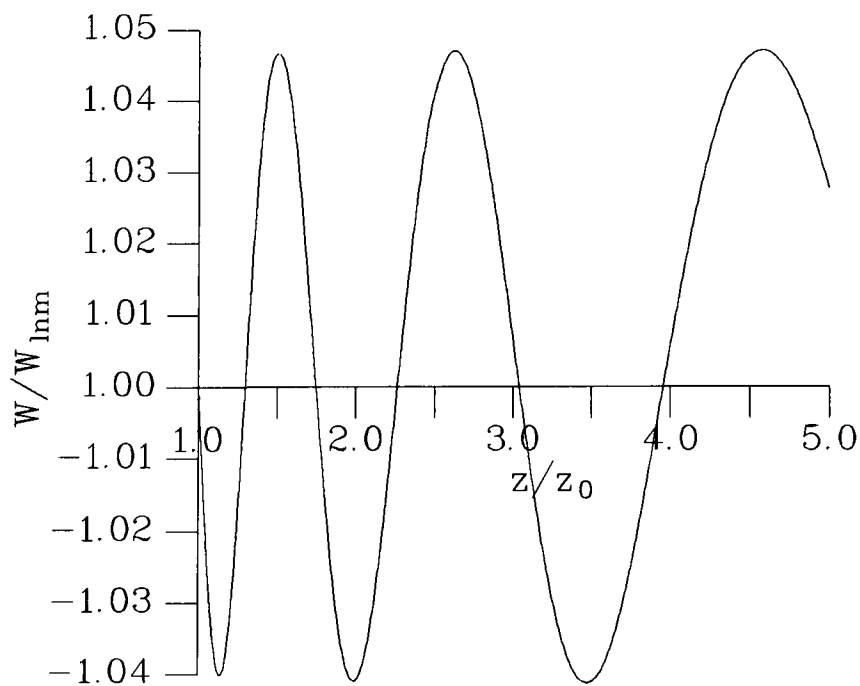


Figure 3.6: The ratio of the beam waist of the total field propagating in a linear taper, to the beam waist of the corresponding lowest-order local-normal-mode, plotted against the taper parameter $d \equiv z/z_0$.

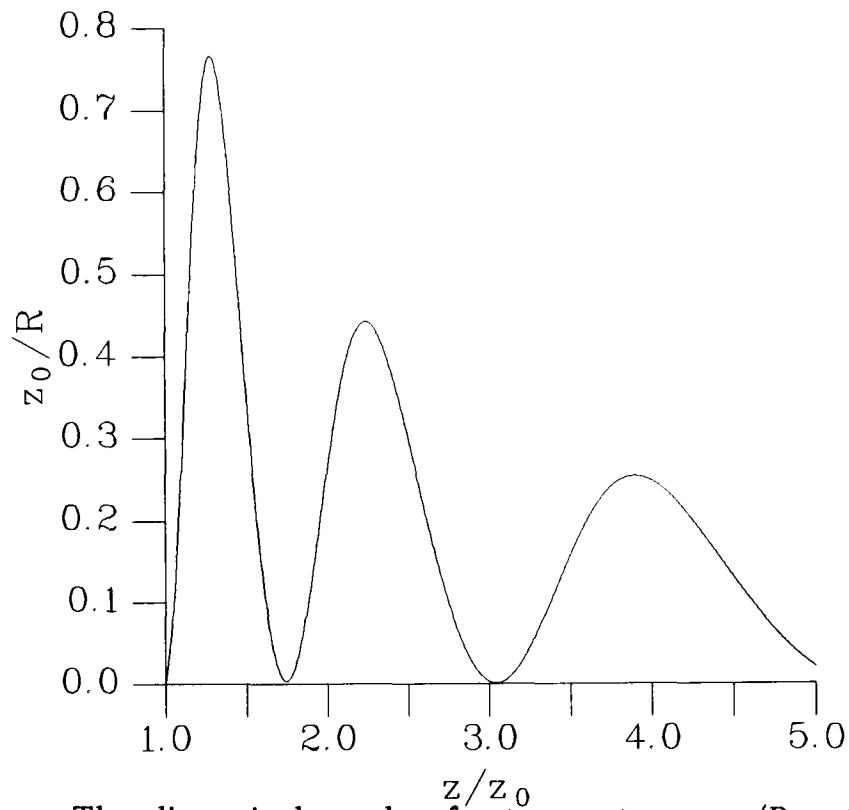


Figure 3.7:

The dimensionless phasefront curvature z_0/R of the total field propagating in a linear taper, plotted against the taper parameter $d \equiv z/z_0$.

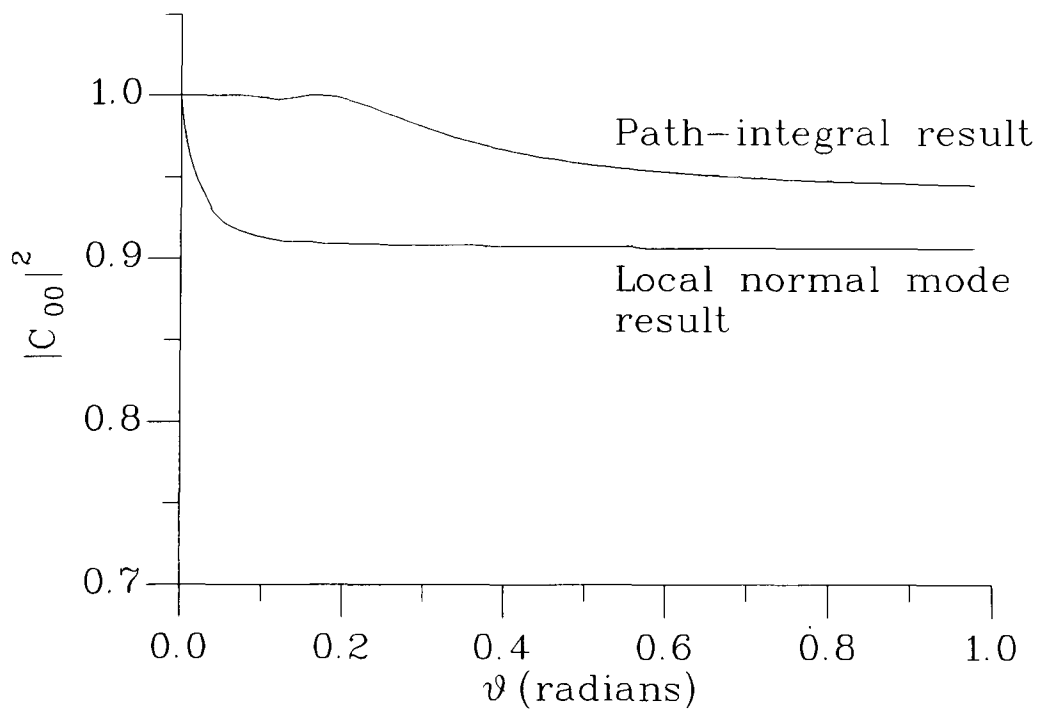


Figure 3.8:

A comparison of the power coupling efficiency prediction of equation (3.62) and the local normal mode analysis of Marcuse (1970).

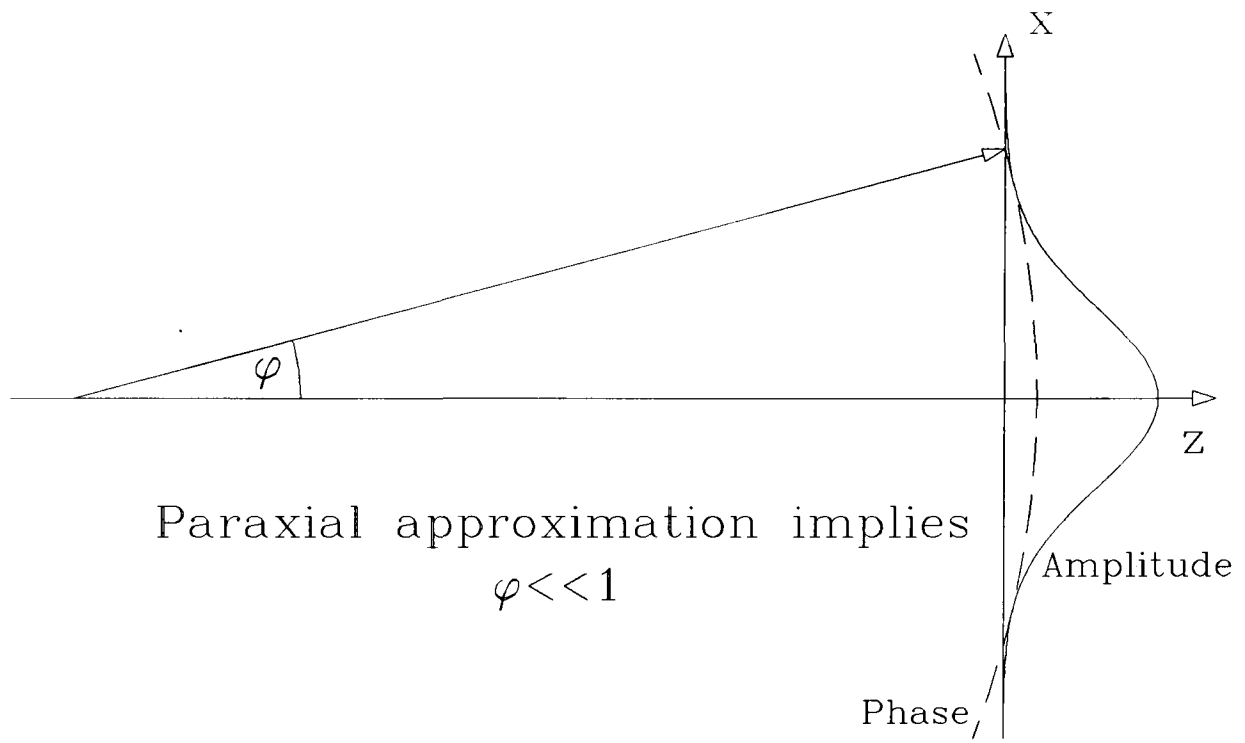


Figure 3.9: The smallness of the value of the angle φ is a measure of the validity of the paraxial approximation.

Chapter 4

Waveguides II: parabolic–refractive–index waveguide tapers of different geometries.

4.1 The symmetric, arbitrarily tapering parabolic–refractive–index waveguide.

The second half of chapter 3 was devoted to the detailed study of the linearly tapering parabolic–refractive–index waveguide, which was modeled by the refractive index distribution,

$$n(x, y, z) = n_0 \left(1 - \frac{1}{2} c^2(z) x^2 - \frac{1}{2} b^2 y^2 \right), \quad (4.1)$$

with

$$c(z) = \frac{1}{z \tan \theta}. \quad (4.2)$$

We now wish to study tapered waveguides of more general geometries, as these occur in waveguide junctions, and more importantly in waveguide sections which interconnect waveguides of different cross-sectional areas and/or shapes. In an integrated optical circuit we ideally want to squeeze as many optical components as possible onto a substrate of any given size, and one way of achieving this, is by minimising the length of all interconnections. It is well known (Tamir, 1990) that if a parabolic horn waveguide is used as a high–coupling–efficiency connector between any two given waveguide sections, it will have a shorter length than the corresponding high–efficiency linearly–tapering waveguide, and it is therefore advantageous to study its coupling properties in detail.

As was explained in chapter 3, the refractive index contour $n(x, 0, z) = n_0/2$ in the xz plane is described by the equation

$$x(z) = \pm 1/c(z), \quad (4.3)$$

and we use this equation to describe the geometry of the arbitrary, symmetrically tapered waveguide (see figure 4.1). Special cases of engineering interest which we will study later

in this chapter, include the parabolic taper, the inverse square law taper, and the exponential taper, described by the equations $x(z) = \pm\sqrt{z/c}$, $x(z) = 1/(c\sqrt{cz})$, and $x(z) = \exp(-cz)/g$, respectively, where c and g are constants.

As the problem is separable in the x and y coordinates, we may consider the partial propagator,

$$K(x, z; x_0, z_0) = \int \delta x(z) \exp\left\{ ik/2 \int_{z_0}^z d\zeta \left[\dot{x}^2(\zeta) - c^2(\zeta)x^2(\zeta) \right] \right\}, \quad (4.4)$$

without loss of generality. In appendix A it was shown that the path integral (4.4) can be evaluated in closed form, by virtue of the fact that it is quadratic in the path variable, $x(\zeta)$; evaluation of this integral gives,

$$K(x, z; x_0, z_0) = \left[\frac{k}{2\pi i} \right]^{1/2} \left[\frac{1}{f(z, z_0)} \right]^{1/2} \exp\left\{ ik/2 \int_{z_0}^z d\zeta \left[\dot{X}^2(\zeta) - c^2(\zeta)X^2(\zeta) \right] \right\}, \quad (4.5)$$

where $X(\zeta)$ is the path of the ray described by geometrical optics, and passing through the two points (x_0, z_0) and (x, z) . We have also seen in (3.46) and (3.47) that $X(\zeta)$ is the solution to the differential equation,

$$\frac{d^2 X(\zeta)}{d\zeta^2} + c^2(\zeta)X(\zeta) = 0, \quad (4.6a)$$

with boundary conditions,

$$X(z_0) = x_0 \quad \text{and} \quad X(z) = x. \quad (4.6b)$$

The function $f(z, z_0)$ obeys the same differential equation as $X(\zeta)$ in its z variable,

$$\frac{\partial^2 f(z, z_0)}{\partial z^2} + c^2(z)f(z, z_0) = 0, \quad (4.7a)$$

with boundary conditions,

$$f(z=z_0, z_0) = 0 \quad \text{and} \quad \left. \frac{\partial f(z, z_0)}{\partial z} \right|_{z=z_0} = 1. \quad (4.7b)$$

Since both the geometrical optics ray path $X(\zeta)$ and the function $f(z, z_0)$ are solutions of the same differential equation, both can be expressed as linear combinations of the two linearly independent solutions of

$$\frac{d^2 \Xi(\zeta)}{d\zeta^2} + c^2(\zeta)\Xi(\zeta) = 0, \quad (4.8)$$

which we will call $\Xi_1(\zeta)$ and $\Xi_2(\zeta)$. Fitting the boundary conditions (4.6b) and (4.7b),

results in

$$X(\zeta) = \frac{(\Xi_1(\zeta)\Xi_2(z_0) - \Xi_1(z_0)\Xi_2(\zeta))x + (\Xi_1(z)\Xi_2(\zeta) - \Xi_1(\zeta)\Xi_2(z))x_0}{\Xi_1(z)\Xi_2(z_0) - \Xi_1(z_0)\Xi_2(\zeta)} \quad (4.9)$$

and

$$f(z, z_0) = \frac{\Xi_1(z)\Xi_2(z_0) - \Xi_1(z_0)\Xi_2(z)}{\Xi_1(z_0)\Xi_2(z_0) - \Xi_1(z_0)\Xi_2(z_0)}. \quad (4.10)$$

As a consequence, we may express $X(\zeta)$ in terms of $f(z, z_0)$, as

$$X(\zeta) = \frac{x f(\zeta, z_0) + x_0 f(z, \zeta)}{f(z, z_0)}. \quad (4.11)$$

It should be noted that the denominator in the expression (4.10) for $f(z, z_0)$ is the negative of the Wronskian of $\Xi_1(\zeta)$ and $\Xi_2(\zeta)$. By virtue of the fact that the differential equation (4.8) has no first derivative term in it, the Wronskian

$$W\{\Xi_1(\zeta), \Xi_2(\zeta)\} \equiv \frac{d\Xi_1(\zeta)}{d\zeta} \Xi_2(\zeta) - \Xi_1(\zeta) \frac{d\Xi_2(\zeta)}{d\zeta}, \quad (4.12)$$

is independent of ζ (Morse and Feshbach, 1953). Making use of this fact it is easy to show that

$$W\{f(z, \zeta), f(\zeta, z_0)\} = f(z, z_0). \quad (4.13)$$

A very important symmetry property of $f(z, z_0)$ which follows directly from (4.10) is,

$$f(z, z_0) = -f(z_0, z). \quad (4.14)$$

Furthermore, if we define

$$F(z, z_0) \equiv \frac{\partial f(z, z_0)}{\partial z}, \quad (4.15)$$

equation (4.10) further implies that,

$$\frac{\partial f(z, z_0)}{\partial z_0} = -F(z_0, z). \quad (4.16)$$

Finally, the function $f(z, z_0)$ also obeys the differential equation,

$$\frac{\partial^2 f(z, z_0)}{\partial z_0^2} + c^2(z_0)f(z, z_0) = 0, \quad (4.17a)$$

with boundary conditions

$$f(z, z_0=z) = 0 \quad \& \quad \left. \frac{\partial f(z, z_0)}{\partial z_0} \right|_{z_0=z} = -1. \quad (4.17b)$$

We are now in a position to evaluate the integral in the exponent of the propagator expression (4.5) in a closed form. The integral is simply the optical path length of the ray of light described by geometrical optics.

Let
$$I = \int_{z_0}^z d\zeta [\dot{X}^2(\zeta) - c^2(\zeta)X^2(\zeta)] \quad (4.18)$$

Using equation (4.6a), we have,

$$-c^2(\zeta)X(\zeta) = \frac{d^2X(\zeta)}{d\zeta^2}. \quad (4.19)$$

If we use equation (4.19), the optical path length expression (4.18) becomes,

$$I = \int_{z_0}^z d\zeta \left\{ \left[\frac{dX(\zeta)}{d\zeta} \right]^2 + X(\zeta) \frac{d^2X(\zeta)}{d\zeta^2} \right\}. \quad (4.20)$$

Integrating (4.20) once by parts, shows that,

$$I = \left[\frac{dX(\zeta)}{d\zeta} X(\zeta) \right]_{\zeta=z_0}^{\zeta=z}, \quad (4.21)$$

which, on using the boundary conditions (4.6b), simplifies to,

$$I = \frac{dX(z)}{dz} x - \frac{dX(z_0)}{dz_0} x_0. \quad (4.22)$$

Substituting for $X(z)$ in terms of (4.11), we find that,

$$I = x \left\{ \frac{x \frac{\partial f(\zeta, z_0)}{\partial \zeta} + x_0 \frac{\partial f(z, \zeta)}{\partial \zeta}}{f(z, z_0)} \right\}_{\zeta=z} - x_0 \left\{ \frac{x \frac{\partial f(\zeta, z_0)}{\partial \zeta} + x_0 \frac{\partial f(z, \zeta)}{\partial \zeta}}{f(z, z_0)} \right\}_{\zeta=z_0}. \quad (4.23)$$

Using the boundary conditions (4.7b), (4.17b) and the symmetry property (4.14), the above result simplifies to,

$$I = x^2 \frac{\partial}{\partial z} \left[\ln f(z, z_0) \right] - x_0^2 \frac{\partial}{\partial z_0} \left[\ln f(z, z_0) \right] - \frac{2xx_0}{f(z, z_0)}. \quad (4.24)$$

The propagator (4.5) can therefore be expressed as,

$$K(x, z; x_0, z_0) = \left[\frac{k}{2\pi i} \right]^{1/2} \left[\frac{1}{f(z, z_0)} \right]^{1/2} \exp \left\{ ik/2 \left(x^2 \frac{\partial (\ln f(z, z_0))}{\partial z} - x_0^2 \frac{\partial (\ln f(z, z_0))}{\partial z_0} - \frac{2xx_0}{f(z, z_0)} \right) \right\}. \quad (4.25)$$

Equations (4.7) and (4.25) completely describe the paraxial wave propagator in an arbitrary, symmetrical, parabolic–refractive–index waveguide, whose geometry is defined by equation (4.3).

4.2 The coupling efficiency of an arbitrary, symmetrical, parabolic-refractive-index taper.

In section 3.4 of chapter 3, we considered the coupling efficiency of the linearly tapering parabolic-refractive-index waveguide which was connected to two matched, uniform, semi-infinite parabolic-refractive-index waveguides. The refractive index distributions which describe the two waveguides which we have defined as the input and output waveguides to the taper, are chosen to be,

$$n_{\text{in}}(x_0) = n_0 \left(1 - \frac{1}{2} a_0^2 x_0^2 \right) \quad \text{for } \zeta \leq z_0, \quad (4.26a)$$

$$n_{\text{out}}(x) = n_0 \left(1 - \frac{1}{2} a^2 x^2 \right) \quad \text{for } \zeta \geq z, \quad (4.26b)$$

respectively. In order to match the refractive index distribution of the input guide to that of the taper at a station $\zeta = z_0$, we must choose,

$$a_0 = c(z_0). \quad (4.26c)$$

Likewise, in order to match the refractive index distribution of the output waveguide at $\zeta = z$, we must choose,

$$a = c(z). \quad (4.26d)$$

Equations (4.26) hold for the arbitrary, symmetrical, parabolic-refractive-index taper, as well as for the linear taper. The modes of the input and output waveguides were derived in section 3.1 of chapter 3, and were shown to be the normalised Gauss-Hermite polynomials (Feynman and Hibbs, 1965). The modes of the input waveguide, $\psi_n(x_0)$, are given by,

$$\psi_n(x_0) = \frac{1}{2^{n/2} (n!)^{1/2}} \left[\frac{ka_0}{\pi} \right]^{1/4} H_n(\sqrt{ka_0} x_0) \exp\left\{ -\frac{ka_0 x_0^2}{2} \right\}, \quad (4.27a)$$

where

$$H_n(\xi) \equiv \sum_{q=0}^{\leq n/2} \frac{(-1)^q n!}{q! (n-2q)!} (2\xi)^{n-2q}, \quad (4.27b)$$

is the Hermite polynomial of order n (Abramowitz and Stegun, 1965, equation 22.3.10).

The modes of the output waveguide, $\varphi_m(x)$, are also given by (4.27), with m , x and a replacing n , x_0 and a_0 respectively. The expression for the amplitude coupling coefficient (3.61), can then be used in conjunction with the taper propagator (4.25) and the uniform waveguide modal field amplitude (4.27), to determine the coupling efficiency between any two input and output mode combinations. Since the explicit calculation is fairly lengthy, we present it in appendix B. The final result for the amplitude coupling coefficient is,

$$C_{mn} = \left[\frac{\sqrt{aa_0}}{2if} \right]^{1/2} \left[\left(\frac{a_0}{2} + \frac{i}{2} \frac{\partial \ln f}{\partial z_0} \right) \left(\frac{a}{2} - \frac{i}{2} \frac{\partial \ln f}{\partial z} \right) - \frac{1}{4f^2} \right]^{-1/2} \times$$

$$\frac{\sqrt{(n!m!)}}{2^n 2^{m/2}} \sum_{p=0}^{\leq n/2} \sum_{q=0}^{\leq m/2} \sum_{r=0}^{\leq (n-2p)/2} \frac{(n+m-2p-2q-2r)!}{p!q!r!(m-2q)!(n-2p-2r)!(n/2-m/2-p-q-r)!} \times$$

$$\frac{\left[\frac{1}{\frac{1}{4} + \frac{i}{4a_0} \frac{\partial \ln f}{\partial z_0}} - 1 \right]^p \left[\frac{1}{if \sqrt{a - i \frac{\partial \ln f}{\partial z}}} \right]^{n-2p-2r} \left[\frac{a^2}{2} - \frac{i}{2} a \frac{\partial \ln f}{\partial z} \right]^{m/2-q}}{\left[\left(\frac{a_0}{2} + \frac{i}{2} \frac{\partial \ln f}{\partial z_0} \right) \left(\frac{a}{2} - \frac{i}{2} \frac{\partial \ln f}{\partial z} \right) - \frac{1}{4f^2} \right]^{n/2+m/2-p-q-r}}$$

for $m+n$ even, (4.28a)

and

$$C_{mn} = 0 \quad \text{for } m+n \text{ odd. (4.28b)}$$

We have used $f \equiv f(z, z_0)$ in (4.28) for compactness. Equation (4.28) proves the statement made in chapter 3, that the even and odd modes of a symmetrical waveguide structure cannot couple to each other. In the special case $m = n = 0$, the amplitude coupling coefficient is given by,

$$C_{00} = \sqrt{2} \left\{ \left\{ \sqrt{\frac{c(z_0)}{c(z)}} \frac{\partial f}{\partial z} - \sqrt{\frac{c(z)}{c(z_0)}} \frac{\partial f}{\partial z_0} \right\} + i \left\{ \sqrt{c(z_0)c(z)} f + \frac{\left[1 + \frac{\partial f}{\partial z_0} \frac{\partial f}{\partial z} \right]}{\sqrt{c(z_0)c(z)} f} \right\} \right\}^{-1/2},$$

(4.29)

where we have made use of equations (4.26) to eliminate the parameters a_0 and a . The lowest-order-mode to lowest-order-mode coupling efficiency is then given by,

$$|C_{00}|^2 = \left\{ \frac{1}{2} + \frac{1}{4} \left[c(z_0)c(z)f^2(z, z_0) + \frac{c(z)}{c(z_0)} \left[\frac{\partial f(z, z_0)}{\partial z_0} \right]^2 + \frac{c(z_0)}{c(z)} \left[\frac{\partial f(z, z_0)}{\partial z} \right]^2 + \left\{ 1 + \frac{\partial f(z, z_0)}{\partial z_0} \frac{\partial f(z, z_0)}{\partial z} \right\}^2 / [c(z_0)c(z)f^2(z, z_0)] \right] \right\}^{-1/2}.$$

(4.30)

Equations (4.28) and (4.30) are new powerful results and (within the paraxial approximation) give an exact expression for the coupling efficiency of an arbitrary, symmetrical, multimode waveguide taper whose refractive index distribution is described by (4.1). These new and exact results have only been made available to us through the path integral analysis. They can easily be used in the optimum design of integrated optical tapered waveguides. Their usefulness becomes even more apparent when we show in section 4.4 that there exist a large number of practically useful taper geometries for which there are closed form solutions to (4.7). Finally, we must point out once again, that the wavenumber k does not appear explicitly in equations (4.28) to (4.30) just as it did not appear in equations (3.62) to (3.64) in chapter 3. The reason for this, is that we have been considering waveguides with an infinite transverse parabolic refractive index profile, which does not possess a finite mode cut-off. As a consequence, all of the above results are strictly applicable to multimode waveguides only.

4.3 The total field propagation in an arbitrary, symmetric, parabolic-refractive-index taper.

When we excite the taper with the lowest order mode of the matched input waveguide, given by (4.27) with $n=0$, the total field amplitude $\psi(x,z;z_0)$ in the tapered waveguide can be found using the propagation rule (3.60) together with the explicit form (4.25) for the propagator.

$$\psi(x,z;z_0) = \int_{-\infty}^{+\infty} dx_0 \left[\frac{ka_0}{\pi} \right]^{1/4} \exp\left\{ -\frac{ka_0 x_0^2}{2} \right\} \left[\frac{k}{2\pi i} \right]^{1/2} \left[\frac{1}{f(z,z_0)} \right]^{1/2} \times \\ \exp\left\{ ik/2 \left(x^2 \frac{\partial(\ln f(z,z_0))}{\partial z} - x_0^2 \frac{\partial(\ln f(z,z_0))}{\partial z_0} - \frac{2xx_0}{f(z,z_0)} \right) \right\}. \quad (4.31)$$

The above integral can be evaluated using (2.51), to give,

$$\psi(x, z; z_0) = \left[\frac{ka_0}{\pi f^2 (a_0^2 + (\partial(\ln f)/\partial z_0)^2)} \right]^{1/4} \exp \left\{ ik(z-z_0) - \frac{i}{2} \arctan \left[\frac{a_0}{\partial(\ln f)/\partial z_0} \right] \right\} \times \\ \exp \left\{ - \frac{ka_0 x^2}{2f^2 (a_0^2 + (\partial(\ln f)/\partial z_0)^2)} + \frac{ikx^2}{2} \frac{\partial(\ln f)/\partial z_0 + \partial(\ln f)/\partial z (a_0^2 f^2 + (\partial f/\partial z_0)^2)}{(a_0^2 f^2 + (\partial f/\partial z_0)^2)} \right\}, \quad (4.32)$$

where we have abbreviated $f(z, z_0)$ to f . The above expression can be directly compared with the corresponding expression for the standard Gaussian beam (2.59), in order to find an expression for the beam waist, $w(z)$, and phasefront radius of curvature, $R(z)$, of the total field in the taper. Comparison shows that,

$$w(z) = \sqrt{\frac{2}{ka_0}} \sqrt{a_0^2 f^2 + \left[\frac{\partial f}{\partial z_0} \right]^2}, \quad (4.33)$$

$$R(z) = \frac{a_0^2 f^2 + \left[\frac{\partial f}{\partial z_0} \right]^2}{\frac{\partial(\ln f)}{\partial z_0} + \frac{\partial(\ln f)}{\partial z} \left[a_0^2 f^2 + \left[\frac{\partial f}{\partial z_0} \right]^2 \right]}. \quad (4.34)$$

Equations (4.32) to (4.34) completely describe the propagation of a centred Gaussian beam which has originated from the lowest order mode of the matched input waveguide in a symmetric, arbitrarily tapered waveguide with a parabolic refractive index distribution. All of the above results are exact within the paraxial approximation and are, to the best of our knowledge, new. The total field for higher order mode excitations can also be easily found, if we use the corresponding higher order mode fields (with $n \geq 1$) in (4.31).

4.4 Geometries for which the taper function $f(z, z_0)$ can be obtained in closed form.

The propagator of a symmetric, parabolic–refractive–index waveguide taper of an arbitrary geometry, can be found in general by using geometrical considerations to specify z_0 and z , and solving equation (4.7a) numerically to obtain $f(z, z_0)$, $\frac{\partial f(z, z_0)}{\partial z}$ and $\frac{\partial f(z, z_0)}{\partial z_0}$. Note that the latter two quantities are not independent, but are related through equation (4.16). Such an approach does not give us the full benefits of the insight that can

be gained by using the technique of path integration in the study of graded-index tapered waveguides. By restricting ourselves to three very broad categories of taper geometries, we can obtain the tapered waveguide propagator in an exact closed form. This is possible because the tapered waveguide geometries which we will shortly consider, are such that we can solve the differential equation (4.7) in closed form.

The first geometry of interest is that of the linearly tapering waveguide, which has been considered in detail in sections 3.3 to 3.5 of chapter 3. In this case the function $c(z)$ is given by equation (4.2) and the taper function $f(z, z_0)$ was found in chapter 3 to be given by (3.56) and (3.53). These results are summarised below:

$$c(z) = \frac{1}{z \tan \theta}, \quad (4.35a)$$

and

$$f(z, z_0) = \frac{\sqrt{zz_0}}{q} \sin[q \ln(z/z_0)], \quad (4.35b)$$

where

$$q \equiv \frac{\sqrt{4 - \tan^2 \theta}}{2 \tan \theta}. \quad (4.35c)$$

The next important class of geometries is that for which the function $c(z)$ is a simple power law function in z ,

$$c(z) = \kappa z^\alpha. \quad (4.36)$$

This function describes a taper whose geometry is given by

$$x(z) = \pm \frac{1}{\kappa} z^{-\alpha} \quad (4.37)$$

The linear taper is a special case of this taper when $\alpha = -1$ and $\kappa = 1/\tan \theta$. The cases $\alpha = \frac{1}{2}$ and $\alpha = 0$ result in solutions to (4.7) which are either Airy or trigonometric functions of z respectively (Abramowitz and Stegun, 1965, section 10.4). Since both the Airy and the trigonometric functions can be expressed in terms of Bessel functions of the first and second kind (Abramowitz and Stegun, 1965, equations 10.1.11 and 10.4.14–21), we attempt to find solutions of (4.7) using the ansatz

$$y(z) = z^\beta H_{\pm m}^\delta(\gamma z^\delta), \quad (4.38)$$

where $H_{\pm m}(\eta)$ satisfies Bessel's equation of order m . It can be readily seen that (4.38) satisfies

$$z^2 \frac{d^2 y}{dz^2} + (1 - 2\beta) z \frac{dy}{dz} + (\beta^2 - m^2 \delta^2 + \gamma^2 \delta^2 z^{2\delta}) y = 0, \quad (4.39)$$

which reduces to equation (4.7) when $\beta = \frac{1}{2}$, $\alpha = \delta - 1$, $\kappa = \gamma\delta$ and $m = \pm \frac{\beta}{\delta}$. Therefore, when $|m| = \frac{1}{2(1+\alpha)}$ is not an integer, the general solutions of (4.39) are linear combinations of the linearly independent solutions,

$$y(z) = \sqrt{z} J_{1/(2+2\alpha)} \left[\frac{\kappa}{1+\alpha} z^{(1+\alpha)} \right] \quad \text{and} \quad \sqrt{z} J_{-1/(2+2\alpha)} \left[\frac{\kappa}{1+\alpha} z^{(1+\alpha)} \right]. \quad (4.40)$$

When $|m| = \frac{1}{2(1+\alpha)}$ is an integer, we must now choose the linearly independent solutions,

$$y(z) = \sqrt{z} J_{1/(2+2\alpha)} \left[\frac{\kappa}{1+\alpha} z^{(1+\alpha)} \right] \quad \text{and} \quad \sqrt{z} Y_{1/(2+2\alpha)} \left[\frac{\kappa}{1+\alpha} z^{(1+\alpha)} \right]. \quad (4.41)$$

It is useful to note that in the case of the linearly tapering waveguide, when $\alpha = -1$, the above ansatz fails and cannot be used at all. Using equation (4.10) together with the expressions for the Wronskian of the Bessel functions of the first and second kind (Abramowitz and Stegun, 1965, equation 9.1.15) we find that the taper function $f(z, z_0)$ for non-integer $\frac{1}{2(1+\alpha)}$ is given by

$$f(z, z_0) = \frac{\pi \sqrt{z z_0}}{2(1+\alpha) \sin \left[\frac{\pi}{2(1+\alpha)} \right]} \left\{ J_{1/(2+2\alpha)} \left[\frac{\kappa}{1+\alpha} z^{(1+\alpha)} \right] J_{-1/(2+2\alpha)} \left[\frac{\kappa}{1+\alpha} z_0^{(1+\alpha)} \right] - J_{-1/(2+2\alpha)} \left[\frac{\kappa}{1+\alpha} z^{(1+\alpha)} \right] J_{1/(2+2\alpha)} \left[\frac{\kappa}{1+\alpha} z_0^{(1+\alpha)} \right] \right\}. \quad (4.42a)$$

In the case of integer $\frac{1}{2(1+\alpha)}$ the taper function $f(z, z_0)$ is given by,

$$f(z, z_0) = -\frac{\pi \sqrt{z z_0}}{2(1+\alpha)} \left\{ J_{1/(2+2\alpha)} \left[\frac{\kappa}{1+\alpha} z^{(1+\alpha)} \right] Y_{1/(2+2\alpha)} \left[\frac{\kappa}{1+\alpha} z_0^{(1+\alpha)} \right] - Y_{1/(2+2\alpha)} \left[\frac{\kappa}{1+\alpha} z^{(1+\alpha)} \right] J_{1/(2+2\alpha)} \left[\frac{\kappa}{1+\alpha} z_0^{(1+\alpha)} \right] \right\}. \quad (4.42b)$$

Equations (4.36), (4.37) and (4.42), together with the general propagator (4.25) completely describe propagation in a wide and rather general class of tapered, graded-index waveguides. This result is new and its importance cannot be over-emphasised.

One further tapered waveguide geometry which we will study using a slightly

adapted form of the above ansatz is the exponential taper. For the sake of clarity, we will postpone discussing this until section 4.6 of this chapter.

Finally, we will briefly mention one more refractive index model which is of interest to integrated optics. This is a waveguide whose walls, or equivalently its contours of constant refractive index, are undulating sinusoidally, as shown in figure 4.2. The refractive index model is,

$$n(x,z) = n_0 \left(1 - \frac{1}{2} c^2 [1 + d^2 \sin^2(\kappa z)] x^2 \right). \quad (4.43)$$

The corresponding differential equation yielding the taper function $f(z, z_0)$ is then,

$$\frac{\partial^2 f(z, z_0)}{\partial z^2} + c^2 [1 + d^2 \sin^2(\kappa z)] f(z, z_0) = 0. \quad (4.44)$$

Using the transformations,

$$u \equiv \kappa z, \quad (4.45a)$$

$$a = \frac{c^2}{\kappa^2} \left[1 + \frac{d^2}{2} \right], \quad (4.45b)$$

and

$$q = \frac{c^2 d^2}{4 \kappa^2}, \quad (4.45c)$$

this can be shown to be equivalent to Mathieu's differential equation (Abramowitz and Stegun, 1965, equation 20.1.1) in the form,

$$\frac{\partial^2 f}{\partial u^2} + [a - 2q \cos(2u)] f = 0. \quad (4.45d)$$

As a consequence, the taper function $f(z, z_0)$ can be expressed in terms of Mathieu functions. Unfortunately, the propagator which results from this analysis turns out not to be useful in the study of electromagnetic wave propagation in the waveguide of interest, for two reasons. The first reason is that the length $2\pi/\kappa$, which describes the periodicity in the waveguide 'wall' undulations, is approximately equal to the wavelength of the light confined by the waveguide, for practical devices such as the distributed feedback waveguide—reflector (Lee, 1986). This is in direct contradiction with the basic assumption, made during the formulation of the propagation problem, that the dielectric constant changes by a negligible amount over displacements of one wavelength (c.f. equation (1.6) in chapter 1). The second way in which this analysis fails, is that the path integral approach to the propagation problem only takes into account forward moving rays and hence waves

(c.f. sections 2.1 to 2.4 in chapter 2). The study of the distributed feedback waveguide must, by the very nature of its operation mechanism, take into consideration reflected, as well as forward moving waves. This can be accomplished in principle, if we were to consider the coupling between the forward and backward wave motion propagators (c.f. equation (2.26) and accompanying comment for the explicit form of the backward wave propagator). Such a task is beyond the scope of this thesis, and should form the basis for further work on this subject. We have discussed this latter waveguide model in order to illustrate the limitations of our method of analysis, and the fact that care should be exercised not to attempt to study waveguide structures which are incompatible with the assumptions made in the formulation of our method.

4.5 The parabolic and inverse-square-law parabolic-refractive-index waveguides.

We now proceed to study a number of specific taper geometries of engineering interest. These include the parabolic and inverse-square-law tapers, as well as the exponential taper which is considered in section 4.6.

The constant refractive index contour $n(x,0,z) = n_0/2$ of a graded-index waveguide with a parabolic geometry is shown in figure 4.3. The corresponding function $c(z)$ is given by,

$$c(z) = \sqrt{c/z}, \quad (4.46)$$

and the constant refractive index contour $n(x,0,z) = n_0/2$ geometry is described by,

$$x(z) = \pm \sqrt{z/c}, \quad (4.47)$$

which is the equation of a parabola. Note that the constant c characterising the parabola has dimensions of inverse length. The corresponding taper function $f(z,z_0)$ is then given by (4.42b) with $a = -\frac{1}{2}$ and $\kappa = \sqrt{c}$, and is restricted to $z > z_0 > 0$.

$$f(z,z_0) = \pi\sqrt{zz_0} \left[Y_1(2\sqrt{cz}) J_1(2\sqrt{cz_0}) - J_1(2\sqrt{cz}) Y_1(2\sqrt{cz_0}) \right]. \quad (4.48)$$

Equations (4.25) and (4.48) then completely specify the propagator of the parabolic taper. We are now in a position to study the coupling mechanism and the propagation of a Gaussian beam in a parabolic taper in some detail. For the sake of brevity, we choose not to examine all of the above quantities in detail, but concentrate on the one which is often of great practical importance in the engineering design of such a taper – its lowest order mode coupling efficiency (Tamir, 1990). This is given by substituting (4.48) into (4.30) and simplifying the latter to obtain,

$$|C_{00}|^2 = \left[1 + \frac{\pi^2 c}{4} \sqrt{zz_0} \left\{ (p_0 - s_0)^2 + (q_0 \sqrt{z/z_0} + r_0 \sqrt{z_0/z})^2 \right\} \right]^{-1/2}, \quad (4.49)$$

where p_0 , q_0 , r_0 and s_0 are the Bessel function cross-products (Abramowitz and Stegun, 1965, equations 9.1.32), defined by,

$$p_0 = Y_0(2\sqrt{cz}) J_0(2\sqrt{cz_0}) - J_0(2\sqrt{cz}) Y_0(2\sqrt{cz_0}), \quad (4.50a)$$

$$q_0 = -Y_1(2\sqrt{cz}) J_0(2\sqrt{cz_0}) + J_1(2\sqrt{cz}) Y_0(2\sqrt{cz_0}), \quad (4.50b)$$

$$r_0 = -Y_0(2\sqrt{cz}) J_1(2\sqrt{cz_0}) + J_0(2\sqrt{cz}) Y_1(2\sqrt{cz_0}), \quad (4.50c)$$

and
$$s_0 = Y_1(2\sqrt{cz}) J_1(2\sqrt{cz_0}) - J_1(2\sqrt{cz}) Y_1(2\sqrt{cz_0}). \quad (4.50d)$$

It is evident from equations (4.49) and (4.50) that the lowest order mode coupling efficiency $|C_{00}|^2$ always lies in the range $0 \leq |C_{00}|^2 \leq 1$, and is equal to 1 when $z = z_0$. In order to plot $|C_{00}|^2$ in a way which is consistent with the corresponding plot for the linear taper in figure 3.4, we specify two new parameters d and θ . d is the ratio of the width of the matched output waveguide at $\zeta = z$ to the width of the matched input waveguide at $\zeta = z_0$, and is given by $d \equiv \frac{a_0}{a} = \sqrt{\frac{cz}{cz_0}}$. θ is the angle between the tapered waveguide axis (z -axis) and the tangent to the constant refractive index contour $n(x, \theta, z) = n_0/2$ at the input plane $\zeta = z_0$, and is given by $\theta = \arctan\left[\frac{1}{2\sqrt{cz_0}}\right]$. The lowest-order-mode to lowest-order-mode coupling efficiency for the parabolic taper, $|C_{00}|^2$, is plotted against both θ and d in figure 4.4. In figure 4.4, it can be clearly seen that there exists a ridge of high coupling efficiency in the region where $|C_{00}|^2$ has

values roughly between 95% and 100%, for relatively large values of both θ and d . This ridge is fairly wide, implying that the design of a high efficiency parabolic taper is possible, even when manufacturing tolerances are taken into account. For values of θ smaller than those in the vicinity of the above ridge, the coupling efficiency oscillates quite rapidly between 95%–100% and approximately 58%. The ridges of high coupling efficiency in this region are narrow and very closely spaced together, which suggests that the design of parabolic tapers with parameters θ and d in this region should be avoided. The presence of these rapid oscillations can easily be explained in terms of the taper geometry. In order to have a small initial taper angle θ , we have to start the parabolic taper a large distance, z_0 , away from the vertex of the complete parabola at $\zeta = \theta$. If the width ratio d is also appreciably greater than unity, the distance away from the vertex, z , at which we have to terminate the parabolic taper is very much larger than z_0 . In other words, for small θ and large d , the criterion $z \gg z_0 \gg 1/c$ is strictly satisfied. A very small change in θ then corresponds to a very large change in cz . As a result, the Bessel functions in expressions (4.50) and hence the coupling efficiency in (4.49) become highly oscillatory.

A comparison between $|C_{00}|^2$ for the parabolic taper and the corresponding function for the linear taper (shown in figure 3.4), shows the same qualitative behaviour as θ and d vary. The main difference is that for the linear taper the peaks of high coupling efficiency are at exactly 100%, and the adjacent minima have very high values, at approximately 95%, whilst for the parabolic taper the peaks of high coupling efficiency vary progressively from 100% at small values of d to approximately 95% when $d = 10$ and the adjacent minima have very low values of approximately 58%. Furthermore, for the linear taper, the region in which the rapid oscillations occur is confined to much smaller values of θ . As a result, it follows from purely geometrical considerations that a parabolic taper is better than a linear taper if we want to design short single-mode tapers having high coupling efficiencies.

We now turn our attention to the taper which is described by,

$$c(z) = \sqrt{c^3 z}. \quad (4.51)$$

Thus defined, the constant c has the dimensions of inverse length. The contours of constant refractive index $n(x, 0, z) = n_0/2$ are now given by,

$$x(z) = \pm \frac{1}{c \sqrt{cz}}, \quad (4.52)$$

which for $z > z_0 > 0$, describes a hyperbola of higher degree (Rektorys, 1969). As the relation between the dimensionless parameters cz and cx is an inverse square law, we will call this taper the inverse-square-law taper, or ISL taper for short. Its geometry is shown in figure 4.5. The function $f(z, z_0)$ is now given by (4.42a), with $a = 1/2$ and $\kappa = c^{3/2}$. The Bessel functions of order $1/3$ can be expressed in a more compact way as the two linearly independent Airy functions, Ai and Bi (Abramowitz and Stegun, 1965, equations 10.4.22–31). The function $f(z, z_0)$ then simplifies to,

$$f(z, z_0) = \frac{\pi}{c} \left[Ai(-cz)Bi(-cz_0) - Bi(-cz)Ai(-cz_0) \right]. \quad (4.53)$$

Equations (4.25) and (4.53) completely specify the propagator of paraxial, scalar waves in an ISL taper. We are now in a position to examine the lowest order mode coupling efficiency of the ISL taper. Substituting (4.53) into (4.30) and after considerable algebraic manipulation, we find that,

$$|C_{00}|^2 = \left[1 + \frac{\pi^2 c}{4} \sqrt{zz_0} \left\{ (p - s)^2 + (q + r)^2 \right\} \right]^{-1/2}, \quad (4.54)$$

where p , q , r and s are now given by the cross-products,

$$p = Ai(-cz)Bi(-cz_0) - Bi(-cz)Ai(-cz_0), \quad (4.55a)$$

$$q = \left\{ Ai(-cz) \frac{1}{\sqrt{cz_0}} \frac{dBi(u)}{du} - Bi(-cz) \frac{1}{\sqrt{cz_0}} \frac{dAi(u)}{du} \right\}_{u=-cz_0}, \quad (4.55b)$$

$$r = \left\{ \frac{1}{\sqrt{cz}} \frac{dAi(v)}{dv} Bi(-cz_0) - \frac{1}{\sqrt{cz}} \frac{dBi(v)}{dv} Ai(-cz_0) \right\}_{v=-cz}, \quad (4.55c)$$

and

$$s = \left\{ \frac{1}{\sqrt{cz}} \frac{dAi(v)}{dv} \frac{1}{\sqrt{cz_0}} \frac{dBi(u)}{du} - \frac{1}{\sqrt{cz}} \frac{dBi(v)}{dv} \frac{1}{\sqrt{cz_0}} \frac{dAi(u)}{du} \right\}_{v=-cz, u=-cz_0}. \quad (4.55d)$$

It is evident from equations (4.54) and (4.55) that $|C_{00}|^2$ always lies in the range

$0 \leq |C_{00}|^2 \leq 1$, and is equal to 1 when $z = z_0$. The parameters against which we plot $|C_{00}|^2$ in figure 4.6 are the ratio, d , of the width of the input matched waveguide at $\zeta = z_0$ to that of the output matched waveguide at $\zeta = z$, and the angle, θ , between the z -axis and the tangent to the contour $n(x, \theta, \zeta) = n_0/2$ at $\zeta = z$. We choose to reverse the role of the input and output waveguides in the case of the ISL taper, in order to present our results in a way which is consistent with the presentation of the results for the linear and parabolic tapers, where the output waveguide is wider than the input one.

Thus, the two new parameters are now given by, $d = \frac{a}{a_0} = \sqrt{\frac{cz}{cz_0}}$ and $\theta = \arctan\left[\frac{1}{2\sqrt{c^3 z^3}}\right]$.

It can be clearly seen in figure 4.6 that the coupling efficiency never reaches a value of 100%, except in the trivial cases of $\theta = 0$, or $d = 1$. Apart from a small number of very narrow and very shallow ridges at very small θ values, $|C_{00}|^2$ falls with increasing values of both θ and d , to a value of approximately 58% at $d = 10$ and $\theta = 1.1$. The presence of ripples in the value of the coupling efficiency in the small θ region is a phenomenon common to all the graded index tapers we have examined, but these ripples are least pronounced in the case of the ISL taper. It is also clear from the absolute values of the lowest order mode coupling efficiency that the ISL taper is inefficient in its single mode operation when compared to either the linear or the parabolic taper. The lack of either peaks or troughs on the coupling efficiency surface shown in figure 4.6 gives little control over the high efficiency design of such a taper.

Unfortunately, we do not know of any other work in which either the parabolic, or the ISL tapers with parabolic transverse refractive index distributions are studied, either theoretically, numerically, or experimentally, and we are therefore unable to produce a comparison of our results to those of an independent investigator. All of the results presented in this section are entirely new.

4.6 The exponential, parabolic–refractive–index waveguide.

We now proceed to consider one further type of taper geometry of engineering importance, the exponentially tapering waveguide. The refractive index contour $n(x,0,z) = n_0/2$ for this taper is shown in figure 4.7. The corresponding function $c(z)$ is given by,

$$c(z) = h \exp(-cz), \quad (4.56)$$

and the geometry of the tapered waveguide is described by the equation,

$$x(z) = \pm \frac{1}{h} \exp(cz). \quad (4.57)$$

Equation (4.7) is now of the form

$$\frac{d^2y}{dz^2} + h^2 \exp(-2cz) y = 0. \quad (4.58)$$

If we make a change of variable from z to $u \equiv \exp(-cz)$, equation (4.58) transforms to

$$u^2 \frac{d^2y}{du^2} + u \frac{dy}{du} + \left[\frac{h}{c}\right]^2 u^2 y = 0. \quad (4.59)$$

Using the ansatz (4.38) we find $\beta = 0$, $m = 0$, $\gamma = h/c$ and $\delta = 1$, which suggests that the two linearly independent solutions of (4.58) are,

$$y(z) = J_0\left[\frac{h}{c} \exp(-cz)\right] \quad \text{and} \quad Y_0\left[\frac{h}{c} \exp(-cz)\right]. \quad (4.60)$$

From this we find that,

$$f(z, z_0) = \frac{\pi}{2c} \left\{ J_0\left[\frac{h}{c} \exp(-cz)\right] Y_0\left[\frac{h}{c} \exp(-cz_0)\right] - J_0\left[\frac{h}{c} \exp(-cz_0)\right] Y_0\left[\frac{h}{c} \exp(-cz)\right] \right\}. \quad (4.61)$$

Equations (4.25), (4.56), (4.57) and (4.61) completely specify the propagator of a general exponential taper. Closed form expressions describing the propagation of a Gaussian beam in an exponentially tapering parabolic–refractive–index waveguide have been derived by Casperson (1985), and we will refer to them for comparison later in this chapter. Substituting equation (4.61) into equation (4.25), and after carrying out some simplifying algebraic manipulations, the lowest order mode coupling efficiency of the exponential taper is found to be given by,

$$|C_{00}|^2 = \left[1 + \frac{\pi^2 h^2}{16c^2} e^{-c(z+z_0)} \left\{ (p_1 - s_1)^2 + (q_1 + r_1)^2 \right\} \right]^{-1/2}, \quad (4.62)$$

where p_1 , q_1 , r_1 and s_1 are the Bessel function cross-products defined by,

$$p_1 = J_0\left(\frac{h}{c} \exp(-cz)\right) Y_0\left(\frac{h}{c} \exp(-cz_0)\right) - J_0\left(\frac{h}{c} \exp(-cz_0)\right) Y_0\left(\frac{h}{c} \exp(-cz)\right), \quad (4.63a)$$

$$q_1 = -J_0\left(\frac{h}{c} \exp(-cz)\right) Y_1\left(\frac{h}{c} \exp(-cz_0)\right) + J_1\left(\frac{h}{c} \exp(-cz_0)\right) Y_0\left(\frac{h}{c} \exp(-cz)\right), \quad (4.63b)$$

$$r_1 = -J_1\left(\frac{h}{c} \exp(-cz)\right) Y_0\left(\frac{h}{c} \exp(-cz_0)\right) + J_0\left(\frac{h}{c} \exp(-cz_0)\right) Y_1\left(\frac{h}{c} \exp(-cz)\right), \quad (4.63c)$$

$$s_1 = J_1\left(\frac{h}{c} \exp(-cz)\right) Y_1\left(\frac{h}{c} \exp(-cz_0)\right) - J_1\left(\frac{h}{c} \exp(-cz_0)\right) Y_1\left(\frac{h}{c} \exp(-cz)\right). \quad (4.63d)$$

Once again, we plot the exponential taper lowest-order-mode coupling efficiency $|C_{00}|^2$ against the ratio d of the width of the output waveguide at $\zeta = z$ to the width of the input waveguide at $\zeta = z_0$, and the angle between the constant refractive index contour $n(x, 0, \zeta) = n_0/2$ and the z -axis at the input plane $\zeta = z_0$, in figure 4.8. In the case of the exponential taper, these parameters are given by, $d = \exp[c(z-z_0)]$ and $\theta = \arctan\left[\frac{c}{h} e^{cz_0}\right]$, respectively. It can be clearly seen that the exponential taper lowest order mode coupling efficiency plot is qualitatively very similar to the corresponding coupling efficiency plot for the linear taper. The main difference between the two plots is that, for a given value of the parameter d , the maximum value of θ for which the coupling efficiency is high for the linear taper, has approximately twice the value of the corresponding maximum value of θ for the exponential taper. Furthermore, the region of small θ and high coupling efficiency, is such that the peaks of the ripples of high coupling efficiency are not all at 100%, but vary between approximately 90% and 100%, for the range of parameters θ and d shown in the plot. Since the region of high coupling efficiency is smaller, the ridges of high coupling efficiency are narrower, and the optimum coupling efficiency that can be achieved for practical tapers is less than 100%, we can conclude that the exponential taper is not as useful as the corresponding linear device. From the discussion in section 4.5 earlier, it also follows that the exponential taper does

not compare favourably with the parabolic taper: its optimum coupling efficiency (around 90%) is marginally less than the corresponding one for the parabolic taper (around 95%), and to achieve it we would have to use long exponential tapers. Nevertheless, it has much better lowest-order-mode coupling efficiency characteristics than the ISL taper which we have also studied in the previous section.

The propagation of a Gaussian beam in an exponential, parabolic-refractive-index taper has been studied in detail by Casperson (1985), who has found exact closed form results for the Gaussian beam amplitude and phase distributions, within the paraxial approximation. We have compared the predictions for the Gaussian beam waist size in equation (4.33), with the taper function $f(z, z_0)$ given by equation (4.61), to the corresponding result derived by Casperson (1985), which can be easily extracted from his equations (4) and (30) to (34). The refractive index distribution model that Casperson uses is given by,

$$n(x, \zeta) = n_0 \left(1 - \frac{1}{2} [F \exp(2\gamma\zeta) - G] x^2 \right), \quad (4.64)$$

where $0 \leq \zeta \leq z$. The main difference between our model and Casperson's is the use of the parameter G , which allows him to vary the initial width of the taper in the plane $\zeta = 0$. In our model, the variation of the initial width of the taper is provided by allowing the input plane of the taper to lie at $\zeta = z_0$, and varying the value of z_0 . Casperson's approach complicates the computations, because what is effectively his function equivalent to our function $f(z, z_0)$, must then be expressed in terms of Bessel functions of non-integer order. When the above is taken into account and we modify Casperson's calculations to allow for non-zero z_0 and $G = 0$, the final result he obtains for the Gaussian beam waist can be written in our notation as,

$$w(z) = \sqrt{\frac{2}{ka_0} \frac{\pi}{2c} \sqrt{a_0^2 p_1^2 + e^2 q_1^2}}, \quad (4.65)$$

where p_1 and q_1 are given by equation (4.63). We have thus found that we can arrive at exactly the same result (4.65) using equations (4.61) and (4.33). Therefore, Casperson's

analysis is completely equivalent to ours.

Our work, which is new, yields exact, closed form expressions for the propagator and coupling efficiencies of the exponential taper, and as a consequence has a much more general applicability than Casperson's, which only considers the propagation of a Gaussian beam in a taper of this geometry. In addition to this, we have been able to obtain the propagation characteristics of a centred Gaussian beam, in a graded-index taper whose geometry is described by an arbitrary power law (4.37). What is even more important though, is that we have been able to obtain for the first time, closed form expressions for the propagator and the coupling efficiency between any two input and output local modes of a graded-index, tapered waveguide with parabolic, ISL, exponential, or arbitrary power-law geometry. Path integration has proved a useful tool as it has enabled us to arrive at exact results for a wider range of taper geometries than ever before.

4.7 Conclusions.

In this chapter we have presented the analysis of a tapered parabolic-refractive-index waveguide, whose contours of constant refractive index are arbitrary curves symmetrically placed around the waveguide axis. We have been able to obtain, in closed form, expressions for the taper propagator, the coupling efficiency between any two local normal modes at the ends of the taper, and the beam waist and radius of curvature of the total field excited by the lowest order local normal mode at the taper input. All the above expressions were determined in terms of an arbitrary function specified in terms of a relatively simple differential equation.

This arbitrary function was determined exactly for the cases where the taper geometry is described by an arbitrary power-law expression, or an exponential expression. The special cases of the parabolic, inverse-square-law and exponential tapers were then examined in some detail, and their lowest-order-mode to lowest-order-mode coupling

efficiency properties were compared to those of the linear taper. The parabolic taper was found to be better than the corresponding linear one in its single-mode operation, while the exponential and inverse-square-law tapers were found to be less useful. Finally, our results on the propagation of a Gaussian beam in the exponential taper were found to be in agreement with those of Casperson (1985).

To the best of our knowledge, there is very little work published on graded-index tapered waveguides of various geometries, and it would therefore be desirable to compare the predictions of this chapter with experimental work on this topic, as well as numerical and Wentzel-Kramers-Brillouin (WKB, see Mathews and Walker, 1970) analyses of these waveguide structures.

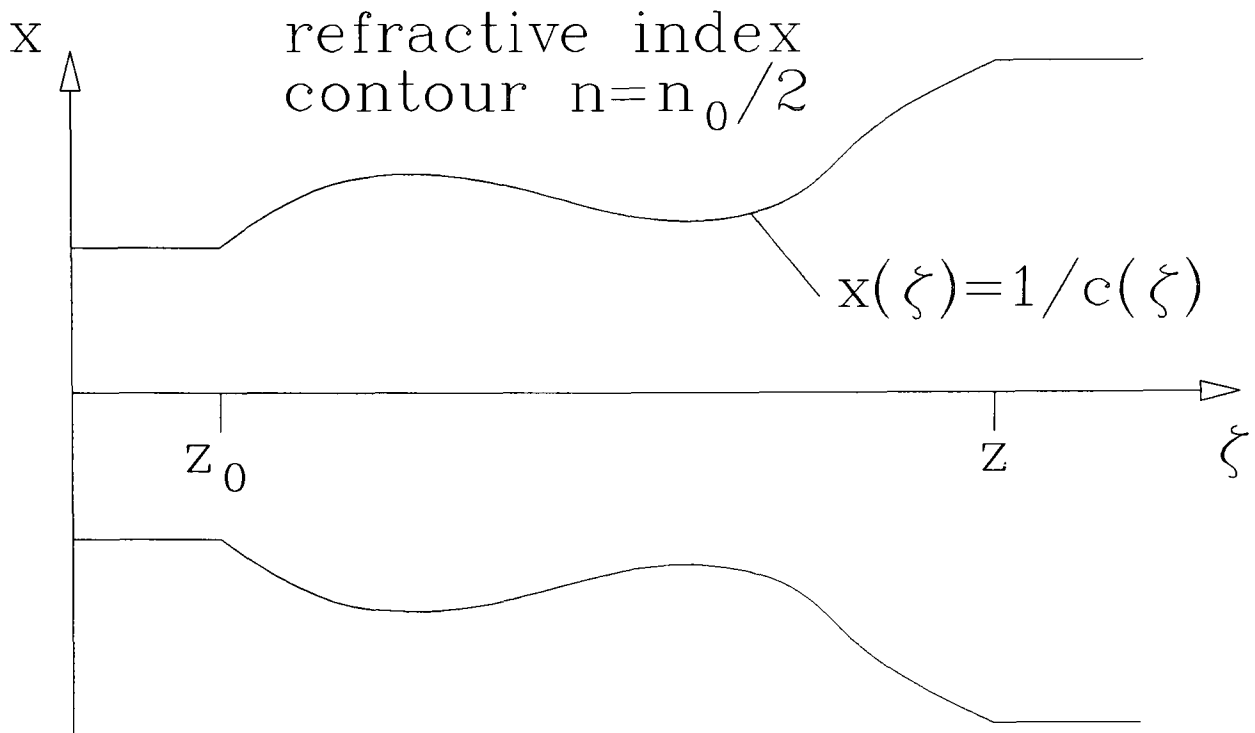


Figure 4.1: The constant refractive index contour $n = n_0/2$ of an arbitrarily tapered parabolic refractive index waveguide.

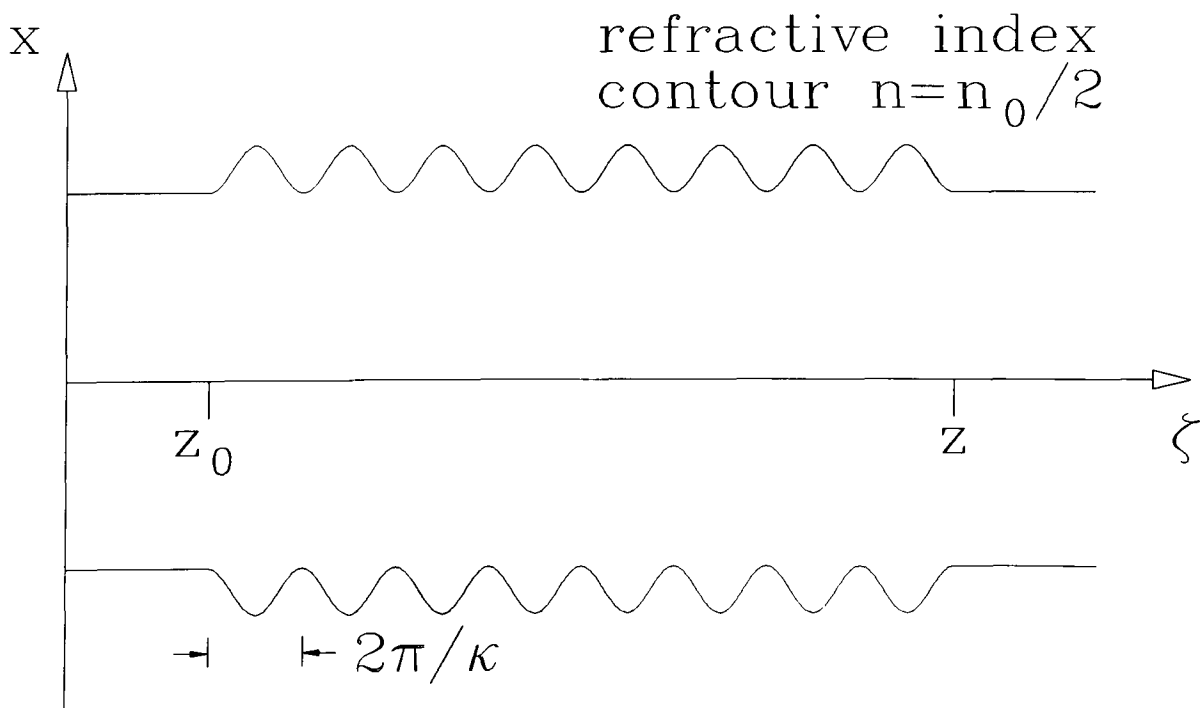


Figure 4.2: The constant refractive index contour $n = n_0/2$ of a parabolic refractive index waveguide with a periodically varying width.

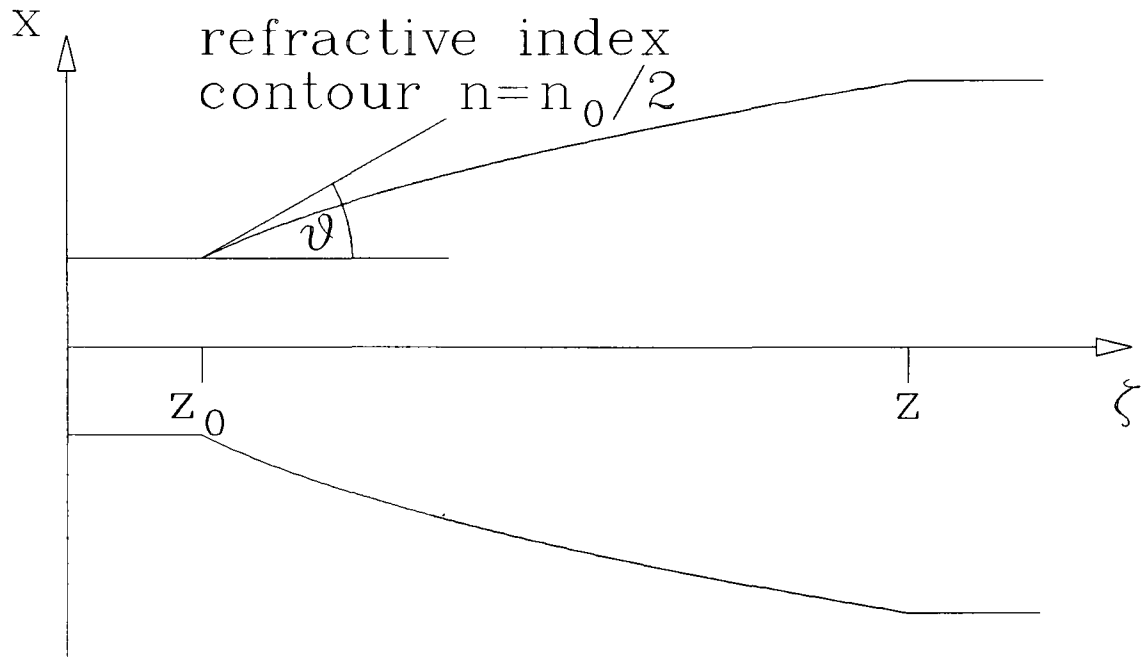


Figure 4.3: The constant refractive index contour $n = n_0/2$ for the parabolic taper.

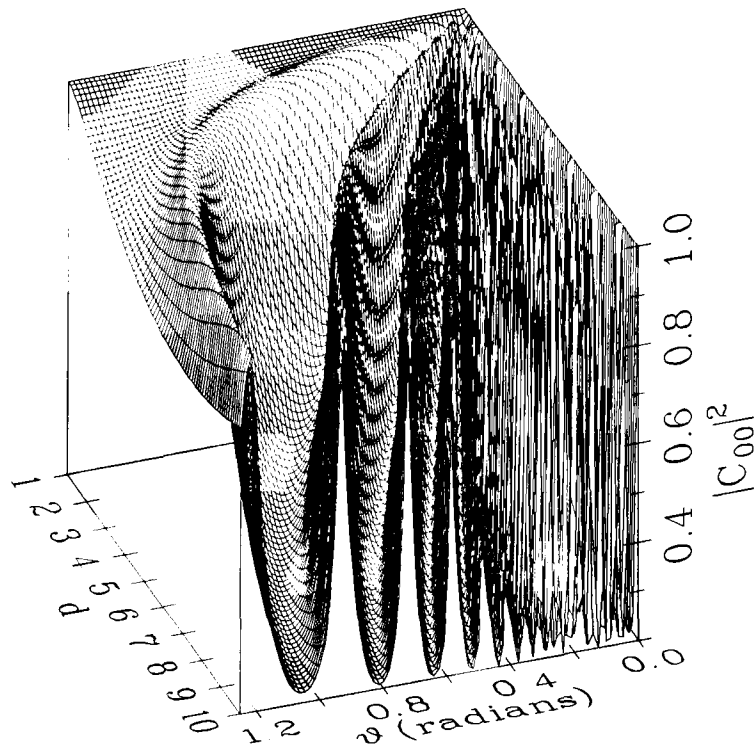


Figure 4.4: The lowest-order-mode to lowest-order-mode power coupling efficiency for the parabolic taper, plotted against the parameters θ and d .

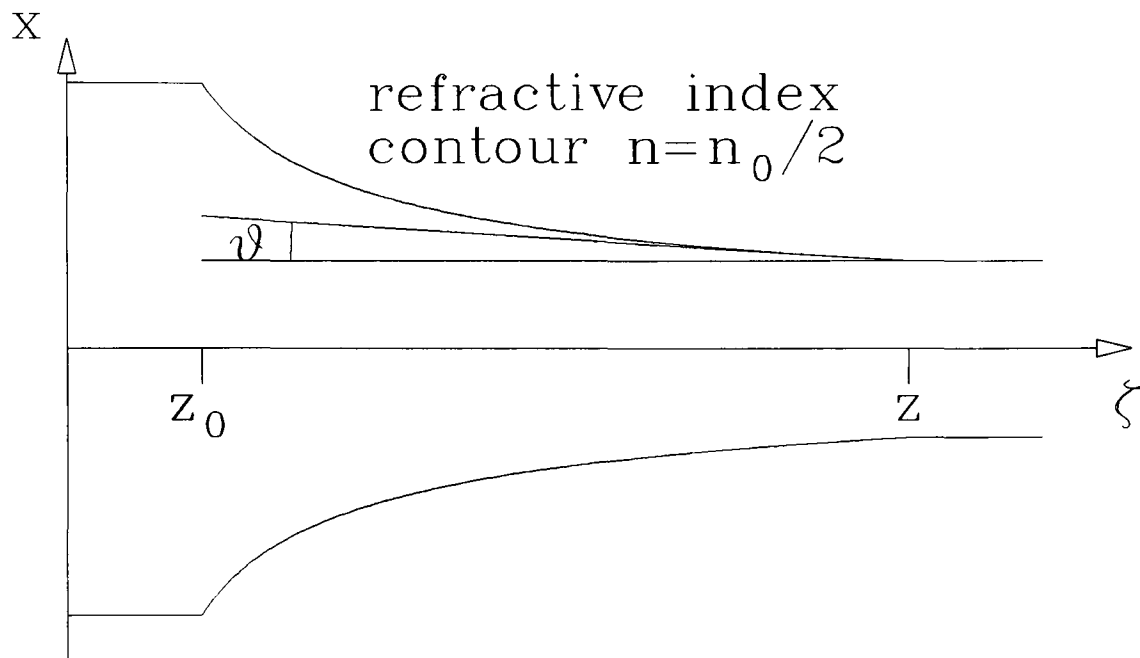


Figure 4.5: The constant refractive index contour $n = n_0/2$ for the inverse-square-law taper.

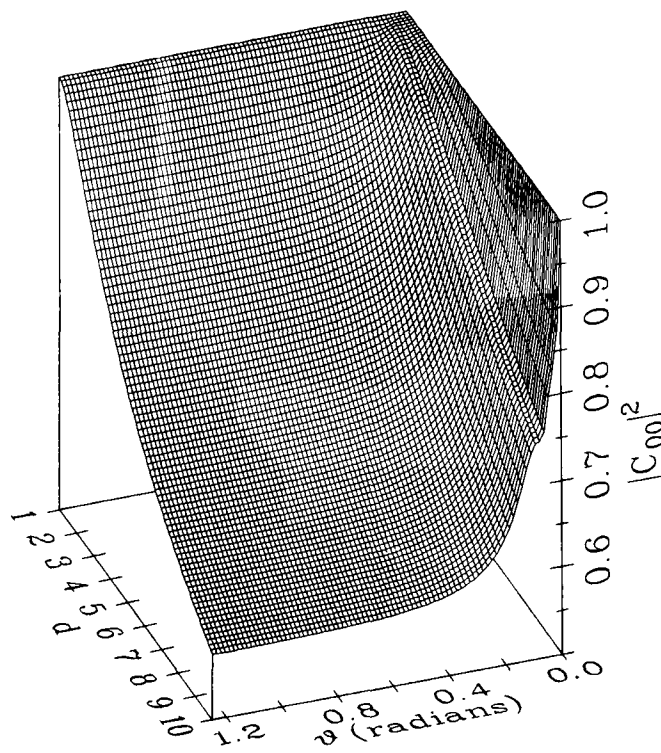


Figure 4.6: The lowest-order-mode to lowest-order-mode power coupling efficiency for the inverse-square-law taper, plotted against the parameters θ and d .

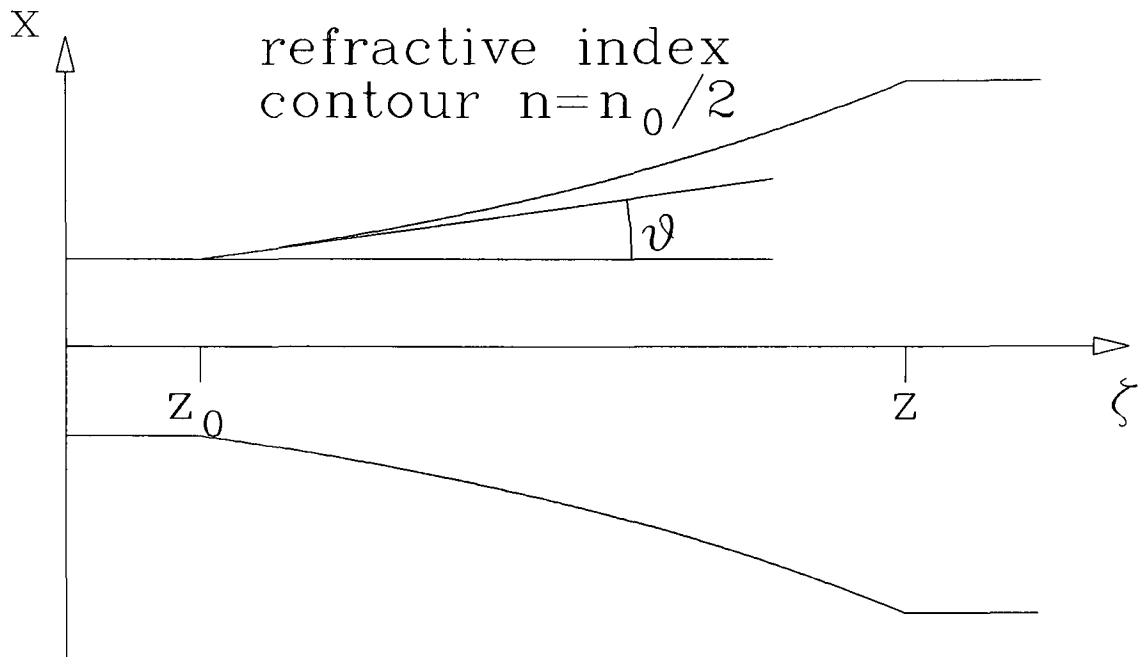


Figure 4.7: The constant refractive index contour $n = n_0/2$ for the exponential taper.

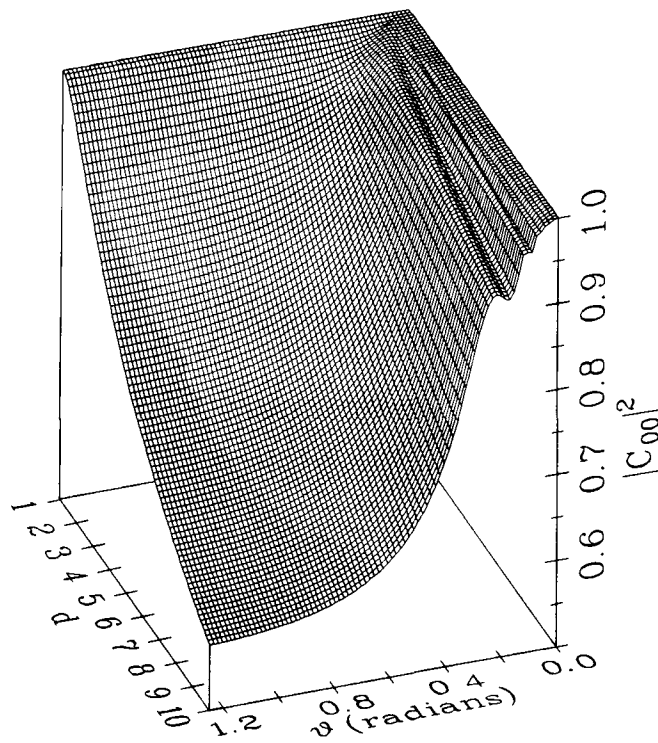


Figure 4.8: The lowest-order-mode to lowest-order-mode power coupling efficiency for the exponential taper, plotted against the parameters θ and d .

Chapter 5.

The coupling between two graded-index waveguides in close proximity.

5.1 Introduction.

The importance of understanding the detailed mechanism of operation of graded-index waveguide junctions was explained at some length in chapter 1. In chapter 1, we also explained that any junction between two graded-index waveguides can be considered to consist of two separate regions: a tapered section where the two waveguides merge into each other, and a section in which the two waveguides are separate but are in close proximity. Away from these two regions the two waveguides can be analysed independently, since the waves propagating in each one of them are no longer coupled (Burns and Milton, 1990). In chapters 3 and 4 we have studied in some detail the propagation of paraxial waves in graded-index waveguide tapers having a wide variety of geometries. In order to be able to adequately model passive graded-index waveguide junctions, we now need to study the problem of propagation in two waveguides whose separation is small, but varies in an arbitrary manner. Such guiding structures do not only occur in the study of waveguide junctions, but are also frequently encountered in optical couplers (Lee, 1986). In what follows we obtain an approximate expression for the propagator of two parallel graded-index waveguides, and suggest ways in which our calculation could be extended to the study of the non-parallel coupled waveguide problem.

5.2 The refractive index distribution used to model the two coupled waveguides.

The refractive index distribution we used to model the single graded-index

waveguide in chapters 2 to 4, was a parabolic distribution of infinite extent and is shown in figure 5.1(a). In order to be consistent with our original waveguide model we now seek to model two coupled graded-index waveguides by a smooth, infinite refractive index distribution, which looks like that of figure 5.1(b). The two peaks in this refractive index distribution correspond to the centres of the two waveguides. The region of low refractive index between the two peaks is a realistic description of the refractive index distribution found between graded-index waveguides formed by diffusion (Lee, 1986) if the depth, $U(z)$, is a rapidly increasing function of the waveguide separation $b(z)$. This is just another way of stating the obvious fact that the two waveguides must be isolated when their separation is very large. A refractive index distribution which satisfies the above description is,

$$n(x,z) = n_0 [1 - a^4(x^2 - b^2(z))^2], \quad (5.1)$$

where we have made use of the fact that the problem is separable in the x and y coordinates (c.f. chapter 3) and thus neglected any y variation in the refractive index. The separation of the two coupled waveguides is now given by $2b(z)$, while the depth, U , of the region of low refractive index between the two waveguides is given by $U(z) = -n_0 a^4 b^4(z)$. By allowing $b(z)$ to be an arbitrary but smooth function of the distance along the paraxial axis z , we are effectively modeling two waveguides of variable separation, ranging from zero to infinity. The depth of the low refractive index region then also ranges from zero to infinity, a consequence of which is that we have two isolated waveguides when their separation is a very large number of wavelengths. Finally, one other advantage of using this refractive index distribution is that both the refractive index and its derivatives are continuous functions of the transverse coordinate x , which enables us to treat the problem analytically.

There are a number of particular forms of the function $b(z)$ which are of great practical importance in engineering. When $b(z) = b$, a constant, the two coupled waveguides are parallel, as is the case in a number of waveguide filters and directional

couplers (Lee, 1986, Snyder and Love, 1983, Tamir (Ed.), 1990). When $b(z)$ is a linear function of the displacement z along the paraxial axis, the relevant optical device consists of two straight, coupled, non-parallel waveguides. A device of this type occurs in tapered velocity couplers and as part of waveguide junctions and branches (Lee, 1986, Snyder and Love, 1983, Tamir (Ed.), 1990). We will first concentrate on obtaining a closed form expression for the propagator of a waveguide structure which has a completely arbitrary separation function $b(z)$. We will then consider the case of two straight, parallel coupled waveguides in some detail, and very briefly look at how we might analyse any other cases of interest.

In order to determine an approximate propagator of the coupled waveguide system described by the refractive index distribution (5.1), we have decided to make use of Feynman's variational method (Feynman and Hibbs, 1965), which we present in section 5.3 below.

5.3 The study of graded-index waveguides having a general transverse refractive index variation.

As was stated in section 2.6 of chapter 2, a model medium with a quadratic refractive index variation can be considered to give a good description of a real waveguide medium. This fact can be exploited by using this quadratic refractive index model as the starting point for a variational estimate of the properties of more complicated systems. Most media that can be used as waveguides in optics share a common feature with the model quadratic medium: the refractive index on the axis of propagation, or optical axis, is higher than that in the surrounding regions. It follows from elementary calculus that the shape of a smooth function, such as the ones that occur in the description of refractive index distributions formed by diffusion processes, near the vicinity of its local maximum is that of a parabola. As a consequence, most graded index waveguides have a refractive

index distribution similar to that modeled by equation (2.65) in the region where most of the wave energy is concentrated. A plot of the refractive index variation of a typical graded index waveguide with distance from the optical axis looks roughly like the one shown in figure 5.2. The propagator and the propagation constant of the lowest order waveguide mode can be found in an approximate way by using the variational method developed by Feynman (Feynman and Hibbs, 1965) and the generalisation introduced by Samathiyakanit (1972). The modes of a waveguide are the various transverse field distributions having zero wavefront curvature which can travel along the waveguide unchanged (Snyder and Love, 1983). The corresponding propagation constant, β , is related to the phase velocity of each mode by $v = \omega/\beta$. The corresponding quantities in quantum mechanics are the eigenfunctions and energy levels of a particle which exists in a potential well. In what follows, the method is formulated in a way which is suitable for the study of dielectric waveguides. In order to calculate the propagator or lowest order mode propagation constant corresponding to a waveguide with an arbitrary refractive index profile, the propagator describing a medium with a functionally similar refractive index profile must be known exactly.

This known, or reference, propagator is chosen to be that of the medium with quadratic variation in the refractive index. It is rather fortunate that the quadratic refractive index waveguide is suitable for use as an archetypal waveguide, since it is the only model for which we can perform the path integral exactly and obtain the propagator in a closed form. In what follows we will denote the quadratic refractive index propagator by K_t and the corresponding optical path length by S_t . Thus,

$$K_t(x, y, z; x_0, y_0, z_0) = \int \int \delta x(z) \delta y(z) \exp\{ikS_t\}, \quad (5.2)$$

where,

$$S_t = \int_{z_0}^z d\zeta \left[\frac{1}{2}\dot{x}^2(\zeta) + \frac{1}{2}\dot{y}^2(\zeta) + n_t(x(\zeta), y(\zeta)) \right], \quad (5.3)$$

and

$$n_t(x, y) = 1 - \frac{1}{2}a^2x^2 - \frac{1}{2}a^2y^2. \quad (5.4)$$

Notice that the refractive index constant n_0 , which appears in (2.65) has been absorbed in

the wavenumber k . The corresponding quantities for the medium, or waveguide under investigation are,

$$K(x, y, z; x_0, y_0, z_0) = \int \int \delta x(z) \delta y(z) \exp\{ikS\}, \quad (5.5)$$

where

$$S = \int_{z_0}^z d\zeta \left[\frac{1}{2} \dot{x}^2(\zeta) + \frac{1}{2} \dot{y}^2(\zeta) + n(x(\zeta), y(\zeta)) \right]. \quad (5.6)$$

and $n(x, y)$ is the arbitrary refractive index distribution for which it is not feasible to evaluate (5.5), but which has a roughly similar variation in x and y to that of $n_t(x, y)$. The refractive indices considered are independent of z since interest is focused on waveguides whose characteristics are invariant along their axis. Equation (5.5) can be re-written in the form,

$$K(x, y, z; x_0, y_0, z_0) = \int \int \delta x(z) \delta y(z) \exp\{ik(S - S_t)\} \exp\{ikS_t\}. \quad (5.7)$$

Dividing both sides by K_t , and omitting the arguments $(x, y, z; x_0, y_0, z_0)$ for brevity, gives,

$$\frac{K}{K_t} = \frac{\int \int \exp\{ik(S - S_t)\} \exp\{ikS_t\} \delta x(z) \delta y(z)}{\int \int \exp\{ikS_t\} \delta x(z) \delta y(z)}. \quad (5.8)$$

Equation (5.8) is the functional analogue of

$$\langle f(x) \rangle = \frac{\int f(x) p(x) dx}{\int p(x) dx}, \quad (5.9)$$

which defines the average of the function $f(x)$ with respect to a probability density function $p(x)$. We may then interpret the right hand side of equation (5.8) as a functional average with the weight $\exp\{ikS_t\}$, playing the role of a probability density function. This averaging is divided by a normalizing factor chosen so that $\langle 1 \rangle = 1$. In general,

$$\langle \mathcal{F}[x(z), y(z)] \rangle \equiv \frac{\int \int \delta x(z) \delta y(z) \mathcal{F}[x(z), y(z)] \exp\{ikS_t\}}{\int \int \delta x(z) \delta y(z) \exp\{ikS_t\}}. \quad (5.10)$$

Using the above definition of a functional average, the unknown expression (5.8) for the

propagator can be written in the form,

$$\frac{K}{K_t} = \left\langle \exp\{ik(S - S_t)\} \right\rangle \quad (5.11)$$

or,

$$K = K_t \langle \exp[ik(S - S_t)] \rangle. \quad (5.12)$$

Equation (5.12) is an exact expression for the propagator. Following Feynman (Feynman and Hibbs, 1965), we analytically continue the expression for the propagator to imaginary propagation distances in order to project out the lowest order mode propagation constant. Omitting any y -dependence in the expression that follow, the normal mode expansion of the propagator is given by (Morse and Feshbach, 1953)

$$K(x, z; x_0, z_0) = \sum_{n=0}^{\infty} \varphi_n(x) \varphi_n^*(x_0) \exp[i\beta_n(z - z_0)], \quad (5.13)$$

where $\varphi_n(x, y)$ and β_n denote the transverse field distribution and propagation constant of the n^{th} mode respectively. The propagation constants for all waveguides are bounded from above (Snyder and Love, 1983). The analytic continuation mentioned above involves making the substitution

$$z - z_0 = i\mu. \quad (5.14)$$

By taking the limit of large and negative μ , and using the fact that for large and negative μ , the exponential term with the biggest propagation constant (which is the lowest order mode propagation constant β_0) dominates the sum in (5.13), we have,

$$\lim_{\mu \rightarrow -\infty} \frac{K(x, i\mu; x_0, 0)}{K_t(x, i\mu; x_0, 0)} = \frac{\varphi_0(x) \varphi_0^*(x_0) \exp[-\beta_0 \mu]}{\varphi_{t0}(x) \varphi_{t0}^*(x_0) \exp[-\beta_{t0} \mu]}, \quad (5.15)$$

where $\varphi_0(x)$, $\varphi_{t0}(x)$, β_0 and β_{t0} are the lowest order mode field distributions (eigenfunctions) and propagation constants (eigenvalues) for the unknown and known, reference, waveguide respectively. In the limit of large and negative μ , equations (5.12) and (5.15) give,

$$\frac{\varphi_0(x) \varphi_0^*(x_0)}{\varphi_{t0}(x) \varphi_{t0}^*(x_0)} \exp[-(\beta_0 - \beta_{t0})\mu] \approx \langle \exp[-k(S - S_t)] \rangle, \quad (5.16)$$

where equations (5.3) and (5.6) show that,

$$k(S-S_t) = k \int_0^\mu d\zeta' \left[n(x(\zeta')) - n_t(x(\zeta')) \right]. \quad (5.17)$$

Taking logarithms on both sides of (5.16) gives,

$$\beta_0 - \beta_{t0} - \frac{1}{\mu} \ln \left[\frac{\varphi_0(x) \varphi_0^*(x_0)}{\varphi_{t0}(x) \varphi_{t0}^*(x_0)} \right] \approx -\frac{1}{\mu} \ln \langle \exp[-k(S-S_t)] \rangle. \quad (5.18)$$

If the approximation is reasonable, then $\varphi_0 \sim \varphi_{t0}$ and the argument of the logarithm in (5.18) is a number of order unity. Also dividing the logarithm by μ produces a term which vanishes as $\mu \rightarrow -\infty$. Thus, for large μ equation (5.18) becomes,

$$\beta_0 - \beta_{t0} \approx -\frac{1}{\mu} \ln \langle \exp[-k(S-S_t)] \rangle. \quad (5.19)$$

It can be seen from equation (5.17) that the argument of the exponential in (5.19) is a real number. In this case the inequality,

$$\langle \exp(x) \rangle \geq \exp(\langle x \rangle), \quad (5.20)$$

which is valid for real x (Feynman and Hibbs, 1965), may be used in (5.19) together with the monotonic behaviour of the logarithmic function, to give,

$$\beta_0 - \beta_{t0} \geq -\frac{1}{\mu} \langle -k(S-S_t) \rangle. \quad (5.21)$$

or

$$-\beta_0 \leq -\beta_{t0} - \frac{k}{\mu} \langle (S-S_t) \rangle. \quad (5.22)$$

If $-\beta_{t0} - \frac{k}{\mu} \langle (S-S_t) \rangle$ is minimized with respect to any variational parameters built into $n_t(x)$, a lower bound for $-\beta_0$ can be established. In quantum mechanics it is well known that variational methods provide a powerful and frequently very accurate method of estimating ground state energy eigenvalues and we expect the use of a corresponding variational principle for the waveguide propagator to yield an accurate estimate of the lowest order mode (ground state) propagation constants as well. Minimizing the quantity $-k \langle (S-S_t) \rangle$ implies that the propagator in (5.12) can be approximated by its first cumulant (Samathiyakanit, 1972), and in this case we have the approximate result

$$K \approx K_t \exp[ik \langle (S-S_t) \rangle]. \quad (5.23)$$

The choice of the medium with quadratic refractive index variation as the reference propagator is dictated by the fact that the propagator is known in closed form and hence

the calculations can be made simple, while at the same time retaining the basic waveguide properties of the medium in question. We will now proceed to make use of the variational method we have just presented in order to calculate the propagator of the two coupled graded-index waveguides modeled by equation (5.1). The method can be used equally well to find the propagator of waveguides with realistic transverse refractive index distribution profiles, such as a Gaussian. In chapter 6, we also employ this method in the study of the propagator of a model random medium.

5.4 The propagator describing two coupled graded-index waveguides.

The propagator of the guiding structure modeled by the refractive index distribution (5.1) is given by,

$$K(x, z; x_0, z_0) = \exp[ik(z-z_0)] \int \delta x(z) \exp\left\{ ik \int_{z_0}^z d\zeta \left[\frac{\dot{x}^2(\zeta)}{2} - a^4 [x^2(\zeta) - b^2(\zeta)]^2 \right] \right\}. \quad (5.24)$$

Since the above path integral contains a quartic term in the path $x(z)$, it cannot be evaluated exactly. We may, though, obtain an approximate closed form expression for the above propagator using Feynman's variational method as explained in the previous section. The trial propagator which we use is that of the arbitrary taper (4.25). This choice is dictated by two properties common to the two waveguide structures: the first is that both the coupled waveguide refractive index distribution (5.1) and the arbitrary taper refractive index distribution (4.1) have maxima close to but not on the z -axis when $b(z)$ is small and the coupling between the two waveguides is significant. This causes most of the wave amplitude to be concentrated near the peaks in the refractive index distribution (Born and Wolf, 1980), and therefore results in both the structures having a guiding property in common. The second common property is that the width of the parabolic refractive index distribution and the separation of the two coupled waveguides, which both

define the extent to which the wave spreads away from the z -axis, can both be varied and may extend to infinity. A further, though non-physical, reason for the above choice for the trial propagator is that the propagator for an arbitrary taper only contains terms which are quadratic in the path $x(z)$, and this enables us to actually do all the necessary calculations in closed form.

The trial propagator is then given by equations (4.4), (4.7) and (4.25), whose content is summarised below. All factors $\exp[ik(z-z_0)]$ which occur in propagator expressions because of the non-zero, constant part n_0 in the refractive index distributions (4.1) and (5.1), are hereafter omitted for brevity.

$$K_t(x, z; x_0, z_0) = \int \delta x(z) \exp\left\{ ik \int_{z_0}^z d\zeta \left[\frac{\dot{x}^2(\zeta)}{2} - \frac{c^2(\zeta)x^2(\zeta)}{2} \right] \right\}, \quad (5.25)$$

Evaluation of the functional integral shows that,

$$K_t(x, z; x_0, z_0) = \left[\frac{k}{2\pi i f} \right]^{1/2} \exp\left\{ ik/2 \left[\frac{\partial \ln f}{\partial z} x^2 - \frac{\partial \ln f}{\partial z_0} x_0^2 - \frac{2xx_0}{f} \right] \right\}, \quad (5.26)$$

where $f \equiv f(z, z_0)$ is defined by differential equation,

$$\frac{\partial^2 f(z, z_0)}{\partial z^2} + c^2(z)f(z, z_0) = 0, \quad (5.27a)$$

and satisfies the boundary conditions,

$$f(z=z_0, z_0) = 0 \quad \text{and} \quad \left. \frac{\partial f(z, z_0)}{\partial z} \right|_{z=z_0} = 1. \quad (5.27b)$$

Feynman's variational technique prescribes that an approximate propagator for the system of the two coupled waveguides is given by (5.23) as,

$$K(x, z; x_0, z_0) \simeq K_t(x, z; x_0, z_0) \exp[ik \langle S - S_t \rangle], \quad (5.28a)$$

where,

$$S = -a^4 \int_{z_0}^z d\zeta [x^2(\zeta) - b^2(\zeta)]^2, \quad (5.28b)$$

$$S_t = -\frac{1}{2} \int_{z_0}^z d\zeta c^2(\zeta)x^2(\zeta), \quad (5.28c)$$

and the averaging implied by the angular brackets, $\langle \rangle$, is defined as before by,

$$\langle h[x(z)] \rangle \equiv \frac{\int \delta x(z) h[x(z)] \exp\left\{ ik \int_{z_0}^z d\zeta \left[\frac{\dot{x}^2(\zeta)}{2} - \frac{c^2(z)x^2(\zeta)}{2} \right] \right\}}{\int \delta x(z) \exp\left\{ ik \int_{z_0}^z d\zeta \left[\frac{\dot{x}^2(\zeta)}{2} - \frac{c^2(\zeta)x^2(\zeta)}{2} \right] \right\}}. \quad (5.28d)$$

In this particular problem the variational "parameter" is the function $c(z)$ which appears in equation (4.1). The question of how to determine this "parameter" is complicated and discussed in the following paragraph.

As we saw in section 5.3, for structures which are uniform along the paraxial propagation axis (z -axis), we must minimise $-\beta_{t0} - \frac{k}{\mu} \langle S - S_t \rangle$, where μ is a large imaginary paraxial propagation distance and β_{t0} is the propagation constant of the lowest order mode of the trial medium. The minimisation is to be done with respect to all the free parameters (variables) built into the trial propagator of the model. In our case, the devices which we are considering, are in general non-uniform along the paraxial propagation axis, and hence we are not in a position to define the concepts of waveguide modes and their corresponding propagation constants. Since we cannot minimise a formally non-existent quantity, a modified version of the variational method which does not rely on the concept of modes would need to be developed. Even if this problem were to be overcome, the free parameters of the parabolic trial medium are no longer variables, but functions like $c(z)$, and hence any minimisation which we decide to perform is a problem of the type encountered in the calculus of variations. The full variational calculation is therefore an extremely difficult problem to consider. An approximate way of performing a variational calculation is as follows: we first consider the simpler problem of two parallel coupled waveguides for which $b(z)$ has the constant value b , and a trial medium which is a single uniform, parabolic refractive index guide. In this case the variational parameter is simply the single variable, c , which replaces the function $c(z)$. In this case we may easily define the propagation constant of the lowest order mode, and this allows us to complete the variational calculation as prescribed in chapter 2. The

optimal value of the parameter c can then be determined in terms of the parameters k , a , and b . One way of completing the variational calculation in an approximate manner, is to match the geometry of the exact and trial refractive index profiles for each and every z -cross-section individually. This corresponds to replacing the variable b in the expression which defines the optimum value of the parameter c for the parallel waveguide problem, by the function $b(z)$. Thus $c(a,b,k)$ becomes $c(a,b(z),k)$, which we denote by $c(z)$. This geometrical matching argument is an ansatz which relates the optimal form of the arbitrary taper function $c(z)$ to the arbitrary separation function $b(z)$. Having determined the arbitrary taper function $c(z)$, the corresponding taper function $f(z,z_0)$ must be then found using the differential equation (5.27). If $\frac{db(z)}{dz} \ll 1$, we may argue that the coupled waveguides separate adiabatically, and this allows us to retain the functional form of the function $f(z,z_0)$ corresponding to the parallel waveguide case, in which we replace the parameter c with the function $c(z)$ in the expression for $f(z,z_0)$. The preceding arguments unfortunately lack in rigour, but represent a plausible solution that makes the calculation tractable.

5.5 The derivation of an approximate closed form expression for the propagator of the coupled waveguides.

In order to calculate an approximate closed form expression for the propagator (5.2) we need to evaluate $\langle S - S_t \rangle$. This average can be expressed solely in terms of $\langle x^2(\zeta) \rangle$ and $\langle x^4(\zeta) \rangle$. The above two averages can easily be computed if we consider the characteristic functional Φ (Feynman and Hibbs, 1965), defined by,

$$\Phi \equiv \left\langle \exp \left\{ ik \int_{z_0}^z d\zeta g(\zeta) x(\zeta) \right\} \right\rangle, \quad (5.29)$$

where $g(\zeta)$ is an arbitrary, continuous function of ζ . Successive functional differentiations of Φ with respect to $g(\zeta)$, show that,

$$\langle x^n(\zeta) \rangle = \frac{1}{(ik)^n} \frac{\delta^n \Phi}{\delta g(\zeta)^n} \Big|_{g(\zeta) \equiv 0}. \quad (5.30)$$

Using the definition of the average given in (5.28d) we can see that the denominator of the full expression for Φ is given in equation (5.26). The numerator, I , of this expression is computed below.

$$I = \int \delta x(z) \exp \left\{ ik \int_{z_0}^z d\zeta \left[\frac{\dot{x}^2(\zeta)}{2} - \frac{c^2(\zeta)x^2(\zeta)}{2} + g(\zeta)x(\zeta) \right] \right\}. \quad (5.31)$$

The above path integral is the propagator of a forced quantum mechanical harmonic oscillator for which the external force g and the spring stiffness c are both arbitrary functions of time. To the best of our knowledge this quantum mechanical problem has never been solved in the past, possibly because it does not apply to any physical problem of interest in mainstream theoretical physics. The propagator (5.31) only differs from that in (5.25) by the presence of a term in the exponent which is linear in $x(\zeta)$. A consequence of this is that if we change the variable of path integration to the function which describes the fluctuation of the path away from the ray path prescribed by geometrical optics (c.f. appendix A), the path integral over the fluctuations is identical to that of equation (A.3) (Schulman, 1981). Thus,

$$I = \left[\frac{k}{2\pi i f} \right]^{1/2} \exp \left\{ ik S_{\text{GO}} \right\}, \quad (5.32)$$

where f is defined in (5.27) and S_{GO} is the optical path length of the ray path $X(\zeta)$ prescribed by geometrical optics.

$$S_{\text{GO}} = \int_{z_0}^z d\zeta \left[\frac{\dot{X}^2(\zeta)}{2} - \frac{c^2(\zeta)X^2(\zeta)}{2} + g(\zeta)X(\zeta) \right]. \quad (5.33)$$

We have seen in appendix A that the geometrical optics ray path $X(\zeta)$ can be derived from an optical Lagrangian,

$$\mathcal{L} = \frac{\dot{X}^2(\zeta)}{2} - \frac{c^2(\zeta)X^2(\zeta)}{2} + g(\zeta)X(\zeta). \quad (5.34)$$

The Euler–Lagrange equation (Goldstein, 1980) corresponding to the above optical Lagrangian and which specifies the geometrical optics path, simplifies to,

$$\frac{d^2 X(\zeta)}{d\zeta^2} + c^2(\zeta)X(\zeta) = g(\zeta), \quad (5.35a)$$

with the boundary conditions,

$$X(z_0) = x_0 \quad \text{and} \quad X(z) = x. \quad (5.35b)$$

The closed form solution for $X(\zeta)$ can be found by writing it as,

$$X(\zeta) = X_1(\zeta) + X_2(\zeta), \quad (5.36)$$

where $X_1(\zeta)$ satisfies the homogeneous differential equation (5.35a) with the inhomogeneous boundary conditions (5.35b), and $X_2(\zeta)$ satisfies the inhomogeneous differential equation (5.35a) with homogeneous boundary conditions. By virtue of the fact that the taper function $f(z, z_0)$ satisfies the same differential equation (5.27a), and the boundary conditions (5.27b), we may express $X_1(\zeta)$ in terms of $f(z, z_0)$, as,

$$X_1(\zeta) = \frac{x f(\zeta, z_0) + x_0 f(z, \zeta)}{f(z, z_0)}. \quad (5.37)$$

$X_2(\zeta)$ can be easily determined using the Green's function, $G(\zeta; \zeta')$, defined by,

$$\left[\frac{d^2}{d\zeta^2} + c^2(\zeta) \right] G(\zeta; \zeta') = \delta(\zeta - \zeta'). \quad (5.38)$$

This Green's function can also be expressed in terms of $f(z, z_0)$. It is a straightforward matter to show that,

$$G(\zeta; \zeta') = \begin{cases} -\frac{f(\zeta, z_0)f(z, \zeta')}{f(z, z_0)} & \text{for } z_0 < \zeta < \zeta' \\ -\frac{f(\zeta', z_0)f(z, \zeta)}{f(z, z_0)} & \text{for } \zeta' < \zeta < z. \end{cases} \quad (5.39)$$

The function $X_2(\zeta)$ is then given by,

$$X_2(\zeta) = \int_{z_0}^z d\zeta' g(\zeta') G(\zeta; \zeta'). \quad (5.40)$$

Combining the results (5.37), (5.39) and (5.40), we obtain the following expression for the geometrical optics ray path $X(\zeta)$,

$$X(\zeta) = \frac{1}{f(z, z_0)} \left[x f(\zeta, z_0) + x_0 f(z, \zeta) - f(\zeta, z_0) \int_{\zeta}^z d\zeta' g(\zeta') f(z, \zeta') - f(z, \zeta) \int_{z_0}^{\zeta} d\zeta' g(\zeta') f(\zeta', z_0) \right]. \quad (5.41)$$

Using equations (5.19) and (5.11), we can then determine S_{G0} to be,

$$\begin{aligned}
S_{G0} = & \frac{1}{2f(z, z_0)} \left\{ \frac{1}{f(z, z_0)} \left[x^2 \int_{z_0}^z d\zeta \left[\left[\frac{\partial f(\zeta, z_0)}{\partial \zeta} \right]^2 - c^2(\zeta) f^2(\zeta, z_0) \right] + \right. \\
& x^2 \int_{z_0}^z d\zeta \left[\left[\frac{\partial f(z, \zeta)}{\partial \zeta} \right]^2 - c^2(\zeta) f^2(z, \zeta) \right] + 2xx_0 \int_{z_0}^z d\zeta \left[\frac{\partial f(\zeta, z_0)}{\partial \zeta} \frac{\partial f(z, \zeta)}{\partial \zeta} - c^2(\zeta) f(\zeta, z_0) f(z, \zeta) \right] - \\
& 2x \int_{z_0}^z d\zeta \left\{ \left[\left[\frac{\partial f(\zeta, z_0)}{\partial \zeta} \right]^2 - c^2(\zeta) f^2(\zeta, z_0) \right] \left[\int_{\zeta}^z d\zeta' g(\zeta') f(z, \zeta') \right] \right\} - \\
& 2x_0 \int_{z_0}^z d\zeta \left\{ \left[\left[\frac{\partial f(z, \zeta)}{\partial \zeta} \right]^2 - c^2(\zeta) f^2(z, \zeta) \right] \left[\int_{z_0}^{\zeta} d\zeta' g(\zeta') f(\zeta', z_0) \right] \right\} - \\
& 2x \int_{z_0}^z d\zeta \left\{ \left[\frac{\partial f(\zeta, z_0)}{\partial \zeta} \frac{\partial f(z, \zeta)}{\partial \zeta} - c^2(\zeta) f(\zeta, z_0) f(z, \zeta) \right] \left[\int_{z_0}^{\zeta} d\zeta' g(\zeta') f(\zeta', z_0) \right] \right\} - \\
& 2x_0 \int_{z_0}^z d\zeta \left\{ \left[\frac{\partial f(\zeta, z_0)}{\partial \zeta} \frac{\partial f(z, \zeta)}{\partial \zeta} - c^2(\zeta) f(\zeta, z_0) f(z, \zeta) \right] \left[\int_{\zeta}^z d\zeta' g(\zeta') f(z, \zeta') \right] \right\} + \\
& \int_{z_0}^z d\zeta \left\{ \left[\left[\frac{\partial f(\zeta, z_0)}{\partial \zeta} \right]^2 - c^2(\zeta) f^2(\zeta, z_0) \right] \left[\int_{\zeta}^z d\zeta' g(\zeta') f(z, \zeta') \right]^2 \right\} + \\
& \int_{z_0}^z d\zeta \left\{ \left[\left[\frac{\partial f(z, \zeta)}{\partial \zeta} \right]^2 - c^2(\zeta) f^2(z, \zeta) \right] \left[\int_{z_0}^{\zeta} d\zeta' g(\zeta') f(\zeta', z_0) \right]^2 \right\} + \\
& 2 \int_{z_0}^z d\zeta \left\{ \left[\frac{\partial f(\zeta, z_0)}{\partial \zeta} \frac{\partial f(z, \zeta)}{\partial \zeta} - c^2(\zeta) f(\zeta, z_0) f(z, \zeta) \right] \left[\int_{\zeta}^z d\zeta' g(\zeta') f(z, \zeta') \right] \left[\int_{z_0}^{\zeta} d\zeta' g(\zeta') f(\zeta', z_0) \right] \right\} + \\
& 2x \int_{z_0}^z d\zeta g(\zeta) f(\zeta, z_0) + 2x_0 \int_{z_0}^z d\zeta g(\zeta) f(z, \zeta) - 2 \int_{z_0}^z d\zeta g(\zeta) f(\zeta, z_0) \int_{\zeta}^z d\zeta' g(\zeta') f(z, \zeta') - \\
& \left. 2 \int_{z_0}^z d\zeta g(\zeta) f(z, \zeta) \int_{z_0}^{\zeta} d\zeta' g(\zeta') f(\zeta', z_0) \right\}. \tag{5.42}
\end{aligned}$$

All the integrals containing the term $-c^2(\zeta)$ in the expression for S_{G0} above can be evaluated by parts. Since it would be too tedious and lengthy to reproduce such calculations here or even in an appendix, we demonstrate the detailed evaluation of only one term, in order to illustrate the method used. All of the above integrals can be performed using the same general approach. Let us consider the evaluation of the integral, J , defined below, and which appears in the fifth line of equation (5.42), i.e.

$$J \equiv \int_{z_0}^z d\zeta \left\{ \left[\frac{\partial f(\zeta, z_0)}{\partial \zeta} \frac{\partial f(z, \zeta)}{\partial \zeta} - c^2(\zeta) f(\zeta, z_0) f(z, \zeta) \right] \left[\int_{z_0}^{\zeta} d\zeta' g(\zeta') f(\zeta', z_0) \right] \right\}. \tag{5.43}$$

The defining differential equation (5.27a) for the function $f(z, z_0)$ can be used to substitute for $-c^2(\zeta) f(\zeta, z_0)$ in the above expression, to give,

$$J = \int_{z_0}^z d\zeta \left\{ \frac{\partial f(\zeta, z_0)}{\partial \zeta} \frac{\partial f(z, \zeta)}{\partial \zeta} \int_{z_0}^{\zeta} d\zeta' g(\zeta') f(\zeta', z_0) + \frac{\partial^2 f(\zeta, z_0)}{\partial \zeta^2} f(z, \zeta) \int_{z_0}^{\zeta} d\zeta' g(\zeta') f(\zeta', z_0) \right\}. \quad (5.44)$$

Integrating the second term in the integrand in (5.44) by parts, finally yields,

$$J = \int_{z_0}^z d\zeta \left\{ \frac{\partial f(\zeta, z_0)}{\partial \zeta} \frac{\partial f(z, \zeta)}{\partial \zeta} \int_{z_0}^{\zeta} d\zeta' g(\zeta') f(\zeta', z_0) - \frac{\partial f(\zeta, z_0)}{\partial \zeta} \left[\frac{\partial f(z, \zeta)}{\partial \zeta} \int_{z_0}^{\zeta} d\zeta' g(\zeta') f(\zeta', z_0) + f(z, \zeta) g(\zeta) f(\zeta, z_0) \right] \right\} + \left[\frac{\partial f(\zeta, z_0)}{\partial \zeta} f(z, \zeta) \int_{z_0}^{\zeta} d\zeta' g(\zeta') f(\zeta', z_0) \right]_{\zeta=z_0}^{\zeta=z}. \quad (5.45)$$

Using the boundary conditions (5.27b) for $f(z, z_0)$, the above expression then simplifies to,

$$J = \int_{z_0}^z d\zeta g(\zeta) f(z, \zeta) f(\zeta, z_0) \frac{\partial f(\zeta, z_0)}{\partial \zeta}. \quad (5.46)$$

The same general approach can be used to evaluate all the integrals in (5.42). If we now use the expression for the Wronskian of $f(z, z_0)$ given in equation (4.13) of chapter 4, we can group some of the resulting terms together to finally obtain,

$$S_{G0} = \frac{1}{2} \left[x^2 \frac{\partial \ln f(z, z_0)}{\partial z} - x_0^2 \frac{\partial \ln f(z, z_0)}{\partial z_0} - \frac{2xx_0}{f(z, z_0)} \right] + \frac{1}{f(z, z_0)} \left[x \int_{z_0}^z d\zeta g(\zeta) f(\zeta, z_0) + x_0 \int_{z_0}^z d\zeta g(\zeta) f(z, \zeta) - \frac{1}{2} \int_{z_0}^z d\zeta \int_{z_0}^{\zeta} d\zeta' g(\zeta) g(\zeta') f(z, \zeta') f(\zeta, z_0) - \frac{1}{2} \int_{z_0}^z d\zeta \int_{z_0}^{\zeta} d\zeta' g(\zeta) g(\zeta') f(z, \zeta) f(\zeta', z_0) \right] \quad (5.47)$$

The above expression for the optical path length can be further simplified if we use the explicit form (5.39) for the Green's function (5.38), to get,

$$S_{G0} = \frac{1}{2} x^2 \frac{\partial \ln f(z, z_0)}{\partial z} - \frac{1}{2} x_0^2 \frac{\partial \ln f(z, z_0)}{\partial z_0} - \frac{xx_0}{f(z, z_0)} + \frac{x}{f(z, z_0)} \int_{z_0}^z d\zeta g(\zeta) f(\zeta, z_0) + \frac{x_0}{f(z, z_0)} \int_{z_0}^z d\zeta g(\zeta) f(z, \zeta) + \frac{1}{2} \int_{z_0}^z d\zeta \int_{z_0}^{\zeta} d\zeta' g(\zeta) g(\zeta') G(\zeta; \zeta'). \quad (5.48)$$

Equations (5.27), (5.32) and (5.48) completely specify the propagator of a forced quantum mechanical harmonic oscillator for which the external force g and the spring stiffness c are both arbitrary functions of time. Using equations (5.26), (5.32) and (5.48), we arrive at the following expression for the characteristic functional Φ .

$$\Phi = \exp\left\{\frac{ikx}{f(z, z_0)} \int_{z_0}^z d\zeta g(\zeta) f(\zeta, z_0) + \frac{ikx_0}{f(z, z_0)} \int_{z_0}^z d\zeta g(\zeta) f(z, \zeta) + \frac{1}{2} \int_{z_0}^z d\zeta \int_{z_0}^z d\zeta' g(\zeta) g(\zeta') G(\zeta; \zeta')\right\} \quad (5.49)$$

Using equation (5.30) and functionally differentiating (5.49) with respect to $g(\zeta)$, then gives the following closed form expressions for $\langle x^2(\zeta) \rangle$ and $\langle x^4(\zeta) \rangle$.

$$\langle x^2(\zeta) \rangle = \left[\frac{xf(\zeta, z_0) + x_0 f(z, \zeta)}{f(z, z_0)} \right]^2 - \frac{f(z, \zeta) f(\zeta, z_0)}{ikf(z, z_0)}, \quad (5.50)$$

and

$$\langle x^4(\zeta) \rangle = \left[\frac{xf(\zeta, z_0) + x_0 f(z, \zeta)}{f(z, z_0)} \right]^4 - 6 \frac{f(z, \zeta) f(\zeta, z_0)}{ikf(z, z_0)} \left[\frac{xf(\zeta, z_0) + x_0 f(z, \zeta)}{f(z, z_0)} \right]^2 + 3 \left[\frac{f(z, \zeta) f(\zeta, z_0)}{ikf(z, z_0)} \right]^2. \quad (5.51)$$

Finally, using equations (5.28), the difference between the optical path lengths of the trial and exact propagators for the coupled waveguide system is given by,

$$ik \langle S - S_t \rangle = -ika^4 \int_{z_0}^z d\zeta b^4(\zeta) + ik \int_{z_0}^z d\zeta [2a^4 b^2(\zeta) + c^2(\zeta)/2] \langle x^2(\zeta) \rangle - ika^4 \int_{z_0}^z d\zeta \langle x^4(\zeta) \rangle. \quad (5.52)$$

Substituting for the terms $\langle x^2(\zeta) \rangle$ and $\langle x^4(\zeta) \rangle$ from equations (5.50) and (5.51), we see that equation (5.52) can be written as,

$$\begin{aligned} ik \langle S - S_t \rangle = & -ika^4 \int_{z_0}^z d\zeta b^4(\zeta) - \frac{ika^4}{f^4(z, z_0)} \int_{z_0}^z d\zeta [xf(\zeta, z_0) + x_0 f(z, \zeta)]^4 - \\ & \frac{3a^4}{ikf^2(z, z_0)} \int_{z_0}^z d\zeta f^2(z, \zeta) f^2(\zeta, z_0) + \frac{6a^4}{f^3(z, z_0)} \int_{z_0}^z d\zeta f(z, \zeta) f(\zeta, z_0) [xf(\zeta, z_0) + x_0 f(z, \zeta)]^2 + \\ & \frac{ik}{f^2(z, z_0)} \int_{z_0}^z d\zeta [2a^4 b^2(\zeta) + c^2(\zeta)/2] [xf(\zeta, z_0) + x_0 f(z, \zeta)]^2 - \\ & \frac{1}{f(z, z_0)} \int_{z_0}^z d\zeta [2a^4 b^2(\zeta) + c^2(\zeta)/2] f(z, \zeta) f(\zeta, z_0). \end{aligned} \quad (5.53)$$

An approximate final closed form expression for the coupled waveguide propagator is then given by combining equations (5.28a), (5.26) and (5.53), and is,

$$\begin{aligned}
K(x, z; x_0, z_0) \simeq & \sqrt{\frac{k}{2\pi i f(z, z_0)}} \exp\left\{ ik \left[(z-z_0) - a^4 \int_{z_0}^z d\zeta b^4(\zeta) + \frac{3a^4}{k^2 f^2(z, z_0)} \int_{z_0}^z d\zeta f^2(z, \zeta) f^2(\zeta, z_0) \right] \right\} \times \\
& \exp\left\{ -\frac{1}{f(z, z_0)} \int_{z_0}^z d\zeta [2a^4 b^2(\zeta) + c^2(\zeta)/2] f(z, \zeta) f(\zeta, z_0) \right\} \times \\
& \exp\left\{ ik/2 \left[x^2 \frac{\partial \ln f(z, z_0)}{\partial z} - x_0^2 \frac{\partial \ln f(z, z_0)}{\partial z_0} - \frac{2xx_0}{f(z, z_0)} \right] \right\} \times \\
& \exp\left\{ \frac{6a^4}{f^3(z, z_0)} \int_{z_0}^z d\zeta f(z, \zeta) f(\zeta, z_0) [xf(\zeta, z_0) + x_0 f(z, \zeta)]^2 \right\} \times \\
& \exp\left\{ \frac{ik}{f^2(z, z_0)} \left[\int_{z_0}^z d\zeta [2a^4 b^2(\zeta) + c^2(\zeta)/2] [xf(\zeta, z_0) + x_0 f(z, \zeta)]^2 - \frac{a^4}{f^2(z, z_0)} \int_{z_0}^z d\zeta [xf(\zeta, z_0) + x_0 f(z, \zeta)]^4 \right] \right\}
\end{aligned} \tag{5.54}$$

To the best of our knowledge, the above approximate but closed form expression for the propagator of a model of two coupled graded-index waveguides is entirely new. The above result is also new in the context of quantum mechanics, where the corresponding problem is that of the anharmonic oscillator. It well known (Schulman, 1981) that the description of the motion of an anharmonic oscillator is closely linked to problems such as instantons in quantum field theory and second order phase transitions in statistical mechanics. Therefore, the above new result is potentially useful outside the context in which it was originally derived.

The propagator (5.54) does not constitute a complete solution of the propagation problem in the coupled graded-index waveguides system, unless the optimal value of the function $c(z)$ and thus of $f(z, z_0)$ is used in (5.54). The problems associated with the determination of the optimal form of these functions were discussed in section 5.4, so we will not dwell on these difficulties further.

We now want to point out that an important general property presented by the propagator (5.54) is that it contains a number of exponential terms, some of which have real exponents, and some of which have imaginary exponents. We know from chapters 3 and 4 that in all cases of interest the function $f(z, z_0)$ is oscillatory in nature. The presence of oscillatory terms in the real exponents implies that at any given transverse coordinate position x , the amplitude of a propagating wave will alternately increase and

then decrease with increasing z . This is precisely what we expect to happen in waveguides which are in close proximity: their fields are coupled and as a consequence, there is energy exchange between them (Snyder and Love, 1983). As we will shortly see, when the waveguides are parallel the exchange is periodic in z .

5.6 The approximate propagator describing two parallel, coupled graded-index waveguides.

When we are considering two parallel, coupled graded-index waveguides, their separation $2b(z)$ is independent of z . We may therefore set $b(z) \equiv b$, and $c(z) \equiv c$, where both b and c are now constants. In this case the taper function $f(z, z_0)$ defined in (5.27) is simply given by,

$$f(z, z_0) = \frac{1}{c} \sin(c(z-z_0)). \quad (5.55)$$

The integrals of $f(z, z_0)$ which appear in the expression for the coupled waveguide propagator (5.54) are simple trigonometric integrals which can be readily evaluated to give,

$$\begin{aligned} K(x, z; x_0, z_0) \simeq & \sqrt{\frac{kc}{2\pi i \sin(c(z-z_0))}} \exp\left\{-\left[\frac{a^4 b^2}{c^2} + \frac{1}{4}\right] \left[1 - c(z-z_0) \cot(c(z-z_0))\right]\right\} \times \\ & \exp\left\{ik(1-a^4 b^4)(z-z_0) + \frac{9ia^4}{8kc^3 \sin(c(z-z_0))} \left[\frac{c(z-z_0)}{\sin(c(z-z_0))} \left[1 - \frac{2}{3} \sin^2(c(z-z_0))\right] - \cos(c(z-z_0))\right]\right\} \times \\ & \exp\left\{\frac{9a^4}{4c^2 \sin^2(c(z-z_0))} \left((x^2+x_0^2) \left[1 - \frac{1}{3} \sin^2(c(z-z_0))\right] - c(z-z_0) \cot(c(z-z_0)) \right) + \right. \\ & \left. 2xx_0 \left[\frac{c(z-z_0)}{\sin(c(z-z_0))} \left[1 - \frac{2}{3} \sin^2(c(z-z_0))\right] - \cos(c(z-z_0)) \right] \right\} \times \\ & \exp\left\{\frac{ikc}{\sin(c(z-z_0))} \left((x^2+x_0^2) \left[\frac{1}{2} \cos(c(z-z_0)) + \left[\frac{a^4 b^2}{c^2} + \frac{1}{4}\right] \left[\frac{c(z-z_0)}{\sin(c(z-z_0))} - \cos(c(z-z_0))\right]\right] + \right. \right. \\ & \left. \left. 2xx_0 \left[-\frac{1}{2} + \left[\frac{a^4 b^2}{c^2} + \frac{1}{4}\right] \left[1 - c(z-z_0) \cot(c(z-z_0))\right]\right] \right) \right\} \times \\ & \exp\left\{-\frac{ik}{\sin^3(c(z-z_0))} \left[\frac{3a^4}{8c}\right] \left((x^4+x_0^4) \left[\frac{c(z-z_0)}{\sin(c(z-z_0))} - \cos(c(z-z_0))\right] \left[1 + \frac{2}{3} \sin^2(c(z-z_0))\right] + \right. \right. \\ & \left. \left. 4xx_0(x^2+x_0^2) \left[1 - \frac{1}{3} \sin^2(c(z-z_0))\right] - c(z-z_0) \cot(c(z-z_0)) \right) + \right. \\ & \left. \left. 6x^2x_0^2 \left[\frac{c(z-z_0)}{\sin(c(z-z_0))} \left[1 - \frac{2}{3} \sin^2(c(z-z_0))\right] - \cos(c(z-z_0))\right] \right) \right\}. \quad (5.56) \end{aligned}$$

The above closed form result for the propagator of two coupled graded-index waveguides is, to the best of our knowledge new. Although the approximate propagator of the anharmonic oscillator in quantum mechanics has been derived in the past using other methods (Schulman, 1981, Wiegel, 1986), Feynman's variational method has never been applied to this problem before.

The propagator (5.56) exhibits the important feature which we have briefly mentioned at the end of the previous section. With the exception of a transient response for small $(z-z_0)$, all the exponential terms in (5.56) are periodic in $(z-z_0)$. This periodicity distance is known in engineering as the beat length, z_b , along the waveguide (Snyder and Love, 1983), and is given by,

$$z_b \equiv 2\pi/c. \quad (5.57)$$

The beat length is an important quantity which we must be able to predict accurately in order to design useful devices such as directional couplers (Lee, 1986, Snyder and Love, 1983, Tamir (Ed.), 1990).

We are now in a position to perform the minimisation required by the variational method in order to obtain c and through (5.57) the beat length z_b . In order to maximise the lowest order mode propagation constant of the coupled waveguide structure, we first need to make the analytic continuation

$$z-z_0 = i\mu, \quad (5.58)$$

and consider the limit of large negative μ . In this limit, we have,

$$\sin(c(z-z_0)) = \sin(i\mu c) \simeq \frac{\exp(-\mu c)}{2i}, \quad (5.59a)$$

and

$$\cos(c(z-z_0)) = \cos(i\mu c) \simeq \frac{\exp(-\mu c)}{2}. \quad (5.59b)$$

The expression for the propagator then becomes,

$$K(x,z;x_0,z_0) \simeq \sqrt{\frac{2ikc}{2\pi i \exp(-c\mu)}} \exp \left[-k\mu + ka^4b^4\mu + \frac{3a^4\mu}{4kc^2} - \left[\frac{a^4b^2}{c^2} + \frac{1}{4} \right] \mu c + \frac{9a^4}{8kc^3} - \left[\frac{a^4b^2}{c^2} + \frac{1}{4} \right] - \left[\frac{a^4b^2}{c^2} - \frac{1}{4} \right] kc (x^2+x_0^2) - \frac{3a^4}{4c^2} (x^2+x_0^2) - \frac{ka^4}{c} (x^4+x_0^4) \right], \quad (5.60)$$

where we have neglected all the terms multiplied by any power of $\exp(+\mu c)$. Taking the natural logarithm of the above expression, dividing by $-\mu$ and letting $\mu \rightarrow -\infty$ finally gives,

$$\beta_0 \simeq \lim_{\mu \rightarrow -\infty} \left[-\frac{1}{\mu} \ln(K(x, z; x_0, z_0)) \right] = (k - c/2) + \left[\frac{a^4 b^2}{c^2} + \frac{1}{4} \right] c - ka^4 b^4 - \frac{3a^4}{4kc^2}. \quad (5.61)$$

The first two terms $k - c/2$ constitute the lowest order mode propagation constant, β_{t0} , of the parabolic waveguide (c.f. chapter 3). According to the formulation of the variational technique, we now need to minimise $-\beta_0$, or equivalently maximise β_0 , with respect to c . Thus, we need to solve,

$$\frac{d\beta_0}{dc} = -\frac{1}{2} - \frac{a^4 b^2}{c^2} + \frac{1}{4} + \frac{3a^4}{2kc^2} = 0, \quad (5.62)$$

for the parameter c . In order to ensure that the value of c given by (5.62) makes β_0 a maximum, it must also satisfy,

$$\frac{d^2\beta_0}{dc^2} = \frac{2a^4 b^2}{c^3} - \frac{9a^4}{2kc^4} < 0, \quad (5.63a)$$

which implies that,

$$c < \frac{9}{4kb^2}. \quad (5.63b)$$

Thus in order to determine c we must solve the cubic equation,

$$c^3 + 2a^4 b^2 c - 3a^4/k = 0, \quad (5.64)$$

for one of its real roots, which must be less than $c < \frac{9}{4kb^2}$. The discriminant of the cubic equation D can be easily determined (Abramowitz and Stegun, paragraph 3.8.2, 1965) and is found to be given by,

$$D = \frac{8a^{12} b^6}{27} + \frac{9a^8}{4k^2}, \quad (5.65)$$

which is always positive. This implies that the cubic equation has only one real root given by (Abramowitz and Stegun, 1965, equation 3.8.2),

$$c = \left[\frac{3a^4}{2k} \right]^{1/3} \left[\left[\sqrt{1 + \left[\frac{2}{3} \right]^5 k^2 a^4 b^6} + 1 \right]^{1/3} - \left[\sqrt{1 + \left[\frac{2}{3} \right]^5 k^2 a^4 b^6} - 1 \right]^{1/3} \right]. \quad (5.66)$$

A change of variable to $t \equiv \left[\left[\frac{2}{3} \right]^5 k^2 a^4 b^6 \right]^{1/6}$, transforms equation (5.66) and the inequality

(5.63b) to,

$$c = \left[\frac{3a^4}{2k} \right]^{1/3} \left[\left[\sqrt{1+t^6} + 1 \right]^{1/3} - \left[\sqrt{1+t^6} - 1 \right]^{1/3} \right], \quad (5.67)$$

and

$$c < \left[\frac{3a^4}{2k} \right]^{1/3} t^{-2}, \quad (5.68)$$

respectively. The inequality (5.68) thus becomes,

$$\left[\sqrt{1+t^6} + 1 \right]^{1/3} - \left[\sqrt{1+t^6} - 1 \right]^{1/3} < t^{-2}. \quad (5.69)$$

The above inequality holds for all values of t in the range $0 \leq t < +\infty$, as can be seen by expanding the left-hand-side of (5.69) into an infinite series into the variable $1/t$. This then shows that the value of c in (5.66) is always the optimum solution to the variational problem, for all values of the parameters a , b and k .

The explicit form of the dimensionless parameter t is worth examining here, because it gives us some insight into the physical parameters governing the coupling mechanism. t is proportional to $(kb/\pi)^{1/3}$, where kb/π is the separation of the two guides measured in units of the wavelength, and to $(a^4b^4)^{1/6}$, where a^4b^4 is the ratio of the depth of the refractive index on the z -axis to its peak value at the centre of the two waveguides. The fractional depth in the refractive index on the z -axis corresponds to the height of the potential barrier in the quantum mechanical problem of electronic motion in a double potential well. The two dimensionless parameters a^4b^4 and kb/π are also known from other work (Landau and Lifshitz, 1977, Wiegel, 1973) to be important in determining c . The qualitative dependence of c on these two parameters predicted by all methods of analysis (including ours) is that the beat length increases monotonically with the separation of the two guides and the fractional depth of the refractive index between them.

The expression for the parameter c (5.66) has a number of important features worth discussing. For the sake of convenience in the discussion below, we define the corresponding dimensionless parameter c' by $c' \equiv \left[\frac{k}{3a^4} \right]^{1/3} c$. We can easily see that,

$$c' = \left[\frac{\sqrt{1+t^6} + 1}{2} \right]^{1/3} - \left[\frac{\sqrt{1+t^6} - 1}{2} \right]^{1/3}. \quad (5.70)$$

A plot of c' against t is shown in figure 5.3. At first sight, we might be justified in speculating that the curve of figure 5.3 resembles an exponential or a Gaussian curve. A non-linear least-squares algorithm shows that the optimum description of the above curve is,

$$c' \simeq \exp \left\{ -0.7 t^{1.58} \right\}, \quad (5.71)$$

which resembles neither an exponential, nor a Gaussian function. We comment later on this. In figure 5.3 we have also plotted for the sake of comparison the curve described by equation (5.71) as well as the exponential and Gaussian curves which best fit the exact solution.

To the best of our knowledge there exists only one other path-integral analysis of motion in a double potential well, and we believe this latter analysis to be cruder than our variational calculation. The approximate method was developed by Wiegel (1973, 1975) in his study of Brownian motion in a field of force, and is called the hopping paths approximation. Briefly, the hopping paths approximation consists of the following logical steps: the Brownian particle (in our case this corresponds to a ray of light) spends most of its time at the bottom of the adjacent potential wells and thus the classical action corresponding to this section of its path can be calculated easily. We then assume that the particle "hops" between the bottom of these two adjacent potential wells at discrete times t_1, t_2, t_3 , etc. A correction factor to the action can be then estimated by assuming that at the above discrete times the particle is in the vicinity of the peak of the potential barrier. The integral over all possible hopping paths is then carried out by integrating the resulting propagator expression over all the time-ordered discrete times $t_1, t_2, t_3, \dots, t_n$. This multiple integral can be found by taking the Laplace transform of the propagator with respect to time, evaluating the resulting expression and finally inverting the Laplace transform at the end, to obtain the final expression for the propagator. The hopping paths

approximation results in c' being described by an exponential function, which does not agree with our result (5.66).

Rather more conventional approximate analyses, such as the weak coupling approximation, using differential equations also tend to give a result which is an exponential function of some kind (Landau and Lifshitz, 1977, Marcuse, 1982, Lee, 1986, Burns and Milton, 1990).

Using equation (5.70) we can see that for large values of the dimensionless parameter t , $c' \sim \frac{2}{3t^2}$. The physical significance of having a large value of t is that it corresponds either to well separated waveguides, or to waveguides separated by a very deep region of low refractive index. Therefore, the limit of large t is that of the weak coupling approximation. Our results predict that the beat length increases as t^2 , whereas most other analyses predict at least an exponential rise for large t . This discrepancy arises from the fact that for large separations and/or well isolated waveguides, the parabolic refractive index distribution which we have used as the starting point in the variational calculation ceases to be an acceptable approximation to the exact refractive index profile shown in figure 5.1(b). Therefore, our result is not as reliable as those resulting from other analyses (Wiegel, 1973, 1975, Landau and Lifshitz, 1977, Marcuse, 1982, Lee, 1986, Burns and Milton, 1990) in the limit $t \gg 1$. Nevertheless, in the limit of small t , or equivalently the case of strongly coupled waveguides, our model is likely to be more reliable than the models referenced above, since its derivation did not involve any simplifying assumptions. Unfortunately, we have been unable to obtain any experimental data in order to check whether our predictions make a better or worse model than the existing ones.

In chapter 3 we saw that much more information can be extracted from the closed form expression for the propagator of any waveguiding structure whose cross-sectional refractive index distribution is invariant along the z -axis. For example we can extract the various modal field profiles, their propagation constants, or study the propagation of

Gaussian beams in this waveguide. Due to the time constraints available for the completion of this thesis, we will only consider one way of extracting the information concerning the two lowest order modes of the two parallel, coupled graded-index waveguides.

The procedure for extracting the information about the modes of the the coupled waveguide system which we will follow is a similar one to that of section 3.1 of chapter 3 (c.f. also Feynman and Hibbs, 1965). Expanding all the trigonometric functions in the expression for the propagator (5.56) into their Maclaurin series in the variable $\exp(-icz)$, and retaining only terms which are at most of first order in this variable, we have,

$$\begin{aligned}
K(x,z;x_0,z_0) \simeq & \sqrt{\frac{k}{\pi}} \frac{c}{\pi} \exp\left\{-\frac{a^4 b^2}{c^2} - \frac{1}{4} + \frac{9a^4}{8kc^3}\right\} \times \\
& \exp\left\{ikz - icz/2 - ika^4 b^4 z + i\left[\frac{a^4 b^2}{c^2} + \frac{1}{4}\right] cz - \frac{3ia^4}{4kc^2} z\right\} \times \\
& \exp\left\{-\frac{3a^4}{4c^2}(x^2+x_0^2) - \frac{kc}{2}(x^2+x_0^2) + \left[\frac{a^4 b^2}{c^2} + \frac{1}{4}\right] kc(x^2+x_0^2) - \frac{3a^4 k}{4c}(x^4+x_0^4)\right\} \times \\
& \exp\left\{\left[-\frac{6a^4}{c^2}icz + 4ikc^2 z\left[\frac{a^4 b^2}{c^2} + \frac{1}{4}\right] + \frac{9a^4}{c^2} + 2kc - 4kc\left[\frac{a^4 b^2}{c^2} + \frac{1}{4}\right] - \frac{a^4 k}{c}(x^2+x_0^2)\right] e^{-icz} xx_0\right\},
\end{aligned} \tag{5.72}$$

where we have set $z_0 = 0$, without loss of generality. Expanding the last exponential term into its infinite power series, rearranging the z -dependent terms and then resumming, yields,

$$\begin{aligned}
K(x,z;x_0,z_0) \simeq & \sqrt{\frac{k}{\pi}} \frac{c}{\pi} \exp\left\{-\frac{a^4 b^2}{c^2} - \frac{1}{4} + \frac{9a^4}{8kc^3}\right\} \times \\
& \exp\left\{ikz - icz/2 - ika^4 b^4 z + i\left[\frac{a^4 b^2}{c^2} + \frac{1}{4}\right] cz - \frac{3ia^4}{4kc^2} z\right\} \times \\
& \exp\left\{-\frac{3a^4}{4c^2}(x^2+x_0^2) - \frac{kc}{2}(x^2+x_0^2) + \left[\frac{a^4 b^2}{c^2} + \frac{1}{4}\right] kc(x^2+x_0^2) - \frac{3a^4 k}{4c}(x^4+x_0^4)\right\} \times \\
& \left[1 + xx_0\left[\frac{9a^4}{c^2} - 4kc\left[\frac{a^4 b^2}{c^2} - \frac{1}{4}\right] - \frac{a^4 k}{c}(x^2+x_0^2)\right] e^{-icz} + O(e^{-2icz})\right].
\end{aligned} \tag{5.73}$$

Comparing the above result to the eigenfunction expansion of the propagator (3.3), we can see that the lowest order mode propagation constant and field profile are given by,

$$\beta_0 \simeq k - c/4 - ka^4b^4 + a^4b^2/c - \frac{3a^4}{4kc^2}, \quad (5.74a)$$

$$\varphi_0(x) \simeq \left[\frac{kc}{\pi} \right]^{1/4} \exp\left\{ -\frac{a^4b^2}{2c^2} - \frac{1}{8} + \frac{9a^4}{16kc^3} \right\} \exp\left\{ \left[\left[\frac{a^4b^2}{c^2} + \frac{1}{4} \right] kc - \frac{3a^4}{4c^2} \right] x^2 - \left[\frac{3a^4k}{4c} \right] x^4 \right\}. \quad (5.74b)$$

respectively. A typical plot of $\varphi_0(x)$ against x is shown in figure 5.4. It is worth pointing out that the two peaks in the field distribution occur at $x \simeq \pm \lambda/2$, while the corresponding peaks in the refractive index distribution occur at $x = \pm \lambda$. This shifting of the position of the peaks of the field amplitude towards each other is a consequence of the strong coupling between the two waveguides. Most conventional analyses of coupled waveguides (e.g. Snyder and Love, 1983) consider the unperturbed fields of each guide in isolation and estimate the coupling parameter c by finding an overlap integral between the modes of the two waveguides. Clearly the presence of this shifting of the field maxima, makes the implicit assumption involved in the conventional coupled mode analyses invalid: we cannot define in any meaningful way the modes of a single waveguide in the presence of a second waveguide in close proximity. The propagation constant of the first excited odd mode is finally given by,

$$\beta_1 \simeq k - 5c/4 - ka^4b^4 + a^4b^2/c - \frac{3a^4}{4kc^2}. \quad (5.75)$$

Due to the fact that the variational technique optimises the fit between the lowest order modes of the exact and trial refractive index distributions, the modal field distributions for higher order modes which we can extract are only crude approximations to the true eigenfunctions. This shortcoming manifests itself even more strongly in the case under study, since here we cannot even write down an expression for the field profile of the first excited mode. This is due to the presence of the term $\frac{a^4k}{c}(x^2+x_0^2)$ in the expression for $\varphi_1(x)\varphi_1^*(x_0)$, (c.f. equation (5.73)), which is not separable in the variables x and x_0 . The expression for the propagation constant of this mode (5.75), provided by the variational technique is however expected to be an accurate upper bound, since the product $\varphi_1(x)\varphi_1^*(x_0)$ is orthogonal to the corresponding lowest order mode product $\varphi_0(x)\varphi_0^*(x_0)$,

for both the exact and approximate eigenfunctions $\varphi_0(x)$ and $\varphi_1(x)$ (Sakurai, 1985). In spite of this failure of the variational method, the presence of a common factor xx_0 in (5.73) enables us to predict that the first excited mode of the coupled waveguide system must have a node at $x = 0$.

Since the lowest order mode is an even mode and the first excited mode is an odd mode, their sum and difference turn out to represent wave distributions which are almost localised in the waveguide centred at the points $x = +b$ and $x = -b$ respectively. The propagation constant difference $\Delta\beta = \beta_0 - \beta_1$ can be seen from expressions (5.74a) and (5.75) to be given by $\Delta\beta = c$, which confirms that the propagator expression (5.56) predicts the periodic exchange of energy between the two coupled waveguides, with a beat length equal to $2\pi/c$.

5.7 The functional form of the optimum function $c(z)$ for a system of two coupled waveguides with variable separation: speculations on a possible way forward?

In section 5.4 of this chapter we have explained that it is not possible in general to use Feynman's variational method in order to obtain the optimum form of the function $c(z)$, for a given waveguide separation function $b(z)$. The only way forward is to make the conjecture that we can match the exact and trial parabolic refractive index distributions in each and every transverse plane to the z -axis, and so write,

$$c(a,b(z),k) = c(z) = \left[\frac{3a^4}{2k} \right]^{1/3} \left[\left[\sqrt{1 + \left[\frac{2}{3} \right]^5 k^2 a^4 b^6(z)} + 1 \right]^{1/3} - \left[\sqrt{1 + \left[\frac{2}{3} \right]^5 k^2 a^4 b^6(z)} - 1 \right]^{1/3} \right]. \quad (5.76)$$

It must be made clear at this stage that substituting expression (5.76) into the propagator (5.56) would clearly be nonsense, unless the parameter $b(z)$ and hence $c(z)$ are slowly varying functions of z so that the expression

$$\frac{d[c(z)z]}{dz} \approx c(z), \quad (5.77)$$

is true to a good approximation for all the values of z in the range of interest. When the above criterion is satisfied, the waveguide system under study is undergoing what Burns and Milton (1990) have described as an adiabatic waveguide transition, and in this case the concept of local normal modes becomes applicable. The correct way of finding the propagator in the general case, is to substitute equation (5.76) into the differential equation (5.27) and find $f(z, z_0)$. Explicit knowledge of the function $f(z, z_0)$, then enables us to substitute it into (5.54) and find the full expression for the propagator of the system of two coupled waveguides with a variable spacing. The differential equation for $f(z, z_0)$ which needs to be solved, is then,

$$\frac{\partial^2 f(z, z_0)}{\partial z^2} + \left[\left[\frac{3a^4}{2k} \right]^{1/3} \left[\left[\sqrt{1 + \left[\frac{2}{3} \right]^5 k^2 a^4 b^6(z)} + 1 \right]^{1/3} - \left[\sqrt{1 + \left[\frac{2}{3} \right]^5 k^2 a^4 b^6(z)} - 1 \right]^{1/3} \right]^2 \right] f(z, z_0) = 0, \quad (5.78)$$

and must satisfy the boundary conditions (5.27b). We have been unable so far to solve the above differential equation in a closed form, whether approximately or exactly. One possible way to proceed is to solve the above differential equation numerically, for a given separation function $b(z)$ and range of values of z . Other possible approaches to the solution of (5.78) could be to use asymptotic expressions for $c(z)$ corresponding to large and small values of the dimensionless parameter t . For large t , equation (5.78) can be approximated by,

$$\frac{\partial^2 f(z, z_0)}{\partial z^2} + \frac{9}{4k^2 b^2(z)} f(z, z_0) = 0. \quad (5.79)$$

Clearly, for any $b(z)$ described by a power law expression in z , the solution of (5.79) is given by equations (4.25) in chapter 4. Unfortunately, the integrals in the expression for the propagator (5.54) cannot be evaluated in closed form for an arbitrary power law expression for $b(z)$, and we must resort to numerical techniques once again. For small values of the parameter t , the differential equation for $f(z, z_0)$ can now be approximated by,

$$\frac{\partial^2 f(z, z_0)}{\partial z^2} + \left[\frac{3a^4}{k} \right]^{2/3} \left\{ 1 - 2^{1/3} \left[\frac{2}{3} \right]^{5/2} k a^2 b^3(z) \right\} f(z, z_0) = 0. \quad (5.80)$$

Once again this differential equation can be solved using the ansatz (4.21) with the modified Bessel equation. The integrals in expression (5.32) for the propagator cannot in general be evaluated in closed form and we again have to resort to numerical techniques, or a WKB analysis. We have not pursued the computational aspects of this work any further, since the existing time constraints do not permit us to do so.

A continuation of this work in the future is planned, since we do not know of any existing work which has examined the propagation of waves in a system of two coupled waveguides with variable, but also arbitrary separation. Even though we have not been able to solve the problem of propagation in two coupled waveguides with variable, arbitrary separation, we are in a position to claim partial success, since we have been able to arrive at new, closed form results for the case of paraxial wave propagation in two parallel waveguides. The above results can be naturally extended to the case in which the two waveguides separate adiabatically (Burns and Milton, 1990).

5.8 Conclusions.

In this chapter we have presented a refractive index model for a coupled, graded-index waveguide system in which the spacing of the two waveguides is variable. This model is shown in equation (5.1) and is plotted in figure 5.1(b). The most important feature which we have tried to build into this model is that the region between the two waveguides should have a refractive index which decreases rapidly when the separation of the two waveguides increases.

We have applied the path-integral formalism to the coupled waveguide system in conjunction with the Feynman variational technique in order to obtain an approximate closed form for its propagator. The trial refractive index distribution which we used in the variational technique was that of an infinite parabolic refractive index tapered waveguide of arbitrary geometry. The closed form expression for the propagator of the coupled

waveguide system with an arbitrary spacing is, to the best of our knowledge, entirely new. One of the intermediate steps in its calculation was the determination of a closed form expression for the propagator of the forced harmonic oscillator for which both the spring stiffness and the external force are arbitrary functions of time – a result also new.

The special case of the propagator of the system of two parallel coupled waveguides was then considered in some detail, and new results were obtained for the beat length of the two waveguides, together with information on the propagation constants and physically sensible mode field profiles of the two lowest order modes of this structure. On theoretical grounds, we concluded that our results predict a better approximation for the beat length compared to that produced by other similar analyses, for strong and intermediate strength coupling between two waveguides.

Finally, some speculations on the ways in which specific non-parallel coupled waveguide geometries can be analysed were presented. Because of time constraints, we have not considered the non-parallel coupled waveguide problem any further. A continuation of work on this topic is planned for the future.

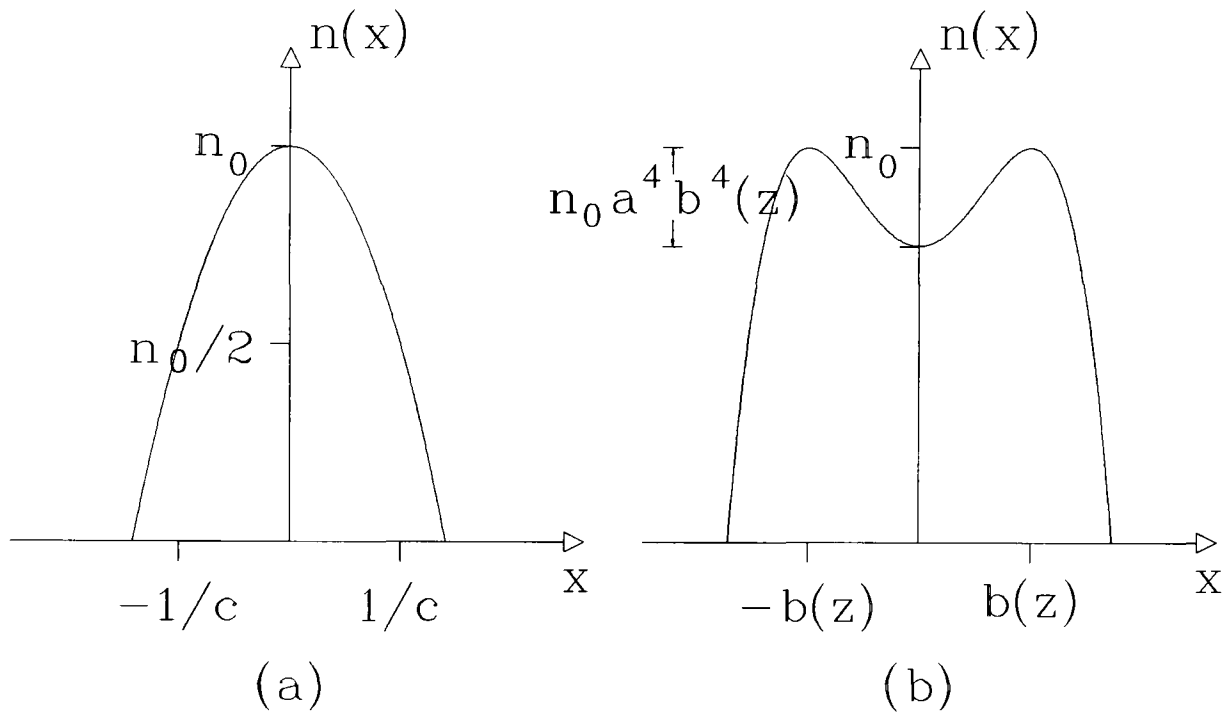


Figure 5.1: (a) The refractive index distribution of a parabolic refractive index waveguide, and (b) the refractive index distribution of the two coupled graded-index waveguides.

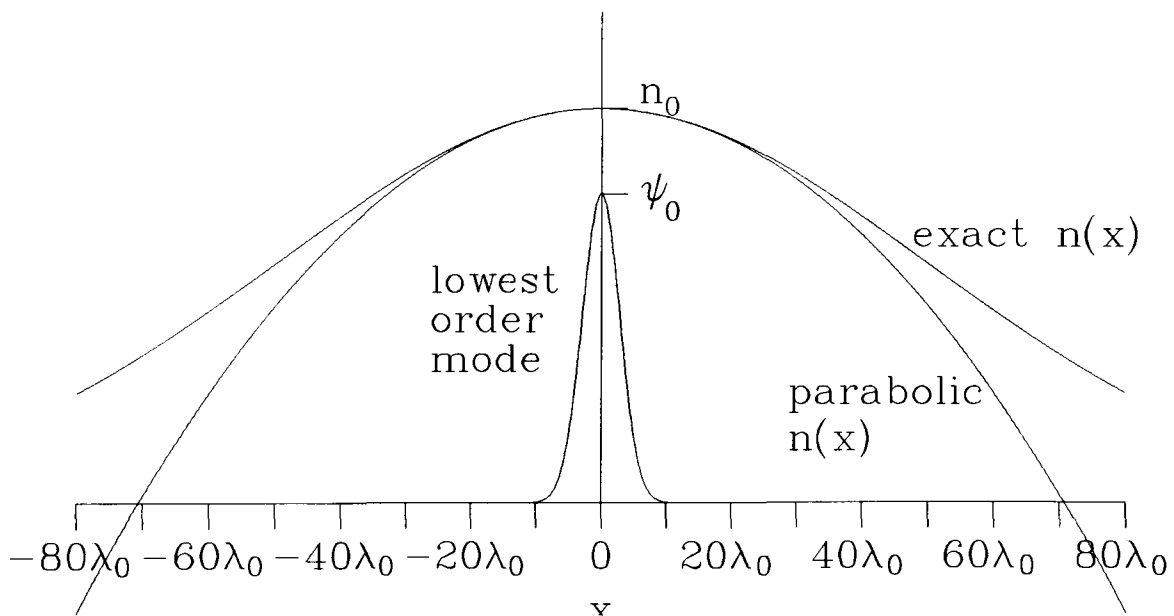


Figure 5.2: The exact refractive index distribution and the approximate parabolic refractive index distribution of a typical graded-index waveguide ($a = 50\lambda_0$) are practically indistinguishable in the region where the lowest order mode field amplitude is significantly different from zero.

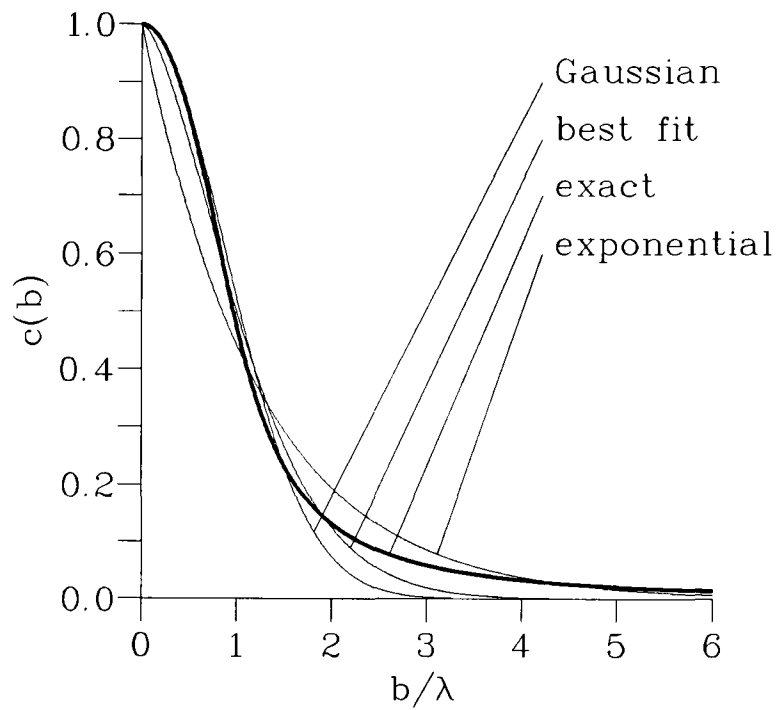


Figure 5.3: The coupling parameter c for the two coupled graded-index waveguide problem, plotted against the guide separation parameter b . The exact curve is shown together with the various fitted exponential-type curves for comparison.

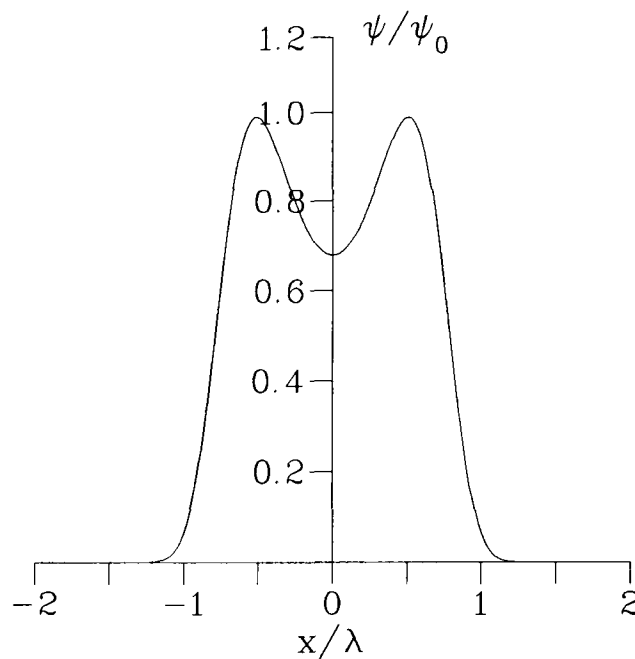


Figure 5.4: The lowest order mode field profile for two coupled graded-index waveguides for which $b = \lambda_0/n_0$ and $a = n_0/(\lambda_0\sqrt{2})$.

Chapter 6

The random medium.

6.1 Introduction.

As we have already mentioned in chapter 1, many integrated optical waveguides are manufactured by diffusing a metal, such as Silver or Titanium, into a substrate such as glass or Lithium Niobate. The process of diffusion occurs through the Brownian motion of the diffusant (Einstein, 1905, 1906), and is intrinsically random. As a result, the averaged diffusant concentration is described by a diffusion equation, but the concentration is subject to random statistical fluctuations. Since the refractive index is to a good approximation a linear function of the diffusant concentration (Lee, 1986), random inhomogeneities appear in the resulting refractive index distribution. A study of wave propagation in practical inhomogeneous media would therefore be incomplete without examining wave propagation in a medium with random refractive index inhomogeneities. The topic of optical wave propagation in a random medium using path integrals has been studied extensively, but by no means exhaustively, elsewhere (Hannay, 1977). In this chapter we will examine the general formalism describing the problem of wave propagation in a medium with random inhomogeneities in its refractive index, and subsequently apply this to Gaussian random media having different spatial correlation functions. The new concept of the *density of modes* will be introduced and used to describe these random media. A significant fraction of the work in this chapter derives from the extensive literature on the propagation of electrons in disordered solids (Edwards and Gulyaev, 1964, Zittartz and Langer, 1966, Jones and Lukes, 1969, Economou, Cohen, Freed and Kirkpatrick, 1971, Edwards and Abram, 1972, Samathiyakanit, 1974).

6.2 The definition of the random medium.

A medium with random refractive index fluctuations is one whose refractive index distribution can be written down as the sum of an "ideal", or desired, non-random refractive index component, which characterises its averaged waveguiding properties, plus a small, undesired, "random" component, which will be defined more precisely in what follows. We assume that the random refractive index inhomogeneities have the following statistical properties: they have an amplitude with a zero mean, and an arbitrary two-point spatial correlation function. Spatial correlation functions involving the coordinates of an odd number of points are assumed to be equal to zero, while those of an even number of points are assumed to be expressible as the product of two-point correlation functions alone. This latter assumption only holds for Gaussian random systems but can be approximately true for systems having different statistics (see for example the discussion on the Kirkwood superposition approximation in Croxton, 1975). As we shall soon see, we will only consider Gaussian random systems in this chapter, for which this assumption holds exactly. The refractive index of the medium can then be written as,

$$n(x,y,z) = \nu(x,y,z) + V(x,y,z), \quad (6.1)$$

where $\nu(x,y,z)$ is the deterministic, or wanted part of the refractive index and $V(x,y,z)$ is the random part which we take to be a random function with a zero mean:

$$\langle V(x,y,z) \rangle = 0, \quad (6.2)$$

The precise meaning of the average $\langle . \rangle$ will be defined later in this section. The two-point spatial correlation function of V will have the form,

$$\langle V(x,y,z)V(x',y',z') \rangle = W(\sqrt{(x-x')^2+(y-y')^2+(z-z')^2}), \quad (6.3)$$

or, writing $\mathbf{r} = (x,y,z)^T$ and using this in (6.3), the abbreviated form of the latter is,

$$\langle V(\mathbf{r})V(\mathbf{r}') \rangle = W(|\mathbf{r}-\mathbf{r}'|). \quad (6.4)$$

Furthermore, higher spatial correlation functions are assumed to be given by,

$$\langle V(\mathbf{r})V(\mathbf{r}')V(\mathbf{r}'') \rangle = 0, \quad (6.5)$$

$$\begin{aligned} \langle V(\mathbf{r})V(\mathbf{r}')V(\mathbf{r}'')V(\mathbf{r}''') \rangle &= W(|\mathbf{r}-\mathbf{r}'|)W(|\mathbf{r}''-\mathbf{r}'''|) + W(|\mathbf{r}-\mathbf{r}''|)W(|\mathbf{r}'-\mathbf{r}'''|) \\ &+ W(|\mathbf{r}-\mathbf{r}'''|)W(|\mathbf{r}'-\mathbf{r}''|), \end{aligned} \quad (6.6)$$

etc.

It is important to note that W is not the same as the two-point spatial correlation function $H(\mathbf{r},\mathbf{r}')$ for the refractive index. The relation between the two is easy to determine if we consider that $\langle V(\mathbf{r}) \rangle = 0$ and note that since ν is deterministic,

$$\langle n(x,y,z) \rangle = \nu(x,y,z). \quad (6.7)$$

Using the definitions (6.1), (6.2), (6.4) and (6.7), it is trivial to show that,

$$\langle n(\mathbf{r})n(\mathbf{r}') \rangle = \langle \nu(\mathbf{r})\nu(\mathbf{r}') + V(\mathbf{r})V(\mathbf{r}') - \nu(\mathbf{r})V(\mathbf{r}') - V(\mathbf{r})\nu(\mathbf{r}') \rangle, \quad (6.8)$$

or,

$$H(\mathbf{r},\mathbf{r}') = \nu(\mathbf{r})\nu(\mathbf{r}') + W(|\mathbf{r}-\mathbf{r}'|). \quad (6.9)$$

For every realisation of the refractive index fluctuation function $V(x,y,z)$, the propagator will have a different functional form. Clearly, there are an infinite number of possible propagators, since there can be an infinite number of functions $V(x,y,z)$ satisfying the above assumptions and definitions. When determining the average of any quantity of interest (we will consider such quantities in the next section), the average is taken over all possible allowable realisations of $V(x,y,z)$, using as a weight the probability functional, which defines the statistics of the random function $V(x,y,z)$ (Feynman and Hibbs, 1965) of $V(x,y,z)$. In this work we will assume that the random function $V(x,y,z)$ obeys Gaussian statistics, partly because this makes the calculations tractable, and partly because the resulting refractive index model is intuitively expected to be realistic. Before seeing how this averaging can be performed, it is instructive to consider the equivalent statistical problem which deals with normally distributed random variables.

Let s be a single normally distributed Gaussian variable of zero mean. Then its probability density function is,

$$p(s) = \mathcal{N}^{-1} \exp\left\{-\frac{s^2}{2\sigma^2}\right\}, \quad (6.10)$$

where σ^2 is the variance of s , and \mathcal{N} is a normalizing factor chosen such that,

$$\int_{-\infty}^{+\infty} ds p(s) = 1. \quad (6.11)$$

The average of any function $f(s)$ is then given by,

$$\langle f(s) \rangle = \int_{-\infty}^{+\infty} ds f(s) p(s). \quad (6.12)$$

We now proceed to extend these definitions to an N -dimensional vector of Gaussian random variables $\mathbf{s} = (s_1, s_2, \dots, s_N)^T$. We must now define a joint probability density function for \mathbf{s} which will depend on a symmetric $N \times N$ covariance matrix $\underline{\kappa}^{-1}$. We write this as,

$$p(\mathbf{s}) = \mathcal{N}^{-1} \exp\left\{-\frac{1}{2} \mathbf{s}^T \underline{\kappa} \mathbf{s}\right\}, \quad (6.13)$$

where \mathcal{N} is now defined by the relation:

$$\mathcal{N}^{-1} \int_{-\infty}^{+\infty} \dots \int_{-\infty}^{+\infty} d^N s \exp\left\{-\frac{1}{2} \mathbf{s}^T \underline{\kappa} \mathbf{s}\right\} = 1. \quad (6.14)$$

Comparison with (6.10) shows that the diagonal element, κ_{ii} , of $\underline{\kappa}$ is simply the inverse variance of the Gaussian random variable s_i , while the off diagonal element, κ_{ij} is the inverse of the cross correlation between the Gaussian random variables s_i and s_j . The average of any function $f(\mathbf{s})$ is then given by,

$$\langle f(\mathbf{s}) \rangle = \int_{-\infty}^{+\infty} \dots \int_{-\infty}^{+\infty} d^N s f(\mathbf{s}) p(\mathbf{s}). \quad (6.15)$$

If we now choose the s_i to be the value of $V(\mathbf{r})$ at $\mathbf{r} = \mathbf{r}_i$ and let $N \rightarrow \infty$, we pass from the set of discrete random variables $s_i = V(\mathbf{r}_i)$ to a set of Gaussian random functions $V(\mathbf{r})$. It is easy to see that equations (6.13) and (6.15) now become,

$$\langle f[V(\mathbf{r})] \rangle = \mathcal{N}^{-1} \int \delta V(\mathbf{r}) f[V(\mathbf{r})] \exp\left\{-\frac{1}{2} \int_{-\infty}^{+\infty} \int_{-\infty}^{+\infty} \int_{-\infty}^{+\infty} d^3 r \int_{-\infty}^{+\infty} \int_{-\infty}^{+\infty} \int_{-\infty}^{+\infty} d^3 r' V(\mathbf{r}) \kappa(\mathbf{r} - \mathbf{r}') V(\mathbf{r}')\right\}, \quad (6.16)$$

where $f[V(\mathbf{r})]$ is a functional depending on $V(\mathbf{r})$, \mathcal{N} is a normalising factor such that $\langle 1 \rangle = 1$ and $\kappa(\mathbf{r} - \mathbf{r}')$ is the analogue of the covariance matrix. Evaluating the

functional integral in (6.16) in its limiting form with $f[V] = V(\mathbf{r}) V(\mathbf{r}')$ and then taking the appropriate limit gives,

$$\langle V(\mathbf{r}) V(\mathbf{r}') \rangle = \kappa^{-1}(\mathbf{r}-\mathbf{r}'), \quad (6.17)$$

where $\kappa^{-1}(\mathbf{r}-\mathbf{r}')$ is the inverse of the function $\kappa(\mathbf{r}-\mathbf{r}')$, defined in such a way that,

$$\int_{-\infty}^{+\infty} \int_{-\infty}^{+\infty} \int_{-\infty}^{+\infty} d^3r' \kappa(\mathbf{r}-\mathbf{r}') \kappa^{-1}(\mathbf{r}'-\mathbf{r}'') = \delta(\mathbf{r}-\mathbf{r}''), \quad (6.18)$$

where $\delta(\mathbf{r})$ is the three-dimensional Dirac delta function. Comparison of equations (6.17) and (6.4) then gives,

$$W(|\mathbf{r}-\mathbf{r}'|) = \kappa^{-1}(\mathbf{r}-\mathbf{r}'). \quad (6.19)$$

Therefore,

$$\int_{-\infty}^{+\infty} \int_{-\infty}^{+\infty} \int_{-\infty}^{+\infty} d^3r W(|\mathbf{r}-\mathbf{r}'|) \kappa(\mathbf{r}'-\mathbf{r}'') = \delta(\mathbf{r}-\mathbf{r}'') \quad (6.20)$$

Equation (6.16) then becomes,

$$\langle f[V] \rangle = \mathcal{N}^{-1} \int \delta V(\mathbf{r}) f[V] \exp\left\{-\frac{1}{2} \int d^3r \int d^3r' V(\mathbf{r}) W^{-1}(|\mathbf{r}-\mathbf{r}'|) V(\mathbf{r}')\right\}. \quad (6.21a)$$

In order to ensure that $\langle 1 \rangle = 1$, \mathcal{N} is given by,

$$\mathcal{N} = \int \delta V(\mathbf{r}) \exp\left\{-\frac{1}{2} \int d^3r \int d^3r' V(\mathbf{r}) W^{-1}(|\mathbf{r}-\mathbf{r}'|) V(\mathbf{r}')\right\}. \quad (6.21b)$$

Equation (6.21a) defines an averaging process for which each of the properties (6.4) to (6.6) holds. The average $\langle . \rangle$, which has been used without definition throughout this section, is therefore an integral part of the refractive index model we have chosen to adopt. Equations (6.1) to (6.6), and (6.21) constitute the basic refractive index model which we will use in this work. In order to completely specify the refractive index model, we must also consider the explicit functional form of the two-point spatial correlation function $W(|\mathbf{r}-\mathbf{r}'|)$. For the time being we will leave this to be completely arbitrary.

6.3 The averaged propagator.

For each particular realisation of the random component of the refractive index

function $V(\mathbf{r})$ the propagator of the random medium $K(\mathbf{r};\mathbf{r}_0)$ is given by substituting the refractive index form (6.1) into the path integral expression for the propagator (2.27), to get,

$$K(x,y,z;x_0,y_0,z_0;[V]) = \Theta(z-z_0) \int \int \delta x(z) \delta y(z) \exp\left\{ ik \int_{z_0}^z d\zeta \frac{1}{2}[\dot{x}^2(\zeta) + \dot{y}^2(\zeta)] + ik \int_{z_0}^z d\zeta [\nu(x(\zeta),y(\zeta),\zeta) + V(x(\zeta),y(\zeta),\zeta)] \right\}, \quad (6.22)$$

where $\Theta(z-z_0)$ is the Heaviside step function. The propagator K in the above equation depends on the particular realisation of the random function $V(x,y,z)$ and should, therefore, be written as $K(x,y,z;x_0,y_0,z_0;[V])$.

Knowledge of the statistics of the random part of the refractive index can now be used to derive information on the various field statistics. Depending on the circumstances (Hannay, 1977), we might need to investigate the various "moments" of the propagating field, such as $\langle \psi \rangle$, $\langle \psi^* \psi \rangle$, $\langle \psi^* \psi \psi^* \psi \rangle$, etc, where the expectations are taken over all the possible realisations of the random medium, and are defined in (6.21). Knowledge of the above quantities requires knowledge of the expectation of the so called propagator moment products such as the first order moment, $\langle K(\boldsymbol{\rho},z,\boldsymbol{\rho}_0,z_0) \rangle$, the second order moment, $\langle K(\boldsymbol{\rho},z,\boldsymbol{\rho}_0,z_0) K(\boldsymbol{\rho}',z,\boldsymbol{\rho}'_0,z_0) \rangle$, etc. The latter expectation is very important as it generates the coherence function on the observation plane z for an arbitrary field in the plane z_0 (Hannay, 1977). In general, it is more difficult to evaluate higher order field moments than lower order ones. Hannay (1977) has examined the statistics of the intensity fluctuations in a thin random phase screen, an extended, uniform random medium, and an irregular optical fibre, using the limiting form of the propagator appropriate to geometrical optics. His calculations mainly involved the computation of the second and fourth order propagator moments. A major simplifying assumption in Hannay's work was that he only considered random media which are completely uncorrelated along the direction of propagation. In what follows we choose to concentrate on calculating the first order moment of the propagator only, for two kinds of

random media: one of zero correlation length along the direction of propagation, and one of infinite correlation length along the direction of propagation. We should, at this stage, point out that any physically realisable random medium in integrated optics should have a correlation length along the direction of propagation which is equal to, or at least has the same length scale as the correlation length in the plane transverse to the direction of propagation. This problem is very difficult to solve and we have not attempted to consider it in this work. Unfortunately, we have not been able to find any information on the typical values of the above correlation length in the literature, and thus we cannot estimate whether either of the two extreme models we have studied is a good approximation to the types of random media which we are likely to encounter in practice. Finally, in the calculations which follow we try to extract as much information as possible from the first order moment of the propagator, but time has not yet allowed extension of this work to the calculation of higher order propagator moments.

The average propagator $G(x, y, z; x_0, y_0, z_0)$ is defined as the average of the propagator $K(x, y, z; x_0, y_0, z_0; [V])$ over the space of all random Gaussian refractive index functions $V(x, y, z)$ using equation (6.21). Thus,

$$G(x, y, z; x_0, y_0, z_0) \equiv N^{-1} \int \delta V(\mathbf{r}) K(x, y, z; x_0, y_0, z_0; [V(x, y, z)]) \exp\left\{-\frac{1}{2} \int d^3r \int d^3r' V(\mathbf{r}) W^{-1}(|\mathbf{r}-\mathbf{r}'|) V(\mathbf{r}')\right\}. \quad (6.23)$$

Equations (6.22) and (6.23) then completely specify the average propagator.

6.4 The evaluation of the functional integral over the space of all random Gaussian refractive index functions $V(x, y, z)$.

The path integral in equation (6.23) can be evaluated using a technique originally employed by Edwards and Abram (1972). After substituting for the specific random medium realisation propagator $K(x, y, z; x_0, y_0, z_0; [V(x, y, z)])$, using (6.22), the order of

functional and path integrations in (6.23) can be reversed to give,

$$G(x, y, z; x_0, y_0, z_0) = \Theta(z - z_0) \times \\ \int \int \delta x(z) \delta y(z) \left\{ \exp \left\{ ik \int_{z_0}^z d\zeta \frac{1}{2} [\dot{x}^2(\zeta) + \dot{y}^2(\zeta)] + ik \int_{z_0}^z d\zeta \nu[x(\zeta), y(\zeta), \zeta] \right\} \times \right. \\ \left. \mathcal{N}^{-1} \int \delta V(\mathbf{r}) \exp \left\{ ik \int_{z_0}^z d\zeta V[x(\zeta), y(\zeta), \zeta] \right\} \exp \left\{ -\frac{1}{2} \int d^3\mathbf{r} \int d^3\mathbf{r}' V(\mathbf{r}) W^{-1}(|\mathbf{r} - \mathbf{r}'|) V(\mathbf{r}') \right\} \right\}. \quad (6.24)$$

The expression I defined by,

$$I \equiv \\ \mathcal{N}^{-1} \int \delta V(\mathbf{r}) \exp \left\{ ik \int_{z_0}^z d\zeta V[x(\zeta), y(\zeta), \zeta] \right\} \exp \left\{ -\frac{1}{2} \int d^3\mathbf{r} \int d^3\mathbf{r}' V(\mathbf{r}) W^{-1}(|\mathbf{r} - \mathbf{r}'|) V(\mathbf{r}') \right\}, \quad (6.25)$$

can now be evaluated using the functional analogue of completing the square. The following linear transformation in the variable of the functional integration must first be made.

$$V(\mathbf{r}) = \varphi(\mathbf{r}) + ik \int_{z_0}^z W(|\mathbf{r} - \mathbf{r}(\zeta)|) d\zeta. \quad (6.26)$$

The Jacobian of the linear transformation is unity, and hence,

$$\delta V(\mathbf{r}) = \delta\varphi(\mathbf{r}). \quad (6.27)$$

Substituting (6.26) and (6.27) in the expression (6.25) yields,

$$I = \mathcal{N}^{-1} \int \delta\varphi(\mathbf{r}) \exp \left\{ ik \int_{z_0}^z d\zeta \varphi[\mathbf{r}(\zeta)] - k^2 \int_{z_0}^z d\zeta \int_{z_0}^z d\zeta' W[|\mathbf{r}(\zeta) - \mathbf{r}(\zeta')|] - \right. \\ \left. \frac{1}{2} \int d^3\mathbf{r} \int d^3\mathbf{r}' \left[\varphi(\mathbf{r}) + ik \int_{z_0}^z d\zeta W[|\mathbf{r} - \mathbf{r}(\zeta)|] \right] W^{-1}(|\mathbf{r} - \mathbf{r}'|) \left[\varphi(\mathbf{r}') + ik \int_{z_0}^z d\zeta' W[|\mathbf{r}' - \mathbf{r}(\zeta')|] \right] \right\}, \quad (6.28)$$

which after expanding the terms in the exponent becomes,

$$\begin{aligned}
I = N^{-1} \int \delta\varphi(\mathbf{r}) \exp \left\{ ik \int_{z_0}^z d\zeta \varphi[\mathbf{r}(\zeta)] - k^2 \int_{z_0}^z d\zeta \int_{z_0}^z d\zeta' W[|\mathbf{r}(\zeta) - \mathbf{r}(\zeta')|] + \right. \\
\left. \frac{k^2}{2} \int d^3\mathbf{r} \int d^3\mathbf{r}' \int_{z_0}^z d\zeta \int_{z_0}^z d\zeta' W[|\mathbf{r} - \mathbf{r}(\zeta)|] W^{-1}(|\mathbf{r} - \mathbf{r}'|) W[|\mathbf{r}' - \mathbf{r}(\zeta')|] - \right. \\
\left. \frac{ik}{2} \int d^3\mathbf{r} \int d^3\mathbf{r}' \int_{z_0}^z d\zeta' \varphi(\mathbf{r}) W^{-1}(|\mathbf{r} - \mathbf{r}'|) W[|\mathbf{r}' - \mathbf{r}(\zeta')|] - \right. \\
\left. \frac{ik}{2} \int d^3\mathbf{r} \int d^3\mathbf{r}' \int_{z_0}^z d\zeta \varphi(\mathbf{r}') W[|\mathbf{r} - \mathbf{r}(\zeta)|] W^{-1}(|\mathbf{r} - \mathbf{r}'|) \right\}. \tag{6.29}
\end{aligned}$$

The definition of W in (6.3), together with the fact that it depends only on the separation $|\mathbf{r} - \mathbf{r}'|$ of the two points \mathbf{r} and \mathbf{r}' , implies that,

$$W(|\mathbf{r} - \mathbf{r}'|) = W(|\mathbf{r}' - \mathbf{r}|). \tag{6.30}$$

By the definition of a functional inverse, it is also true that,

$$\int d^3\mathbf{r}' W(|\mathbf{r} - \mathbf{r}'|) W^{-1}(|\mathbf{r}' - \mathbf{r}''|) = \delta(\mathbf{r} - \mathbf{r}''). \tag{6.31}$$

Using (6.30) and (6.31) in (6.29), we obtain,

$$\begin{aligned}
I = N^{-1} \int \delta\varphi(\mathbf{r}) \exp \left\{ - \frac{k^2}{2} \int_{z_0}^z d\zeta \int_{z_0}^z d\zeta' W[|\mathbf{r}(\zeta) - \mathbf{r}(\zeta')|] - \right. \\
\left. \frac{1}{2} \int d^3\mathbf{r} \int d^3\mathbf{r}' \varphi(\mathbf{r}) W^{-1}(|\mathbf{r} - \mathbf{r}'|) \varphi(\mathbf{r}') \right\}. \tag{6.32}
\end{aligned}$$

The first term in the exponent of (6.32) is independent of $\varphi(\mathbf{r})$ and can therefore be taken out of the functional integral. Substituting for N from (6.21b), expression (6.32) then becomes,

$$\begin{aligned}
I = \exp \left\{ - \frac{k^2}{2} \int_{z_0}^z d\zeta \int_{z_0}^z d\zeta' W[|\mathbf{r}(\zeta) - \mathbf{r}(\zeta')|] \right\} \times \\
\frac{\int \delta\varphi(\mathbf{r}) \exp \left\{ - \frac{1}{2} \int d^3\mathbf{r} \int d^3\mathbf{r}' \varphi(\mathbf{r}) W(|\mathbf{r} - \mathbf{r}'|) \varphi(\mathbf{r}') \right\}}{\int \delta V(\mathbf{r}) \exp \left\{ - \frac{1}{2} \int d^3\mathbf{r} \int d^3\mathbf{r}' V(\mathbf{r}) W(|\mathbf{r} - \mathbf{r}'|) V(\mathbf{r}') \right\}}, \tag{6.33}
\end{aligned}$$

and hence,

$$I = \exp \left\{ - \frac{k^2}{2} \int_{z_0}^z d\zeta \int_{z_0}^z d\zeta' W[|\mathbf{r}(\zeta) - \mathbf{r}(\zeta')|] \right\}. \tag{6.34}$$

Substituting this back into the expression for the average propagator (6.24), finally gives,

$$G(x, y, z; x_0, y_0, z_0) = \Theta(z - z_0) \int \int \delta x(z) \delta y(z) \exp \left\{ ik \int_{z_0}^z d\zeta \frac{1}{2} [\dot{x}^2(\zeta) + \dot{y}^2(\zeta)] + ik \int_{z_0}^z d\zeta \nu[x(\zeta), y(\zeta), \zeta] - \frac{k^2}{2} \int_{z_0}^z d\zeta \int_{z_0}^z d\zeta' W[|\mathbf{r}(\zeta) - \mathbf{r}(\zeta')|] \right\}. \quad (6.35)$$

Expression (6.35) is the path integral expression for the average propagator corresponding to the random medium defined in section 6.2. All the statistical information concerning the random medium under study, was assumed to be contained in the Gaussian amplitude statistics and the two-point correlation function. The fact that the amplitude distribution of the random part of the refractive index is Gaussian has enabled us to "complete the square" in the functional integral. Equation (6.35) is an important result since it directly links the hitherto arbitrary two-point correlation function W to the average propagator.

6.5 The density of propagation modes.

Before proceeding to consider the average propagator of a random medium with specific two-point spatial correlation functions, we will concentrate on examining the ways in which useful information can be extracted from the propagator.

Some pieces of information can be extracted from the average propagator in an almost trivial way. For example, the average field distribution at a plane $\zeta = z$ can be related to the input field distribution, $\psi(x_0, y_0)$ at a plane $\zeta = z_0$ using,

$$\langle \psi(x, y, z; z_0) \rangle = \int_{-\infty}^{+\infty} dx_0 \int_{-\infty}^{+\infty} dy_0 G(x, y, z; x_0, y_0, z_0) \psi(x_0, y_0), \quad (6.36)$$

where $G(x, y, z; x_0, y_0, z_0)$ is given by equation (6.35).

Two very important pieces of information which can be extracted from the average propagator are the phase velocity of a scalar, paraxial wave and to what extent this wave is attenuated when propagating along a given direction in space.

Before casting the above ideas into more concrete, mathematical language, it is useful to look briefly at the physical picture of what is happening when a wave propagates

in a random medium. It is more instructive to concentrate on the geometrical ray description rather than the wave description of paraxial optics. It is also easier to visualise propagation in a medium illuminated by a uniform plane wave and in which the deterministic part of the refractive index distribution is constant. The above simplifications can be made without changing the nature of the phenomenon under study. In the absence of random refractive index inhomogeneities, the rays would have moved in parallel straight line trajectories. In the present case though, whenever a ray encounters a refractive index inhomogeneity, it will be slightly deflected from its straight line path by a process of refraction, regardless of whether the local refractive index is slightly higher or lower than its average value. High local refractive index deviations are unlikely to occur because of their Gaussian amplitude probability distribution, as well as the underlying assumption of a weakly inhomogeneous medium made throughout our work. Each ray suffers multiple small deflections, but in general keeps propagating roughly along its original direction of propagation, as shown in figure 6.1. A very small number of rays suffer multiple refractions in such a way that they eventually end moving in a direction approximately orthogonal to their original direction of propagation, or even more rarely, in a direction opposite to their original direction of propagation. It is precisely this small number of rays which contributes to the attenuation of the propagating wave. The end result is that the optical wave suffers a little attenuation, and its propagation constant along the overall axis of propagation is no longer uniquely defined, but is spread around the value it would have had in the corresponding non-random uniform medium. Another consequence of the way the geometrical rays travel in such a random medium is that the amplitude and phase distributions of the wave in any plane normal to the paraxial axis are now non-uniform. As a result the intensity distribution on such a plane exhibits significant fluctuations. In order to study this intensity distribution, we need to consider second order field moments, which is beyond the scope of this work.

The effective propagation constant and the attenuation of the optical wave are

related to each other via the Kramers–Kronig (or dispersion) relations (Mathews and Walker, 1970), and as such we do not need to consider them separately. We choose to concentrate on the study of the effective propagation constant probability density, $N(\beta)$, which bears a direct analogy with the density of states in solid state physics (Ashcroft and Mermin, 1976). This concept is new in optics.

By analogy with the density of states in quantum mechanics, we define the density of propagation modes, $N(\beta)$, in such a way that $N(\beta) d\beta$ is the probability amplitude that a ray of frequency ω , travelling in the direction parallel to the paraxial axis (z -axis), will move with a propagation constant lying between β and $\beta + d\beta$. The density of propagation modes can be extracted from the trace of the average propagator for both a uniform random medium and a waveguide with random refractive index inhomogeneities. The explicit dependence of the density of propagation modes on the trace of the propagator is different in the two cases, and we will shortly consider both of them below. Before we proceed any further, it is necessary to give a physical interpretation to the trace of the propagator.

In the next two paragraphs only, for the sake of simplicity in our arguments we take the medium in which the optical wave is propagating to be a non-random waveguide. The results derived can be extended to a random medium easily. Writing the propagator in terms of its modal eigenfunction expansion (3.3), we have,

$$K(x, y, z; x_0, y_0, z_0) = \sum_{n=0}^{\infty} \sum_{m=0}^{\infty} \varphi_{nm}(x, y) \varphi_{nm}^*(x_0, y_0) \exp[i\beta_{nm}(z - z_0)] \Theta(z - z_0). \quad (6.37)$$

Then, taking the trace of the above propagator (3.13),

$$\text{Tr} K(x, y, z; x_0, y_0, z_0) = \int_{-\infty}^{+\infty} dx_0 \int_{-\infty}^{+\infty} dy_0 K(x=x_0, y=y_0, z; x_0, y_0, z_0). \quad (6.38)$$

and using the orthonormality of the mode eigenfunctions, the above result reduces to,

$$\text{Tr } K(x, y, z; x_0, y_0, z_0) = \sum_{n=0}^{\infty} \sum_{m=0}^{\infty} \exp[i\beta_{nm}(z-z_0)] \Theta(z-z_0). \quad (6.39)$$

The mathematical steps (6.37) to (6.39) which we used to arrive at the trace of the propagator can be given the following physical interpretation: $|K(x, y, z; x_0, y_0, z_0)|^2 dx_0 dy_0$ is the probability for a geometrical ray originating in the little element of area $dx_0 dy_0$ centred around (x_0, y_0, z_0) to pass through the element of area $dx dy$ centred on (x, y, z) . Setting $x = x_0$ and $y = y_0$ and integrating over all the $x_0 y_0$ plane, then gives the probability amplitude for a ray originating at any point on this plane to have the same transverse position in the xy plane. Equation (6.39) though shows that the trace of the propagator can also be interpreted as a sum of uniform plane waves moving along the z -axis, each with a propagation constant corresponding to the propagation constant of each of the waveguide modes. Given that in the geometrical optics picture a ray is defined to be the normal to a wavefront (Born and Wolf, 1980), each (n, m) component of the trace of the propagator may then be interpreted as the probability amplitude for a ray moving parallel to the z -axis to go from the $\zeta = z_0$ plane to the $\zeta = z$ plane with an effective propagation constant, β_{nm} , corresponding to the (n, m) mode of the guide. In other words, the trace of the propagator describes "equivalent" rays travelling parallel to the z -axis with different effective wavenumbers assigned to them.

In the case of a non-random waveguide, such as the one considered in the previous paragraph, the density of modes is, by definition, given by,

$$N(\beta) = \sum_{n=0}^{\infty} \sum_{m=0}^{\infty} \delta(\beta - \beta_{nm}). \quad (6.40)$$

Equations (6.39) and (6.40) suggest that the density of propagation modes can be derived from the propagator by a simple Fourier transform. Taking the Fourier transform of the expression for the trace of the waveguide propagator (6.39) with respect to $(z-z_0)$, gives,

$$\mathfrak{F}_\beta [Tr K] = \int_{-\infty}^{+\infty} d(z-z_0) \exp[-i\beta(z-z_0)] \sum_{n=0}^{\infty} \sum_{m=0}^{\infty} \exp[i\beta_{nm}(z-z_0)] \Theta(z-z_0). \quad (6.41)$$

The above integral can be evaluated if we introduce a positive and imaginary infinitesimal quantity, ϵ , to β_{nm} , and make the change of variable $z = z-z_0$.

$$\mathfrak{F}_\beta [Tr K] = \sum_{n=0}^{\infty} \sum_{m=0}^{\infty} \lim_{\epsilon \rightarrow 0} \int_0^{+\infty} dz \exp[-\epsilon z - i(\beta - \beta_{nm})z]. \quad (6.42)$$

Thus,

$$\mathfrak{F}_\beta [Tr K] = \sum_{n=0}^{\infty} \sum_{m=0}^{\infty} \lim_{\epsilon \rightarrow 0} \frac{-i}{\beta - \beta_{nm} - i\epsilon}. \quad (6.43)$$

We now need to make use of the following identity,

$$\lim_{\epsilon \rightarrow 0} \frac{1}{x \pm i\epsilon} \equiv P\left[\frac{1}{x}\right] \mp i\pi\delta(x), \quad (6.44)$$

where P is the principal part of any integral of the above expression we may take. Hence,

$$\mathfrak{F}_\beta [Tr K] = \sum_{n=0}^{\infty} \sum_{m=0}^{\infty} -iP\left[\frac{1}{\beta - \beta_{nm}}\right] + \pi\delta(\beta - \beta_{nm}), \quad (6.45)$$

and

$$\sum_{n=0}^{\infty} \sum_{m=0}^{\infty} \delta(\beta - \beta_{nm}) = \frac{1}{\pi} \Re e[\mathfrak{F}_\beta [Tr K]]. \quad (6.46)$$

Comparing (6.40) with (6.46), we can see that the density of propagation modes in the medium is related to the trace of the propagator by,

$$N(\beta) = \frac{1}{\pi} \Re e[\mathfrak{F}_\beta [Tr K]]. \quad (6.47)$$

The above expression can be generalised to a random, guiding, translationally invariant medium.

In a uniform medium, such as free space or the uniform random medium, equation (6.47) is no longer valid. The reason for this is that in a uniform medium, the trace of the propagator has an $\frac{1}{r}$ amplitude dependence in order for the propagating fields to satisfy the radiation boundary condition at infinity. As we have seen in section 2.5 of chapter 2,

this $\frac{1}{r}$ term becomes $\frac{1}{z}$ in the paraxial approximation. We now want to derive an equivalent expression to (6.47) for uniform media. We know that in free space (or in the non-random medium case), a wave of frequency ω has a unique propagation constant $k = \frac{\omega}{c}$. Its density of propagation modes is then given by,

$$n_0(\beta) = \delta(\beta - k). \quad (6.48)$$

Following the same steps as in the guiding medium case, we try to extract equation (6.48) from the free space propagator (2.54), while at the same time ensuring that a plausible physical interpretation is given to all the mathematical steps involved in the process. The free space propagator is given by,

$$K_0(x, y, z, x_0, y_0, z_0) = \Theta(z - z_0) \frac{k}{2\pi i(z - z_0)} \exp\left\{ik(z - z_0) + \frac{ik}{z - z_0}[(x - x_0)^2 + (y - y_0)^2]\right\}. \quad (6.49)$$

Setting $x = x_0$ and $y = y_0$ and making the change of variable $z \equiv z - z_0$, we have,

$$K_0(x = x_0, y = y_0, z, x_0, y_0, 0) = \Theta(z) \frac{k}{2\pi i z} \exp[ikz]. \quad (6.50)$$

Evidently, integrating the above expression over the entire $x_0 y_0$ plane yields a result which is formally infinite. It is perfectly legitimate though, to define the trace of the propagator of a uniform medium per unit cross-sectional area, S , which is given by,

$$\text{Tr } K_0(x_0, y_0, z, x_0, y_0, 0) / S = \Theta(z) \frac{k}{2\pi i z} \exp[ikz]. \quad (6.51)$$

As we have already mentioned, the trace of the propagator has an $\frac{1}{z}$ amplitude dependence. In order to extract information on the density of modes from (6.51), we need to consider an object which describes an equivalent uniform plane wave propagating along the z -axis, just as the trace of the propagator of a guiding medium was found to be a superposition of uniform plane waves in equation (6.39). In the language of quantum mechanics this is equivalent to the statement that uniform plane waves are momentum eigenstates. In the geometrical optics picture we need to account for the spreading of the rays which originate from a point source, so that all of them travel in the same direction, namely parallel to the paraxial axis. Multiplying both sides of the above expression by z , then accounts for the spreading of the rays. Taking the Fourier transform of the resulting

expression with respect to β , then gives,

$$\mathfrak{F}_\beta \left[\beta \operatorname{Tr} K_0(x_0, y_0, \beta, x_0, y_0, 0) \right] = kS/2 \int_{-\infty}^{+\infty} d\beta \Theta(\beta) \frac{1}{\pi i} \exp[ik\beta - i\beta\beta]. \quad (6.52)$$

Introducing a small positive infinitesimal quantity, ϵ , in the exponent, evaluating the integral and using the identity (6.44), then yields,

$$\mathfrak{F}_\beta \left[\frac{2\beta}{kS} \operatorname{Tr} K_0(x_0, y_0, \beta, x_0, y_0, 0) \right] = \frac{1}{\pi} P \left[\frac{1}{k-\beta} \right] - i \delta(\beta-k). \quad (6.53)$$

A comparison of (6.48) and (6.53) shows that, for a uniform medium the density of propagation modes is to be defined by,

$$N(\beta) = -\mathfrak{Im} \left\{ \mathfrak{F}_\beta \left[\frac{2\beta}{kS} \operatorname{Tr} K_0(x_0, y_0, \beta, x_0, y_0, 0) \right] \right\}. \quad (6.54)$$

Once again, the above expression can be directly generalised to a uniform random medium. We are now in a position to study various random media with specific two-point spatial correlation functions W .

6.6 The random medium which has a zero correlation length along the direction of propagation.

The random medium with zero correlation length along the direction of propagation is, as we shall shortly see, the simplest possible random medium which we can study. The simplicity of its analysis has made this random medium the subject of many studies of propagation in random media (Klyatskin and Tatarskiĭ, 1970, Hannay, 1977, Dashen, 1979). These analyses usually concentrate on calculating higher order propagator moments, which is a topic we will not enter into. Another way of looking at this random medium model is to consider it as a continuum of random phase screens, each completely uncorrelated with the rest.

The random parts of the refractive index, $V(x, y, z)$, are taken to be completely uncorrelated along the paraxial propagation axis (z -axis), and exhibit a Gaussian

correlation, with a finite correlation length L , in the plane transverse to the paraxial axis. The appropriately normalised two-point correlation function W is given by,

$$W(|\mathbf{r}-\mathbf{r}_0|) = \frac{W_0}{2\pi L^2} \delta(z-z_0) \exp\left[-\frac{(x-x_0)^2 + (y-y_0)^2}{2L^2}\right]. \quad (6.55)$$

The average propagator (6.35) corresponding to the above correlation functions is then given by,

$$\begin{aligned} G(x,y,z;x_0,y_0,z_0) = & \Theta(z-z_0) \int \int \delta x(z) \delta y(z) \times \\ & \exp\left\{ ik \int_{z_0}^z d\zeta \frac{1}{2} [\dot{x}^2(\zeta) + \dot{y}^2(\zeta)] + ik \int_{z_0}^z d\zeta \nu[x(\zeta), y(\zeta), \zeta] - \right. \\ & \left. \frac{k^2}{2} \int_{z_0}^z d\zeta \int_{z_0}^z d\zeta' \frac{W_0}{2\pi L^2} \delta(\zeta-\zeta') \exp\left[-\frac{(x(\zeta)-x(\zeta'))^2 + (y(\zeta)-y(\zeta'))^2}{2L^2}\right] \right\}. \end{aligned} \quad (6.56)$$

Carrying out the ζ' integral in the exponent of (6.56) is trivial because of the presence of the Dirac delta function in the integrand. The resulting term is independent of the paths $x(\zeta)$ and $y(\zeta)$ and can therefore be taken outside the path integral to give,

$$\begin{aligned} G(x,y,z;x_0,y_0,z_0) = & \Theta(z-z_0) \exp\left\{-\frac{W_0 k^2 (z-z_0)}{4\pi L^2}\right\} \int \int \delta x(z) \delta y(z) \times \\ & \exp\left\{ ik \int_{z_0}^z d\zeta \frac{1}{2} [\dot{x}^2(\zeta) + \dot{y}^2(\zeta)] + ik \int_{z_0}^z d\zeta \nu[x(\zeta), y(\zeta), \zeta] \right\}. \end{aligned} \quad (6.57)$$

The above result for the average propagator can be written in a more instructive and compact way as,

$$G(x,y,z;x_0,y_0,z_0) = \exp\left\{-\frac{W_0 k^2 (z-z_0)}{4\pi L^2}\right\} K(x,y,z;x_0,y_0,z_0; [V(x,y,z) \equiv 0]). \quad (6.58)$$

The above result is very simple and powerful. It states that in the case of random refractive index fluctuations whose correlation length in the direction of propagation is infinitesimally small, the phase of the propagator remains, on average, unperturbed. The amplitude of the propagator though, decreases exponentially with the distance travelled in the medium. For any given particular realisation of the random medium, the phasefronts of the propagating wave are however distorted. It is only when we average over all the possible realisations of the random medium that the phase error is found to have a zero

mean. In order to determine root-mean-square phase error on any given wavefront, we need to study higher order propagator moments (Hannay, 1977).

The average propagator in (6.58) can be directly used to determine the attenuation suffered by each waveguide mode as it propagates along the waveguide axis (z -axis). The transmission and reflection coefficients describing the total transmitted and the total reflected power from a waveguide of length $(z-z_0)$ are,

$$T = \exp\left\{-\frac{W_0 k^2 (z-z_0)}{2\pi L^2}\right\}, \quad (6.59a)$$

and,

$$R = 1 - \exp\left\{-\frac{W_0 k^2 (z-z_0)}{2\pi L^2}\right\}, \quad (6.59b)$$

respectively. The attenuation constant (Davidson, 1978) of this waveguide is then given by,

$$\alpha = \frac{W_0 k^2}{4\pi L^2} \quad \text{Np/m.} \quad (6.60a)$$

The same attenuation constant expressed in decibels per metre is then,

$$A = \frac{5W_0 k^2}{\pi L^2 \ln 10} \quad \text{dB/m.} \quad (6.60b)$$

Unfortunately, no information exists in the literature on the attenuation caused by random refractive index fluctuations in integrated optical waveguides. We can get a feel though for the magnitude of the mean square amplitude of these fluctuations, by doing the following order of magnitude calculation. All the numerical data quoted below have been taken from Table 7.1 in Lee (1986). The typical lower bound to the attenuation constant for integrated optical waveguides fabricated by a diffusion process is 1 dB/cm. The typical operating free space wavelength for these waveguides is $0.63 \mu\text{m}$. Finally, a typical value for the maximum refractive index n_0 is around 1.5. If we take into account that there are other loss mechanisms in an integrated optical waveguide other than scattering losses by random refractive index inhomogeneities, this puts an upper bound on the magnitude of W_0/L^2 , namely, $W_0/L^2 < 10^{-12} \text{ m}$.

The next piece of information that can be extracted from the average propagator expression (6.58), is the density of modes. By making the assumption that the deterministic part of the refractive index ν is independent of z , we are effectively

studying a waveguide structure having a uniform cross-sectional refractive index distribution along its length. This enables us to write down the propagator in terms of its eigenmode expansion (6.37). The density of modes for such a waveguide structure (6.47), is then given by,

$$N(\beta) = \frac{1}{\pi} \Re \int_{-\infty}^{+\infty} d\beta_3 \exp(-i\beta\beta_3) \int_{-\infty}^{+\infty} dx_0 \int_{-\infty}^{+\infty} dy_0 \sum_{n=0}^{\infty} \sum_{m=0}^{\infty} \varphi_{nm}(x_0, y_0) \varphi_{nm}^*(x_0, y_0) \exp(i\beta_{nm}\beta_3) \Theta(\beta_3) \times \exp\left\{-\frac{W_0 k^2 (z-z_0)}{4\pi L^2}\right\}. \quad (6.61)$$

Using the fact that the eigenmodes $\varphi_{nm}(x, y)$ are normalised, the final result for the density of propagation modes is,

$$N(\beta) = \sum_{n=0}^{\infty} \sum_{m=0}^{\infty} \frac{\frac{k^4 W_0^2}{4\pi^3 L^4}}{\frac{k^4 W_0^2}{4\pi^2 L^4} + (\beta - \beta_{nm})^2}. \quad (6.62)$$

The shape of the density of propagation modes is therefore a sum of Lorentzians, each being centred on the corresponding non-random waveguide mode propagation constant β_{nm} . Using the typical values for λ_0 , n_0 , and W_0/L^2 quoted above, the full width at half maximum of the Lorentzian curve (6.62) in units of k , is approximately 3×10^{-6} . The plot of $N(\beta)$ against β/k is shown in figure 6.2. The value for the full width at half maximum estimated above is a measure of the spectral spread which the propagation constant of each mode suffers, due to scattering by the random refractive index inhomogeneities. This is quite small, but nevertheless not difficult to detect using similar techniques to those used to determine intermodal dispersion in waveguides (Lee, 1986).

As we have mentioned before, the random waveguide model we have studied in this section has been the subject of extensive investigations by other researchers in the field. The specific results presented here are, to the best of our knowledge, entirely new.

6.7 The random medium which is completely correlated along the direction of propagation.

An alternative Gaussian random medium, which has received no study in the context of optical wave propagation, is the one in which the correlation function of the random part of the refractive index is independent of z . This implies that each particular realisation of the random refractive index inhomogeneity is invariant with respect to translations along the z -axis. Therefore, each particular realisation of the medium can be thought of as consisting of random, high or low refractive index rods of arbitrary cross section, parallel to the z -axis. One particular realisation of this random medium is shown in figure 6.3. This is the exact opposite of the random medium we have considered in the previous section, since the medium under study now has an infinite correlation length along the direction of propagation. In order to keep all other parameters the same between the two media, we choose the correlation function to be given by,

$$W(|\mathbf{r}-\mathbf{r}_0|) = \frac{W_0}{2\pi L^2} \exp\left[-\frac{(x-x_0)^2 + (y-y_0)^2}{2L^2}\right]. \quad (6.63)$$

The corresponding quantum mechanical problem is that of electronic motion in a two-dimensional disordered solid, in which the random potential is time-invariant. Our analysis closely follows that of Samathiyakanit (1972). The results presented at the end of this analysis are, nevertheless, new, since Samathiyakanit did not complete the calculation required by the Feynman variational technique (Feynman and Hibbs, 1965) in his paper. This work is also closely related to the work of Feynman on the polaron problem (1955).

As we have pointed out earlier, a physically realisable random medium in integrated optics should have a correlation length along the direction of propagation which is equal to, or at least has the same length scale as the correlation length in the plane transverse to the direction of propagation. What we choose to study instead, are the two extreme cases of random media with zero and infinite correlation length along the direction

of propagation, in the hope that we can gain some insight into the propagation mechanism in a physically realisable medium. The quantum mechanical problem corresponding to this physically realisable random medium in optics, is that of the motion of an electron in a disordered system in which the random potential has finite temporal and spatial correlation times and lengths respectively. This latter problem has also not been studied at all.

We are now in a position to write down the average propagator of the random medium defined by (6.63). As we shall soon see, the calculation of this propagator is rather lengthy and complicated, so for the sake of simplicity we choose $\nu(x, y, z) = 1$, $z_0 = 0$ and use the notation $\rho \equiv \begin{bmatrix} x \\ y \end{bmatrix}$. The average propagator is then given by,

$$G(\rho, z; \rho_0, 0) = \Theta(z) \exp(ikz) \int \delta\rho(z) \exp\left\{ ik/2 \int_0^z d\zeta \dot{\rho}^2(\zeta) - \right. \\ \left. k^2/2 \int_0^z d\zeta \int_0^z d\zeta' \frac{W_0}{2\pi L^2} \exp\left[-\frac{[\rho(\zeta) - \rho(\zeta')]^2}{2L^2} \right] \right\}. \quad (6.64)$$

The above path integral cannot be calculated exactly, and for this reason we will attempt to evaluate it approximately using Feynman's variational method (c.f. chapter 5, section 5.3). For simplicity of notation the term $\Theta(z) \exp(ikz)$ will not be written in the equations explicitly during the calculations. The trial path integral to be used in the variational calculation is that of the two dimensional non-local harmonic oscillator (Feynman and Hibbs, 1965, Samathiyakanit, 1972). A non-local harmonic oscillator is one in which the force and therefore the potential energy depend not on the instantaneous position coordinates of the oscillator, but instead on all its past positions. The context in which the non-local harmonic oscillator usually appears is in the study of the motion of atoms in a crystal lattice, where the pairwise interactions between the atoms can be modeled by harmonic oscillators. The propagator for such a non-local oscillator is,

$$G_t(\rho, z; \rho_0, 0; \omega) = \int \int \delta^2\rho(z) \exp\left\{ ik/2 \int_0^z d\zeta \dot{\rho}^2(\zeta) - \frac{ik\omega^2}{4z} \int_0^z d\zeta \int_0^z d\zeta' [\rho(\zeta) - \rho(\zeta')]^2 \right\} \quad (6.65)$$

where ω is an oscillation frequency which can be regarded as a free variational parameter.

Using equation (5.23) we may then write,

$$G(\rho, z; \rho_0, 0) \approx G_t(\rho, z; \rho_0, 0; \omega) \exp\{ik \langle S - S_t \rangle\}, \quad (6.66)$$

where

$$S = \int_0^z d\zeta \frac{1}{2} \dot{\rho}^2(\zeta) + ik/2 \int_0^z d\zeta \int_0^z d\zeta' \frac{1}{2\pi L^2} \exp\left[-\frac{[\rho(\zeta) - \rho(\zeta')]^2}{2L^2}\right], \quad (6.67)$$

$$S_t = \int_0^z d\zeta \frac{1}{2} \dot{\rho}^2(\zeta) - \frac{\omega^2}{4z} \int_0^z d\zeta \int_0^z d\zeta' [\rho(\zeta) - \rho(\zeta')]^2, \quad (6.68)$$

and the functional average $\langle . \rangle$ is now defined by,

$$\langle f \rangle = \frac{\int \int \delta^2 \rho(z) f \exp(ikS_t)}{\int \int \delta^2 \rho(z) \exp(ikS_t)}. \quad (6.69)$$

It should be noted that there exists a "similarity" between the trial optical path length (6.68) and the optical path length (6.67) we are trying to analyse. Both the correlation terms are non-local and have a minimum at $\rho(\zeta) = \rho(\zeta')$. In order to evaluate (6.66) we must now determine $\langle S \rangle$, $\langle S_t \rangle$ and G_t . Since only the difference $\langle S \rangle - \langle S_t \rangle$ is of interest and the first term in the expressions for S and S_t above is identical, the functional average of only the second terms need be considered below. In what follows $\langle S \rangle$ will be taken to mean the functional average of the second term in the expression (6.67), while S will be taken to be the whole of the expression (6.67). Similar considerations apply to $\langle S_t \rangle$ and S_t .

We must now calculate the three quantities $\langle S_t \rangle$, $\langle S \rangle$ and G_t . We first show that we can reduce the calculation of $\langle S_t \rangle$ and $\langle S \rangle$ to the calculation of the terms $\langle \rho(\zeta) \rangle$ and $\langle \rho(\zeta) \cdot \rho(\zeta') \rangle$, and evaluate the latter two using the method of characteristic functionals, introduced in chapter 5. G_t can be evaluated fairly easily once the above expectations have been computed, because as we shall shortly see we will have already evaluated S_t for the geometrical optics ray path, during the previous calculations. The path integral over the fluctuations around the geometrical optics ray path can also be

determined in a fairly easy manner, since the optical path length expression is quadratic in the ray path.

Using equation (6.68), we can see that we may directly write down the expression for $\langle S_t \rangle$, as,

$$\langle S_t \rangle = -\frac{\omega^2}{4z} \int_0^z d\zeta \int_0^z d\zeta' \langle [\rho(\zeta) - \rho(\zeta')]^2 \rangle. \quad (6.70a)$$

$$\text{or, } \langle S_t \rangle = -\frac{\omega^2}{4z} \int_0^z d\zeta \int_0^z d\zeta' \left\{ \langle \rho^2(\zeta) \rangle + \langle \rho^2(\zeta') \rangle - 2\langle \rho(\zeta) \cdot \rho(\zeta') \rangle \right\}. \quad (6.70b)$$

The corresponding expression for $\langle S \rangle$ may also be written down directly, using equation (6.67).

$$\langle S \rangle = ik/2 \int_0^z d\zeta \int_0^z d\zeta' \frac{1}{2\pi L^2} \left\langle \exp \left[-\frac{[\rho(\zeta) - \rho(\zeta')]^2}{2L^2} \right] \right\rangle. \quad (6.71)$$

In order to transform $\langle S \rangle$ into a similar form to (6.70), we first need to expand the Gaussian term under the integral sign as a Fourier transform with respect to $\rho(\zeta) - \rho(\zeta')$; this yields,

$$\langle S \rangle = ik/2 \int_0^z d\zeta \int_0^z d\zeta' \int_{-\infty}^{+\infty} \frac{d^2\kappa}{(2\pi)^2} \exp(-\kappa^2 L^2/2) \langle \exp[i\kappa \cdot (\rho(\zeta) - \rho(\zeta'))] \rangle, \quad (6.72)$$

where κ is the Fourier variable conjugate to $\rho(\zeta) - \rho(\zeta')$. Now S_t is a quadratic action, so that the $\exp(ikS_t)$ term is Gaussian in ρ . We may now use the well known fact that all the moments of a Gaussian distribution can be expressed in terms of the first and second moments only (Feynman and Hibbs, 1965). Expanding the term $\langle \exp[i\kappa \cdot (\rho(\zeta) - \rho(\zeta'))] \rangle$ into a power series with respect to $\rho(\zeta) - \rho(\zeta')$, averaging term by term, using the fact that the distribution is Gaussian, and resumming, gives,

$$\langle \exp[i\kappa \cdot (\rho(\zeta) - \rho(\zeta'))] \rangle = \exp \left[i\kappa \cdot \langle \rho(\zeta) - \rho(\zeta') \rangle - \frac{1}{2} \left[\frac{1}{2} \kappa^2 \langle [\rho(\zeta) - \rho(\zeta')]^2 \rangle - \kappa_x^2 \langle x(\zeta) - x(\zeta') \rangle^2 - \kappa_y^2 \langle y(\zeta) - y(\zeta') \rangle^2 \right] \right], \quad (6.73)$$

where $\kappa = (\kappa_x, \kappa_y)$. It is obvious by symmetry considerations on both $W(|\rho(\zeta) - \rho(\zeta')|)$ and S_t that $\langle x(\zeta) - x(\zeta') \rangle = \langle y(\zeta) - y(\zeta') \rangle$. Using this together with the fact that

$\kappa^2 = \kappa_x^2 + \kappa_y^2$ we may substitute (6.73) into (6.72) to obtain,

$$\begin{aligned} \langle S \rangle = ik/2 \int_0^z d\zeta \int_0^z d\zeta' \int_{-\infty}^{+\infty} \frac{d^2\kappa}{(2\pi)^2} \exp(-\kappa^2 L^2/2) \times \\ \exp\left[i\kappa \cdot [\langle \rho(\zeta) \rangle - \langle \rho(\zeta') \rangle] - \frac{1}{2}\kappa^2 \left[\langle \rho^2(\zeta) \rangle - \langle \rho(\zeta) \cdot \rho(\zeta') \rangle - \langle x(\zeta) - x(\zeta') \rangle^2 \right] \right]. \end{aligned} \quad (6.74)$$

The κ -integral can then be evaluated to give,

$$\langle S \rangle = ik/2 \int_0^z d\zeta \int_0^z d\zeta' \frac{1}{4\pi A} \exp\left[-\frac{B^2}{4A} \right], \quad (6.75a)$$

where,

$$A = \frac{1}{2} \left[L^2/2 + \langle \rho^2(\zeta) \rangle - \langle \rho(\zeta) \cdot \rho(\zeta') \rangle - [\langle x(\zeta) \rangle - \langle x(\zeta') \rangle]^2 \right] \quad (6.75b)$$

and

$$B = \langle \rho(\zeta) \rangle - \langle \rho(\zeta') \rangle. \quad (6.75c)$$

The calculation of $\langle \rho(\zeta) \rangle$ and $\langle \rho(\zeta) \cdot \rho(\zeta') \rangle$ can now be performed using the method of characteristic functionals, explained in detail in chapter 5. As this calculation is fairly lengthy, we present it in appendix C. The final results for $\langle S_t \rangle$, A and B are,

$$\langle S_t \rangle = \frac{i}{k} [(\omega z/2) \cot(\omega z/2) - 1] + \frac{1}{4} \{ (\omega z/2) \cot(\omega z/2) - [(\omega z/2) \operatorname{cosec}(\omega z/2)]^2 \} |\rho - \rho_0|^2, \quad (6.76)$$

$$A = L^2/4 + \frac{i}{k\omega} \frac{\sin[\omega(\zeta - \zeta')/2] \sin[\omega(z - (\zeta - \zeta')/2)]}{\sin(\omega z/2)}, \quad (6.77a)$$

and

$$B = \frac{\sin[\omega(\zeta - \zeta')/2] \cos[\omega(z - (\zeta + \zeta')/2)]}{\sin(\omega z/2)} (\rho - \rho_0), \quad (6.77b)$$

which are valid for $\zeta \geq \zeta'$ (see appendix C). Note that from equation (6.77a) the following important property of A which will be used later in the calculations can be inferred:

$$A(z, \zeta - \zeta'; \omega) = A(z, z - (\zeta - \zeta'); \omega) \quad (6.78)$$

Finally, the trial propagator G_t needs to be determined in closed form. By virtue of the fact that the optical path length is quadratic in ρ , we may use the method for integrating quadratic functionals (Feynman and Hibbs, 1965, Schulman, 1981), presented

in section 2.6 of chapter 2, to write,

$$G_t(\rho, z; \rho_0, 0; \omega) = F(\omega, z) \exp\{ikS_{t_{G_0}}\}, \quad (6.79)$$

where $F(\omega, z)$ is a function independent of the geometrical optics ray path and its endpoints, and $S_{t_{G_0}}$ is the optical path length corresponding to the geometrical optics ray path. $S_{t_{G_0}}$ can be derived from equation (C.20) in appendix C, by setting $f(\zeta) \equiv 0$. In order to determine $F(\omega, z)$ we make use of the fact that as $\omega \rightarrow 0$, the propagator must be reduce to that of free space. Thus,

$$\lim_{\omega \rightarrow 0} F(\omega, z) = \frac{k}{2\pi iz} \quad (6.80)$$

In Feynman and Hibbs (1965) it is shown that the propagator described by equations (6.65) and (6.79) can be obtained to within a multiplicative constant from the propagator of a local simple harmonic oscillator centred at ρ_1 ,

$$G_t(\rho, z; \rho_0, 0) = \int \delta\rho(z) \exp\left\{ik/2 \int_0^z d\zeta [\dot{\rho}^2(\zeta) - \omega^2 |\rho(\zeta) - \rho_1|^2]\right\}, \quad (6.81)$$

by integrating the origin ρ_1 of the harmonic oscillator over all possible positions in space. Thus,

$$\begin{aligned} & \int \int d^2\rho_1 \int \delta\rho(z) \exp\left\{ik/2 \int_0^z d\zeta [\dot{\rho}^2(\zeta) - \omega^2 |\rho(\zeta) - \rho_1|^2]\right\} \\ &= \frac{\pi}{ik\omega^2} \int \delta\rho(z) \exp\left\{ik \int_0^z d\zeta \frac{1}{2}\dot{\rho}^2(\zeta) - \frac{ik\omega^2}{4z} \int_0^z d\zeta \int_0^z d\zeta' [\rho(\zeta) - \rho(\zeta')]^2\right\} \\ &= \frac{\pi}{ik\omega^2} \int \delta\rho(z) \exp\{ikS_t\} \end{aligned} \quad (6.82)$$

The multiplicative factor F of the non-local oscillator can thus be related to the corresponding factor for the local harmonic oscillator, which is known from chapter 2. Making use of this fact, equation (6.82), and the limiting property (6.80), we arrive at the result,

$$F(\omega, z) = \frac{k}{2\pi iz} \left[\frac{\omega z/2}{\sin(\omega z/2)} \right]^2, \quad (6.83)$$

which is in agreement with the corresponding result in Samathiyakanit (1974). Equations (C.20) with $f(\zeta) \equiv 0$, (6.79) and (6.83) completely specify the non-local harmonic oscillator propagator. We are now in a position to substitute this propagator, together

with equations (6.75) to (6.78) in (6.66) to arrive at the approximate, but closed form result for the average random medium propagator,

$$G(\rho, z; \rho_0, 0) \approx \Theta(z) \exp(ikz) \frac{k}{2\pi iz} \left[\frac{\omega z/2}{\sin(\omega z/2)} \right]^2 \times \\ \exp \left\{ \{ (\omega z/2) \cot(\omega z/2) - 1 \} - \frac{W_0 k^2}{8\pi} \int_0^z d\zeta \int_0^\zeta d\zeta' A(z, \zeta - \zeta'; \omega)^{-1} \exp \left[- \frac{B^2(\rho - \rho_0; z, \zeta, \zeta'; \omega)}{4 A(z, \zeta, \zeta'; \omega)} \right] + \right. \\ \left. \frac{ik}{4z} \{ (\omega z/2) \cot(\omega z/2) + [(\omega z/2) \operatorname{cosec}(\omega z/2)]^2 \} |\rho - \rho_0|^2 \right\}. \quad (6.84)$$

As was explained in chapter 5, we now need to determine the value of the variational parameter ω which makes the above propagator a good approximation to the true propagator for the uniform random medium. This can be achieved by making the exponent of the trace of the above propagator an extremum with respect to ω . It should be noted that since the medium we are considering is uniform on average, only one mode of propagation exists, and therefore the analytic continuation of the variable z (c.f. section 5.3, chapter 5) is not necessary for the variational technique to work. By its very nature this work is almost entirely numerical, and we devote the next section of this chapter to it.

It is important to note though, that substituting for A and B in equation (6.84) shows that the exponent of the propagator contains both real and imaginary terms, resulting in the expected attenuation factor which we met in section 6.6. Here though, we have an additional phase shift term, which is ρ -dependent, and which can be interpreted as wavefront distortion. Average wavefront distortion is a phenomenon which we did not observe in the random medium with zero correlation length along the direction of propagation. The presence of average wavefront distortion is expected on intuitive grounds in the random medium with infinite, or long correlation length along the direction of propagation: in order to account for this phenomenon, we have to picture the long rod-like random refractive index inhomogeneities along the direction of propagation as a bunch of weakly guiding, coupled waveguides. Most of the wave amplitude tends to concentrate around the rods of high refractive index due to their guiding property (Born and Wolf, 1980), and then oscillate between such guides due to the fact that they are in

close proximity to each other and hence are coupled. This process significantly differs from the propagation mechanism which is governed solely by diffraction and for this reason both the average wave amplitude and phase tend to become distorted.

Finally, before we leave this section we must look at the general form that the density of propagation modes takes. The density of propagation modes corresponding to the above propagator is given by substituting the propagator expression (6.84) into the uniform medium density of modes expression (6.54) to get,

$$N(\beta) = -\frac{2}{k} \Im m \int_0^{+\infty} dz \frac{k}{2\pi i} \left[\frac{\omega z/2}{\sin(\omega z/2)} \right]^2 \exp\left\{ (\omega z/2) \cot(\omega z/2) - 1 \right\} - \frac{W_0 k^2}{8\pi} \int_0^z d\zeta \int_0^\zeta d\zeta' \frac{1}{A(z, \zeta - \zeta'; \omega)} + i(k - \beta)z. \quad (6.85)$$

Care is needed in evaluating the above expression, because as we will soon see the variational parameter ω turns out to be a function of z . We will consider the approximate numerical evaluation of the above expression in section 6.9.

6.8 The numerical calculation of the variational parameter ω of the propagator of the random medium which is completely correlated along the direction of propagation.

In order to determine the variational parameter ω , we need to differentiate the exponent of the trace of the propagator with respect to ω , set this expression equal to zero, and finally solve the resulting transcendental equation. It is important that all the terms which explicitly depend on ω appear in the exponent. The trace of the propagator is the expression which appears in the integrand of equation (6.85). Thus, we need to find the extremum of,

$$J \equiv (\omega z/2) \cot(\omega z/2) - 1 + \ln \left[\frac{\omega z/2}{\sin(\omega z/2)} \right]^2 - \frac{W_0 k^2}{8\pi} \int_0^z d\zeta \int_0^\zeta d\zeta' \frac{1}{A(z, \zeta - \zeta'; \omega)} + i(k - \beta)z. \quad (6.86)$$

with respect to ω . Substituting for $A(z, \zeta; \omega)$ from equation (6.77), the above expression

becomes,

$$J = (\omega z/2) \cot(\omega z/2) - 1 + \ln \left[\frac{\omega z/2}{\sin(\omega z/2)} \right]^2 + i(k-\beta)z - \frac{W_0 k^2}{8\pi} \int_0^z d\zeta \int_0^\zeta d\zeta' \frac{1}{\frac{L^2}{4} + \frac{i}{k\omega} \frac{\sin(\omega(\zeta-\zeta')/2) \sin(\omega(z-\zeta+\zeta')/2)}{\sin(\omega z/2)}}. \quad (6.87)$$

The integral in (6.87) can be evaluated exactly, to give,

$$J = i(k-\beta)z - 1 + (\omega z/2) \cot(\omega z/2) + \ln \left[\frac{\omega z/2}{\sin(\omega z/2)} \right]^2 - \frac{W_0 k^3 z}{2\pi} \frac{\tan^{-1} \sqrt{\tan(\omega z/4) \frac{(k\omega L^2/2) \tan(\omega z/4) - i}{(k\omega L^2/2) - i \tan(\omega z/4)}}}{\sqrt{1 + (k\omega L^2/2) - i (k\omega L^2) \cot(\omega z/2)}}. \quad (6.88)$$

We may now define the dimensionless parameters,

$$t \equiv \tan(\omega z/4), \quad (6.89a)$$

$$\alpha \equiv 2kL^2/z, \quad (6.89b)$$

and

$$\beta \equiv \frac{W_0 k^3 z}{4\pi}, \quad (6.89c)$$

which transform (6.88) to,

$$J = (1/t-t) \tan^{-1} t + 2 \ln(\tan^{-1} t) + 2 \ln(1/t+t) - 2\beta \frac{\tan^{-1} \sqrt{t \frac{\alpha t \tan^{-1} t - i}{\alpha \tan^{-1} t - i t}}}{\sqrt{1 + (\alpha \tan^{-1} t)^2 - i \alpha (1/t-t) \tan^{-1} t}}, \quad (6.90)$$

where we have dropped the term $i(k-\beta)z - 1$ which is independent of ω and will therefore vanish when we differentiate J with respect to ω . In order to determine ω we need to solve,

$$\frac{dJ}{d\omega} = 0. \quad (6.91)$$

Since ω is related to t through (6.89a),

$$\frac{dJ}{d\omega} = \frac{dJ}{dt} \frac{dt}{d\omega} = (z/4) \sec^2(\omega z/4) \frac{dJ}{dt} = \frac{z}{4} (1+t^2) \frac{dJ}{dt}. \quad (6.92)$$

We thus need to solve,

$$\frac{z}{4} (1+t^2) \frac{dJ}{dt} = 0, \quad (6.93)$$

for t . Assuming that $z \neq 0$, equations (6.90) and (6.93) give,

$$\frac{2}{\tan^{-1} t} - \frac{(1+t^2)^2}{t^2} \tan^{-1} t - \frac{1-t^2}{t} - \frac{\beta}{\sqrt{1 + (\alpha \tan^{-1} t)^2 - i \alpha (1/t-t) \tan^{-1} t}} \times \left[\frac{2\alpha^2 t (1+t^2) (\tan^{-1} t)^2 - \alpha^2 t (1-t) \tan^{-1} t + (1-t) (1+t^2) - i \alpha \{ (1+t^2) (1-t+2t^2) \tan^{-1} t - (1-t^3) \}}{\{ \alpha (1+t^2) \tan^{-1} t - 2it \} \sqrt{t^2 ((\alpha \tan^{-1} t)^2 - 1) - i \alpha t (1+t^2) \tan^{-1} t}} - \frac{2\alpha^2 t^2 \tan^{-1} t + i \alpha \{ (1+t^2)^2 \tan^{-1} t - t(1-t^2) \}}{t^2 ((\alpha \tan^{-1} t)^2 + 1) - i \alpha t (1-t^2) \tan^{-1} t} \right] = 0. \quad (6.94)$$

The above equation is a complex-valued transcendental equation and its solution can only be pursued numerically. The solution technique we chose was a Newton–Raphson method analytically extended to complex-valued functions and variables. By fixing the values of the two real dimensionless parameters α and β , we applied the Newton–Raphson method to obtain the corresponding value of t . Equation (6.94) turned out to have multiple-valued solutions in t . The main numerical problem we encountered was that the solution returned by the algorithm to determine t , tended to jump between different basins of attraction in the complex plane. To determine a continuous function of t in the two variables α and β , we executed the following logical steps in our algorithm. For small values of β the random refractive index inhomogeneities are very weak, and in this case our model requires that ω and thus t must also be very small. We thus chose the smallest t -solution corresponding to small values of the parameter β , used an extrapolation scheme to determine the starting value of t in the iteration process, and finally applied the complex Newton–Raphson scheme. This method has given us continuous surface plots in which the real and imaginary parts of $\omega z/4 = \tan^{-1}t$ are plotted against α and β . These latter plots can be seen in figures 6.4 and 6.5 respectively. As the numerical method is computationally very intensive we have chosen to plot a limited section of the surface plots for $10^{-2} \leq \alpha, \beta \leq 1$, on logarithmic α and β axes.

6.9 The density of propagation modes of the random medium which is completely correlated along the direction of propagation.

Equations (6.89) and (6.94), as well as the plots in figures 6.4 and 6.5 clearly show that the optimum value of ω is dependent on the length of the random medium z . Therefore, given the statistical specification of the random medium, we should write ω as $\omega(z)$. Bearing this in mind, the density of propagation modes (6.85) can be computed

numerically. Unfortunately, because the calculation giving $\omega(z)$ is numerically intensive, the exact determination of the density of propagation modes turns out to be prohibitively time consuming on the available computing resources. Even if the calculation were to be executed on a more powerful computer we have found that for very large values of z , even the complex Newton–Raphson method with the extrapolation scheme for obtaining the initial value of t in the iteration process, failed in unpredictable ways.

In order to proceed with an approximate calculation of the density of modes we must make a physically justifiable guess for the closed form expression for the variational parameter ω . The only such guess can be made if we look at the two non–local optical path length terms in the average random medium propagator (6.64) and the trial propagator (6.65). The reason we have chosen the trial action to have the specific form shown in (6.65) was that both the non–local terms have a minimum at $\rho(\zeta) = \rho(\zeta')$. We may now claim that in order to make the two terms as similar as possible, we need to equate their curvature at $\rho(\zeta) = \rho(\zeta')$, which determines the value of ω ,

$$\omega = \sqrt{i \frac{W_0 k z}{2 \pi L^4}}. \quad (6.95)$$

The above expression for ω gives a reasonable approximation to the value of $\omega(z)$ found using the numerical technique described in the previous section, for small β , but ceases to be a good approximation for large values of β . Large values of β correspond to very large values of the length of the random medium z , which, using a stationary phase argument, are not expected to contribute significantly to the integral expression for the density of propagation modes (6.85). We now define the following dimensionless parameters,

$$u \equiv kz, \quad (6.96a)$$

$$b \equiv \beta/k, \quad (6.96b)$$

$$l \equiv kL, \quad (6.96c)$$

and

$$p \equiv \sqrt{\frac{ik^2 W_0}{2 \pi}}. \quad (6.96d)$$

We can also define a dimensionless density of propagation modes by,

$$P(b) db = N(\beta) d\beta. \quad (6.96e)$$

Making use of the result (6.88) for the exponent of the density of propagation modes (6.85), we find that,

$$N(\beta) d\beta = P(b) db = \frac{1}{\pi} \int_0^{+\infty} du \Re e \left[\left[\frac{p\sqrt{u^3}/2l^2}{\sin(p\sqrt{u^3}/2l^2)} \right]^2 \exp \left\{ i(1-b)u + \left[\frac{p\sqrt{u^3}}{2l^2} \right] \cot \left[\frac{p\sqrt{u^3}}{2l^2} \right] - 1 - \frac{p^2u}{i} \frac{\tan^{-1} \left[\frac{\tan(p\sqrt{u^3}/4l^2) \frac{(p\sqrt{u}/2) \tan(p\sqrt{u^3}/4l^2) - i}{(p\sqrt{u}/2) - i \tan(p\sqrt{u^3}/4l^2)} \right]}{\sqrt{1 + p^2u/4 - ip\sqrt{u} \cot(p\sqrt{u^3}/2l^2)}} \right\} \right] db. \quad (6.97)$$

A plot of the dimensionless density of modes, $P(b)$, against b for $l = 30$ and $k^2 W_0 = 10^{-3}$ is shown in figure 6.6. The chosen values of the parameters correspond to $L \simeq 4.775 \lambda$ and $W_0/L^2 \simeq 1.11 \times 10^{-6}$. Using the definition (6.4) and two-point correlation function (6.63), we can see that the value of W_0/L^2 implies that the order of magnitude of the random refractive index inhomogeneities is, $\langle \delta n/n_0 \rangle \simeq 10^{-3}$. Once again, we can see that the density of propagation modes is sharply peaked around the non-random uniform medium propagation constant k , and that the spread of the propagation modes is very small. Using a non-linear least squares fitting procedure provided in the NAGTM workstation library, it was found that curve of figure 6.6 is best approximated by a Lorentzian rather than a Gaussian curve (the optimum residual mean square error for the Lorentzian fit was approximately one half that of the Gaussian fit). The equation that was found to best describe the curve in figure 6.6 was, though neither a Lorentzian nor a Gaussian, but,

$$N(b) \simeq 1507 \times \exp \left\{ - \left[\frac{|b-1|}{3.1 \times 10^{-4}} \right]^{1.251} \right\}. \quad (6.98)$$

What is important to stress here, is that the Lorentzian fit which is an acceptable analytical description for the density of propagation modes, shows that the latter does not change appreciably when the correlation length along the paraxial axis of propagation varies from zero to infinity. This is an important new result for the weakly inhomogeneous random medium that has come out of our analysis.

6.10 Conclusions.

In this chapter we have given the definition of a model Gaussian random medium which is potentially applicable to integrated optical waveguides formed by a process of diffusion. We then derived a path–integral expression for the average propagator of such a random medium, and found the propagator to be dependent on the two–point correlation function of the random refractive index inhomogeneities. The concept of the density of propagation modes, which is new to optics, was then introduced together with its probabilistic interpretation in the context of geometrical optics.

Subsequently, we applied the above formalism to two random media: one with a zero correlation length along the direction of propagation and one with an infinite correlation length along the direction of propagation. The path–integral expression for the propagator of the latter medium was evaluated in an approximate form using Feynman’s variational technique (Feynman and Hibbs, 1965), as adapted by Samathiyakanit (1972). The corresponding expression for the density of modes was obtained numerically. The propagator and density of modes of the random medium with a zero correlation length along the direction of propagation were evaluated exactly in closed form. We found that the shape of the density of propagation modes did not differ dramatically for the two types of random media we considered, a result we believe to be new.

The other new result which we have demonstrated, is that the average phasefront distortion is a phenomenon which strongly depends on the value of the random refractive index inhomogeneity correlation length along the direction of propagation. No average phasefront distortion was found to exist for the random medium with a zero correlation length along the direction of wave propagation, in contrast to the random medium with an infinite correlation length. As most of the work on random media tends to assume that this correlation length is zero for the sake of simplicity in the analysis (c.f. section 6.6), this phenomenon is not very well understood. The average phasefront distortion is an

important quantity in optical engineering, because it significantly degrades the coupling efficiency of most optical coupling devices, such as lenses, tapered waveguides, etc. We will reserve any suggestions for further work and its possible engineering significance and applications until chapter 7.

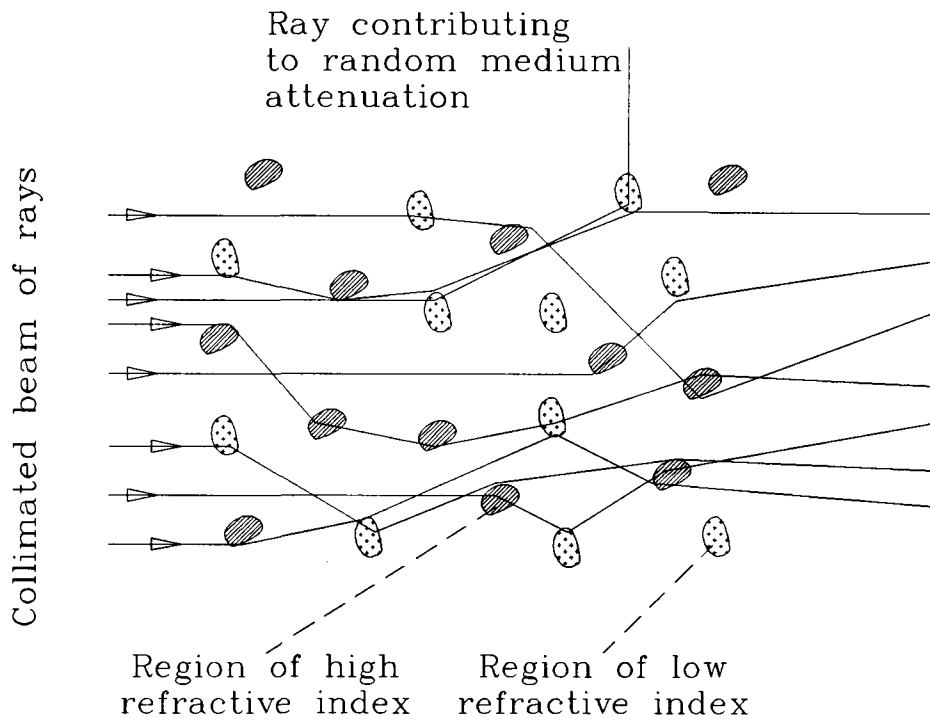


Figure 6.1:

A pencil of collimated rays propagating in a weakly inhomogeneous random medium emerges with most of the rays travelling roughly along their original direction of propagation.

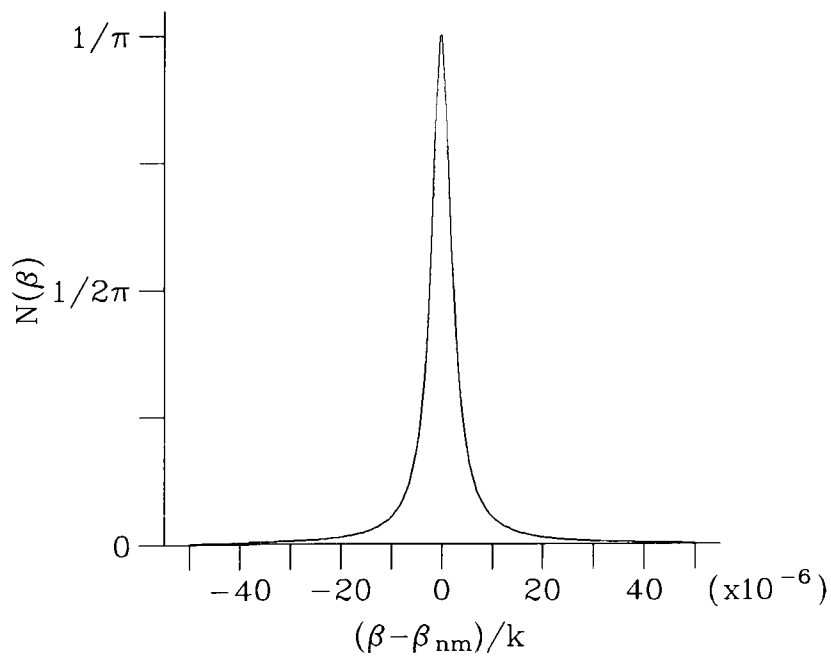


Figure 6.2:

The density of propagation modes for the random medium with a zero refractive index inhomogeneity correlation length along the direction of propagation. We have chosen $\lambda_0 = 0.63\mu m$ and $W_0/L^2 = 10^{-12}$.

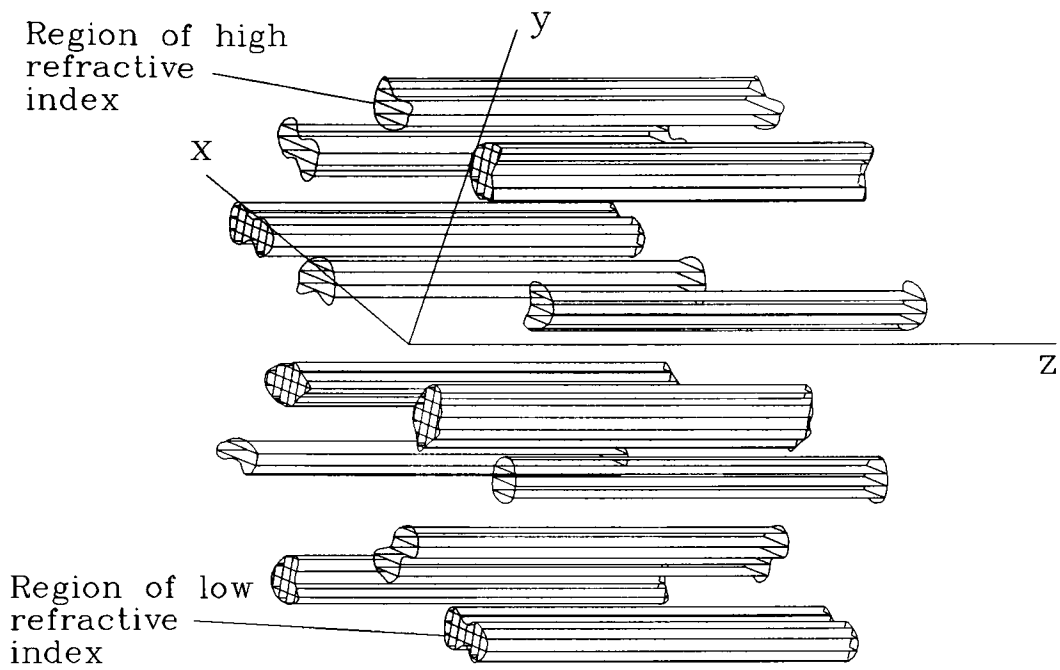


Figure 6.3: A schematic picture of the random refractive index inhomogeneities in a random medium with an infinite refractive index inhomogeneity correlation length along the direction of propagation. The typical cross-sectional sizes and separation of the regions of high and low refractive index is $\sim L$.

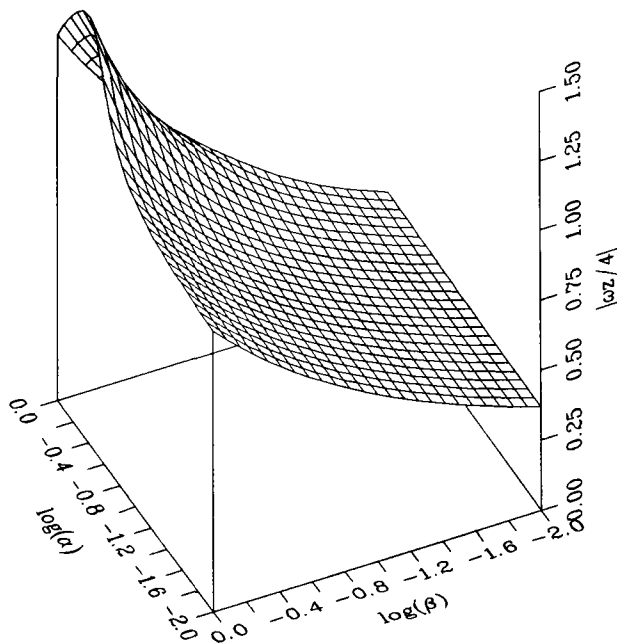


Figure 6.4: The magnitude distribution of the complex, dimensionless variational parameter $\omega z/4$ plotted against the two dimensionless parameters α and β .

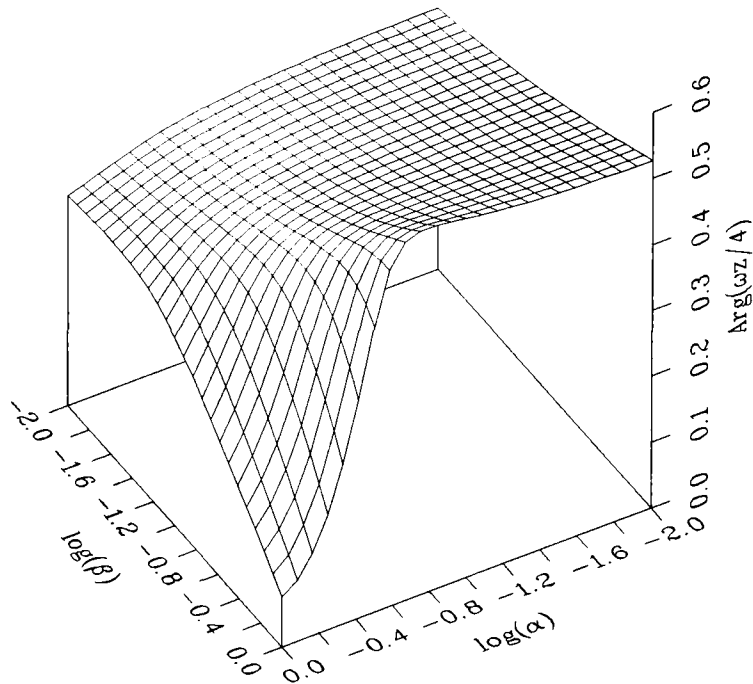


Figure 6.5: The phase distribution of the complex, dimensionless variational parameter $\omega z/4$ plotted against the two dimensionless parameters α and β .

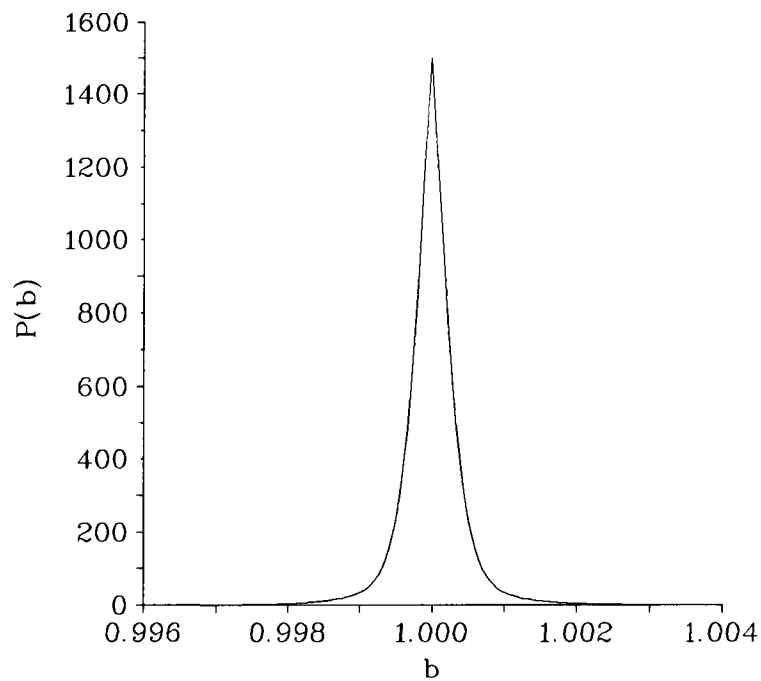


Figure 6.6: The dimensionless density of propagation modes $P(b)$ plotted against $b \equiv \beta/k$ for the random medium with an infinite refractive index inhomogeneity correlation length along the direction of propagation. We have chosen $l = 30$ and $k^2 W_0 = 10^{-3}$.

Chapter 7.

Conclusions and Further Work.

7.1 A general overview of the work presented in the thesis.

In chapter 1 we looked at the reasons for studying the propagation of optical waves in passive graded-index dielectric waveguides, the main one being that they are an essential component in the realisation of modern integrated-optical communications systems. Furthermore, we pointed out that the majority of graded-index waveguide geometries of practical significance, such as tapered waveguide sections, tapered couplers and waveguide junctions, are difficult to study analytically. Most waveguide structures in the above categories were seen to consist of three basic building blocks: single isolated waveguides, tapered waveguides, and coupled waveguides having a variable spacing (see figures 1.1 and 1.2). We then introduced some of the most important existing methods of analysis for such waveguide structures (see e.g. Feit and Fleck, 1978, Snyder and Love, 1983, Marcuse, 1982), and pointed out that these usually use the paraxial and weak guidance approximations. We subsequently used Maxwell's equations to derive the differential equation which describes paraxial, scalar wave propagation in weakly inhomogeneous media, in order to quantify the conditions of its validity. Finally, we presented the well-known analogy between paraxial, scalar wave optics and the quantum mechanical motion of a non-relativistic, spin-0 particle, which forms the basis of all the work in this thesis (c.f. Table 1.1).

In chapter 2 we gave the definition of a path integral and a brief summary of its past use in the various branches of theoretical physics. The analogy between wave optics and quantum mechanics first presented in chapter 1 was then extended to geometrical optics and classical mechanics. This more general analogy between optics and mechanics

was then used to derive a path–integral description of paraxial, scalar wave propagation in weakly inhomogeneous media, starting from Fermat’s principle. The properties and the probabilistic interpretation of the propagator of the paraxial, scalar wave equation were then presented in some detail. Finally, the path–integral description of wave optics and quantum mechanics was shown to provide a conceptually unifying framework for describing, not only the analogy between optics and mechanics, but also the way in which the transition can be made between geometrical optics and wave optics, classical mechanics and wave mechanics, and vice–versa (see figure 2.3).

The well known results for the propagator of paraxial, scalar waves in free space as well as the propagator of a model dielectric waveguide with a parabolic refractive index distribution of infinite extent in the directions transverse to the direction of propagation, were then derived in order to illustrate a couple of simple applications of path integration. The propagation of a general Gaussian beam in free space was studied using the expression for the free space propagator, and the expressions for the beam amplitude properties arrived at, were found to be in a much more compact form than those arrived at by more conventional analyses (Yariv, 1991). Furthermore, we argued that the infinite parabolic refractive index waveguide can be used as an accurate model for a number of practical devices such as a graded–index fibre, but more importantly it can be considered as an archetypal waveguide model for dielectric waveguides formed by a process of diffusion.

Chapters 3 and 4 were mainly concerned with the study of a number of parabolic–refractive–index waveguide geometries. The first waveguide structure considered was the one introduced in chapter 2, and which models a waveguide whose cross–section is uniform along its length. Two methods for extracting information on the various mode field distributions and their corresponding propagation constants were presented for uniform waveguide structures, and their application was illustrated for the uniform parabolic–refractive–index waveguide. The propagation of a Gaussian beam in this waveguide was considered in some detail using the propagator expression derived in

chapter 2. Once again, new compact results describing the propagation of a general Gaussian beam in such a model waveguide were derived.

The remainder of chapter 3 and the entire chapter 4 were then devoted to the study of tapering parabolic refractive index waveguides. In chapter 3 we derived, in closed form, the propagator of a waveguide whose contours of constant refractive index are straight lines, symmetrically inclined around the guide axis, chosen to be the z -axis of a Cartesian coordinate system. Throughout this thesis we used the constant refractive index contour lines specified by $n(x, \theta, z) = n_0/2$, where n_0 is the maximum value of the refractive index, in order to describe the geometry of the tapered waveguide. The waveguide described above was thus named a linear taper. The various expressions for the coupling efficiency between the lowest order and first even excited modes of the waveguides with matched refractive index distributions at the two ends the linear taper, were obtained in closed form. In particular, we looked at the expression for the coupling efficiency between the two lowest order local modes of the input and output waveguides, and used this to arrive at a practical design criterion (c.f. equation (3.65)) specifying the condition for optimum lowest order mode operation of a multimode linear taper. The propagation of a Gaussian beam in a linear taper was also considered in some detail. We studied the propagation of a Gaussian beam excited by the lowest order mode of matched input waveguide, which enabled us to specify when the approximate local normal mode analysis is applicable to the study of the graded-index linear taper. Furthermore, we were able to verify a posteriori the validity of the paraxial approximation. All the results on the linear graded-index taper are new, and unlike most conventional analyses (Marcuse, 1970, Snyder and Love, 1983), they are exact within the approximation of paraxial propagation in a weakly guiding medium.

In chapter 4 we obtained a closed form expression for the propagator of an arbitrarily tapered, parabolic-refractive-index waveguide, in terms of a single unknown function, which for most geometries of interest can be easily determined in closed form.

The coupling efficiency between any combination of modes of the matched input and output waveguides to this taper, as well as the propagation characteristics of the Gaussian beam excited by the lowest order mode of the input matched waveguide, were also obtained in terms of this unknown function. For the special cases where the geometry of the contours of constant refractive index can be described in terms of a power law, or an exponential function in z , the unknown function mentioned above was shown to be given by simple cross-product expressions of Bessel functions. The cases of parabolic, inverse-square-law and exponential geometries were finally studied in some detail. We concluded that as far as their lowest order mode operation is concerned, the parabolic taper was found to be the optimum geometry having a very high coupling efficiency for short taper lengths. The linear taper was also found to be useful in its single mode operation, provided the taper length is not a critical parameter in the design process. All the results in this section are believed to be new, with the exception of the propagation characteristics of a Gaussian beam in an exponentially tapering waveguide, for which perfect agreement was found to exist between our predictions and those of Casperson (1985).

In chapter 5, we looked at the problem of propagation in a medium whose refractive index distribution models a pair of graded-index waveguides in close proximity. Our model allows for a variable separation between the two coupled waveguides, while at the same time attempting to incorporate a realistic dependence of the refractive index distribution between the two waveguides with their distance of separation (see figure 5.1). In order to evaluate the path integral and arrive at a closed form expression for the propagator, we first had to present the Feynman variational technique (Feynman and Hibbs, 1965). This technique is a useful method for finding the approximate propagator of a medium with a refractive index distribution which has a number of similarities with a trial refractive index distribution. The main requirements are that the two waveguiding structures are invariant along the axis of propagation, and that the trial refractive index

distribution is one for which we know how to evaluate the path integral expression for its propagator exactly. We used the arbitrarily tapered parabolic refractive index waveguide propagator as the starting point of the variational method and were able to arrive at a new, closed form result for the approximate propagator of the system of two coupled waveguides having an arbitrary separation distance. As in the case of the arbitrary taper, this propagator expression was found to depend on an arbitrary function specified by a partial differential equation. The variational technique requires the determination of the optimal value of the various parameters built into the trial refractive index distribution, which can only be determined in a rigorous manner for the parallel waveguide case. We proposed an ansatz which attempts to match the trial and the coupled waveguide refractive index distributions at each and every z -cross-section, and which allows us to determine, in principle, this unknown function. We then proceeded to examine the parallel coupled graded-index waveguide case in more detail. We were able to arrive at new results for the beat length, the propagator, and information on the propagation constants of the first two of modes of such a waveguide structure. We were also able to arrive at an approximate expression for the lowest order mode field profile. Our new results were found, on theoretical grounds, to be more accurate compared to existing analyses (Wiegel, 1973, 1975, 1986, Landau and Lifshitz, 1977), when the coupling between the two waveguides is either strong, or of intermediate strength. It is worth pointing out that these are precisely the two cases which are of interest in optical engineering. One of the intermediate steps in the calculation of the propagator of the two coupled graded-index waveguides, was the determination of the propagator of the forced harmonic oscillator for which both the spring stiffness and the external force are arbitrary functions of time – a result also new.

The penultimate chapter in this thesis (chapter 6) was concerned with propagation in a random medium. After a brief explanation behind the motivation for the study of propagation in a random medium in the context of integrated optics, we presented a refractive index model for a Gaussian random medium. The average propagator for such a

medium having an arbitrary refractive index inhomogeneity correlation function, was then derived in some detail. Averages of products of propagators, which are useful in determining the various statistics of the field distributions in random media, were not considered in this work. Instead, we concentrated on obtaining as much information as possible from the average propagator. To do this, we introduced the concept of the density of propagation modes, which bears a direct analogy with the density of states in solid state physics. This concept is new in optics, and we therefore had to provide a physical interpretation for it, based on the probabilistic interpretation of the propagator in terms of geometrical rays. Two distinct random media characterised by their refractive index inhomogeneity correlation functions were examined in this chapter. The first one is the random medium which has a zero correlation length along the direction of wave propagation. This random medium is very easy to analyse, and this is the reason why it has been the subject of almost all other studies of propagation in random media known to us (Klyatskin and Tatarskiĭ, 1970, Hannay, 1977, Dashen, 1979). The density of modes and attenuation constant of the random medium with zero correlation length along the direction of propagation were determined, and these are believed to be new results. One of the important new conclusions we reached was that such a medium does not, on average, give rise to any phasefront distortion.

The second medium on which we focused our attention was the random medium which has an infinite random refractive index inhomogeneity correlation length along the direction of propagation. The analysis of this section of chapter 6 is largely based on Samathiyakanit's (1972) incomplete calculation of the average propagator of an electron moving in a disordered solid. The analysis of this random medium makes use of Feynman's variational technique, using as a trial propagator that of the non-local harmonic oscillator. Although the expressions for the average propagator and the density of propagation modes derived are in agreement with those of Samathiyakanit (1972), they are new in the context of the optical propagation problem. A suitable choice of dimensionless

parameters was made to enable us to perform the minimisation calculation required by the variational technique. The complete variational calculation is a new result presented for the first time in this thesis. In this way we were able to determine numerically the optimum value of the free variational parameter, which in this problem was chosen to be the spring stiffness of the non-local harmonic oscillator. As the optimum value of the variational parameter was found to be dependent on the z -coordinate variable (the distance of propagation into the random medium), the exact calculation of the density of propagation modes was found to be computationally intensive, to the point where we could not complete it using the available computing resources. A physically justifiable guess for the value of this parameter was then made, which enabled us to compute an estimated density of propagation modes. The shape of the curve of the density of propagation modes was found to be similar to the corresponding curve for the random medium with zero correlation length along the direction of propagation. One of the important results which could be directly observed from the average propagator expression of the random medium with an infinite correlation length along the direction of propagation, was that, on average, a propagating wave suffers wavefront distortion as well as attenuation, in contrast to the case of zero correlation length when only attenuation is observed. Quantitative information on the average phasefront distortion is important in optical engineering, as phasefront distortion severely degrades the coupling efficiency performance of devices used as couplers or connectors. The physical reason for the presence of wavefront distortion is well understood. For each realisation of the random medium, the refractive index inhomogeneities form parallel, randomly positioned "tubes" along the z -axis, having a uniform, random cross-section (see figure 6.3). Some of these "tubes" have a refractive index which is higher than that of the surrounding region and thus act as a collection of parallel waveguides, each having a different set of modal propagation constants. Therefore, their presence does not only concentrate the wave amplitude in the vicinity of each of these guides, but also results in the various parts of the wave

propagating at different speeds, in a manner which is even more complicated by the fact that these waveguides are coupled. On average, the wave amplitude as well as its surfaces of constant phase are distorted, which is in agreement with the results of chapter 6.

7.2 Suggested further work.

There are a number of topics related to the work in this thesis which deserve further study, some of them being a continuation of the work we presented, and some being completely new. In the next few paragraphs, we will try to list the six main areas in which further work is either planned, or is desirable.

(a) The predictions of the path–integral analysis on the coupling efficiency of parabolic–refractive–index waveguides of various geometries should be compared to experimental work on the subject, WKB and numerical analyses. This would provide us with a framework for checking the usefulness of our results in comparison to other existing methods of analysis. If the tapers are sufficiently slowly varying, a WKB analysis could prove very useful in solving the differential equation (4.7) for the taper function $f(z, z_0)$ approximately, for an even greater variety of taper geometries than those considered in this thesis.

(b) The problem of wave propagation in a pair of non–parallel coupled waveguides, whose distance of separation varies arbitrarily, has by no means been exhaustively covered in chapter 5. Further work resulting in approximate closed form expressions for the propagator of specific coupled waveguide geometries will undoubtedly be a valuable contribution to the subject of mathematical modeling in optics. The possibility of modifying the variational technique so that an Euler–type equation can be found for non–parallel waveguide geometries, is also something that should be looked into seriously.

(c) More realistic refractive index models describing graded–index waveguides

formed by a diffusion process can be examined approximately, by making use of Feynman's variational technique. As in many other problems in physics (see e.g. Feynman, 1955, Hannay, 1977, Wiegel, 1986), use of path integration in conjunction with the Feynman variational technique, results in obtaining approximate solutions to problems for which results are unobtainable by other means. Such work, resulting in closed form results, is expected to complement existing numerical methods of analysis by providing the designer of optical circuits with more insight into the propagation mechanism relevant to the waveguide structure of interest.

(d) The propagators of straight, uniform waveguides (c.f. chapters 2 and 3), tapered waveguides (c.f. chapters 3 and 4), and coupled waveguides (c.f. chapter 5 and paragraph (a) above) can be cascaded together using their Markov property, in order to yield the propagator of a wide variety of graded-index waveguide junctions and couplers. In this sense, the results presented in chapters 2 to 5 in this thesis can be used as an analytical tool in the study of fairly complex graded-index waveguide structures, which in the past could only be studied numerically. Using this approach a simulation software package used for analysing graded-index waveguide networks could be written. Such a simulation programme might be less accurate in its predictions than more conventional numerical simulation schemes (e.g. the beam propagation method – see chapter 1), but would probably prove to be much faster in the study of very complex optical networks.

(e) An extension of the work of chapter 6 to the study of random media with a finite refractive index inhomogeneity correlation length along the direction of wave propagation, would be valuable, not only in the context of optics, but also in more general wave propagation studies. The cases when this correlation length is small, large, and comparable to either the wavelength, or the correlation length in the plane transverse to the direction of wave propagation, deserve particular attention if we are to gain any better insight into the mechanisms of wave propagation in random media. An important question which any future research on this subject should try to address, is whether there

exists some critical correlation length along the direction of propagation, at which phasefront distortion becomes significant. Serious consideration should finally be given to any future work which is going to yield information on higher order field statistics for these more complicated random media. Such work will be a natural extension of Hannay's work (Hannay, 1977) on the random medium with zero refractive-index-inhomogeneity correlation length along the direction of wave propagation.

(f) One of the reasons behind the reluctance of a large number of people to use path integration as a practical tool for doing many types of calculations, is the fact that at present the only way of evaluating path integrals numerically is using fairly naive Monte-Carlo methods (Schulman, 1981, Hawkins, 1987, 1988, Troudet and Hawkins, 1988). We strongly feel that much research into the efficient numerical evaluation of path integrals is needed before they gain the same acceptance that differential equations have. Depending on the wavelength and the characteristic length scales of the medium in which propagation takes place, an efficient computational scheme could neglect a very large number of paths which deviate significantly from the ray paths specified by geometrical optics. Similarly, an efficient computational scheme should be able to identify other classes of paths whose omission for any computations does not result in any significant loss of accuracy in the final result. Examples of such paths might be fractal paths of certain fractal dimensions (Amir-Azizi, Hey and Morris, 1987), given the dimensionality of the system we are studying.

7.3 Conclusions.

The use of path integration in the study of paraxial, guided wave optics was suggested by a significant number of people over the past twenty years (Eichmann, 1971, Eve, 1976, Schulman, 1981, Marcuse, 1982, Hawkins, 1987, 1988, Troudet and Hawkins, 1988). As a rule, all these researchers either demonstrated that the path-integral

formulation of paraxial, scalar wave optics is possible, or have applied path integration to the study of fairly simple waveguide structures. In this thesis, we have demonstrated that the technique of path integration can be successfully applied to the study of more complicated graded-index waveguide structures, which are useful from the engineering point of view. The results obtained on arbitrarily tapered graded-index waveguides and the strongly coupled graded-index waveguides of variable separation are not only new, but cannot be readily obtained using any other method of analysis. We feel, therefore, that we are in a position to claim that the work presented in this thesis is the first successful application of path integration to non-trivial problems in optics. The main limitation of our work is that we have only considered refractive index profiles in which the refractive index takes non-physical values at large distances away from the waveguide axis. This, as we explained at some length in chapters 2 and 3 does not compromise the usefulness of our results, so long as we confine our model to multimode waveguides. Results such as the high lowest order mode coupling efficiency criterion for the linear taper, the beat length of two strongly coupled parallel graded-index waveguides and the attenuation constant of a waveguide with random refractive index inhomogeneities are testimony to the fact that a seemingly complex mathematical technique can produce simple, but nevertheless valuable practical information which can be used in the design of integrated optical waveguide systems.

Before closing this thesis, we feel that it is necessary to spell out the advantages and disadvantages of using path integration over more conventional methods of solving the paraxial wave equation.

Let us begin with the disadvantages first. The instances in which the path integral can be evaluated exactly are very few indeed (Schulman, 1981, Wiegel, 1986). Usually, we must be contented with an approximate solution to the problem, obtained using either a perturbative or a variational approach (Feynman and Hibbs, 1965). The calculations involved in solutions of the above type are, as is evident from a fair number of the

calculations presented in this thesis, often lengthy and complex, but not necessarily difficult. Lastly, there exist many more well established and accurate computational techniques for solving differential equations than path integrals.

On the other hand, path integrals have a large number of advantages compared to differential equations, which for certain kinds of problems outweigh their disadvantages. First and foremost, it is intuitively much easier to think in terms of ray paths and the contribution of their optical path length to the propagator on a global basis (even in the presence of boundaries), rather than considering the local relationships between a function and its derivatives, together with the additional problem of treating the boundary conditions as an afterthought. This point is stated more elegantly by DeWitt–Morette, Low, Schulman and Shiekh (1986), where they use path integration to find the propagator of scalar waves diffracted over a wedge. This advantage is, to some extent, a subjective one, as it depends on our personal perspective of the way any physical problem should be solved: the path integral description of optics unifies geometrical and wave optics in a way which is intuitive and much more satisfactory compared to differential equations (c.f. figure 2.3).

In many instances, the above advantage turns out to be an objective one, as the path–integral representation allows us to see at a glance the paths of the system which are important. For example, the semi–classical WKB method can be generalised if we take into account that only paths in the vicinity of the ray path specified by geometrical optics, for which $\delta S \sim \lambda/2\pi$, contribute significantly to the propagator. By writing these paths in the form of *Fermat path + fluctuation* and expanding the optical path length S up to second order in the fluctuation, we can obtain an approximate form of the propagator,

$$K \cong \sum N[\textit{Fermat path}] \times \exp\{ikS[\textit{Fermat path}]\}, \quad (7.1)$$

where N is the integral over the fluctuations, and the sum is over all the Fermat paths for the optical system in question. Approximate propagators obtained using the generalised semi–classical WKB approximation, have a non–perturbative character and

often lead to non-analytic results (Wiegel, 1986, section 5.1). Furthermore, use of the Feynman variational technique presented in chapter 5, outweighs the disadvantage of having a very limited number of path integrals which can be evaluated exactly, as it often leads to results which are unobtainable by other means (e.g. see Hannay, 1977, chapter 6; Feynman, 1955; and the propagators of the arbitrary taper and the strongly coupled graded-index waveguides in chapter 5 of this thesis).

Another important advantage we have found in using path integrals is that it allows parallels to be drawn between different areas of physics, which are seemingly very different from each other. The analogy between quantum mechanics and paraxial wave optics which we have used throughout this thesis, is not a particularly good example, as it is also evident from the differential equation formulations of the two subjects. The analogies between the above two subjects and subjects such as Brownian motion and polymer dynamics, to name but a few, are examples which put the case for using path integrals more strongly (c.f. Wiegel, 1986, especially section 5.3).

One further advantage of using path or functional integrals is that it is sometimes possible to extract useful information out of various path-integral expressions, without actually having to evaluate the functional integral itself. We have been fortunate to come across such a problem in section 6.4 of this thesis, in the calculation of the average propagator of a Gaussian random medium.

The use of differential equations in the description of the physical world has arisen from Newton's efforts to create the branch of physics known today as Newtonian mechanics. Similarly, the use of path integration has arisen, three hundred years later, out of Feynman's effort to describe quantum mechanical motion, while still using the Newtonian idea of a trajectory or a path. Given the three centuries which separate the path integration from differential equations, it is not at all surprising that the available analytical and numerical techniques for the former are not as well developed as for the latter. Today, differential equations and path integrals tend to be regarded as

complementary methods for doing calculations only in the various branches of theoretical physics. In time, it is our opinion that both differential equations and path integrals will gain equal acceptance as calculational tools in many more areas of science and engineering.

Appendix A

Evaluation of the path integral in equation (3.44).

We will now evaluate the path integral in equation (3.44) for an arbitrary function $c(z)$. The approach presented here follows closely that of Schulman (1981). The path taken by a ray of light in the geometrical optics limit, is that for which Fermat's principle requires the exponent of the integrand in equation (3.44) to be an extremum. The method used here integrates the fluctuations about the geometrical optics path in a functional integral which is quadratic in the fluctuations and their derivatives, just as we did in chapter 2 for the case where $c(z) = \text{constant}$.

By analogy with Mechanics, we will call the integrand in the exponent in (3.44) an optical Lagrangian; this has the form

$$L[x, z] = \frac{1}{2} \dot{x}^2 - \frac{1}{2} c^2(z) x^2. \quad (\text{A.1})$$

The solution of the Euler–Lagrange equation (Goldstein, 1980)

$$\frac{d^2x}{dz^2}(z) + c^2(z) x(z) = 0, \quad (\text{A.2})$$

gives the ray path, $X(z)$, prescribed by geometrical optics. Defining the variation about the geometrical optics path as $\xi(z) \equiv x(z) - X(z)$, it is easy to see that equation (3.44) becomes

$$K(x, z, x_0, z_0) = \exp\left\{ ik/2 \int_{z_0}^z d\zeta [\dot{X}^2(\zeta) - c^2(\zeta) X^2(\zeta)] \right\} \times \\ \oint \delta\xi(z) \exp\left\{ ik/2 \int_{z_0}^z d\zeta [\dot{\xi}^2(\zeta) - c^2(\zeta) \xi^2(\zeta)] \right\}, \quad (\text{A.3})$$

where the variation, $\xi(\zeta)$, vanishes at the end–points z and z_0 . The path integral in (A.3) now only depends on the variables z and z_0 . The terms in the exponent which are linear in $\xi(\zeta)$ vanish by virtue of the fact that $X(z)$ is the solution of the optical Euler–Lagrange equation. Therefore, in order to evaluate (A.3) we need both the solution to equation (A.2) and the functional form of the following path integral:

$$I = \oint \delta\xi(z) \exp\left\{ ik/2 \int_{z_0}^z d\zeta \left[\dot{\xi}^2(\zeta) - c^2(\zeta) \xi^2(\zeta) \right] \right\}. \quad (\text{A.4})$$

Writing I in its limiting form (Feynman and Hibbs, 1965), we have

$$I = \lim_{N \rightarrow \infty} \int_{-\infty}^{+\infty} \dots \int_{-\infty}^{+\infty} d\xi_1 \dots d\xi_{N-1} \left[\frac{k}{2\pi i \epsilon} \right]^{N/2} \exp\left\{ ik \sum_{j=0}^{N-1} \left[\frac{(\xi_{j+1} - \xi_j)^2}{2\epsilon} - \frac{1}{2} \epsilon c_j^2 \xi_j^2 \right] \right\}, \quad (\text{A.5})$$

where

$$\epsilon \equiv \frac{z - z_0}{N} \quad (\text{A.6})$$

and

$$c_j \equiv c[z_0 + \frac{j}{N}(z - z_0)]. \quad (\text{A.7})$$

We now define an $(N-1)$ dimensional vector

$$\eta = \begin{bmatrix} \xi_1 \\ \vdots \\ \xi_{N-1} \end{bmatrix} \quad (\text{A.8})$$

and the $(N-1) \times (N-1)$ matrix σ by

$$\sigma = \frac{k}{2\epsilon i} \begin{bmatrix} 2 & -1 & 0 & 0 & \dots & 0 & 0 \\ -1 & 2 & -1 & 0 & \dots & 0 & 0 \\ 0 & -1 & 2 & -1 & & & \\ \vdots & \vdots & & \ddots & & & \vdots \\ 0 & 0 & & & & 2 & -1 \\ 0 & 0 & & & & -1 & 2 \end{bmatrix} + \frac{ik\epsilon}{2} \begin{bmatrix} c_1^2 & & & & & & \\ & c_2^2 & & & & & \\ & & \ddots & & & & \\ & & & \ddots & & & \\ & & & & & & \\ & & & & & & c_{N-1}^2 \end{bmatrix}, \quad (\text{A.9})$$

in order to re-write equation (A.5) in the following form:

$$I = \lim_{N \rightarrow \infty} \left[\frac{k}{2\pi i \epsilon} \right]^{N/2} \int d^{N-1} \eta \exp(-\eta^T \sigma \eta), \quad (\text{A.10})$$

where we have used the fixed endpoint condition $\xi_0 = \xi_N = 0$. The integral in equation (A.10) can easily be evaluated by performing a linear, unitary transformation which diagonalises σ . The resulting $(N-1)$ Gaussian integrals are easily evaluated to give,

$$I = \lim_{N \rightarrow \infty} \left[\frac{k}{2\pi i \epsilon} \right]^{N/2} \frac{\pi^{(N-1)/2}}{\det \sigma}, \quad (\text{A.11})$$

or

$$I = \lim_{N \rightarrow \infty} \left[\frac{k}{2\pi i} \frac{1}{\epsilon} \frac{1}{\left[\frac{2i\epsilon}{k} \right]^{N-1} \det \sigma} \right]^{1/2}. \quad (\text{A.12})$$

A function $f(z, z_0)$ of the two variables z and z_0 may then be defined by

$$f(z, z_0) = \lim_{N \rightarrow \infty} \left[\epsilon \left[\frac{2i\epsilon}{k} \right]^{N-1} \det \sigma \right]. \quad (\text{A.13})$$

Using equation (A.9) we have:

$$\left(\frac{2i\epsilon}{k}\right)^{N-1} \det \sigma = \det \left\{ \begin{array}{c} \left[\begin{array}{cccccccc} 2 & -1 & 0 & 0 & \dots & 0 & 0 \\ -1 & 2 & -1 & 0 & \dots & 0 & 0 \\ 0 & -1 & 2 & -1 & & & \\ \vdots & \vdots & & \ddots & & & \vdots \\ 0 & 0 & & & & 2 & -1 \\ 0 & 0 & & & & -1 & 2 \end{array} \right] - \epsilon^2 \left[\begin{array}{ccc} c_1^2 & & 0 \\ & c_2^2 & \\ & & \ddots \\ & & & c_{N-1}^2 \end{array} \right] \end{array} \right\}. \quad (\text{A.14})$$

If we now define the minor of order j in the above equation to be p_j , then by straightforward expansion of the determinants it can be seen that the following recursion relation exists between the minors:

$$p_{j+1} = (2 - \epsilon^2 c_{j+1}^2) p_j - p_{j-1}. \quad (\text{A.15})$$

Multiplying all the terms in equation (A.15) by ϵ and rearranging the terms, we get,

$$\frac{(\epsilon p_{j+1} - 2\epsilon p_j + \epsilon p_{j-1})}{\epsilon^2} = -c_{j+1}^2 (\epsilon p_j). \quad (\text{A.16})$$

In the limit $N \rightarrow \infty$ (i.e. $\epsilon \rightarrow 0$), the finite difference equation (A.16) becomes a differential equation and the function which obeys this differential equation is the one defined in (A.13).

$$\lim_{N \rightarrow \infty} \epsilon p_j = \lim_{N \rightarrow \infty} f(z_0 + \frac{j}{N}(z - z_0), z_0) = f(\zeta, z_0). \quad (\text{A.17})$$

The initial values for $f(z, z_0)$ are easy to calculate:

$$f(z_0, z_0) = \lim_{\epsilon \rightarrow 0} (\epsilon p_0) = 0, \quad (\text{A.18})$$

$$\left. \frac{\partial f(z, z_0)}{\partial z} \right|_{z=z_0} = \lim_{\epsilon \rightarrow 0} \left[\frac{\epsilon(p_1 - p_0)}{\epsilon} \right] = \lim_{\epsilon \rightarrow 0} (2 - \epsilon^2 c_1^2 - 1) = 1. \quad (\text{A.19})$$

The differential equation obeyed by $f(z, z_0)$ is, therefore,

$$\frac{\partial^2 f}{\partial z^2}(z, z_0) + c^2(z) f(z, z_0) = 0. \quad (\text{A.20})$$

Combining the results of equations (A.3), (A.12), and (A.13), we have,

$$K(x, z; x_0, z_0) = \left[\frac{k}{2\pi i} \right]^{1/2} \left[\frac{1}{f(z, z_0)} \right]^{1/2} \exp \left\{ ik/2 \int_{z_0}^z d\zeta [\dot{X}^2(\zeta) - c^2(\zeta) X^2(\zeta)] \right\}, \quad (\text{A.21})$$

where $X(\zeta)$ is the geometrical optics ray path satisfying

$$\frac{d^2 X(\zeta)}{d\zeta^2} + c(\zeta) X(\zeta) = 0, \quad (\text{A.22})$$

with the boundary conditions

$$X(z_0) = x_0 \quad \text{and} \quad X(z) = x, \quad (\text{A.23})$$

and $f(z, z_0)$ is defined by equations (A.18) to (A.20).

Appendix B

The coupling coefficient C_{mn} for the arbitrary, symmetric, parabolic–refractive–index waveguide.

The general amplitude coupling coefficient, C_{mn} , describing the excitation of the m^{th} mode at the taper output (at $\zeta = z$), due to the presence of the n^{th} mode at the taper input (at $\zeta = z_0$) is given by equation (3.61). Substituting equations (4.25) and (4.27a) into (3.61), gives

$$C_{mn} = \int_{-\infty}^{+\infty} dx \int_{-\infty}^{+\infty} dx_0 \left\{ \frac{1}{2^{m/2} (m!)^{1/2}} \left[\frac{ka}{\pi} \right]^{1/4} H_m(\sqrt{ka} x) \exp\left\{ -\frac{kax^2}{2} \right\} \right\} \times \\ \left\{ \left[\frac{k}{2\pi i f(z, z_0)} \right]^{1/2} \exp[ik(z-z_0)] \exp\left\{ \frac{ik}{2} \left[x^2 \frac{\partial}{\partial z} \left[\ln f(z, z_0) \right] - x_0^2 \frac{\partial}{\partial z_0} \left[\ln f(z, z_0) \right] - \frac{2xx_0}{f(z, z_0)} \right] \right\} \right\} \times \\ \left\{ \frac{1}{2^{n/2} (n!)^{1/2}} \left[\frac{ka_0}{\pi} \right]^{1/4} H_n(\sqrt{ka_0} x_0) \exp\left\{ -\frac{ka_0 x_0^2}{2} \right\} \right\}, \quad (\text{B.1})$$

where $f(z, z_0)$ is given by (4.7), and a and a_0 are related to $c(z)$ and $c(z_0)$ by,

$$a = c(z) \quad \text{and} \quad a_0 = c(z_0). \quad (\text{B.2})$$

Thus,

$$C_{mn} = \frac{k}{\pi} \left\{ \frac{\sqrt{aa_0}}{2^{m+n+1} i f(z, z_0) m! n!} \right\}^{1/2} \exp[ik(z-z_0)] \int_{-\infty}^{+\infty} dx \int_{-\infty}^{+\infty} dx_0 H_m(\sqrt{ka} x) H_n(\sqrt{ka_0} x_0) \times \\ \exp\left\{ -\left(\frac{ka}{2} - \frac{ik}{2} \frac{\partial}{\partial z} \left[\ln f(z, z_0) \right] \right) x^2 - \left(\frac{ka_0}{2} + \frac{ik}{2} \frac{\partial}{\partial z_0} \left[\ln f(z, z_0) \right] \right) x_0^2 - \left(\frac{ik}{f(z, z_0)} \right) xx_0 \right\}. \quad (\text{B.3})$$

We now need to evaluate an integral of the form,

$$J = \int_{-\infty}^{+\infty} dx \int_{-\infty}^{+\infty} dy H_m(\beta x) H_n(\alpha y) \exp\left[-Ay^2 - Bx^2 - Cxy \right], \quad (\text{B.4})$$

where,

$$\alpha = \sqrt{ka}, \quad (\text{B.5})$$

$$\beta = \sqrt{ka_0}, \quad (\text{B.6})$$

$$A = \frac{ka_0}{2} + \frac{ik}{2} \frac{\partial}{\partial z_0} \left[\ln f(z, z_0) \right], \quad (\text{B.7})$$

$$B = \frac{ka}{2} - \frac{ik}{2} \frac{\partial}{\partial z} \left[\ln f(z, z_0) \right], \quad (\text{B.8})$$

and

$$C = \frac{ik}{f(z, z_0)}. \quad (\text{B.9})$$

Performing the y -integration first, we have

$$J = \int_{-\infty}^{+\infty} dx H_m(\beta x) \exp \left[-Bx^2 + \frac{C^2}{4A} x^2 \right] \int_{-\infty}^{+\infty} dy H_n(\alpha y) \exp \left[-A \left[y + \frac{Cx}{2A} \right]^2 \right]. \quad (\text{B.10})$$

Making the change of variable,

$$u = \sqrt{A} \left[y + \frac{Cx}{2A} \right], \quad (\text{B.11})$$

in the y -integral, and using

$$H_n(u+v) = \frac{1}{2^{n/2}} \sum_{s=0}^n \frac{n!}{(n-s)!s!} H_{n-s}(\sqrt{2} u) H_s(\sqrt{2} v), \quad (\text{B.12})$$

(Spiegel, 1968, equation 27.26), yields,

$$J = \int_{-\infty}^{+\infty} dx H_m(\beta x) \exp \left[-Bx^2 + \frac{C^2}{4A} x^2 \right] \times \frac{1}{2^{n/2}} \sum_{s=0}^n \frac{n!}{(n-s)!s!} H_{n-s} \left(-\frac{\alpha C}{A\sqrt{2}} x \right) \frac{1}{\sqrt{A}} \int_{-\infty}^{+\infty} du H_s \left[\frac{\alpha\sqrt{2}}{\sqrt{A}} u \right] \exp[-u^2]. \quad (\text{B.13})$$

The u -integral in equation (B.13) is given by Abramowitz and Stegun (1965, equation 22.13.18),

$$\int_{-\infty}^{+\infty} du H_s(yu) \exp[-u^2] = \begin{cases} \sqrt{\pi} (y^2 - 1)^{s/2} s! / (s/2)! & s \text{ even.} \\ 0 & s \text{ odd.} \end{cases} \quad (\text{B.14})$$

Thus, equation (B.13) becomes

$$J = \int_{-\infty}^{+\infty} dx H_m(\beta x) \exp \left[-Bx^2 + \frac{C^2}{4A} x^2 \right] \frac{1}{2^{n/2}} \times \sum_{p=0}^{\leq n/2} \frac{n!}{(n-2p)!(2p)!} H_{n-2p} \left(-\frac{\alpha C}{A\sqrt{2}} x \right) \frac{1}{\sqrt{A}} \sqrt{\pi} \left[\frac{2\alpha^2}{A} - 1 \right]^p \frac{(2p)!}{p!}. \quad (\text{B.15})$$

Making the further change of variable

$$w = \sqrt{\frac{AB - C^2/4}{A}} x, \quad (\text{B.16})$$

and substituting into equation (B.15), gives after some simplification

$$J = \sqrt{\frac{\pi}{AB - C^2/4}} \frac{1}{2^{n/2}} \sum_{p=0}^{\leq n/2} \frac{n!}{(n-2p)!p!} \left[\frac{2\alpha^2}{A} - 1 \right]^p \times \int_{-\infty}^{+\infty} dw H_m \left[\sqrt{\frac{A}{AB - C^2/4}} \beta w \right] H_{n-2p} \left[\frac{-\alpha C}{\sqrt{2A} \sqrt{AB - C^2/4}} w \right] \exp[-w^2]. \quad (\text{B.17})$$

In order to evaluate the integral in equation (B.17), we have to make use of the explicit series expansion for the Hermite polynomials given in equation (4.27b). Equation (B.17) then reduces to

$$J = \sqrt{\frac{\pi}{AB - C^2/4}} \frac{1}{2^{n/2}} \sum_{p=0}^{\leq n/2} \frac{n!}{(n-2p)!p!} \left[\frac{2\alpha^2}{A} - 1 \right]^p \times \sum_{q=0}^{\leq m/2} \frac{(-1)^q m!}{(m-2q)!q!} \left[\frac{2\beta\sqrt{A}}{\sqrt{AB - C^2/4}} \right]^{m-2q} \sum_{r=0}^{\leq (n-2p)/2} \frac{(-1)^r (n-2p)!}{(n-2p-2r)!r!} \left[\frac{-\sqrt{2}\alpha C}{\sqrt{A} \sqrt{AB - C^2/4}} \right]^r \times \int_{-\infty}^{+\infty} dw w^{n+m-2p-2q-2r} \exp[-w^2]. \quad (\text{B.18})$$

The w -integral is

$$\int_{-\infty}^{+\infty} dw w^{n+m-2p-2q-2r} \exp[-w^2] = \begin{cases} \frac{\sqrt{\pi}(n+m-2p-2q-2r)!}{2^{n+m-2p-2q-2r} r! (n/2+m/2-p-q-r)!} & \text{if } n+m \text{ is even.} \\ 0 & \text{if } n+m \text{ is odd.} \end{cases} \quad (\text{B.19})$$

It is evident from equations (B.18) and (B.19) that even modes only excite even modes and odd modes only excite odd modes.

Substituting equation (B.19) into equation (B.18), and using equations (B.5) to (B.9) to simplify the resulting expression, we can easily obtain the final expression for C_{mn} . Denoting $f \equiv f(z, z_0)$, this final expression is given by,

$$\begin{aligned}
C_{mn} &= \left[\frac{\sqrt{aa_0}}{2if} \right]^{1/2} \left[\left(\frac{a_0}{2} + \frac{i}{2} \frac{\partial \ln f}{\partial z_0} \right) \left(\frac{a}{2} - \frac{i}{2} \frac{\partial \ln f}{\partial z} \right) - \frac{1}{4f^2} \right]^{-1/2} \times \\
&\frac{\sqrt{(n!m!)}}{2^n 2^{m/2}} \sum_{p=0}^{\leq n/2} \sum_{q=0}^{\leq m/2} \sum_{r=0}^{\leq (n-2p)/2} \frac{(n+m-2p-2q-2r)!}{p!q!r!(m-2q)!(n-2p-2r)!(n/2-m/2-p-q-r)!} \times \\
&\frac{\left[\frac{1}{\frac{1}{4} + \frac{i}{4a_0} \frac{\partial \ln f}{\partial z_0}} - 1 \right]^p \left[\frac{1}{if \sqrt{a - i \frac{\partial \ln f}{\partial z}}} \right]^{n-2p-2r} \left[\frac{a^2}{2} - \frac{i}{2} a \frac{\partial \ln f}{\partial z} \right]^{m/2-q}}{\left[\left(\frac{a_0}{2} + \frac{i}{2} \frac{\partial \ln f}{\partial z_0} \right) \left(\frac{a}{2} - \frac{i}{2} \frac{\partial \ln f}{\partial z} \right) - \frac{1}{4f^2} \right]^{n/2+m/2-p-q-r}}.
\end{aligned}$$

(B.20)

Appendix C

The determination of the functional averages in chapter 6.

The averages $\langle \rho(\zeta) \rangle$ and $\langle \rho(\zeta) \cdot \rho(\zeta') \rangle$ can be easily determined if we introduce the following characteristic functional,

$$\Phi = \left\langle \exp \left\{ ik \int_0^z d\zeta f(\zeta) \cdot \rho(\zeta) \right\} \right\rangle. \quad (\text{C.1})$$

where $f(\zeta)$ is an arbitrary two-dimensional vector function of ζ . We can extract the two averages from the characteristic functional, by differentiating Φ with respect to $f(\zeta)$ and then setting $f(\zeta) \equiv 0$. Thus,

$$\langle \rho(\zeta) \rangle = \frac{1}{ik} \frac{\delta \Phi}{\delta f(\zeta)} \Big|_{f(\zeta) \equiv 0}, \quad (\text{C.2})$$

and

$$\langle \rho(\zeta) \cdot \rho(\zeta') \rangle = -\frac{1}{k^2} \frac{\delta^2 \Phi}{\delta f(\zeta) \cdot \delta f(\zeta')} \Big|_{f(\zeta) \equiv 0}. \quad (\text{C.3})$$

It is now necessary to derive the explicit form of equations (C.2) and (C.3) in order to evaluate the average optical path length expressions (6.70) and (6.75). Using the definition of the average in (6.69), the characteristic functional can be written as,

$$\Phi = \frac{\int \delta \rho(z) \exp \left\{ ik \left[S_t + \int_0^z d\zeta f(\zeta) \cdot \rho(\zeta) \right] \right\}}{\int \delta \rho(z) \exp [ik S_t]}. \quad (\text{C.4})$$

The path integral in the numerator of (C.4) is readily interpreted as the propagator of the non-local harmonic oscillator in a spatially uniform external force field. We may define for convenience the modified optical path length S_t' by,

$$S_t' = S_t + \int_0^z d\zeta' f(\zeta') \cdot \rho(\zeta'). \quad (\text{C.5})$$

Since S_t is quadratic in $\rho(\zeta)$, then S_t' is also quadratic in $\rho(\zeta)$. It was shown in chapter 2 that for Gaussian path integrals such as the ones on the right hand side of equation (C.4), the change of variable of integration from the ray path $\rho(z)$ to the deviation $\eta(z)$ from the geometrical optics ray path $\tilde{\rho}(z)$, results in,

$$\int \delta \rho(z) \exp[ikS[\rho(\zeta)]] = \exp[ikS_{G_0}(\rho, \rho_0, z)] \times \oint \delta \eta(z) \exp[ik(S[\eta(\zeta)] - \text{all linear terms in } [\eta(\zeta)])], \quad (\text{C.6})$$

whence,

$$\int \delta \rho(z) \exp[ikS[\rho(\zeta)]] = \exp[ikS_{G_0}(\rho, \rho_0, z)] \text{ (Function of } z \text{ and parameters only)}. \quad (\text{C.7})$$

$S_{G_0}(\rho, \rho_0, z)$ depends on the endpoints of the ray path and is computed using the geometrical optics path $\tilde{\rho}(z)$. Using (C.7) and the fact that equation (C.5) shows that S_t' and S_t differ by only a linear term in ρ , (C.4) becomes,

$$\Phi = \frac{\exp[ikS_{t'_{G_0}}(\rho, \rho_0, z)] \int \delta \eta(z) \exp[ikS_t[\eta(\zeta)]]}{\exp[ikS_{t_{G_0}}(\rho, \rho_0, z)] \int \delta \eta(z) \exp[ikS_t[\eta(\zeta)]]} \quad (\text{C.8})$$

Hence,
$$\Phi = \exp\{ik[S_{t'_{G_0}}(\rho, \rho_0, z) - S_{t_{G_0}}(\rho, \rho_0, z)]\}, \quad (\text{C.9})$$

where $S_{t'_{G_0}}(\rho, \rho_0, z)$ is computed using the geometrical optics path and $\tilde{\rho}(z)$ is the solution of the Euler–Lagrange equations with an optical Lagrangian given by,

$$L = \frac{1}{2} \dot{\rho}^2(z) - \frac{\omega^2}{4z} \int_0^z d\zeta' [\rho(z) - \rho(\zeta')] + f(z) \cdot \rho(z). \quad (\text{C.10})$$

$S_{t_{G_0}}(\rho, \rho_0, z)$ is then computed using the corresponding geometrical optics path found with $f(z) \equiv 0$. Substituting equation (C.9) into equations (C.2) and (C.3) and using the fact that only $S_{t'_{G_0}}$ depends functionally on $f(z)$ when carrying out the functional differentiations, we find that,

$$\langle \rho(\zeta) \rangle = \frac{1}{ik} \frac{\delta}{\delta f(\zeta)} \exp\{ik[S_{t'_{G_0}}(\rho, \rho_0, z) - S_{t_{G_0}}(\rho, \rho_0, z)]\} \Big|_{f(\zeta) \equiv 0}, \quad (\text{C.11})$$

or,
$$\langle \rho(\zeta) \rangle = \frac{\delta S_{t'_{G_0}}}{\delta f(\zeta)} \Big|_{f(\zeta) \equiv 0}. \quad (\text{C.12})$$

Similarly,

$$\langle \rho(\zeta) \cdot \rho(\zeta') \rangle = \left[\frac{\delta^2 S_{t'_{G_0}}}{\delta f(\zeta) \cdot \delta f(\zeta')} + \frac{\delta S_{t'_{G_0}}}{\delta f(\zeta)} \frac{\delta S_{t'_{G_0}}}{\delta f(\zeta')} \right] \Big|_{f(\zeta) \equiv 0}. \quad (\text{C.13})$$

It is evident from equations (C.12) and (C.13) that we now need to evaluate the optical path length $S_{k'_{G_0}}(\rho, \rho_0, z)$, which in turn requires knowledge of $\tilde{\rho}(z)$. As it has been pointed out above, $\tilde{\rho}(z)$ is the solution of the Euler–Lagrange equation with L given by

equation (C.10). The resulting differential equation is,

$$\frac{d^2 \tilde{\rho}}{d\zeta^2}(\zeta) + \frac{\omega^2}{z} \int_0^z d\zeta' [\tilde{\rho}(\zeta) - \tilde{\rho}(\zeta')] - f(\zeta) = 0, \quad (\text{C.14})$$

which gives,

$$\frac{d^2 \tilde{\rho}}{d\zeta^2}(\zeta) + \omega^2 \tilde{\rho}(\zeta) = \frac{\omega^2}{z} \int_0^z d\zeta' \tilde{\rho}(\zeta') + f(\zeta). \quad (\text{C.15})$$

The above equation can be solved using the Green's function for the classical harmonic oscillator, subject to the boundary conditions $\tilde{\rho}(0) = \rho_0$ and $\tilde{\rho}(z) = \rho$. This latter Green's function satisfies the ordinary differential equation,

$$\left(\frac{d^2}{d\zeta^2} + \omega^2 \right) g(\zeta, \zeta') = \delta(\zeta - \zeta'), \quad (\text{C.16})$$

and vanishes at the two boundaries $\zeta = 0$ and $\zeta = z$. It is given by,

$$g(\zeta, \zeta') = -\frac{1}{\omega \sin(\omega z)} [\sin(\omega(z-\zeta)) \sin(\omega \zeta') \Theta(\zeta - \zeta') + \sin(\omega(z-\zeta')) \sin(\omega \zeta) \Theta(\zeta' - \zeta)] \quad (\text{C.17})$$

where Θ is the Heaviside step function. The general solution of (C.15) which satisfies the correct boundary conditions, is,

$$\begin{aligned} \tilde{\rho}(\zeta) = \frac{1}{\sin(\omega z)} \left[\rho \sin(\omega \zeta) + \rho_0 \sin(\omega(z-\zeta)) \right] + \omega^2/z \int_0^z d\zeta' g(\zeta, \zeta') \int_0^z d\zeta'' \tilde{\rho}(\zeta'') + \\ \int_0^z d\zeta' g(\zeta, \zeta') f(\zeta'). \end{aligned} \quad (\text{C.18})$$

The first term on the right hand side of equation (C.18) is the solution of the homogeneous differential equation (C.15) and it satisfies the boundary conditions, while the second and third terms are the solutions to the inhomogeneous problem and vanish at the endpoints $\zeta = 0$ and $\zeta = z$. The latter is guaranteed by the boundary conditions chosen for the Green's function $g(\zeta, \zeta')$. Equation (C.18) is an integral equation with degenerate kernel (Mathews and Walker, 1970) and can be easily solved to give,

$$\begin{aligned} \tilde{\rho}(\zeta) = \frac{1}{\sin(\omega z)} \left[\rho \sin(\omega \zeta) + \rho_0 \sin(\omega(z-\zeta)) \right] - 4 \sin(\omega(z-\zeta)/2) \sin(\omega \zeta/2) \left[(\rho + \rho_0) \sin(\omega z/2) - \right. \\ \left. \frac{2}{\omega} \int_0^z d\zeta' f(\zeta') \sin(\omega \zeta'/2) \sin(\omega(z-\zeta')/2) \right] + \int_0^z d\zeta' g(\zeta, \zeta') f(\zeta'). \end{aligned} \quad (\text{C.19})$$

Substituting the solution (C.19) for $\tilde{\rho}(\zeta)$ into equations (C.5) and (6.68) and after

considerable but straightforward algebraic manipulation, the result for $S_{t'_{G0}}$ is,

$$\begin{aligned}
 S_{t'_{G0}}(\rho, \rho_0, z) = & \frac{\omega}{4} \cot(\omega z/4) |\rho - \rho_0|^2 + \\
 & \frac{\omega}{2 \sin \omega z} \left[2\rho/\omega \int_0^z d\zeta f(\zeta) \left[\sin(\omega z) - 2 \sin(\omega z/2) \sin(\omega(z-\zeta)/2) \sin(\omega \zeta/2) \right] + \right. \\
 & 2\rho_0/\omega \int_0^z d\zeta f(\zeta) \left[\sin(\omega(z-\zeta)) - 2 \sin(\omega z/2) \sin(\omega(z-\zeta)/2) \sin(\omega \zeta/2) \right] - \\
 & \left. 2/\omega^2 \int_0^z d\zeta \int_0^\zeta d\zeta' f(\zeta) \cdot f(\zeta') \left[\sin(\omega(z-\zeta)) \sin(\omega \zeta') - \right. \right. \\
 & \left. \left. 4 \sin(\omega(z-\zeta)/2) \sin(\omega \zeta/2) \sin(\omega(z-\zeta')/2) \sin(\omega \zeta'/2) \right] \right], \quad (C.20)
 \end{aligned}$$

and holds for $\zeta \geq \zeta'$. $S_{t_{G0}}(\rho, \rho_0, z)$ can be found by simply setting $f(\zeta) \equiv 0$. Using equations (C.20), (C.2), (C.3), and substituting the results for $\langle \rho(\zeta) \rangle$ and $\langle \rho(\zeta) \cdot \rho(\zeta') \rangle$ into equations (6.70) and (6.75), gives,

$$\langle S_t \rangle = \frac{i}{k} [(\omega z/2) \cot(\omega z/2) - 1] + \frac{1}{4} \{(\omega z/2) \cot(\omega z/2) - [(\omega z/2) \operatorname{cosec}(\omega z/2)]^2\} |\rho - \rho_0|^2, \quad (C.21)$$

$$A = L^2/4 + \frac{i}{k\omega} \frac{\sin[\omega(\zeta - \zeta')/2] \sin[\omega(z - (\zeta - \zeta')/2)]}{\sin(\omega z/2)}, \quad (C.22)$$

and

$$B = \frac{\sin[\omega(\zeta - \zeta')/2] \cos[\omega(z - (\zeta + \zeta')/2)]}{\sin(\omega z/2)} (\rho - \rho_0), \quad (C.23)$$

which are valid for $\zeta \geq \zeta'$.

References.

- Abramowitz M. and Stegun I.A., 1965, *Handbook of Mathematical Functions*, New York: Dover.
- Amir–Azizi S., Hey A.J.G., and Morris T.R., 1987, ‘Quantum Fractals,’ *Complex Systems*, **1**, 923–938.
- Arfken G., 1985, *Mathematical Methods for Physicists*, 3rd Edition, Orlando: Academic.
- Ashcroft N.W. and Mermin N.D., 1976, *Solid State Physics*, Philadelphia: Saunders.
- Born M. and Wolf E., 1980, *Principles of Optics*, 6th Edition, Oxford: Pergamon.
- Boyd J.T., (Ed.), 1991, *Integrated Optics, Devices and Applications*, New York: IEEE Press.
- Burns W.K. and Milton A.F., 1990, *Waveguide Transitions and Junctions*, in Tamir Th. (Ed.), *Guided–Wave Optoelectronics*, 2nd Edition, Berlin: Springer–Verlag.
- Casperson L.W., 1985, ‘Beam Propagation in Tapered Quadratic–Index Waveguides: Analytical Solutions,’ *Journal of Lightwave Technology*, **LT–3**, 264–272.
- Constantinou C.C. and Jones R.C., 1991a, ‘Path–integral analysis of the linearly tapered graded–index waveguide,’ *Journal of Physics D: Applied Physics*, **24**, 839–848.
- Constantinou C.C. and Jones R.C., 1991b, ‘Path–integral analysis of tapered, graded–index waveguides,’ *Journal of the Optical Society of America A*, **8**, 1240–1244.
- Croxtan C.A., 1975, *Introduction to Liquid State Physics*, London: Wiley.
- Cullen T.J. and Wilkinson C.D.W., 1984, ‘Radiation losses from single–mode optical Y–junctions formed by silver–ion exchange in glass,’ *Optics Letters*, **9**, 134–136.
- Daniell P.J., 1918, ‘A general form of integral,’ *Annals of Mathematics*, **19**, 279–294.
- Daniell P.J., 1919, ‘Integrals in an infinite number of dimensions,’ *Annals of Mathematics*, **20**, 281–288.
- Daniell P.J., 1920, ‘Further properties of the general integral,’ *Annals of Mathematics*, **21**, 203–220.

- Dashen R., 1979, 'Path integrals for waves in random media,' *Journal of Mathematical Physics*, **20**, 894–920.
- de Gennes P.G., 1969, 'Some conformation problems of long macromolecules,' *Reports on Progress in Physics*, **32**, 187–205.
- DeWitt–Morette C., Low S.G., Schulman L.S. and Shiekh A.Y., 1986, 'Wedges I,' *Foundations of Physics*, **16**, 311–349.
- Dirac P.A.M., 1933, 'The Lagrangian in quantum mechanics,' *Physikalische Zeitschrift der Sowietunion*, **3**, 64–72.
- Dirac P.A.M., 1958, *The Principles of Quantum Mechanics*, 4th Edition, Oxford: Clarendon.
- Economou E.N., Cohen M.H., Freed K.F. and Kirkpatrick E.S., 1971, 'Electronic Structure of Disordered Materials: A Review of Current Theoretical Understanding,' in *Amorphous and Liquid Semiconductors*, Tauc J. (Ed.), New York: Plenum.
- Edwards S.F. and Peierls R.E., 1954, 'Field equations in functional form,' *Proceedings of the Royal Society*, **A224**, 24–33.
- Edwards S.F., 1958, 'A new method for the evaluation of Electric Conductivity in Metals,' *Philosophical Magazine*, **3**, 1020–1031.
- Edwards S.F., 1963, 'The statistical dynamics of homogeneous turbulence,' *Journal of Fluid Mechanics*, **18**, 239–273.
- Edwards S.F. and Gulyaev Y.B., 1964, 'The density of states of a highly impure semiconductor,' *Proceedings of the Physical Society*, **83**, 495–496.
- Edwards S.F., 1965, 'The statistical mechanics of polymers with excluded volume,' *Proceedings of the Physical Society*, **85**, 613–624.
- Edwards S.F., 1967, 'Statistical mechanics with topological constraints,' *Proceedings of the Physical Society*, **91**, 513–519.
- Edwards S.F. and Abram R.A., 1972, 'The nature of the electronic states of a disordered system,' *Journal of Physics C: Solid State Physics*, **5**, 1183–1206.

- Edwards S.F., 1975, 'Functional problems in the theory of polymers,' in *Functional Integration and its Applications*, Arthurs, A.M., (Ed.), 1974 Conference, Oxford: Clarendon.
- Eichmann G., 1971, 'Quasi-geometric optics of media with inhomogeneous index of refraction,' *Journal of the Optical Society of America*, **61**, 161–168.
- Einstein A., 1905, 'Investigations on the Theory of the Brownian Movement,' *Annalen der Physik*, **17**, 549–559, reprinted in Einstein A., 1956, *Investigations on the Theory of the Brownian Movement*, New York: Dover.
- Einstein A., 1905, 'On the Theory of the Brownian Movement,' *Annalen der Physik*, **19**, 371–381, reprinted in Einstein A., 1956, *Investigations on the Theory of the Brownian Movement*, New York: Dover.
- Eisberg R. and Resnick R., 1985, *Quantum Physics*, 2nd Edition, New York: Wiley.
- Eve M., 1976, 'The use of path integrals in guided wave theory,' *Proceedings of the Royal Society of London*, **A347**, 405–417.
- Feit M.D. and Fleck J.A., 1978, 'Light propagation in graded-index optical fibres,' *Applied Optics*, **17**, 3990–3998.
- Feynman R.P., 1942, 'The principle of least action in quantum mechanics,' *Ph.D. Thesis*, Princeton University, [unpublished].
- Feynman R.P., 1948, 'Space-time approach to non-relativistic quantum mechanics,' *Reviews of Modern Physics*, **20**, 367–387.
- Feynman R.P., 1950, 'Mathematical formulation of the quantum theory of electromagnetic interaction,' *Physical Review*, **80**, 440–457.
- Feynman R.P., 1951, 'An operator calculus having applications in quantum electrodynamics,' *Physical Review*, **84**, 108–126.
- Feynman R.P., 1955, 'Slow electrons in a polar crystal,' *Physical Review*, **97**, 660–665.
- Feynman R.P., 1957, 'Atomic theory of the λ transition in Helium,' *Physical Review*, **91**, 1291–1301.

- Feynman R.P. and Hibbs A.R., 1965, *Quantum Mechanics and Path Integrals*, New York: McGraw–Hill.
- Feynman R.P., 1972, *Statistical Mechanics*, Reading, Massachusetts: Benjamin.
- Gel'fand I.M. and Yaglom A.M., 1960, 'Integration in functional spaces and its applications in quantum physics,' *Journal of Mathematical Physics*, **1**, 48–69.
- Goldstein H., 1980, *Classical Mechanics*, 2nd Edition, Reading, Massachusetts: Addison–Wesley.
- Hannay J.H., 1977, 'Paraxial Optics and Statistical Problems of Wave Propagation,' *Ph.D. Thesis*, Cambridge University, [unpublished].
- Hawking S.W., 1979, 'Path integral approach to gravity,' in *General Relativity*, Hawking S.W. and Israel W., (Eds.), Cambridge: Cambridge University Press.
- Hawkins R.J., 1987, 'Propagation properties of single–mode dielectric waveguide structures: a path integral approach,' *Applied Optics*, **26**, 1183–1188.
- Hawkins R.J., 1988, 'Propagator–based calculation of the properties of dielectric waveguide structures,' *Applied Optics*, **27**, 2033–2037.
- Jones R. and Lukes T., 1969, 'A path integral approach to disordered systems,' *Proceedings of the Royal Society*, **A309**, 457–472.
- Kac M., 1959, *Probability and related topics in the Physical Sciences*, London: Interscience.
- Keller J.B. and McLaughlin D.W., 1975, 'The Feynman integral,' *American Mathematics Monthly*, **82**, 451–465.
- Klyatskin V.I. and Tatarskiĭ V.I., 1970, 'The parabolic equation approximation for propagation of waves in a medium with random inhomogeneities,' *Soviet Physics JETP*, **31**, 335–339.
- Kreyszig E., 1983, *Advanced Engineering Mathematics*, 5th Edition, New York: Wiley.
- Landau L.D. and Lifshitz E.M., 1977, *Quantum Mechanics : Non–relativistic Theory*, 3rd Edition, Oxford: Pergamon.

- Lee D.L., 1986, *Electromagnetic Principles of Integrated Optics*, New York: Wiley.
- Lee S.W., 1978, 'Path integrals for solving some electromagnetic edge diffraction problems,' *Journal of Mathematical Physics*, **19**, 1414–1422.
- Maiman T.H., 1960, 'Stimulated Optical Radiation in Ruby,' *Nature*, **187**, 493–494.
- Marchand E.W., 1978, *Graded Index Optics*, New York: Academic.
- Marcuse D., 1970, 'Radiation Losses of the Dominant Mode in Round Dielectric Waveguides,' *Bell Systems Technical Journal*, **49**, 1665–1693.
- Marcuse D., 1982, *Light Transmission Optics*, 2nd Edition, New York: Van Nostrand Reinhold.
- Mathews J. and Walker R.L., 1970, *Mathematical Methods of Physics*, 2nd Edition, Menlo Park: Benjamin/Cummings.
- Matthews P.T. and Salam A., 1955, 'Propagators of quantised field,' *Il Nuovo Cimento*, **11**, 120–134.
- Melles Griot, 1990, *Optics Guide 5*, Product Catalogue, ISSN 1051–4384.
- Miller S.E., 1969, 'Integrated Optics: An Introduction,' *Bell Systems Technical Journal*, **48**, 2059–2069.
- Milton and Burns, 1977, 'Mode Coupling in Optical Waveguide Horns,' *IEEE Journal of Quantum Electronics*, **QE-13**, 828–835.
- Morse P.M. and Feshbach H., 1953, *Methods of Theoretical Physics*, New York: McGraw–Hill.
- Sakurai J.J., 1985, *Modern Quantum Mechanics*, Menlo Park, California: Benjamin Cummings.
- Samathiyakanit V., 1972, 'Path–integral theory of a model disordered system,' *Journal of Physics C: Solid State Physics*, **7**, 2849–2876.
- Schulman L.S., 1981, *Techniques and Applications of Path Integration*, New York: Wiley.

- Senior J.M., 1985, *Optical Fiber Communications, Principles and Practice*, Englewood Cliffs, NJ: Prentice–Hall.
- Sherrington D., 1971, ‘Auxiliary fields and linear response in Lagrangian many–body theory,’ *Journal of Physics C: Solid State Physics*, **4**, 401–416.
- Snyder A.W. and Love J.D., 1983, *Optical Waveguide Theory*, London: Chapman and Hall.
- Spiegel M.R., 1968, *Mathematical Handbook*, Schaum’s Outline Series in Mathematics, New York: McGraw–Hill.
- Tamir Th. (Ed.), 1990, *Guided–Wave Optoelectronics*, 2nd Edition, Berlin: Springer–Verlag.
- Troudet Th. and Hawkins R.J., 1988, ‘Monte Carlo simulation of the propagation properties of single mode dielectric waveguide structures,’ *Applied Optics*, **27**, 765–773.
- Wiegel F.W., 1973, *Doctoral Thesis*, University of Amsterdam, [unpublished].
- Wiegel F.W., 1975, ‘Path Integral Methods in Statistical Mechanics,’ *Physics Reports*, **16**, 57–114.
- Wiegel F.W., 1986, *Introduction to Path–Integral Methods in Physics and Polymer Science*, Singapore: World Scientific.
- Wiener N., 1921a, *Proceedings of the National Academy of Sciences USA*, **7**, 253–262.
- Wiener N., 1921b, *Proceedings of the National Academy of Sciences USA*, **7**, 294–303.
- Wiener N., 1923, *Journal of Mathematical Physics*, **2**, 131–145.
- Wiener N., 1924, ‘The average value of a functional,’ *Proceedings of the London Mathematical Society*, **22**, 454–467.
- Wiener N., 1930, ‘Generalized harmonic analysis,’ *Acta Mathematica*, **55**, 117–258.
- Wilson K.G., 1971, ‘Renormalization Group & Critical Phenomena,’ *Physical Review*, **84**, 3174–3195.
- Wu H–D. and Barnes F.S., (Ed.), 1991, *Microlenses, Coupling Light to Optical Fibres*, New York: IEEE Press.

Yariv A., 1991, *Optical Electronics*, 4th Edition, Philadelphia: Saunders College Publishing.

Zittartz J. and Langer J.S., 1966, 'Theory of Bound States in a Random Potential,' *Physical Review*, **148**, 741–747.